Agilent Posters at ASMS 2017

Agilent Technologies

AUTOMATION

High-throughput (sub-2.5 second) direct injection using a modified RapidFire 365 HTMS system

Peter Rye[1], Arrin Katz[2], William LaMarr[2], Can Ozbal[2]
[1]Agilent Technologies
[2]PureHoney Technologies, Inc.

ASMS 2017
MP-354

Introduction

The role of mass spectrometry in early drug discovery and especially in functional biochemical and binding assays is well established. Even fast techniques such as UHPLC or SPE-MS face challenges when primary screens of several hundred thousand compounds need to be performed. At a throughput of 8 seconds per sample, an Agilent RapidFire 365 system can analyze 10,000 samples in 24 hours. However, a large screen of several hundred thousand compounds still requires many weeks of effort. We have modified a RapidFire system to facilitate the direct injection of samples at a throughput of less than 2.5 seconds per sample enabling the analysis of 35,000 samples in 24 hours.

Experimental

Modifications to RapidFire plumbing

- 10 mL sample loop (between V1 port 2 and 5) was replaced with a 2 mL sample loop
- Tubing attached to V1 port 1 was disconnected
- Tubing attached to V2 port 2 was connected to V1 port 1
- To recycle mobile phase for pumps 2 and 3:
  - Plumb a tube from V2 port 2 to a recycling bottle
  - Submerge the intake lines for pumps 2 and 3 into the recycling bottle
  - Direct the waste line from pump 2 into the recycling bottle
- To disengage flow for the peristaltic pump (pump 4), the conduits were detached from the rollers

Modifications to RapidFire configuration files

- A copy of the configuration files folder was made
- The configuration files "Pump2" and "Pump3" were individually modified such that the "MIN_ALLOWABLE_PRESSURE=0.00;"
- The configuration file "SampleInterface" was modified such that the valve positions were set as
  - STATE1=[0,0,0,...
  - STATE2=[1,1,0,...
  - STATE3=[0,0,0,...
  - STATE4=[0,0,0,...
  - STATE5=[0,0,0,...
- The configuration file "Column Changer" was modified such that "auto column switch = 0", not 1
- The configuration file "Sipper" was modified such that "sip sensor present = 0", not 1

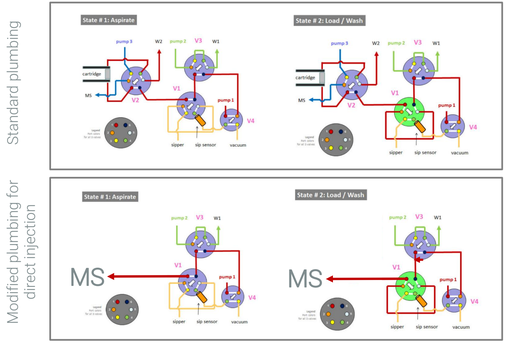

Flowpath diagrams for the standard state 1 (aspirate, top left) and 2 (load/wash, top right) and the modified state 1 (aspirate, bottom left) and 2 (elute, bottom right). In standard mode the RapidFire aspirates sample from the plate into the sampling loop during state 1 and loads/washes the sample onto the cartridge during state 2. In direct injection mode the RapidFire aspirates sample from the plate into the sampling loop during state 1 and elutes that sample to the mass spectrometer (MS) during state 2.

Experimental

RapidFire Method: Direct Injection Mode

Pump 1: 1.25 ml/min
Pump 2: 0.1 ml/min
Pump 3: 0.1 ml/min
State 1 (aspirate): 150 msec
State 2 (elute): 500 msec
Elute buffer: 90% acetonitrile + 0.1% formic acid

RapidFire Method: Standard Mode

Pump 1: 1.5 ml/min
Pump 2: 1.25 ml/min
Pump 3: 1.25 ml/min
State 1 (aspirate): 150 msec
State 2 (load/wash): 3000 msec
State 3 (extra wash): 0 msec
State 4 (elute): 3000 msec
State 5 (reequilibrate): 500 msec
Load/wash buffer: water + 0.1% trifluoroacetic acid (TFA)
Elute buffer: 80% acetonitrile + 0.1% TFA
Cartridge type: D

MS Method: 6470 Triple Quadrupole

Standard small molecule conditions were used. No optimization was done.

Results and Discussion

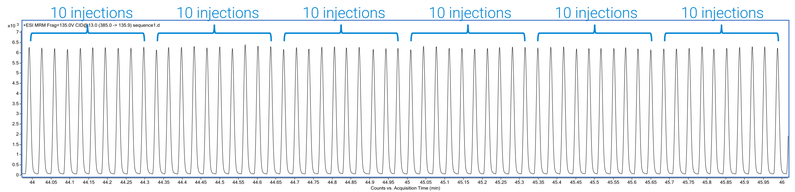

Representative MRM chromatogram data for S-adenosylhomocysteine (SAH), demonstrating the sampling and measurement of 60 injections in ~2 minutes.

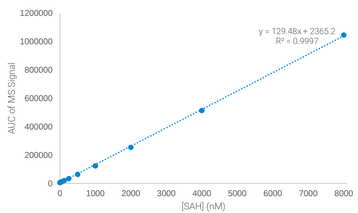

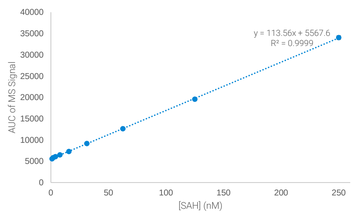

Concentration response curve for SAH. Thirteen 2-fold serial dilutions of SAH were made in water + 0.1% formic acid starting from concentration of 8000 nM. Each of these 14 stock solutions (8000, 4000, 2000, 1000, 500, 250, 125, 62.50, 31.25, 15.62, 7.81, 3.91, 1.95, and 0.98 nM) was aliquoted into a multi-well plate for analysis. One hundred replicate measurements were conducted on each concentration requiring a 52 minute run time. Data were integrated and exported in 1 minute using RapidFire Integrator. Error bars are shown and indicate the standard error of the mean. The plot of the entire concentration range is shown on the left. A zoom-in of the lower concentration data is shown on the right.

Results and Discussion

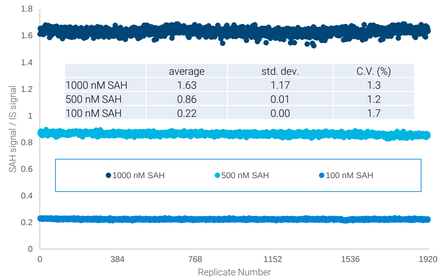

	average	std. dev.	C.V. (%)
1000 nM SAH	1.63	1.17	1.3
500 nM SAH	0.86	0.01	1.2
100 nM SAH	0.22	0.00	1.7

Replicate data for three concentrations of SAH. Bulk solutions of 100, 500, and 1000 nM SAH were made and each was supplemented with 500 nM internal standard (S-adenosylmethionine). Each solution was aliquoted into a multi-well plate for analysis. For each of the three plates, 1,920 replicate measurements were made requiring a 72 minute run time. Data for each run were integrated and exported in 1 minute using RapidFire Integrator. The AUC for the SAH MS signal was divided by the AUC of the internal standard MS signal.

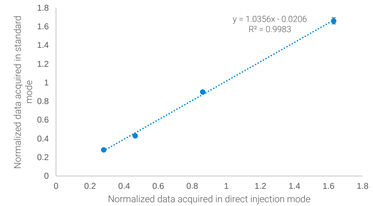

Correlation between standard mode and direct injection mode MS data. Four solutions of SAH were made (125, 250, 500, and 1000 nM) and each was supplemented with 500 nM internal standard (SAM). Ninety-six replicates of each solution were measured with the RapidFire in direct injection mode first and standard mode second. The normalized data for each mode were plotted against each other.

Conclusions

- The RapidFire system was modified to perform direct injection of samples to improve the throughput of the system further.
- The throughput of the modified system was ~2.2 seconds per sample, representing a 3- to 5-fold improvement over standard configuration analyses.
- The modified system demonstrated:
  - A broad and linear concentration response over nearly 4 orders of magnitude with an R^2=0.9997.
  - C.V.s were between 1 and 2% for 1,920 replicate measurements, of three different concentrations, showing excellent reproducibility
  - Near perfect correlation with data acquired in standard mode. R^2=0.9983 over 4 test concentrations
- The RapidFire system could be converted between modes in less than 5 minutes.
- The ability to interconvert the RapidFire system between modes allows the user to balance the throughput and sensitivity of their specific screens.

BIOLOGICAL RESEARCH

AOX1 regulates xenobiotic metabolism in Bladder cancer (BCa): Implications for Bladder cancer

Venkatrao Vantaku[1], Sri Ramya Donepudi[2], Vasanta Putluri[2], Rajapaksha Kimal[1], Cristian Coarfa[1,2], Shyam M Kavuri[3], Vadiraja Bhat[5] Arun Sreekumar[1,2], Yair Lotan[4], Nagireddy Putluri[1,2]

[1] Molecular and Cell Biology and Dan L. Duncan Cancer Center, Baylor College of Medicine, Houston, TX
[2]Advanced Technology Core, Dan L. Duncan Cancer Center, Baylor College of Medicine, Houston, TX
[3] Lester and Sue Smith Breast Center, Baylor College of Medicine, Houston, TX
[4]Department of Urology, University of Texas Southwestern, Dallas, TX
[5]Agilent Technologies, Wilmington, DE.

ASMS 2017
WP-441

Baylor College of Medicine

Agilent

Introduction

Bladder cancer (BCa), the most common cancer of the urinary tract, has higher incidence in men compared to women in western countries. [1]

Etiologically, occupational exposures (aromatic amine and polycyclic aromatic hydrocarbon exposures), tobacco smoking are well known to contribute to the occurrence of BCa. [2]

AOX1(Aldehyde oxidae1) is a cytosolic phase –I xenometabolic enzyme actively participating in cellular metabolism and xenobiotic metabolism of aldehyde containing compounds, N-Heterocycles, azodyes, nitropolycyclic aromatic hydrocarbons.

Bladder cancer development

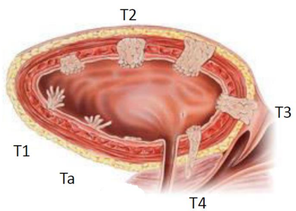

Five stages of bladder neoplasm development, beginning at the bottom of the bladder and continuing in a clockwise manner.

Experimental

The Agilent 6490 LC/TQ and 6550 QTOF LC-MS system were used to generate the analytical results.

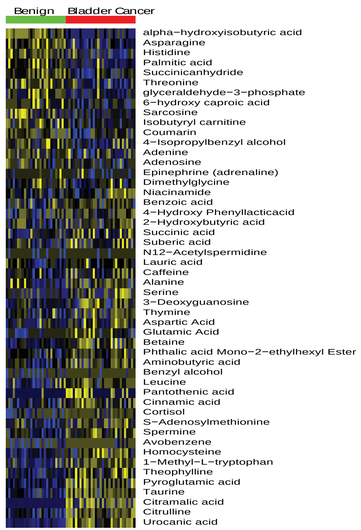

Heat map of the altered xenobiotic metabolites in clinically diagnosed BCa tissues.

Expression of AOX1 by TMA

Tissue micro array TMA of 175 from different grade patients show the high expression of AOX1 in low grade than high grade.

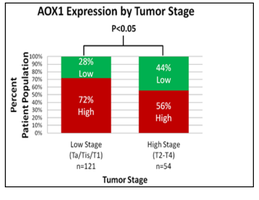

Results and Discussion

Altered xenobiotic metabolites in BCa tissues.

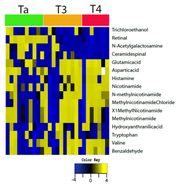

Heat map of the stages wise altered xenobiotic metabolites in different of clinically diagnosed BCa tissues.

Down regulation of AOX1 in BCa progression

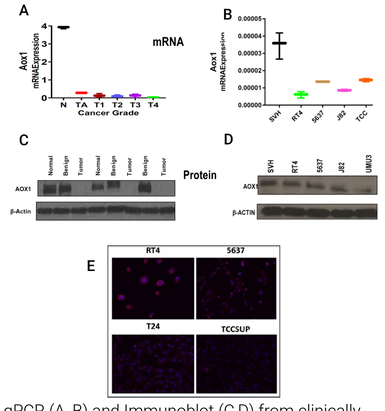

qPCR (A, B) and Immunoblot (C,D) from clinically diagnosed different stage patients and different grade cell lines confirms that the high grade tumors are losing the AOX1. Immuno fluorescence staining (E) of different grade cell lines suggests the low grade cell lines having high expression of AOX1 than high grade cell lines

Switching of AOX1 associated metabolites in KD and OE BCa cell lines

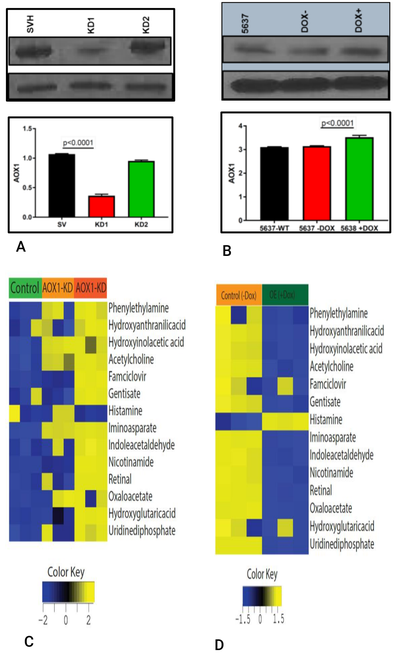

A and B: Immunoblot confirms the knock down and over expression of AOX1 in benign cell lines (SVHUC) and cancer cell lines (5637) respectively. C and D show the switching of AOX1 associated metabolites in knock down and over expressed cells.

Results and Discussion

Negative correlation of AOX1 with EZH2

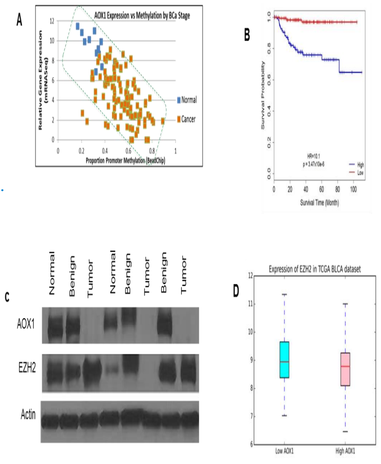

A) show the high methylation in cancer patients having low AOX1 expression. B) Kaplan-Meier curve of EZH2 from TCGA data set. C) immunoblot of patients AOX1 and EZH2 shows the negative correlation of AOX1 with EZH2. D) Correlation analysis of AOX1 with EZH2 using public data sets validated the significant negative correlation.

Reactivation of AOX1 in methylation inhibited BCa cell lines

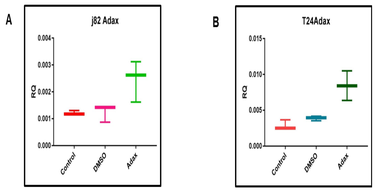

BCa cell lines (J82, T24) treated with methylation inhibitors show the over expression suggesting the AOX1 inhibition in high grade cancer through hyper methylation.

Conclusions

- Xenobiotic metabolites are altered during bladder cancer development.
- Loss of AOX1 xenobiotic enzyme and alteration in its associated metabolites during BCa progression.
- Loss of AOX1 expression in higher stages of BCa is probably due to methylation associated epigenetic modification. Further studies are going on to elucidate the loss of AOX1 and its implications in BCa development.

References

[1] Ferlay, J., et al., Estimates of worldwide burden of cancer in 2008: GLOBOCAN 2008. Int J Cancer, 2010. 127(12): p. 2893-917

[2] Marsit, C.J.et al., Carcinogen exposure and gene promoter hypermethylation in bladder cancer, 2006 ,Carcinogenesis, p.112–116

Reprogramming the SNO-Proteome in the brain of the *Shank3*-KO model of Autism Spectrum Disorder

Haitham Amal[1], Boaz Barak[2], Vadiraja Bhat[3], John S. Wishnok[1], Guoping Feng[2] and Steven R. Tannenbaum[1].

[1] Departments of Biological Engineering and Chemistry, Massachusetts Institute of Technology, Cambridge, MA 02139, USA.
[2] McGovern Institute for Brain Research, Cambridge, MA 02139, USA.
[3] Agilent Tech. Inc. Wilmington, DE.

ASMS 2017
TP-574

Massachusetts Institute of Technology

Agilent

Introduction

Protein S-nitrosation (SNO-protein) is the nitric oxide-mediated posttranslational modification of cysteine thiols.

It is an important regulatory mechanism of protein function in both physiological and pathological pathways.

We used SNOTRAP, which is a direct tagging strategy allowing enrichment of SNO-proteins in Mass Spec.

There is no evidence in the literature for SNO as a factor in Autism and *Shank3*-KO model.

Experimental

SNOTRAP was used, which is a direct tagging strategy allowing enrichment and identification of SNO-proteins using Agilent ChipCube with a 6550 iFunnel Q-TOF LC/MS.

4 groups of mice were included: 6weeks-KO, 6weeks-WT, adults-KO, and adults-WT.

Two different brain regions were analyzed, cortex and striatum.

GO analysis was done using DAVID software and protein-protein interactions analysis using STRING

References

Senevirante U, etal. JACS. 2013.
Senevirante U, etal. PNAS. 2016.

Results and Discussion

SNO-proteins:

	KO	WT	Shared between KO and WT
Adults Cortex	168 (60%)	91 (33%)	19 (7%)
Adults Striatum	267 (67%)	122 (30%)	12 (3%)
6 weeks Cortex	241 (48%)	168 (34%)	88 (18%)
6 weeks Striatum	222 (42%)	201 (20%)	106 (20%)

Results and Discussion

Protein-Protein interactions/adults-KO-cortex:

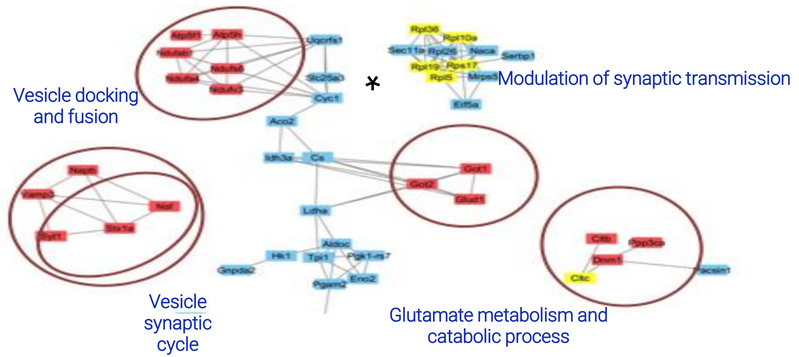

SNO-Calcineurin in the cortex leads to increased Phosphorylation of Synapsin-1 and CREB

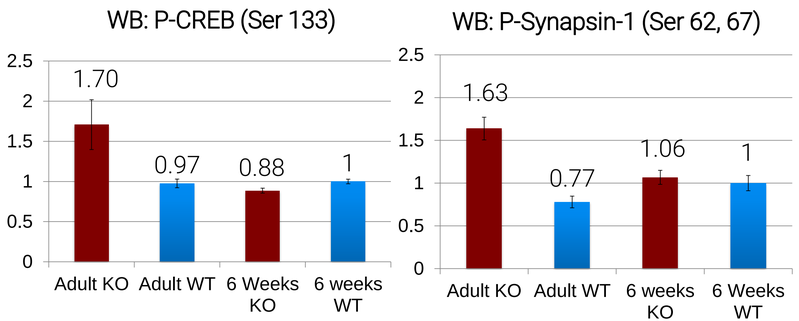

Results and Discussion

Targeted proteins and suggested mechanisms:

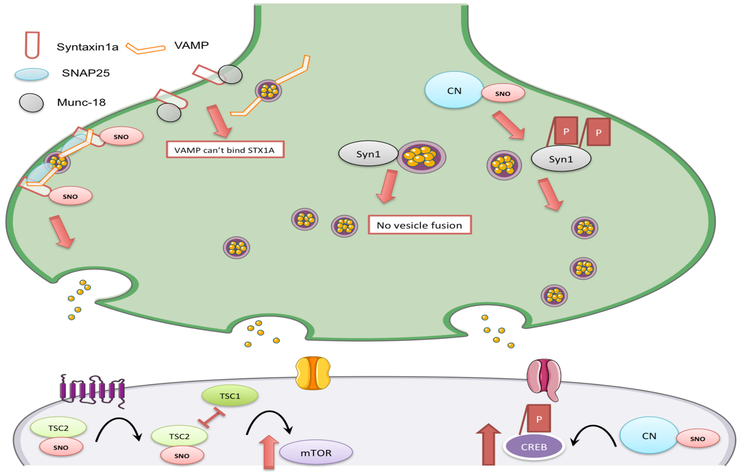

Conclusions

1. The cortex and the striatum in 6 weeks and adults *Shank3*-KO mice are regions subjected for elevated levels of SNO-proteins.
2. S-Nitrosylation of Calcineurin in the pre-synapse leads to facilitation of vesicle release and increase in P-Synapsin1 and in the post-synapse to increase in P-CREB.
3. NO is involved in the imbalanced neurotransmission in *Shank3*-KO model.

Metabolomics Study Reveals the Composition Differences between Chinese Green Tea and Black Tea Cultivars

Pengliang Li[1]; Weidong Dai[1]; Meiling Lu[2]; Zhi Lin[1]

[1]Tea Research Institute, Chin. Acad. of Agric. Sci., Hangzhou, China;

[2]Agilent Technologies (China) Co. Ltd, Beijing, China

ASMS 2017
WP - 166

Introduction

Green tea and black tea are the two most widely consumed tea types in the world, and they are manufactured from appropriate tea cultivars in China. In other words, each tea cultivar has its own suitability for manufacturing. However, the metabolite differences between green tea and black tea cultivars are unclear. The objective of this study is to elucidate such differences by liquid chromatography-mass spectrometry (LC-MS) based metabolomics approach and understand the particular metabolic pathway involved, providing fundamental guidance for tea manufacturing.

Method

Sample Preparation

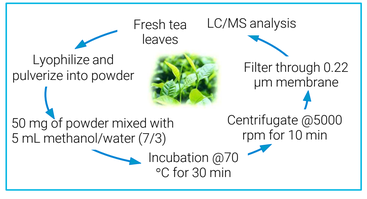

LC Conditions

Agilent 1290 Infinity II UHPLC with built-in degasser
Autosampler with temperature control
Column temperature control compartment.
Column: Zorbax Eclipse Plus C18, 100 × 2.1 mm, 1.8 μm; Column Temperature: 35°C
Mobile Phase:
Solvent A– 0.1% formic acid in H_2O; Solvent B–MeOH; Flow rate: 0.4 mL/min;
Injection volume: 3.0 μL;
Needle backflush: 5 sec with pure methanc
Gradient elution profiles:
0-4 min: 10-15% B; 4-7 min: 15-25% B;
7-9 min: 25-32% B; 9-16 min: 32-40% B;
16-22 min: 40-55% B; 22-28 min: 55-95%B
28-30 min: 95% B; 30-31 min: 95%-10% B
31-35 min: 10% B

Experimental

ESI-Q-TOF MS Conditions

Agilent 6540 Q-TOF with Dual JetStream ESI;
Polarity: positive ionization;
Drying gas temperature: 300°C;
Drying gas flow rate: 8 L/min;
Nebulizer gas pressure: 35 psi;
Sheath gas temperature: 350°C;
Sheath gas flow rate: 11 L/min;
Capillary voltage: 3500 V ;
TOF scan range: m/z of 100-1200;
Auto MS/MS scan range: 50-1200
Collision energy: 20 eV, 30 eV
Reference ions: 121.0509, 922.0098

Workflow for Metabolomics Analysis

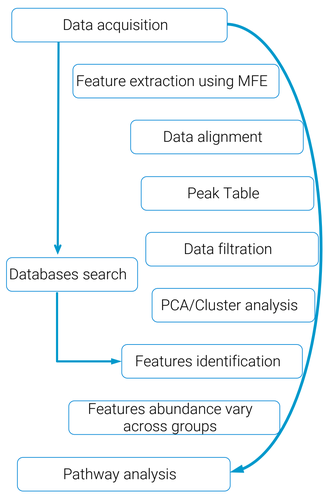

Fig. 1. Schematic diagram showing the workflow for metabolomics analysis.

Results and Discussion

Feature Extraction and Dataset Validation

An optimized UHPLC gradient elution was applied for separation of thousands of compounds in the tea extract followed by detection using accurate Q-TOF/MS under scanning mode. The acquired scanning data were initially subjected to recursive molecular feature extraction (MFE) using MassHunter Profinder software (B.08.00) to extract reliable compounds. As shown in Fig. 2, both the total ion chromatograms and the randomly selected compounds in the QC samples showing excellent repeatability with retention time deviation within ±0.1 min, mass accuracy within ± 3 ppm, and the abundance within ±20% with 40 hours of continuing data acquisition, demonstrating the dataset is very reliable.

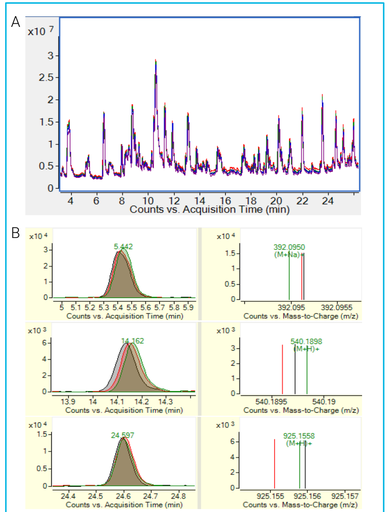

Fig. 2. Overlapping the total ion chromatograms (A) and selected extracted ion chromatograms (B) for QCs obtained during the 40 hours experimental span demonstrating excellent repeatability in retention time, mass accuracy, and peak abundance.

Principle Component Analysis and Cluster Analysis

The compound features were aligned across the dataset in MPP (v14.5) and subjected to chemometric analysis. Principal component analysis and cluster analysis separated the 10 cultivars into 2 groups—green tea (Anjibaicha, Fuzao 2, Longjing43, Zhongcha108/102) and black tea (Fuyun6, Gaoyaqi, Ningzhou2, Wannong95, and Zhuyeqi12)—on the basis of their suitability for manufacturing (Fig.3). The green tea cultivars had higher levels of amino acids and flavonoid glycosides, whereas the black ones contained higher levels of catechins, dimeric catechins, phenolic acids, and alkaloids (Fig.3-B).

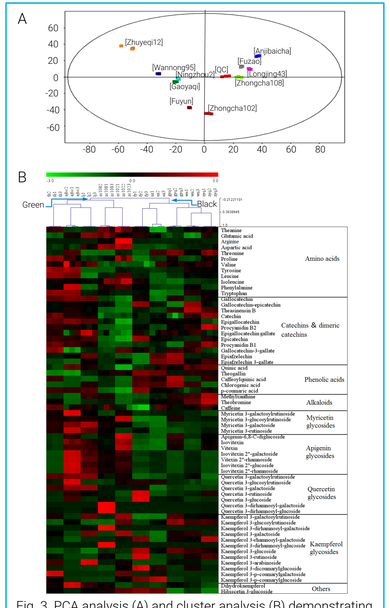

Fig. 3. PCA analysis (A) and cluster analysis (B) demonstrating the clear separation of two groups of tea cultivars.

Results and Discussion

Tentatively Identified Features

Table 1. Summary of compounds tentatively identified (Selected)

Compound name	RT (min)	m/z_{exp}	m/z err (ppm)	MS^2 fragments
Catechins and dimeric catechins (12)				
Gallocatechin[a]	5.33	307.0812	-0.3	223, 195,163,139
Gallocatechin-epicatechin	6.76	595.1448	0.3	305, 291,287,139
Theasinensin B	7.07	763.1502	-0.4	595, 443,305,139
Procyanidin B1[a]	8.50	579.1495	-0.3	409, 291,289,127
Epigallocatechin[a]	8.76	307.0813	0	289, 153, 139
Catechin[a]	8.96	291.0863	-0.3	139, 123, 95
Procyanidin B2[a]	9.55	579.1495	-0.3	409, 301,289,127
Epigallocatechin gallate[a]	10.15	459.0923	0.2	441, 289,153,139
Epicatechin[a]	11.30	291.0865	0.3	207, 139, 123, 55
Gallocatechin 3-gallate[a]	11.58	459.0923	0.2	289, 181,153,139
Epiafzelechin[a]	13.24	275.0915	0.4	191, 139, 107, 55
Epiafzelechin 3-gallate	15.65	427.1022	-0.5	275,153, 139,107
Flavonoid glycosides (32)				
Hibiscetin 3-glucoside	8.20	497.0930	0.8	335, 303,291,153
Apigenin-6,8-C-diglucoside[a]	12.52	595.1660	0.3	559, 475,307,153
Myricetin 3-galactosylrutinoside	14.63	789.2086	0.3	627, 481,319,145
Myricetin 3-glucosylrutinoside	15.14	789.2080	-0.5	627, 481, 319
Myricetin 3-galactoside[a]	15.38	481.0976	-0.2	319, 127, 85
Myricetin 3-rutinoside	15.55	627.1559	0.2	481, 319, 85
Vitexin[a]	16.04	433.1131	0.2	313, 139, 85
Isovitexin 2''-galactoside	16.28	595.1654	-0.7	433, 313, 139
Vitexin 2''-rhamnoside	16.38	579.1707	-0.3	433, 313, 85
Isovitexin 2''-glucoside	16.64	595.1658	0	433, 313, 139, 85
Quercetin 3-galactosylrutinoside	17.32	773.2131	-0.5	611,465,303,145
Quercetin 3-glucosylrutinoside	17.45	773.2131	-0.5	611, 465, 303
Isovitexin[a]	17.45	433.1130	0	313, 283,121, 81
Isovitexin 2''-rhamnoside	17.78	579.1710	0.2	433, 367,313,283
Quercetin 3-dirhamnosylgalactoside	18.18	757.2179	-0.9	611, 465, 303
Quercetin 3-galactoside[a]	18.25	465.1027	-0.2	303, 165, 91
Quercetin 3-dirhamnosylglucoside	18.51	757.2180	-0.8	611, 465, 303
Quercetin 3-rutinoside[a]	18.59	611.1607	0	465, 303, 85
Quercetin 3-glucoside[a]	18.60	465.1015	-2.8	325, 185, 85, 55
Kaempferol 3-galactosylrutinoside	19.23	757.2183	-0.4	595, 449,287,331
Kaempferol 3-glucosylrutinoside	20.13	757.2184	-0.3	595, 449,287,331
Kaempferol 3-dirhamnosylgalactoside	20.23	741.2234	-0.4	595, 449, 287
Kaempferol 3-galactoside[a]	20.36	449.1074	-1.1	309, 185, 123
Kaempferol 3-rhamnosylgalactoside	20.38	595.1659	0.2	449, 287
Kaempferol 3-dirhamnosylglucoside	20.90	741.2231	-0.8	595, 449, 287
Kaempferol 3-glucoside[a]	21.02	449.1079	0	287, 85
Kaempferol 3-rutinoside[a]	21.10	595.1663	0.8	449, 287,147,331
Kaempferol 3-arabinoside[a]	21.38	419.0975	0.5	287
Dihydrokaempferol	21.92	289.0710	4.2	153, 107, 65
Kaempferol 3-p-coumarylgalactoside	24.47	595.1451	0.8	287, 147, 119, 55
Kaempferol 3-p-coumarylglucoside	24.68	595.1452	1.0	287, 147, 91, 331
Kaempferol 3-dicoumarylglucoside	26.61	741.1814	0	455,287,147,477

note[a] : confirmed by authentic standards.

Pathway Analysis

Pathway analysis of the identified 64 compounds showed clear differences in flavones/flavonols/flavonoids biosynthesis and amino acids metabolism between green and black tea cultivars. Further mapping of the flavonoids biosynthesis pathway demonstrated that the precursor of flavonoids, phenylalanine, was at higher levels in green tea cultivars, which was consistent with the higher levels of the downstream metabolites, *p*-coumaric acid and flavone/ flavonol glycosides (Fig. 4). The higher contents of amino acids and flavone/flavonol glycosides contributing to the higher umami and moderate astringency might explain why Anjibaicha, Fuzao 2, Longjing 43, and Zhongcha 102/108 are suitable for manufacturing green teas (the samples at the right side of Fig. 3-A).

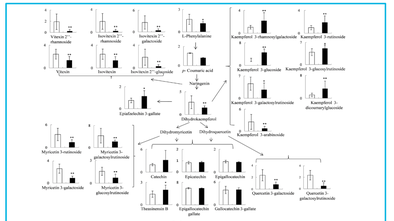

Fig. 4. Metabolic pathway of flavonoid compounds in the green and black tea cultivars. The data are shown as mean ± SD. The white and black columns represent the green and black tea cultivars, respectively. *: $p < 0.05$, **: $p < 0.01$.

Conclusions

- Non-targeted metabolomic analysis was reliably performed for 10 tea cultivars via UHPLC-Q-TOF/MS.
- The 10 tea cultivars were clearly divided into two groups according to their suitability for manufacturing. The green tea cultivars displayed higher levels of amino acids and flavonoid glycosides, whereas the black tea cultivars contained higher levels of catechins and their dimers, phenolic acids, and alkaloids.
- Thirty-two compounds, primarily flavone/flavonol glycosides, were significantly different between the green and black tea cultivars. The flavonoids pathway was inclined toward the synthesis of flavonoid glycosides and synthesis of catechins in green and black tea cultivars, respectively.

Development of a metabolomics platform for unbiased biomarker research in Inborn Errors of Metabolism

Sara Violante[1], Daniel Cuthbertson[3], Carol Ball[3], Sander Houten[1,2] and Chunli Yu[1]

[1]Department of Genetics and Genomic Sciences, [2]Icahn Institute for Genomics and Multiscale Biology, Icahn School of Medicine at Mount Sinai, 1425 Madison Avenue, Box 1498, New York, NY 10029, USA; [3]Agilent Technologies, 5301 Stevens Creek Blvd., Santa Clara, CA 95051.

ASMS 2017
WP-432

Icahn School of Medicine at Mount Sinai

Agilent

Introduction

Metabolomics approach to Inborn Errors of Metabolism

Inborn errors of metabolism (IEM) are rare inherited disorders, affecting genes involved in intermediary metabolism. The deficiency of an enzyme in a specific metabolic pathway will lead to accumulation of metabolites upstream, and deficiency of metabolites downstream of the metabolic block[1]. These are individually rare but collectively common diseases, usually presenting in the neonatal period or infancy.

In this study, we focus on two well-known IEMs, medium-chain acyl-CoA dehydrogenase deficiency (MCADD) and maple syrup urine disease (MSUD). The MCAD enzyme is crucial in the fatty acid oxidation pathway, handling the breakdown of medium-chain acyl-CoAs. The main diagnosis markers are medium-chain acylcarnitines (plasma), acylglycines and dicarboxylic acids (urine). MSUD is a deficiency of the branched-chain alpha-ketoacid dehydrogenase complex. As a result, valine, leucine and isoleucine cannot be fully degraded. Isoleucine transamination produces alloisoleucine, one of the main diagnostic markers for MSUD along with other urinary organic acids.

Over the past years, untargeted mass spectrometric analysis of metabolites i.e. metabolomics has become a powerful tool for biomarker research and the study of disease mechanisms[2]. This is very appealing as an approach for deepening medical knowledge of metabolic disease. Furthermore, it has the potential to discover other compounds which relate to known metabolic disease and impacted metabolic pathways.

Here we present a metabolomics approach for simultaneous and unbiased analysis of plasma metabolites

Experimental

Sample Preparation

Plasma samples (30 µL) from controls (n=7) and subjects with MCADD (n=7) or MSUD (n=7) were deproteinized in 80% ice-cold methanol. Dyphenydramide and hexanedioic 2,2,5,5-D4 acid (200 pg/µL) were included in the methanol solution as internal standards. After centrifugation at 21,000*xg* for 10 min, 150 µL of the supernatant was dried under N_2 flow and resuspended in 100 µL of the initial mobile phase: 98% water + 2% acetonitrile (ACN) + 0.1% formic acid (FA). Sulfamethoxazole (200 pg/µL) was added as instrument performance standard.

Methods

A 33 min chromatographic gradient using mobile phases A: 0.1% FA in water and B: 0.1% FA in ACN on an Agilent 1290 Infinity LC system equipped with a quaternary pump, multisampler, and thermostatted column compartment was used.

Time (min)	%A	%B	Flow
0	98	2	0.4
4	98	2	0.4
30	5	95	0.4
33	5	95	0.4

A volume of 1 µL of sample was injected on to a Zorbax Eclipse Plus C18 (3.5 µm, 4.6 x 100 mm) column and data was acquired in MS scan mode at 8076 transients /spectrum (in positive and negative ion mode) on the 6550 series Accurate Mass Quadrupole Time-of-Flight (QTOF) LC/MS systems using a dual Agilent Jet Stream source for sample introduction. A reference ion solution of m/z 121.050873 and 922.009798 (HP-0921 in ACN) was used for mass correction.

Data analysis

Data analysis was performed using MassHunter Qualitative Analysis B.07. Batch recursive metabolite feature extraction was performed using MassHunter Profinder B.08 software, followed by differential metabolite analysis and identification using Mass Profiler Professional 14.5 software. Unpaired t-tests were performed for MCADD and MSUD against the controls with a Benjamini-Hochberg FDR correction applied (p corr < 0.05).

Results and Discussion

Partial Least Squares Discrimination Analysis (PLS-DA)

An initial PLS-DA analysis of the collected data was performed to evaluate whether the data distribution was influenced by external factors such as sample preparation or sample handling. Figure 1 shows the PLS-DA plots for the data acquired in positive (A) and negative mode (B). The samples cluster by condition (Controls, MCADD and MSUD). This indicates that there is minimal interference from external factors and that the differences observed are due to the distinct sample phenotypes.

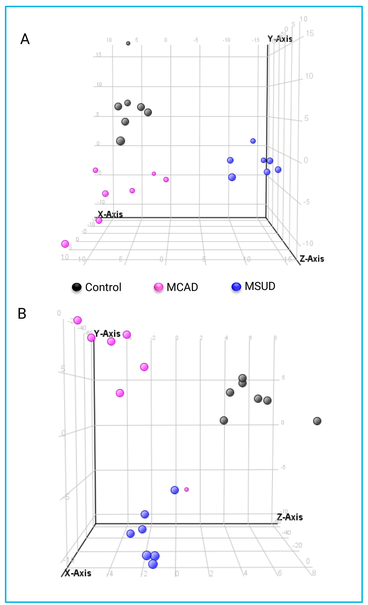

Figure 1.Partial Least Squares Discrimination Analysis plots in positive (A) and negative ion mode (B).

Differentially expressed compounds in MSUD or MCAD

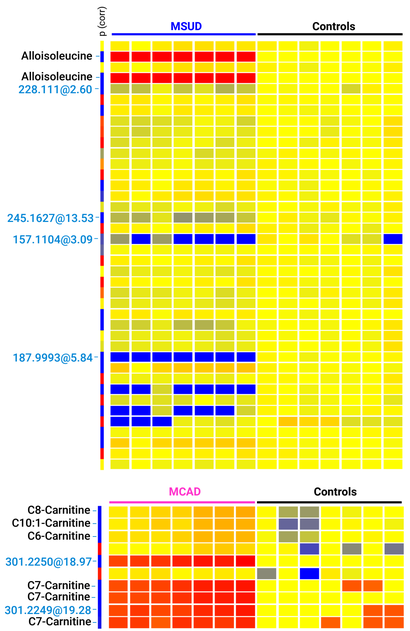

Figure 2. Heatmap of entities differentially expressed in MSUD and MCAD against controls in positive ion mode (negative ion mode not shown). Colors indicate up- or down-regulation relative to controls (red and blue, respectively). Each row represents one compound (entity) and each column represents one sample. Unpaired t-tests were performed with Benjamini-Hochberg FDR correction (p corr < 0.05). P-value (p corr) is indicated on the left bar with blue representing the lowest p corr and red the highest.

Results and Discussion

Known markers of disease found elevated in MSUD and MCAD patient samples

In MSUD samples, the most differentially elevated compound was annotated as alloisoleucine (Figure 2 and 3) which is exclusively found in MSUD patients. Deficiency of the branched-chain alpha-ketoacid dehydrogenase complex will result in the transamination of 2-keto-methylvaleric acid and subsequent production of alloisoleucine.

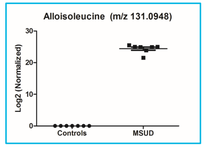

Figure 3. Scatter plot of alloisoleucine in MSUD patients vs controls.

In MCAD samples, we found some of the common markers of the disease differentially elevated: octanoylcarnitine (C8), hexanoylcarnitine (C6) and decenoylcarnitine (C10:1). We were also able to detect and annotate other compounds such as heptanoylcarnitine (C7) and octanoic acid (not shown in heatmap). This metabolomics approach allowed us to detect the main biomarkers of MCAD deficiency in one single test (Figure 2 and 4).

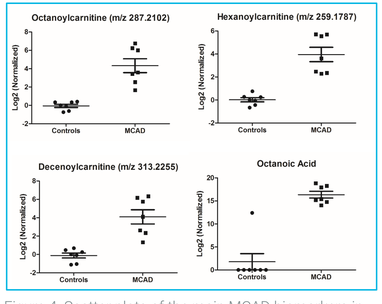

Figure 4. Scatter plots of the main MCAD biomarkers in patients vs controls.

Biomarker discovery

Importantly, we were able to identify potentially novel compounds significantly elevated in MCADD and significantly decreased in MSUD (highlighted in blue in Figure 2 and two examples shown in Figure 5). Studies are still underway for the correct annotation and confirmation of their identities.

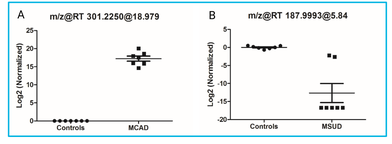

Figure 5. Scatter plots of potential novel compounds in MCAD (A) and MSUD (B).

Conclusions

- We have demonstrated that our untargeted metabolomics platform correctly identifies the main known disease markers of MCADD (medium-chain acylcarnitines and fatty acids) and MSUD (alloisoleucine).
- Additional compounds were found that correlate with the know MCAD and MSUD markers. Studies of these compounds continue with the goal of correct compound annotation.
- An unbiased analysis based on a mass spectrometry platform shows great potential for biomarker research and disease understanding.

References

[1]Lanpher B, Brunetti-Pierri N, Lee B (2006) Nat Rev Genet.

[2]Goodacre R, Vaidyanathan S, Dunn WB, Harrigan GG, Kell DB (2004) Trends Biotechnol.

Bladder Cancer Metabolomics Using the UPLC/MS-based AbsoluteIDQ p180 Kit

Vasanta Putluri[1]; Sri Ramya Donepudi[1]; Feng Jin[1]; Suman Maity[1]; Venkatrao Vantaku[1]; VADIRAJA BHAT[2]; Arun Sreekumar[1]; Nagireddy Putluri[1]

[1]Baylor College of Medicine, Houston, TX;
[2]Agilent Technologies, Inc., Santa Clara, CA

ASMS 2017
WP-433

Introduction

Bladder cancer (BCa) incidence and mortality rates vary substantially among racial and ethnic groups. Most notably, European-Americans (EA) have a higher incidence, while African-Americans (AA) experience higher mortality rates and poorer survival.1 Biocrates is a targeted quantitative metabolomics kit p180. The LC/TQ based AbsoluteIDQ® p180 Kit is an easy-to-use research assay for quantifying up to 188 endogenous metabolites from 5 different compound classes (i.e. acylcarnitines, amino acids, hexoses, phospho- and sphingolipids and biogenic amines). The assay requires very small sample amounts (10 µL) and shows excellent reproducibility.

We carried out targeted, quantitative metabolomic analysis by electrospray ionization tandem MS using the AbsoluteIDQ p180 Kit (Biocrates Life Sciences AG). Samples were anonymized and analyses were carried out on a Agilent 6490 and 6495 LC/TQ Systems. Quantification of the metabolites of the biological sample was achieved by reference to appropriate internal standards. The analytic process to derive metabolite concentrations was performed using the MetIDQ software package (Biocrates Life Sciences AG).

Experimental

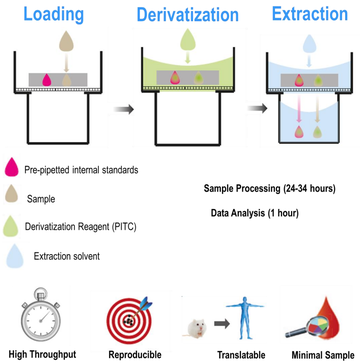

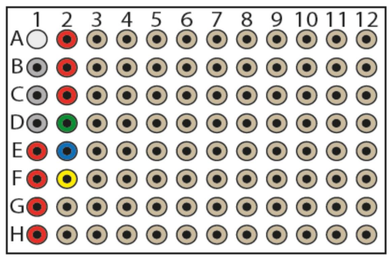

Results and Discussion

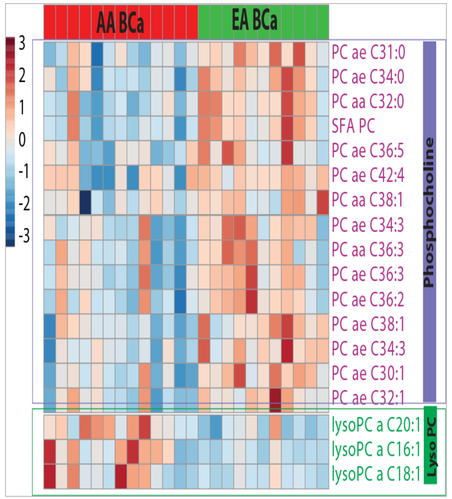

Figure 1 . Heat map showing altered lipids in AA from EA BCa tissues (Concentrations measured in uM).

African American BCa – High lyso PC

African American BCa – Lower PC

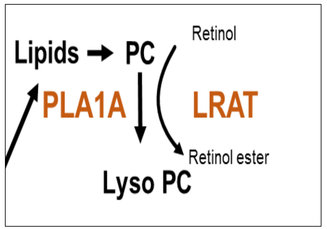

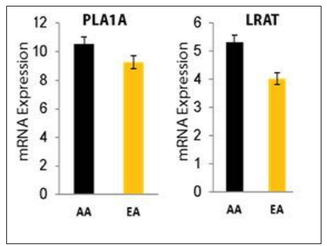

Figure-5 mRNA expressions shows higher levels of PLA1A, and LRAT in AA from EA BCa tissues

Results and Discussion

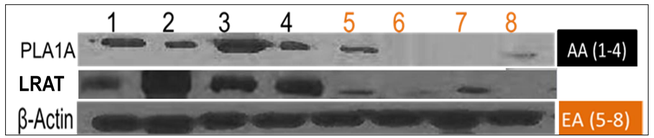

Figure-4 Western blots showing higher expression of PLA1, in AA from EA BCa tissues

Conclusions

- Altered lipid metabolism between AA BCa from EA BCa.
- Phospholipase A1 (PLA1A), Lecithin retinol acyltransferase (LRAT), two key enzymes required for conversion of (PC) into LPC were significantly elevated in AA BCa tissues. Consistent with this finding, global levels of PC were significantly lower in AA BCa tumors than EA BCa tissues.
- In summary, these data show that the lipid metabolism is altered in AA BCa tissues, resulting in accumulation of key metabolites that could result in oncogenic transformation and/or disease progression

References

1. Urology. 2011 Sep 78 (3): 544-549. doi: 10.1016/j.urology.2011.02.042
2. http://www.biocrates.com/
3. Clin Cancer Res. 2016 Oct 19. doi: 10.1158/1078-0432.CCR-16-1647

Metabolic Changes in Lung Tissue of Tuberculosis-Infected Mice Using GC/Q-TOF

Mª Fernanda Rey-Stolle[1], Vineel P Reddy[2], Santiago Angulo[1], Adrie JC Steyn[2,3,4], Sofia Nieto[5], Nathan Eno[5] and Coral Barbas[1]

[1]CEMBIO, Facultad de Farmacia, Universidad CEU San Pablo, Madrid, Spain;
[2]Department of Microbiology, University of Alabama at Birmingham, Birmingham, AL;
[3]KwaZulu-Natal Research Institute for TB and HIV (KRITH), Durban, South Africa;
[4]UAB Center for Free Radical Biology, University of Alabama at Birmingham, Birmingham, AL;
[5]Agilent Technologies Inc., Santa Clara, CA

ASMS 2017
MP-447

CEU Centro de Excelencia en Metabolómica y Bioanálisis CEMBIO Universidad San Pablo

Agilent

Introduction

The global burden of tuberculosis (TB) is vast, with an estimated 9.6 million new TB cases and 1.5 million deaths due to the disease in 2014 alone [1]. Using metabolomics, new TB biomarkers can be identified to make progress in our understanding of the disease. In this study, we used a mouse model of Mtb infection to determine the metabolic profile of uninfected and infected lung tissues.

To identify new pathophysiological pathways involved in infection as well as biomarkers of TB, the untargeted metabolomics study was performed using uninfected and infected lung tissue at 9 weeks following infection. After initial compound annotation, low-energy EI data were used to confirm the molecular ions and identify molecular formulas of putatively identified compounds and unknowns, respectively.

Experimental

Mice were infected with 5x104 CFU of Mycobacterium tuberculosis (Mtb) H37Rv via the intratracheal route. The dried extracts of lung tissue were derivatized by O-methoximation followed by trimethylsilylation. GC/MS analysis was performed using an Agilent 7890B GC system coupled to a novel high resolution 7250 GC/Q-TOF, equipped with EI source allowing low-energy ionization (Figure 1). In addition to the new low-energy EI source, the 7250 GC/Q-TOF system is capable of higher resolving power (25,000 at m/z 272) and improved mass accuracy, as compared to 7200 GC/Q-TOF due to longer (1.5 m) flight tube and higher dynamic range while maintaining high resolving power. Instrument parameters are shown in Table 1.

Locked (RTL) Fiehn method was used to facilitate compound identification when using Fiehn.L RI library for initial compound identification. In addition, NIST.L as well as an accurate mass Metabolomics PCDL were also used to identify additional hits. Feature detection was performed using SureMass signal processing in Agilent MassHunter Unknowns Analysis B.08.00. Statistical analysis was performed in Mass Profiler Professional (MPP) version 13.0. Pathway Architect, an extension tool for MPP, was used to identify biochemical pathways associated with TB infection.

Experimental

Figure 1. Agilent 7250 GC/Q-TOF

GC and MS Conditions:	
Column	DB-5MS, 30 m, 0.25 mm, 0.25 µm, DuraGuard, 10m
Injection volume	1 µL
Split ratio	10:1
Split/Splitless inlet temperature	250 °C
Oven temperature program	60 °C for 1 min 10 °C/min to 325 °C, 9.5 min hold
Carrier gas	Helium at 1 mL/min constant flow
Transfer line temperature	290 °C
Ionization mode	Standard EI at 70 eV; low electron energy EI at 17 eV, 15 eV and 12 eV
Source temperature	200°C
Quadrupole temperature	150°C
Mass range	50 to 950 m/z
Spectral acquisition rate	5 Hz

Table 1. GC/Q-TOF conditions

Results and Discussion

Experimental setup and feature detection

To identify new pathophysiological pathways involved in infection as well as biomarkers of TB, an untargeted metabolomics study was performed using uninfected and infected lung tissue extracts at 9 weeks following infection.

Following feature detection and library search performed in the Unknowns Analysis (Figure 2), the results were exported as .CEF files for further processing in MPP.

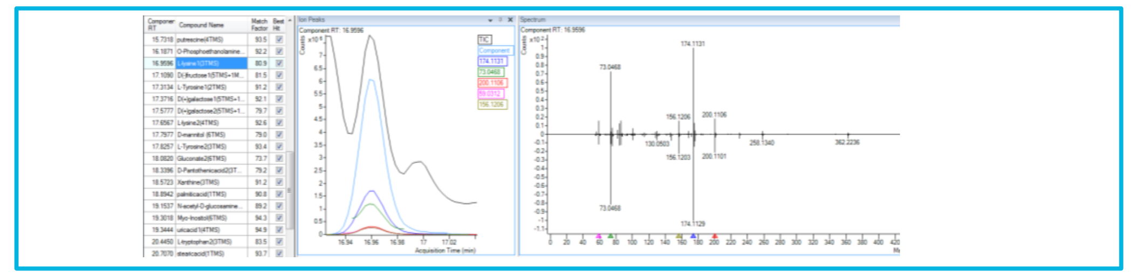

Figure 2. Feature detection and library search performed in Unknowns Analysis (using PCDL as an example)

Differential Analysis

In MPP, Principal Component Analysis (PCA) was utilized to evaluate clustering of the data. Distinct clusters, that represent clear separation between uninfected control and infected tissues were formed (Figure 3).

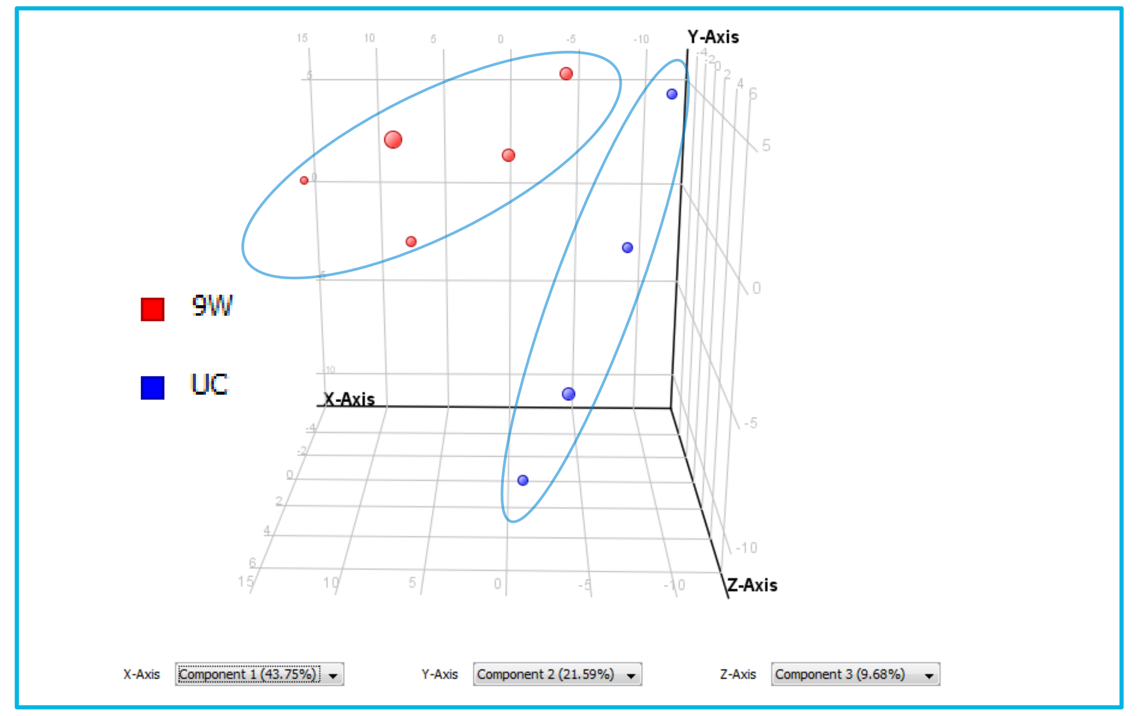

Figure 3. PCA plot. Distinct clusters from uninfected control (UC, blue circles) and 9 weeks following the infection (9W, red circles) lung tissues were observed.

Differential Analysis

Significant changes in the metabolome of lung tissue between infected and uninfected mice were further evaluated in MPP using Fold Change Analysis (Figure 4) as well as Heatmap (Figure 5). Alteration in profiles of many metabolites, in particular, amino acids and nucleobases have been observed. In addition, a change in the profiles of itaconic acid and kynurenine, have also been detected.

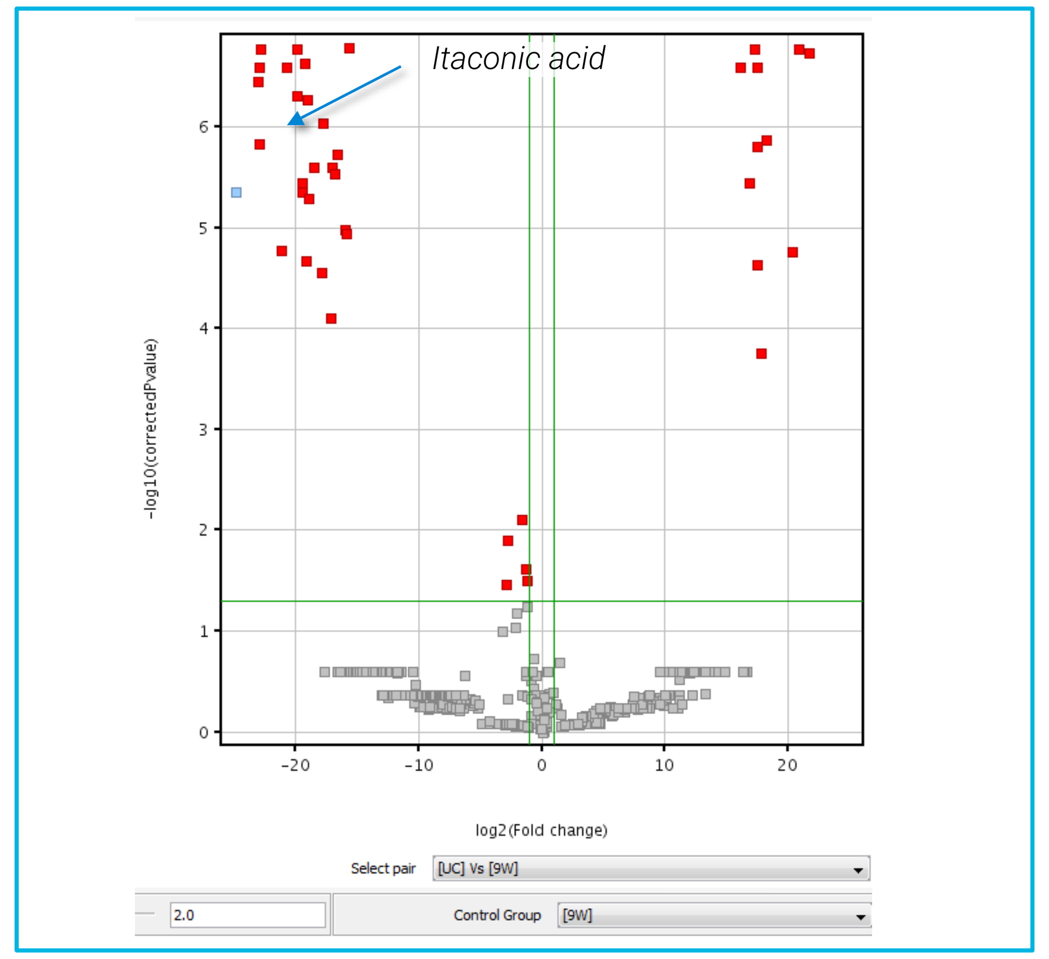

Figure 4. Volcano plot visualizing of log of fold change vs. log of p-Value for uninfected lung tissue vs. 9 weeks following TB infection.

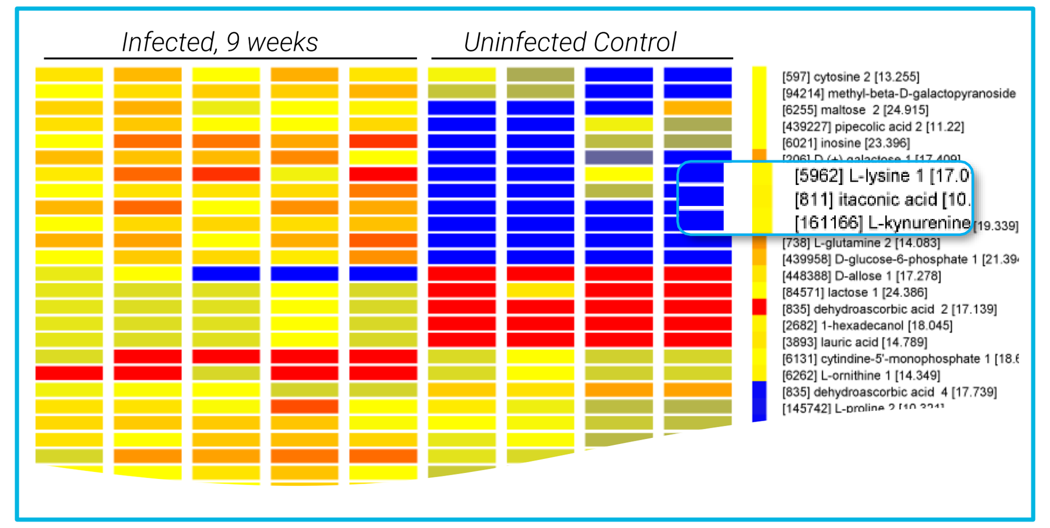

Figure 5. Heat map that highlights differentially regulated metabolites between uninfected and infected lung tissues

In addition, Pathway Architect was used to identify the biochemical pathways potentially associated with TB infection. Pathways of purine and pyrimidine metabolism as well as NAD biosynthesis II were among most significant. One of the examples is shown on Figure 6.

Unknowns identification and confirmation of tentative hits

After initial compound annotation and differential analysis in MPP, low-energy EI spectra were used to confirm the molecular ions and identify molecular formulas of putatively identified differential compounds and unknowns, respectively (Figure 7).

Results and Discussion

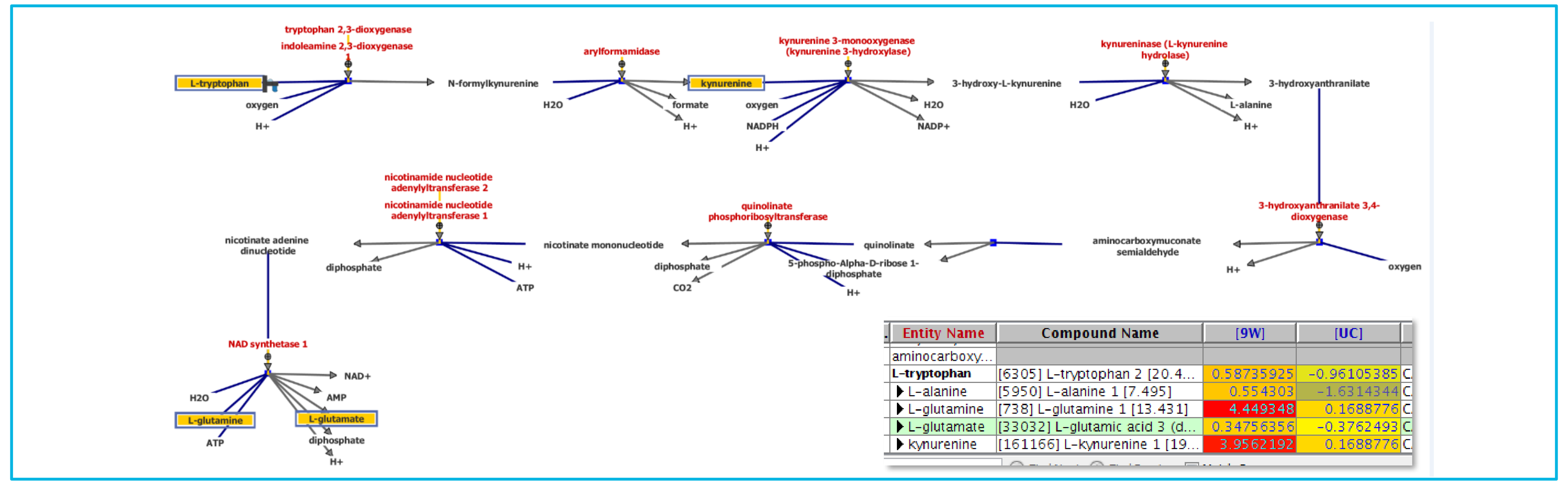

Figure 6. Example of Pathway Analysis Results: NAD Biosynthesis II

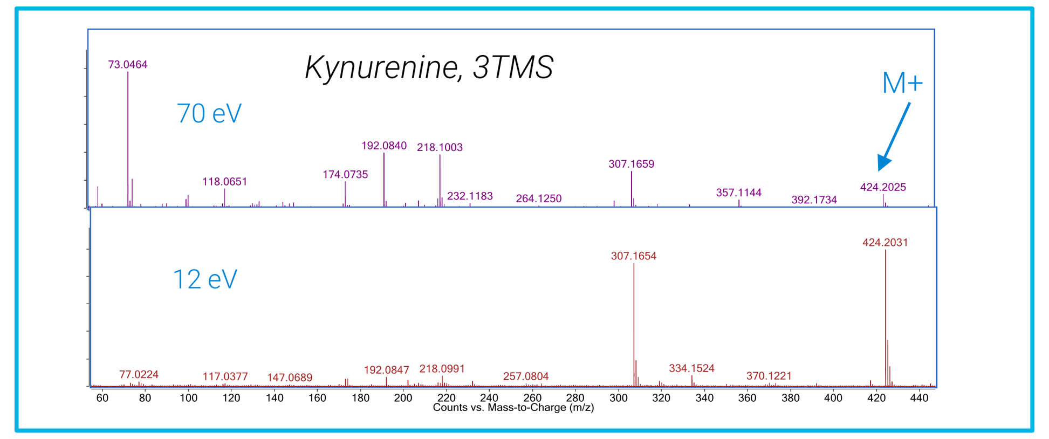

Figure 7. Confirmation of the molecular ion using low electron energy.

The first step in attempt to elucidate structure of unknowns was to use low electron energy to help identify molecular ion. MS/MS was further obtained at optimal electron energy to maximize the absolute abundance of M⁺ use as a precursor. Unknown compound MS/MS spectra were then extracted using Find by Targeted MS/MS algorithm in Qual. The results were evaluated in Molecular Structure Correlator (MSC) (Figure 8).

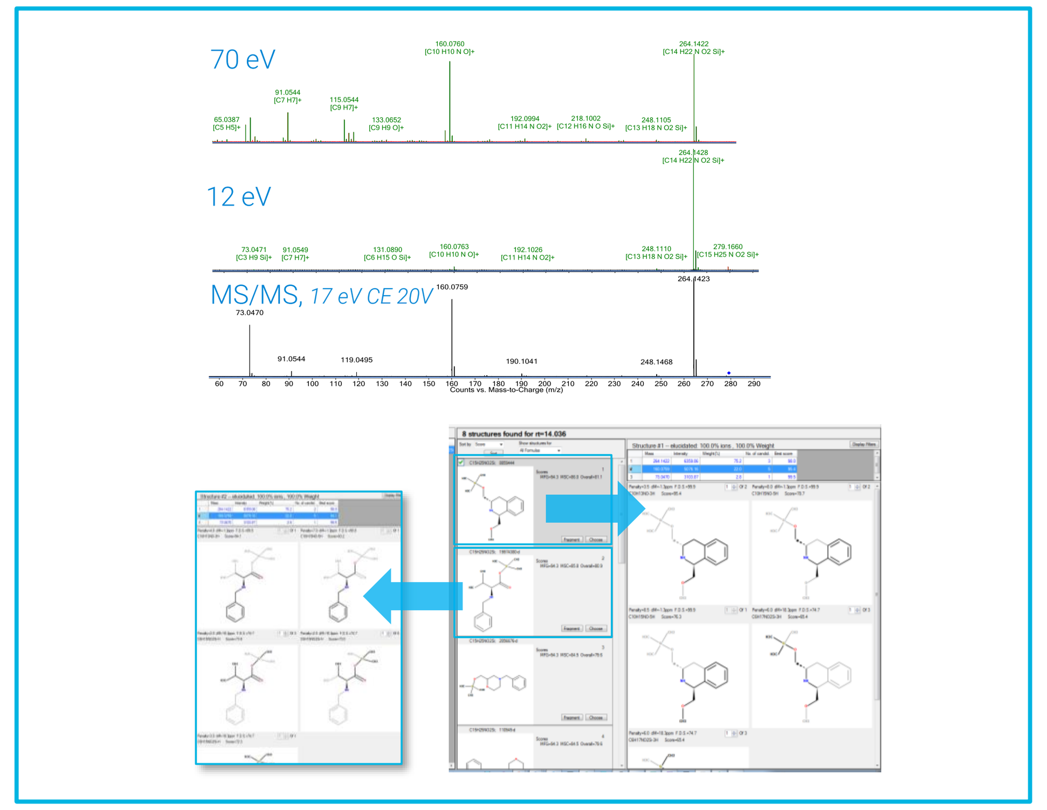

Figure 8. Structure elucidation of unknown compound using low electron energy and MS/MS with Molecular Structure Correlator (MSC). Shown are possible structures of an unknown compound.

Conclusions

The untargeted metabolomics study demonstrated an alteration in amino acids profile, as well as a change in kynurenine and itaconic acid profiles. Interestingly, itaconic acid is not generally classified as a mammalian metabolite, however, it has recently been shown to likely play a role in macrophage-based immune response [2].

Reference

[1] World Health Organization (http://www.who.int/mediacentre/factsheets/fs104/en/)
[2] Cheryl L. Strelko, Wenyun Lu, et al. J. Am. Chem. Soc., 2011, 133 (41), 16386–16389

Improved LC/TQ Analysis of Vitamin D Metabolites in Biological Samples Using Enhanced Matrix Removal Sample Preparation

Derick Lucas and Limian Zhao

Agilent Technologies Inc., 2850 Centerville Rd., Wilmington, DE, 19808

ASMS 2017
TP-459

Agilent
Trusted Answers

Introduction

Vitamin D is routinely analyzed by monitoring 25-hydroxyvitamin D2 and D3 (25-OH D2 and D3) metabolites in biological samples such as plasma and serum. While analysis by mass spectrometry affords high analytical sensitivity and selectivity for target analytes, biological samples contain interferants, namely phospholipids, which hinder analytical performance if not removed. This is a common issue associated with standard sample preparation protocols such as protein precipitation (PPT).

Agilent Captiva EMR—Lipid facilitates PPT and lipid cleanup for dirty biological samples such as plasma and serum. Both 96-well plate and 1 mL cartridges contain a non-drip frit allowing *in-situ* PPT. Precipitated proteins are filtered as the eluent passes through the EMR—Lipid sorbent for cleanup. Lipids are removed through a combined mechanism of size-exclusion and hydrophobic interaction, delivering purified eluents ready for analysis.

Accuracy and precision were assessed intra- and interday to ensure rugged method performance. Captiva EMR—Lipid provided effective *in situ* protein precipitation and clean extracts, demonstrated with matrix effect, standard post-column infusion, and phospholipid experiments, resulting in improved method reliability and robustness.

Simplified Pass-Through Cleanup Protocol

Add crashing solvent to cartridge or 96-well plate

↓

Add biological sample: plasma, serum etc.

↓

Elute with Vacuum or Positive Pressure

↓

Transfer eluent for Analysis or Post-Treatment

Experimental

Instrument Parameters

The validation of vitamin D metabolites was performed on an Agilent 1290 Infinity II UHPLC coupled to an Agilent 6460 Triple Quadrupole LC/MS.

LC Conditions

- Column: Agilent InfinityLab Poroshell 120 EC-C18, 2.1 x 50 mm, 2.7 µm (p/n 699775-902) with 2.1 x 5 mm guard (p/n 821725-911)
- Column Temp: 30°C
- Injection volume: 20 µL
- Mobile Phase A: H_2O + 0.1% formic acid
  B: Methanol + 0.1% formic acid
- Flow: 0.5 mL/min
- Gradient: Hold 0.5 min at 75% B, ramp to 98% B at 4 min, hold at 98% to 5 min.

MS Conditions

- Dynamic MRM was used for quantitation and post-column infusion experiments.
- Phospholipids were monitored with precursor ion scan using a *m/z* 184 product ion.
- See references for more details.

Procedure for Vitamin D Metabolites

Steps	Operation parameters
Add Sample to 96-well sample plate (*p/n A696001000*)	100 µL
Add I.S. working solution to appropriate wells	10 µL
Cover with plate cover and vortex	1 min
Add ACN with 1% FA to Captiva EMR–Lipid plate	400 µL
Use 96-well liquid handler to simultaneously transfer sample mixture to Captiva EMR-Lipid plate (p/n 5190-1000)	110 µL
Aspirate the sample mixture in EMR-Lipid plate by pipetting	3–5 times
Insert CapiVac collar (p/n A796) between EMR-Lipid plate and collection plate	
Apply vacuum for elution at 1 drop/3-5 s	2–4 in. Hg
Increase vacuum to drain the tube	10 in. Hg
Put plate cover on collection plate and place in autosampler for analysis	

Table 1. Detailed protocol for sample preparation of vitamin D metabolites in serum/plasma using Captiva EMR-Lipid 96-well plates.

Results and Discussion – Pass-Through Lipid Removal

Benefits of Captiva EMR-Lipid

- Simple, selective, and efficient pass-through removal of lipids.
- Outstanding recovery and precision.
- Amenable to PPT workflows (offline and *in-situ*).
- Elution by vacuum, positive pressure, or centrifuge.
- New frit design resists clogging by precipitates.
- Accommodates a wide range of analyte classes which can be directly analyzed after elution (*see poster MP-395, TP-451, and references*).

Phospholipid Removal by Captiva EMR-Lipid

Cleanup with Captiva EMR-Lipid delivers purified extracts ready for analysis. Lipids are selectively retained using a novel sorbent while analytes of interest pass-through for analysis.

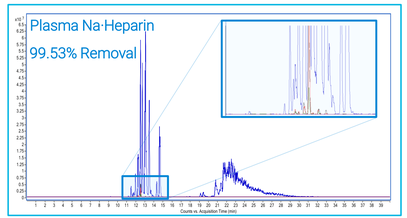

Figure 1. Phospholipid analysis product ion scan overlay of *m/z* = 184. Blue trace = PPT. Green, red, and black traces = Agilent Captiva EMR–Lipid (n = 3).

- Provides >99% phospholipid removal
  - Accommodates a wide range of biological sample types and anti-coagulants (*see poster TP-451 and references*).

Standard Post-Column Infusion: Captiva EMR-Lipid Versus Protein Precipitation

- Elimination of suppression zones gives higher signal response and reproducibility.

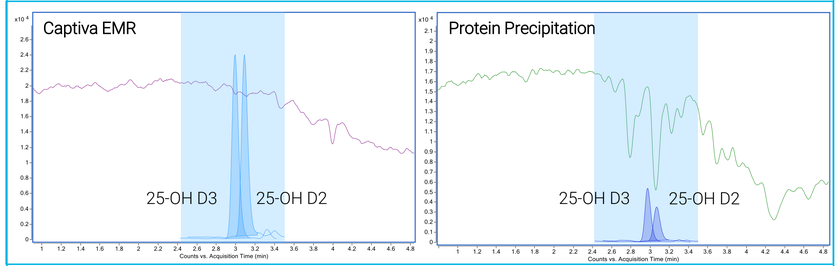

Figure 2. A 50 ng/mL solution of 25-OH D2 and D3 was pumped through a T-in after the LC column using a syringe pump with the LC method running simultaneously. Blank plasma samples were then injected producing suppression zones where matrix/lipids elute.

Results and Discussion – Quantitative Analysis of Vitamin D Metabolites

Method Accuracy and Precision for 25-OH D2 and D3

Conc. ID	25-OH D2 (ng/mL)	25-OH D3 (ng/mL)
LLOQ	10	20
LQ	20	30
MQ	250	250
HQ	500	500
ULOQ	750	750

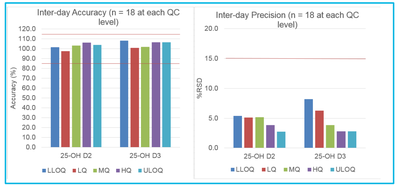

Figure 3. Summary of inter-day verification of vitamin D metabolites in human serum over 3 days. Each day consists of 6 replicates at each level.

Captiva EMR Delivers Excellent Calibration Reproducibility

Calibration curves were run in duplicate for each intra-day evaluation, one set before the QC's and one after.

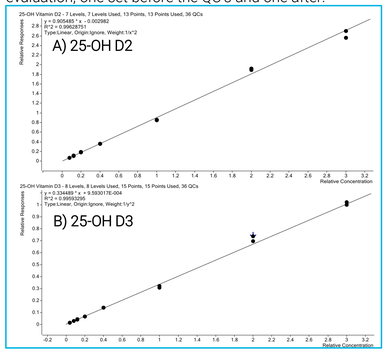

Figure 4. Duplicate calibration curves from 20–750 ng/mL for 25-OH D2 (A) and from 10–750 ng/mL for 25-OH D3 (B).

Target Analytes

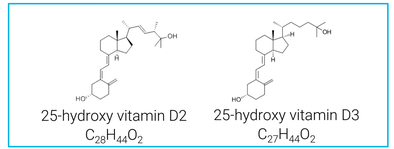

Figure 5. 25-OH D2 and D3 standards and isotopically labeled d_3 internal standards were used in this study.

Conclusions

- A method using Captiva EMR-Lipid was successfully implemented for the verification of vitamin D2 and D3 metabolites in human serum.
- The product contains a new sorbent chemistry which selectively traps lipids and allows analytes to pass through unretained for analysis.
- Captiva EMR-Lipid removes >99% of phospholipids for a wide range of biological sample types and anti-coagulants.
- A non-drip feature allows in-situ PPT or offline PPT.
- Gives high recovery and precision for a wide range of analyte types and classes.
- Future applications and formats will target the clean-up and multi-residue analysis of highly complex samples such as meat, dairy products, oils, etc.

References

1. L. Zhao, D. Lucas. Vitamin D Metabolite Analysis in Biological Samples Using Agilent Captiva EMR-Lipid. *Agilent Technologies Application Note*, publication number 5991-7956EN, 2017.
2. L. Zhao, D. Lucas. Quantitative LC/MS/MS Analysis of Drugs in Human Serum With Agilent Captiva EMR-Lipid Cleanup. *Agilent Technologies Application Note*, publication number 5991-8007EN, 2017.
3. US Food and Drug Administration, *Guidance for Industry Bioanalytical Method Validation,* 2001.

Effect of Stress on Eucalyptus Plant Metabolome

Seetaramanjaneyulu Gundimeda[1], Daniela Feltrim[2], Paulo Muzzaferra[2]

[1]Agilent Technologies, Inc., Bangalore, Karnataka, India
[2]Plant Biology department, State University of Campinas, Brazil

ASMS 2017
WP - 475

Agilent
Trusted Answers

Introduction

Changing atmospheric conditions can have an effect on the metabolome of plants. Effects of higher amounts of carbon dioxide in atmosphere and increase in temperature due to global warming on the plants has been a topical research area for scientists. In this regard, the metabolome of Eucalyptus plant under various stress conditions has been studied. Stem samples of two plant species, Eucalyptus globulus and Eucalyptus grandis were collected. Metabolites were extracted from 25mg of powdered plant samples and data was acquired on a Agilent 6550 iFunnel Q-TOF LC/MS instrument. Statistical analysis is then performed on Mass Profiler Professional (MPP) 14.5.

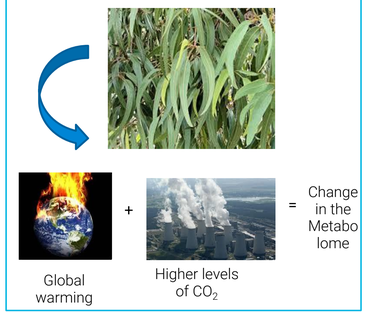

Experimental

Eucalyptus globulus and *Eucalyptus grandis* were exposed to temperatures 10^{0}C, 20 ^{0}C and 30 ^{0}C with CO_2 levels 300 ppm and 700 ppm. Metabolome at temperature, 20 ^{0}C with CO_2 levels 300 ppm was taken as a reference to compare metabolome at different stress conditions. Ion pair chromatography is used to profile aminoacids, sugars, sugar phosphates and secondary plant metabolites. Organic acids were profiled using polyfluoro phenyl propyl (PFP) column. The standards were injected in to LC-MS and a databased with RT information was created to identify compounds from the extracts.

Experimental

Work flow

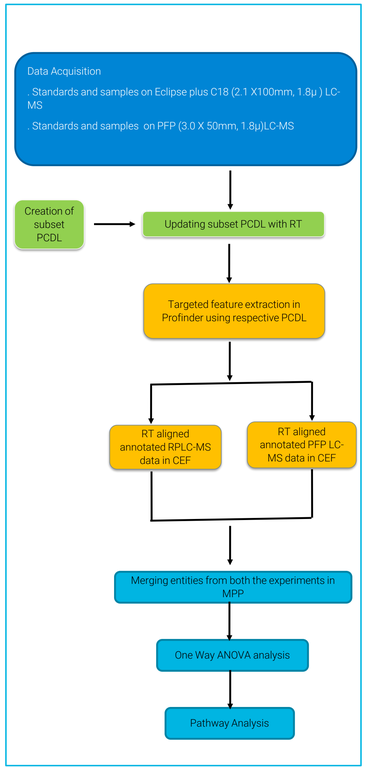

Experimental

Creating a Subset PCDL in Agilent PCDL Manager

MassHunter PCDL Manager has an option to create a custom made database. For targeted metabolite analysis, a subset PCDL from PCDL Manager was created (Figure 1 and 2). This database contained 113 polar metabolites of interest. The database was updated with RT information and used for metabolite identification.

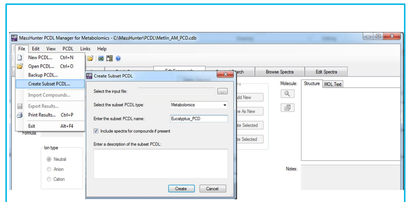

Figure1. Screen shot demonstrating the creation of Subset PCDL

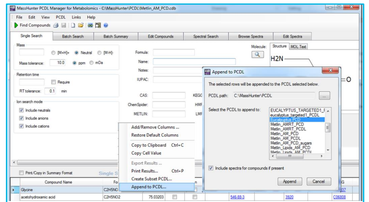

Figure 2. Screen shot showing populating the database by appending the compounds from Metlin PCDL.

RT alignment by Profinder

Profinder aligns the chromatograms and extracts molecular feature information. Metabolite identification and RT alignment is done using the new subset PCDL (Figure 3).

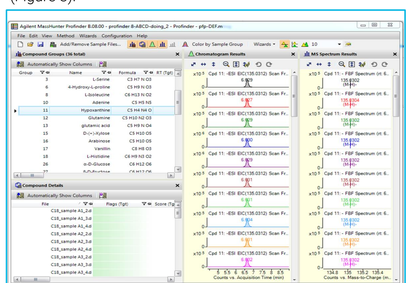

Figure 3. Screen shot showing the identified and aligned metabolite peaks from Profinder

One-Way ANOVA Analysis

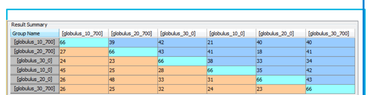

Figure 4. Screen shot demonstrating the results of ANOVA analysis

Table. 1

Compound	Fold change
Raffinose	2.1067336
L-Aspartic Acid	-2.1581993

A total of 70 compounds were identified from LC-MS data. The entities in blue color in figure 4 are statistically relevant. Compounds that are dysregulated under CO_2 stress at 20^{0}C and at 30^{0}C are given in Table.1, and Table.2 respectively.

Table. 2

Compound	Fold change
L-Phenylalanine	2.0747588
Sucrose	-4.1717052
Epicatechin	-6.2781463
myo-Inositol	2.3631005
Caffeine	-2.3471994
Maltose	-3.9184706
D-(+)-Xylose	3.5330777
Sucrose 6'-phosphate	-2.71323
UDP-glucose	-2.1591082
L-Valine	2.0792863
Caffeic Acid	2.1044834
Myricetin	2.4883027

Results and Discussion

Correlation and clustering analysis

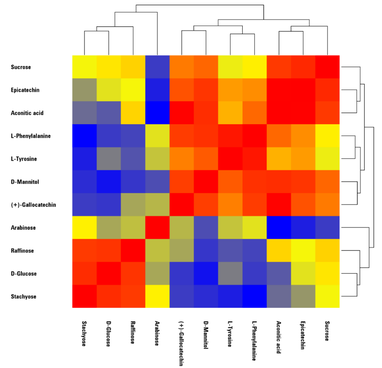

Clustering analysis (Figure 5) divides the entities into groups. Based on their correlation coefficient values, entities are arranged on a heat map with red colour showing positive correlation and blue colour representing negative correlation. Epicatechin exhibited a positive correlation with Acotinic acid as shown in Figure 5A where as it showed a negative correlation with Arabinose as shown in Figure 5B

Figure. 5A

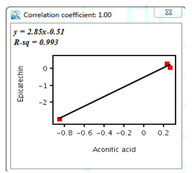

Figure. 5B

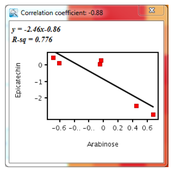

Figure. 5 Clustering analysis of 11selected entities

Pathway analysis

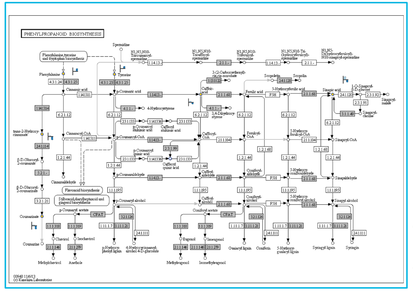

Table 3. Partial list of pathways and matched entities found in the comparison of samples taken from Eucalyptus globulus at 20^{0}C and samples taken at 30^{0}C with 300 ppm CO_2 in both cases

Pathway	Matched entities
Phenyl alanine metabolism	8
Phenyl propanoid biosynthesis	6
Cyanoamino acid metabolism	5
Alanine, Aspartate and glutamate metabolism	4
Glycine, serine and Threonine metabolism	4
Tyriosine metabolism	2
Flavanoid biosynthesis	2
Fructose and Mannose metabolism	2

Conclusions

- Metabolomic changes are more pronounced when CO_2 is associated with higher temperatures.
- Pathway analysis helped in identifying the conditions where starch synthesis is effected

Examining the Structural Influence of Site Specific Phosphorylation by Ion Mobility-Mass Spectrometry

Rebecca S. Glaskin[1] and Caroline S. Chu[2]
[1]Agilent Technologies, Inc., Wilmington, Delaware
[2]Agilent Technologies, Inc., Santa Clara, California

ASMS 2017
MP-382

Agilent
Trusted Answers

Introduction

Phosphorylation is a reversible post-translational modification influencing protein folding and activity occurring on approximately one-third of eukaryotic proteins. A challenge is to determine the sites, abundances, and roles of these modifications in biological samples; often occurring at low abundance and not efficiently ionized and fragmented. Using ion mobility mass spectrometry (IM-MS) facilitates improved peptide identification. Ions are separated on the size-to-charge ratio. The ability to distinguish conformations allows for the separation of isobaric and isomeric species, such as phosphopeptide positional isomers which are difficult to distinguish by MS alone. The workflow utilized contains an automated single-field collisional cross section (CCS) measurement coupled with 4D feature extraction allowing for exportation of conformation specific fragmentation spectra with its collision cross section values. Here we present an automated workflow using automated sample preparation from digestion to phosphopeptide enrichment for ion mobility spectrometry (IMS) analysis.

Experimental

Sample Preparation

Bovine α and β-casein and commercial PhosphoMixes 1-3 Light Phosphopeptide Standards were obtained from Sigma-Aldrich. Bovine α and β-casein were denatured, reduced, alkylated with iodoacetamide, digested with trypsin, and desalted with C18 cartridges in an automated fashion with the use of the Agilent AssayMAP Bravo in accordance with a previous protocol.[1] The resulting phosphopeptides were enriched with Fe(III)-NTA cartridges according to the Agilent AssayMAP Phosphopeptide Enrichment v2.0 App. The individual PhoshoMixes were diluted to 6.66 pmol•µL^{-1} in 20% acetonitrile 0.1% formic acid. Aproximately 1 µg of the digested α and β-casein, 1 µg of the flow thru and eluate from the phosphopeptide enrichment, and 6.66 pmol of the individual PhosphoMixes were used for analysis.

Experimental

Instrumental Analysis

For sample analysis, the Nanodapter was placed onto the Infinity II 1290 binary pump to provide nanoflow rates to the G1992A nano interface on the 6560 IM-Q-TOF. On the IM-Q-TOF the dual ion funnel interface and rear ion funnel are operated at 100 and 150 V peak-to-peak, respectively. The instrument was operated in Alternating Frames, where MS1 and MS2 analyses can be obtained in a single acquisition.

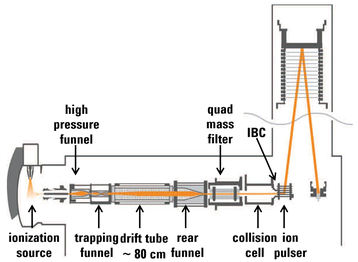

Figure 1. Schematic of the 6560 IM-Q-TOF

LC and IM-Q-TOF Conditions	Value
Drying gas flow (L•min^{-1})	5
Drying gas temperature (°C)	325
Capillary voltage (V)	1375
Mass range (*m/z*)	100 to 1700
Trapping column	75 µm × 2 cm, C18, 3 micron, 100 Å
Analytical column	75 µm × 25 cm, C18, 2 micron, 100 Å
Column temperature (°C)	45
Flow rate (nL•min^{-1})	300
Mobile phases	A) Water 0.1% formic acid B) Acetonitrile 0.1% formic acid
LC gradient	5 minutes 3% B 45 minutes 35% B 55 minutes 75% B 60 minutes 3% B

Table 1. LC-IM-Q-TOF Instrument Parameters

Results and Discussion

Data Analysis.

Feature finding was performed using Molecular Feature Extraction (MFE) followed by sequence matching for α- and β-casein in MassHunter BioConfirm. Ion mobility data was analyzed in IM-MS Browser, using iMFE for compound extraction (with MS/MS spectra) and determining collisional cross section (CCS) values using Single Field CCS calibration.

Analysis of α and β-casein

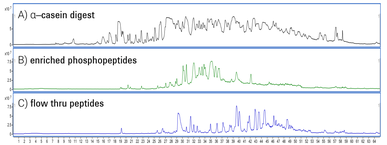

Figure 2. Total Ion Chromatograms of A) α-casein digest resulting from the automated digestion; B) enriched phosphopeptides, and C) peptides found in the flow thru resulting from the AssayMap Bravo phosphorylation enrichment.

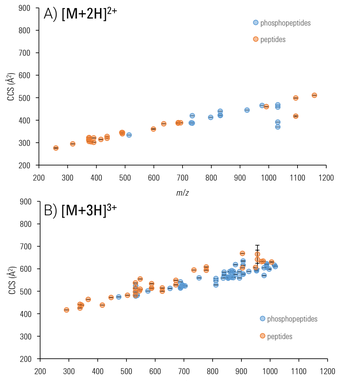

Figure 3. CCS as a function of *m/z* for A) $[M+2H]^{2+}$ and B) $[M+3H]^{3+}$ charge states of peptides and phosphopeptides resulting from the tryptic digestion of α and β−casein. Error bars correspond to the standard deviation obtained from triplicate measurements.

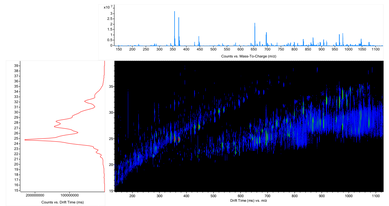

Figure 4. Two-dimensional plot displaying drift time as function of *m/z* for the summation of all the frames resulting from the α-casein digest phosphorylation enrichment.

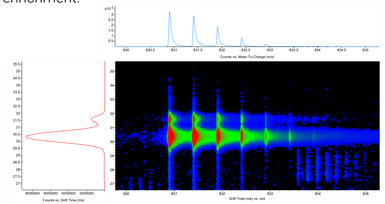

Figure 5. Two-dimensional plot displaying drift time as function of *m/z* for the $[M+2H]^{2+}$ ions of the following phoshopeptide from α-casein, ^{106}VPQLEIVPNpSAEER^{119}, where p corresponds to site of phosphorylation on the following serine residue.

Analysis of Commercial PhosphoMixes

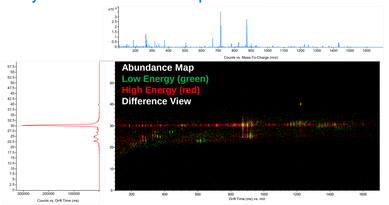

Figure 6. Two-dimensional plot displaying an overlay of the Alternating Frames acquisition, low and high energy fragmentation channels, with the drift time vs. *m/z* plotted for the $[M+2H]^{2+}$ ions of the following phosphopeptide from PhosphoMix 2, ADEPSSEEpSDLEIDK, where p corresponds to site of phosphorylation on the following serine residue.

Results and Discussion

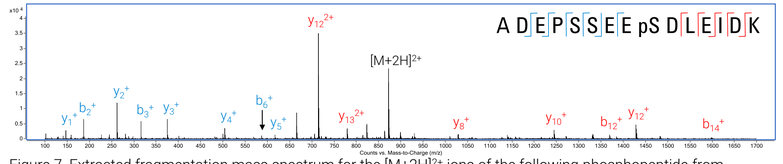

Figure 7. Extracted fragmentation mass spectrum for the $[M+2H]^{2+}$ ions of the following phosphopeptide from PhosphoMix 2, ADEPSSEEpSDLEIDK, where p corresponds to site of phosphorylation on the following serine residue. Phosphorylated residues are shown in red, while nonphosphorylated residues are displayed in blue.

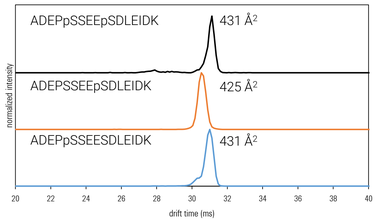

Figure 8. Drift time distributions and corresponding CCS values for three $[M+2H]^{2+}$ phosphopeptides with the same peptide sequences with varying number and location of phosphorylation sites.

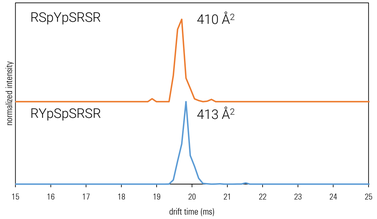

Figure 9. Drift time distributions and corresponding CCS values for two $[M+3H]^{3+}$ phosphopeptides with the same number and position of phosphorylation sites but different peptide sequence.

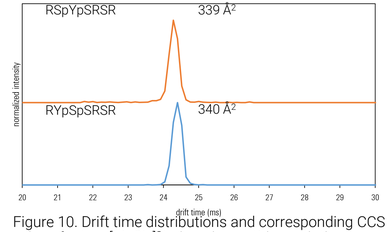

Figure 10. Drift time distributions and corresponding CCS values for two $[M+2H]^{2+}$ phosphopeptides with the same number and position of phosphorylation sites but different peptide sequence.

Conclusions

- Automated workflow from sample preparation and phosphopeptide enrichment to analysis by IMS-MS
- Phosphopeptides are more compact than non-phosphorylated peptides of similar *m/z*
- Differences in CCS values were found with peptides with varying number and location of phosphorylation sites, as well as peptides with varying sequences with the same number and position of phosphorylation sites

References

[1]Russell, J. and Murphy, S. Agilent AssayMAP Bravo Technology Enables Reproducible Automated Phosphopeptide Enrichment from Complex Mixtures Using High-Capacity Fe(III)-NTA Cartridges. *Agilent Technologies Application Note*, publication number 5991-6073EN, 2016.

Acknowledgement: Dawn Stickle for all her assistance and guidance with data acquisition and processing.

Analysis of Per/Polyfluoroalkyl Substances (PFASs) in Biological Fluid using a Novel Lipid Removing Sorbent and LC/TQ

Tarun Anumol, Joan Stevens, and Xiaomi Xu

Agilent Technologies, Wilmington, DE 19808, USA

ASMS 2017
MP-395

Agilent Trusted Answers

Introduction

Per/Polyfluoroalkyl substances (PFASs) are widely used in manufacture and industry because of their desirable properties. They find uses as surfactants, fire-retardants, non-stick cookware and other applications. Their unique properties also make them persistent with long half-lives. Studies have shown that the longer (C-chain>7) PFAS can be bio-accumulative. PFASs are ubiquitous and known to be found in blood and serum. A method was developed for the detection of PFASs in plasma using a novel lipid removing sorbent Captiva EMR-Lipid in a flow through format and Agilent 6495 Triple Quadrupole LC/MS.

Experimental

Sample Preparation:

Captiva Enhanced Matrix Removal-Lipid (EMR-Lipid) is a newly developed phospholipid removing sorbent available in a 96-well or 1 mL cartridge format. Captiva EMR-Lipid allows for in-well protein precipitation, filtration and clean-up for lipid-containing samples, like plasma, serum, whole blood.

Captiva EMR-Lipid Mechanism of Lipid Capture

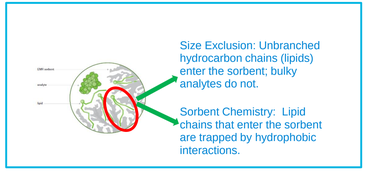

Procedure: PFAs Extraction from Plasma:

Add 400 µL of Acetonitrile with 1% Formic Acid to Captiva EMR-Lipid 1 mL cartridge

Add 100 µL of spiked or blank plasma, pre-spun

In-well mixing

Pull low vacuum, 2-4 psi, 1 drop/3-5 sec

Collect in polypropylene* test tubes

Inject directly into LC/MSMS, using polypropylene* autosampler vials

* Polypropylene collection tubes and autosampler vials are recommended since PFASs will stick to glass

Experimental

Procedure: Phospholipid Removal Evaluation:

Protein Precipitation:

Add 400 µL of Acetonitrile with 1% Formic Acid into a test tube

Add 100 µL of blank plasma, pre-spun

Vortex on a Heidolph Multi Reax® at 800-1000 rpm, 5 minutes

Centrifuge at 5000 rpm, 5 min

Pipette the supernant to an autosampler vial for analysis

Captiva EMR-Lipid:

Add 400 µL of Acetonitrile with 1% Formic Acid to Captiva EMR-Lipid 1 mL cartridge

Add 100 µL of blank plasma, pre-spun

In-well mixing

Pull low vacuum, 2-4 psi, 1 drop/3-5 sec

Collect in polypropylene test tubes

Inject directly into LC/MSMS

LC/MSMS Instrument Conditions:

LC/MSMS: Agilent 1290 Infinity II LC, 6495 Triple Quadrupole LC/MS with iFunnel Technology

Injection volume: 4 µL

Column: Poroshell EC120 C-18, 2.1 x 50 mm, 2.7 µm

Ionization: Negative Electrospray

Table 2. MRM transitions for 22 PFASs

Compound Name	(m/z) Precursor Ion	(m/z) Product Ion	Collision Energy (eV)
PFTrDA	663	618.7	8
PFDoA	613	268.7	20
N EtFOSAA	584	526	20
10:2 FTA	577	463	6
N Me FOSAA	570	511.8	24
PFUdA	563	519	8
PFDA	513	468.6	8
PFDA	513	218.7	16
PFOS	498.9	99	50
PFOS	498.9	80	50
PFNA	462.9	418.9	5
PFNA	462.9	169	17
PFOA	412.9	368.9	5
PFHxS	398.9	99	45
6:2 FTA	377	293	18
PFHpA	362.9	319	5
PFHxA	313	268.6	4
PFBS	298.9	98.9	29
PFPeA	263	218.7	0
PFBA	213	168.7	4
PFTeDA	712.9	668.5	8

Table 1. MRM transitions for 11 Phospholipids

(m/z) Precursor Ion	(m/z) Product Ion	Collision Energy (eV)
808.4	184.4	30
806.4	184.4	30
786.4	184.4	30
784.4	184.4	30
760.4	184.4	30
758.4	184.4	30
704.4	184.4	30
524.4	184.4	30
522.4	184.4	30
520.4	184.4	30
496.4	184.4	30

Results and Discussion

Table 3. Per/Polyfluoroalkyl (PFASs) General Compound Structures:

PFAS Compounds Used in Study			
PFBA	PFOA	PFDA	PFTrDA
PFPeA	PFHxS	PFOS	PFTeDA
PFHxA	8-2 FTA	PFUdA	PFHxDA
PFBS	10-2 FTA	PFDoA	PFODA
6-2 FTA	PFNA	PFDS	
PFHpA	Me-FOSAA	Et-FOSAA	

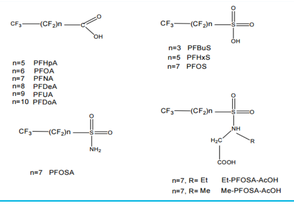

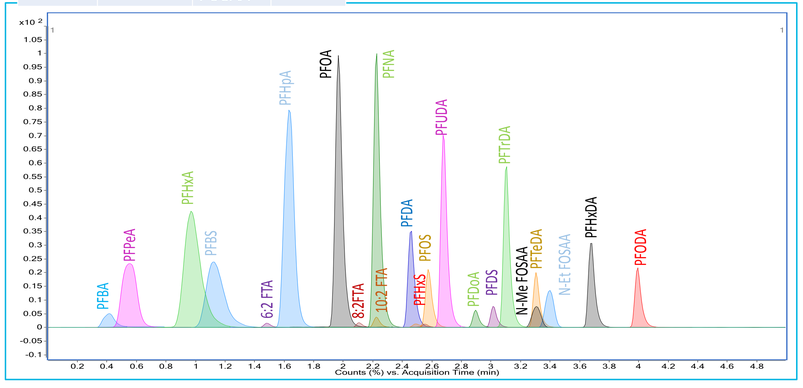

Figure 1. LC/MSMS Chromatogram of Twenty Two Per/Polyfluoroalkyl (PFASs) is the study, 5 ng/mL

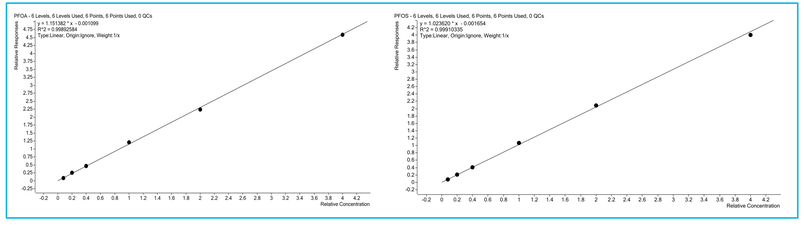

Figure 2. Calibration curves for PFOA and PFOS, calibration curve range 0.1-10 ng/mL

Results and Discussion

Chromatography and Coefficient of Determination, r^2:

Figure 1 represents the exceptional chromatography for the 22 PFASs studied at 5 ng/mL. Separation was achieved in 5 minutes. Figure 2 represents the calibration curves observed for all the PFASs in the study, PFOA and PFOS are shown. For all PFASs the coefficient of determination was > 0.992.

Recovery and RSD:

The recovery and relative standard deviation for the 22 PFASs were determined at 5 and 20 ng/mL shown in Figure 3. The overall recovery was between 75-125% for both 5 and 20 ng/mL. Relative standard deviation was 0.8-14% for 5 and 20 ng/mL.

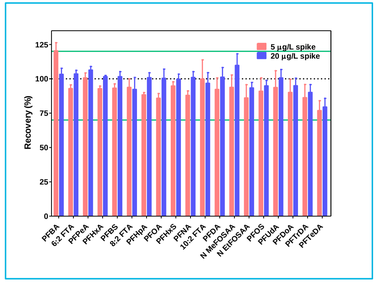

Figure 3. Recovery and RSD for the PFASs evaluated in the study at 5 and 20 ng/mL

Phospholipid Removal by Captiva EMR-Lipid versus Protein Precipitation:

Captiva EMR-Lipid, a novel phospholipid removing sorbent available in a SPE cartridge format allows for in-situ protein precipitation and phospholipid removal as the extract passes through the sorbent during elution. Figure 4 shows the overall phospholipid removal of Captiva EMR-Lipid when compared to protein precipitation, overlay. Captiva EMR-Lipid removes ~99% of the phospholipids based on peak area determined from the LC/MSMS MRM method for 11 phospholipids.

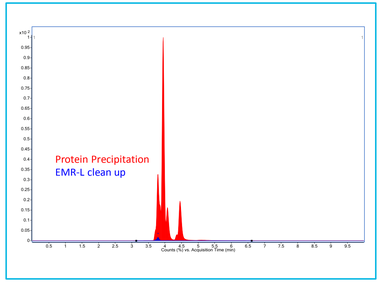

Figure 4. Overlay of the MRM chromatogram after protein precipitation and Captiva EMR-Lipid clean-up, evaluation of 11 phospholipids

Conclusions

Captiva EMR-Lipid for the Removal of Phospholipids and PFASs Analyte Recovery from Plasma:

- Efficient removal of phospholipids, with in-situ protein precipitation
- Sensitive and selective ionization with Agilent 6495 Triple Quadrupole LC/MS with iFunnel Technology
- Excellent recovery and low RSDs
- Acceptable for multi-compound/residue extraction in a cartridge format

Metabolomic Studies of Pyrazinamide in Mycobacterium Tuberculosis Using an Ion-pairing Reversed-Phase Q-TOF LC/MS Approach

Yuqin Dai[1], Travis E. Hartman[2], Steven M. Fischer[1] and Kyu Y. Rhee[2,3]

[1]Agilent Technologies, 5301 Stevens Creek Blvd, Santa Clara, CA 95051

[2]Division of Infectious Diseases, Department of Medicine, and [3]Department of Microbiology and Immunology, Weill Cornell Medical College, New York, NY 10065, USA

ASMS 2017
MP - 512

Agilent
Trusted Answers

Introduction

Tuberculosis (TB) is both the leading cause of deaths due to an infectious disease and the leading cause of deaths due to a curable disease[1]. However, drug resistance[1] is increasing while the pipeline of new drugs stagnates, and knowledge of existing drugs remains incomplete. Pyrazinamide (PZA) is a frontline TB drug[1] whose mechanism of action remains among the most poorly understood.

Here, we present a high-performance ion-pairing reversed-phase (IP-RP) Q-TOF LC/MS method that has enabled the biologically unbiased study of the impact of PZA on the Mycobacterium tuberculosis metabolome. Coupled with batch feature extraction and multivariate statistical analysis software, this workflow enabled the discovery of activity-specific metabolic changes that may help explain PZA's unique metabolic effects.

Experimental

LC/MS Metabolomics Workflow

A Q-TOF LC/MS metabolomics workflow (Figure 1) was developed.

Figure 1. LC/MS metabolomics workflow for high quality data acquisition and analyses .

LC/MS Method

The ion-pairing reversed-phase (IP-RP) chromatography method[2] was used to achieve a wide coverage of metabolite classes and improve retention time reproducibility. LC/MS analyses were performed using an Agilent 1290 Infinity UHPLC system coupled to an Agilent 6545 LC/Q-TOF with either Dual Electrospray (ESI) or Dual AJS source.

Sample Preparation

Virulent M. tuberculosis cells were grown on hydrophilic Durapore membrane filters, and transferred to plates containing PZA. At various time points, filters were harvested for extraction. Metabolism was quenched by plunging the filters into 2:2:1 acetonitrile:methanol:water at −20 °C.

Quenched cells were lysed and then sterile filtered twice and snap frozen on dry ice. At the time of analysis, samples were vortexed, centrifuged, and transferred to the HPLC vials for direct injection into the LC/MS system. Table 1 summarizes the sample information of six biological groups. Each sample was injected twice as technical replicates.

Table 1. Summary of the sample information

pH \ Treatment	Untreated samples	PZA (bacteriostatic)	PZA (bactericidal)
pH 6.6 (little or no activity)	Control pH6.6 (triplicate)	PZA(s)_pH6.6 (triplicate)	PZA(c)_pH6.6 (triplicate)
pH 5.5 (Activity)	Control pH5.5 (triplicate)	PZA(s)_pH5.5 (triplicate)	PZA(c)_pH5.5 (triplicate)

Results and Discussion

The Agilent 6545 Q-TOF delivers accurate mass and isotope ratio measurement

Accurate mass measurement is critical for compound confirmation and molecular formula generation for unknown compounds, but is not sufficient by itself[3]. Isotope ratios provide essential orthogonal information that can greatly reduce the number of plausible molecular formulas, and increase confidence in the result. Figure 2 demonstrates the excellent mass accuracy of the Agilent 6545 Q-TOF.

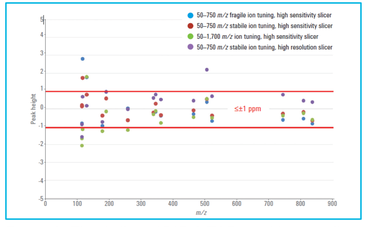

Figure 2. The Agilent 6545 Q-TOF provides excellent mass accuracy, with mass errors <±1 ppm for 54 out of 64 mass measurements

The relative isotope abundance (RIA) is defined as M+1/M ($^{13}C_1/^{12}C$), where M represents the monoisotopic ion. The RIA errors were calculated as:

RIA error (%) = 100 x (RIA_{exp} − RIA_{theo})/RIA_{theo}

Figure 5 shows the RIA errors from the data acquired using extended dynamic range mode with the high resolution slicer. Overall, the RIA errors were below (10 %) for monoisotopic ions (M) with peak intensities in the range of $3.8 \times 10^3 \sim 3.5 \times 10^5$ (Figure 3A), and the first isotopic ions (M+1) with peak intensities in the range of $1.8 \times 10^2 \sim 4.3 \times 10^4$ (Figure 3B). The mean RIA error was −3.69 %. Similar results were also obtained for the data acquired under the high-sensitivity slicer mode. These results clearly demonstrate that the 6545 Q-TOF delivers superior relative isotopic abundance measurements compared to an orbital-trapping FTMS[4].

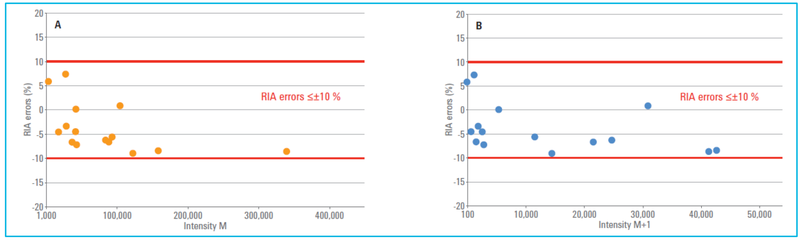

Figure 3. The Agilent 6545 Q-TOF delivers accurate relative isotope abundance measurements. A) Intensity M represents the peak height of the monoisotopic ion (^{12}C). B) Intensity M+1 represents the peak height of the isotopic ion ($^{13}C_1$).

Agilent MassHunter Profinder – Batch Targeted Feature Extraction

The Profinder Batch Targeted Feature Extraction provides a useful workflow for biological pathway-driven data analysis. In this study, Agilent Pathways to PCDL (B.07.00) software was used to create an Agilent PCDL file (.cdb) from KEGG metabolic pathways specific to M. tuberculosis strain H37Rv. Figure 4 illustrates that 73 out of 111 metabolites were found from the raw data. The compound-centric view in Profinder provides useful insight into the quality of the analytical data across different biological groups as well as the reproducibility of replicates within a sample group.

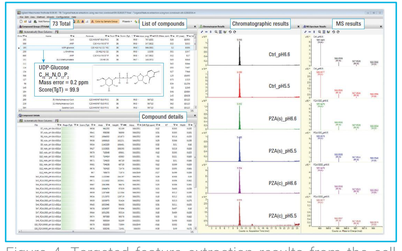

Figure 4. Targeted feature extraction results from the cell extracts in the control and PZA-treated biological groups.

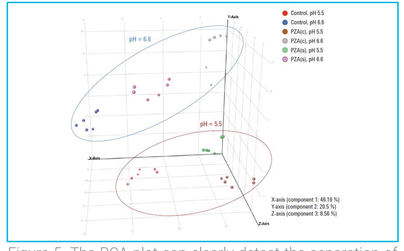

Figure 5. The PCA plot can clearly detect the separation of the treatment groups at two different pH conditions.

MPP – differential analysis of PZA-specific metabolic changes

MPP is a powerful chemometrics software with many statistical tools that allow researchers to get biological insight from complex data faster and easier. Figure 5 illustrates that PCA clearly detected the separation of biological groups with cell growth at two different pH conditions. Furthermore, PCA captures the overall variability in the metabolome of actively dividing cells taken from neutral pH in comparison with the lower variability of the nongrowing condition (pH 5.5).

A volcano plot provides a pair-wise comparison between two different biological groups where the results can be visualized by fold-change and significance simultaneously. Figure 6 shows the volcano plot of the metabolites in the PZA(s)-treated samples versus the control at pH 5.5 with a cutoff of p <0.05 and fold change (FC) >1.5. Fifty-four of the 73 metabolites displayed statistical significance, and 28 of them showed at least 1.5 fold changes in the abundance in the PZA(s)-treated samples compared to the control at pH 5.5. Using this approach, we were able to detect statistically significant metabolites among the treatments.

Results and Discussion

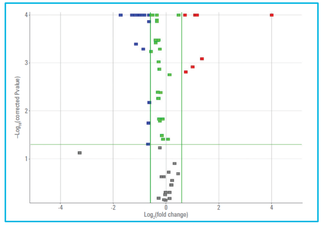

Figure 6. The volcano plot of the metabolites in the PZA-treated samples versus the control at pH 5.5.

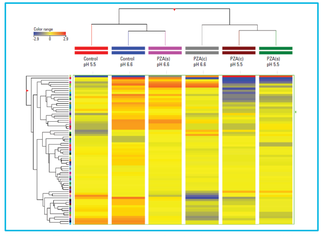

Figure 7. Hierarchical clustering on conditions and entities. The color range bar indicates the relative intensity of each metabolite.

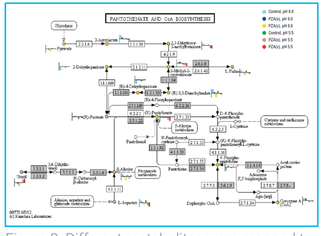

Figure 8. Different metabolites were mapped to the pantothenate and CoA biosynthesis pathway.

Hierarchical clustering is one of the most widely used clustering techniques for unsupervised analysis of mass abundance data. Figure 7 shows the hierarchical clustering result performed on both conditions and entities. The metabolites are displayed as a heat map, and the relative abundance is indicated by color. The tree branching clearly distinguishes the metabolic profile of PZA-treated cells incubated at pH 5.5 from those incubated at pH 6.6. Consistent with PZA's selective activity at pH 5.5, we observed a grouping of PZA(s)-treated cells at pH 6.6 with those of the control samples.

Pathway Analysis using Pathway Architect in MPP

By mapping the differential metabolites and overlaying the abundance results onto curated pathways, it is possible to view pathways enriched with metabolites. This facilitates a quick view of whether the pathway was significantly affected in response to the drug treatments or cell growth conditions. In this study, we found 23 pathways with at least five or more statistically significant metabolites. Figure 8 shows the pantothenate and CoA biosynthesis pathway in which 15 metabolites were found.

Conclusions

- Agilent 6545 Q-TOF delivered excellent mass accuracy and accurate isotope ratio measurement
- IP-RP Q-TOF LC/MS method provided a robust, high analytical performance including reproducibility, chromatographic separation, and wide coverage of endogenous metabolite classes
- Combined with Agilent Profinder and MPP software, this workflow enabled the identification of a specific metabolic biosignature for PZA-treated Mycobacterium tuberculosis that may help to explain PZA's unique metabolic effects.

References

1. Zhang, Y.; Mitchison, D. The curious characteristics of pyrazinamide: a review. Int. J. Tuberc. Lung Dis. 2003, 7(1), 6-21.
2. Dai. Y. 2016 Metabolomics Conference Poster #267
3. Kind, T.; Fiehn, O. Metabolomics database annotation via query of elemental compositions: Mass accuracy is insufficient even at less than 1 ppm. BMC Bioinformatics 2006, 7, 234.
4. Xu, Y.; et al. Evaluation of accurate mass and relative isotopic abundance measurements in the LTQ-Orbitrap Mass Spectrometer for Future Metabolomics Database Building. Anal. Chem. 2010, 82, 5490-5501.

Utilizing an Accurate Mass and Retention Time Library to Facilitate Bio-Marker Discovery in the Human Cerebrospinal Fluid Proteome

Cole Michel[1]; Richard Reisdorph[1]; Enrique Alvarez[1]; Vadiraja Bhat[2]; Paul Goodley[2]; Nichole Reisdorph[1]
[1]University of Colorado Anschutz Medical Campus, Aurora, CO;
[2]Agilent Technologies, Inc, Wilmington, DE;

ASMS 2017
MP-633

University of Colorado Anschutz Medical Campus

Agilent

Introduction

Cerebrospinal fluid (CSF) can be challenging to analyze in protein biomarker discovery experiments for several reasons, including interference from high abundant proteins and sample availability. One strategy to overcome these challenges includes building accurate mass and retention time (AMRT) libraries using LC/MS/MS followed by quantitation using peptide-level abundances. Peptide masses that are differentially expressed between groups are identified using the AMRT library. This approach can potentially improve reproducibility, lower CV's, and increase analytical sensitivity when compared to MS/MS quantification strategies.

Experimental- Sample Prep

Sample preparation: Pooled human CSF from control and MS patients (PPMS) was used. Samples were concentrated using 3 kDa Amicon molecular weight cut-off filters, before being immunodepleted with a MARS Hu-14 column from Agilent. The flow-through fraction was then digested overnight using the FASP method. Samples were then cleaned-up using C18 spin columns. Samples were re-suspended in 3% ACN 0.1% Formic Acid. A BCA assay was performed and all samples were diluted to a final concentration of 0.15µg/uL.

Experimental

Nanodaptor Configuration with 1290 Binary and Cap Pumps

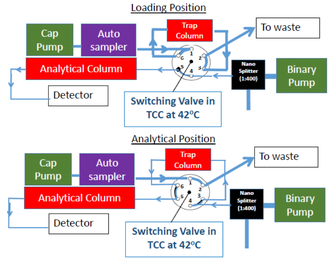

Experimental- LC/MS^n

LC-MS analysis: Peptide fractions were analyzed in triplicate using a nano UHPLC ESI 6550 iFunnel LC/Q-TOF with a 60min gradient.

For MS/MS spectral library generation, the peptide mixture was further fractionated using high pH reverse phase liquid chromatography and concatenated to get 15 fractions.

Data analysis: The data was searched against the human SwissProt database using SpectumMill. An AMRT library was developed using in-house software.

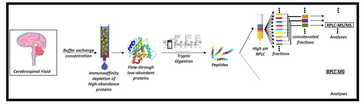

Results and Discussion

42 injections of 15 concatenated fractions

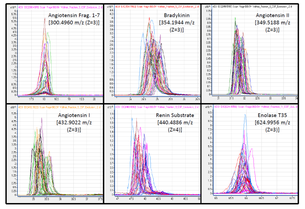

Retention Time Reproducibility over 2 weeks samples and fractions

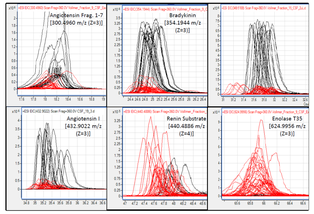

Black = 21 Sample injections [scan rate 1.5] (Renin and Enolase NF)

Red = 42 injections of concatenated fractions [scan rate 10]

Spectrum Mill Summary of High pH Fraction, MS/MS spectral library

Total Distinct Peptides	Total protein groups with > 2 Distinct Peps	Total possible proteins with > 2 Distinct Peps	Total protein groups	Total possible proteins	Total Proteins	Spectrum Mill Cut-offs
50044	4651	5005	7614	7968	9600	fdr < 1%, Peptide score > 0 & SPI > 0%, Protein Score > 0
39240	2964	3199	3941	4176	5239	fdr < 1%, Peptide score > 8 & SPI > 50%, Protein Score > 10
36531	2506	2715	3632	3841	4931	fdr < 1%, Peptide score > 9 & SPI > 50%, Protein Score > 10
32875	2006	2189	3425	3609	4703	fdr < 1%, Peptide score > 10 & SPI > 50%, Protein Score > 10
38405	2964	3199	3106	3341	3903	fdr < 1%, Peptide score > 8 & SPI > 50%, Protein Score > 13
35572	2506	2715	2673	2882	3406	fdr < 1%, Peptide score > 9 & SPI > 50%, Protein Score > 13
31680	2006	2189	2231	2415	2832	fdr < 1%, Peptide score > 10 & SPI > 50%, Protein Score > 13
28794	1833	1995	2086	2248	2638	fdr < 1%, Peptide score > 10 & SPI > 70%, Protein Score > 13

Differential analysis on PPMS vs Control

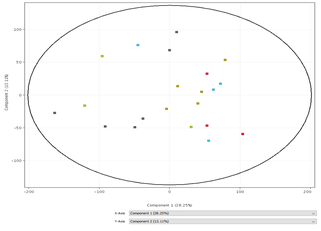

PCA non-averaged interpretation of Disease States using all peptides (17538 peps) (3 control, 5 GAD, 4 NMO, 3 Sarcoid, 6 PPMS)

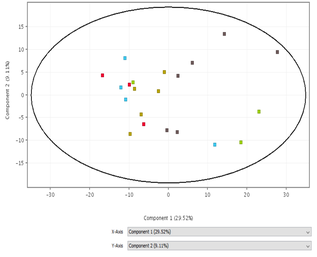

PCA non-averaged interpretation of Disease States using all proteins (506 proteins) (3 control, 5 GAD, 4 NMO, 3 Sarcoid, 6 PPMS)

Results and Discussion

Number of ID's in MPP ID Browser

- 17,538 total compounds extracted from all 21 samples using Profinder v.8.0
- 6,454 peptides identified in ID browser using the MS/MS runs on all 21 samples (36.8% of total compounds identified)
- 10,547 total peptides identified in ID browser using the MS/MS runs on all 21 samples and the High pH fractionation library; 4,093 or 163% more peptides were identified due to the library approach (60.1% of total compounds identified)

Differential analysis: PPMS vs. Control MS vs. MS/MS Analysis

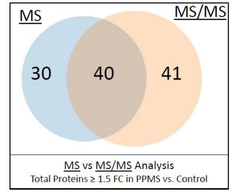

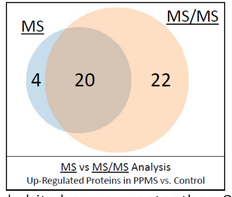

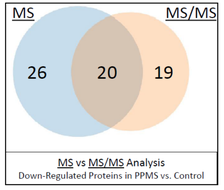

- 42 proteins with multiple peptide hits have a greater than 2.0 fold change in PPMS vs. Control MS-only analysis (27 are down-regulated and 15 are up-regulated in PPMS)
- 70 proteins with multiple peptide hits have a greater than 1.5 fold change in PPMS vs Control MS-only analysis (46 are down-regulated and 24 are up-regulated in PPMS)
- 81 proteins with multiple peptide hits have a greater than 1.5 fold change in PPMS vs. Control MS/MS analysis (39 are down-regulated and 41 are up-regulated in PPMS)
- Differential proteins identified were consistent with previous studies and included complement and CSF-specific proteins

Conclusions

We present a reproducible and sensitive method of performing relative quantitation of CSF proteins. This method comprises depletion of high abundant proteins followed by high pH reverse phase chromatography to separate proteins; fractions are analysis using MS and MS/MS to generate an AMRT library. A total of 10,547 peptides were identified using a 60 minute gradient on a nano-UHPLC system. Over 70 proteins were identified as being differentially expressed in PPMS vs Control samples. Future directions include confirming protein identifications and expanding the sample size.

Higher Order Structure of Intact Proteins by Capillary Electrophoresis Native Ion Mobility Mass Spectrometry

Caroline S. Chu[1] ,Pat D. Perkins[1], Andy Gieschen[2]
[1]Agilent Technologies, Inc., Santa Clara, CA;
[2]Agilent Technologies Inc., La Jolla, CA

ASMS 2017
ThP-603

Agilent
Trusted Answers

Introduction

Capillary electrophoresis (CE) mass spectrometry is emerging as a robust and analytical sensitivity technology for the study of protein structure, requiring very little starting material. In order to study protein structure, often times this is done using native MS where the protein is buffer exchanged into an aqueous buffer at pH 7, usually ammonium acetate or online buffer exchanged with size exclusion chromatography (SEC) and sprayed into the MS by ESI or nanoESI[1]. However, challenges arise when samples are limited especially in early development, Pharmacokinetics and drug metabolism (PKDM) studies. Here we present the use of capillary electrophoresis for online electrophoretic mobility separation coupled to MS and IM-MS for high order structure analysis of intact

Experimental

Proteins were buffered exchanged using ammonium acetate and analyzed on a 6530 Q-TOF and a 6560 IM-QTOF MS. The 7100 CE can interface to both instruments and controlled by MassHunter acquisition software for introducing the sample under both native and denaturing MS conditions. A 1260 II isocratic pump with a 1:100 splitter delivered the sheath liquid. Data under denaturing and native MS conditions were processed and deconvoluted using the Maximum Entropy algorithm in BioConfirm.

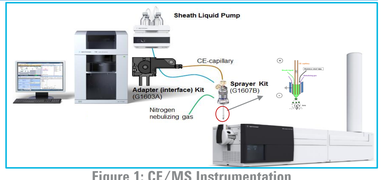

Figure 1: CE/MS Instrumentation

CE-MS of a Commercial Antibody-Drug-Conjugate Mimic

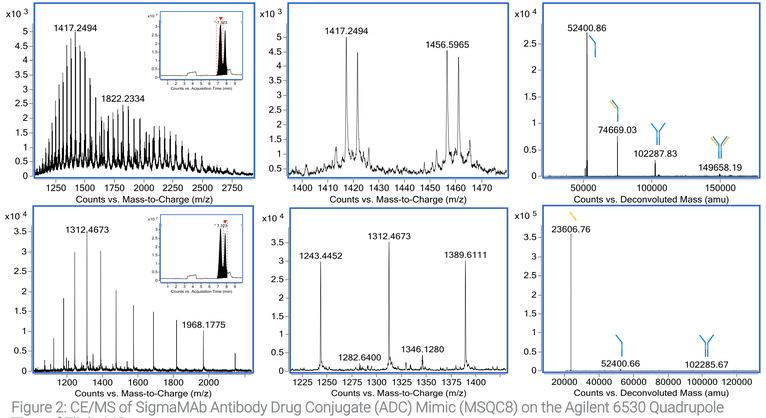

Figure 2: CE/MS of SigmaMAb Antibody Drug Conjugate (ADC) Mimic (MSQC8) on the Agilent 6530 Quadrupole Time of Flight MS

(Left to Right) Mass spectrum of the charge envelope of ADC (Total Ion Chromatogram, TIC, in inset) at retention time 7.3 mins (top) and 7.8 mins (bottom), zoomed spectrum of the highest z state, and deconvoluted mass spectrum with putative assignments. BGE: 30% Acetic Acid in water, Sheath Liquid: 0.1% Formic Acid, 0.005%(v/v) of 2.5 mM HP-921 (G1969-85001) in 50:50 Methanol:Water at 4 µL/min.

CE-MS of Intact Monoclonal Antibodies

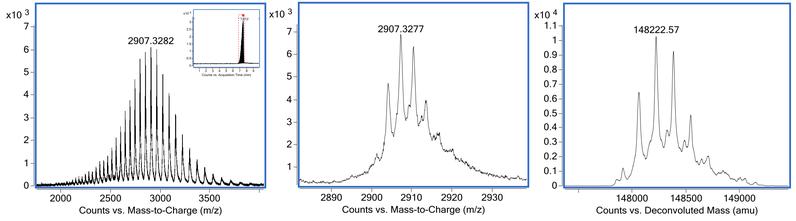

Figure 3: CE/MS of Trastuzumab on the Agilent 6530 Quadrupole Time of Flight MS

(Left to Right) Mass spectrum of the charge envelope of Trastuzumab (TIC, in inset), zoomed spectrum of the highest z state, and deconvoluted mass spectrum. BGE: 30% Acetic Acid in water, Sheath Liquid: 0.1% Formic Acid, 0.005%(v/v) of 2.5 mM HP-921 (G1969-85001) in 50:50 Methanol:Water at 4 µL/min.

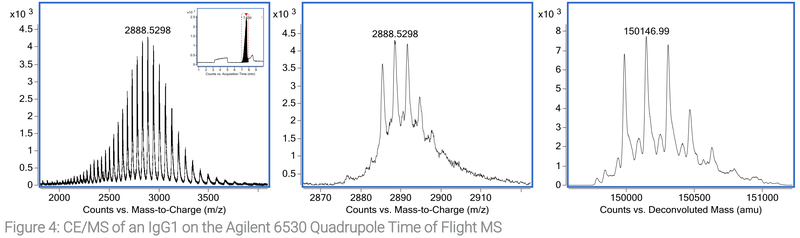

Figure 4: CE/MS of an IgG1 on the Agilent 6530 Quadrupole Time of Flight MS

(Left to Right) Mass spectrum of the charge envelope of IgG1 (TIC, in inset), zoomed spectrum of the highest z state, and deconvoluted mass spectrum. BGE: 30% Acetic Acid in water, Sheath Liquid: 0.1% Formic Acid, 0.005%(v/v) of 2.5 mM HP-921 (G1969-85001) in 50:50 Methanol:Water at 4 µL/min.

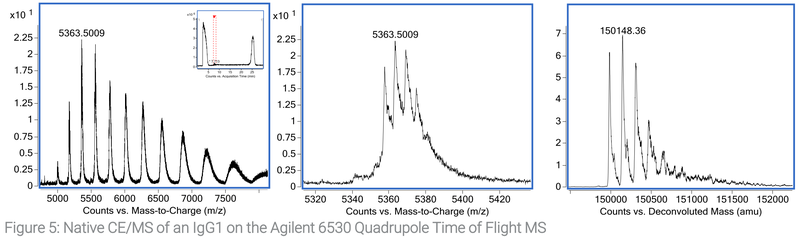

Figure 5: Native CE/MS of an IgG1 on the Agilent 6530 Quadrupole Time of Flight MS

(Left to Right) Mass spectrum of the charge envelope of IgG1 (TIC, in inset), zoomed spectrum of the highest z state, and deconvoluted mass spectrum. BGE: 25 mM Ammonium Acetate, Sheath Liquid: 100 mM Ammonium Acetate at 1 µL/min.

CE-MS of Proteins using Ion Mobility

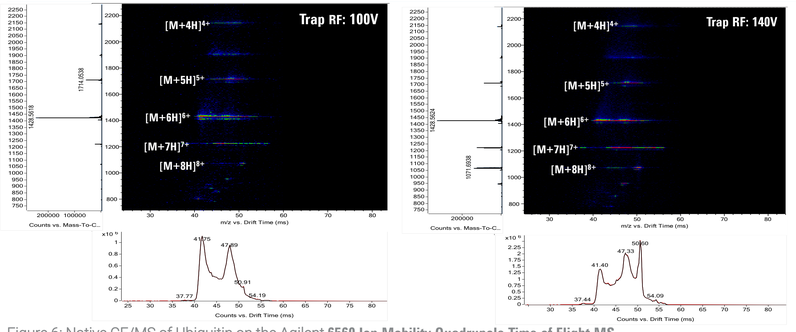

Figure 6: Native CE/MS of Ubiquitin on the Agilent **6560 Ion Mobility Quadrupole Time of Flight MS**

Mass spectrum of the charge envelope of ubiquitin, abundance map, and drift spectrum at trap RF 100V (left) and RF 140V. More unfolding is observed at higher trap RF. BGE: 200 mM Ammonium Acetate, Sheath Liquid: 0.1% Formic Acid, in 20% Methanol in water at 5 µL/min.

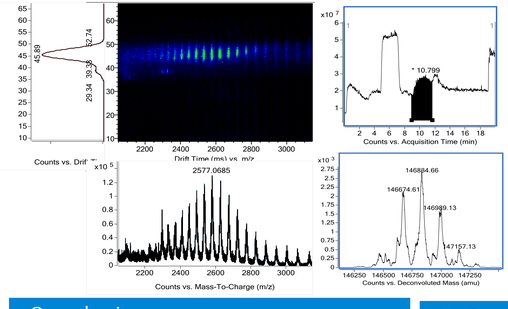

Figure 7: CE/MS of a commercial IgG1 on the Agilent 6560 Ion Mobility Quadrupole Time of Flight MS

Drift spectrum, abundance map, mass spectrum of the IgG1.Deconvoluted mass spectrum (right bottom) and TIC (top right). BGE: 1% Formic Acid, Sheath Liquid: 0.1% Formic Acid, 20% Methanol in water.

Conclusions

- Novel CE/MS methods developed for both low pH and native pH 7 for protein structure characterization using an Agilent 7100 CE and 6500 QTOF MS.
- Using ion mobility provides additional information for high order structure with CE under Native MS
- Native CE/MS of a Mab and non-covalent complexes

References

- [1]Heck, Albert JR. "Native mass spectrometry: a bridge between interactomics and structural biology." *Nature methods* 5.11 (2008): 927.
- [2]Han, Mei, et al. "Intact mass analysis of monoclonal antibodies by capillary electrophoresis–Mass spectrometry." *Journal of Chromatography B* 1011 (2016): 24-32.

Enhanced Lipids Removal from Biological Matrices to Prepare Samples for LC/MS/MS Analysis

Limian Zhao and Derick Lucas

Agilent Technologies Inc., 2850 Centerville Rd., Wilmington, DE, 19808

ASMS 2017

TP- 451

Agilent Trusted Answers

Introduction

Lipids, especially phospholipids (PPLs), in biological matrices can significantly impact bioanalysis quality by LC/MS/MS. The unremoved phospholipids and matrix interferences can cause significant ion suppression, resulting in lower detection limits and poor method reliability, resulting in lower productivity and eventual financial losses.

Agilent Enhanced Matrix Removal–Lipid (EMR–Lipid) is a series of new products utilizing a novel sorbent material that selectively removes major lipid classes from sample matrix without unwanted analyte loss. The lipid removal mechanism is a combination of size exclusion and hydrophobic interaction between the long aliphatic chain of the lipid substances and the EMR–Lipid sorbent. The selective interaction mechanism allows efficient removal of phospholipids and other classes of lipids from biological fluids after PPT.

Captiva EMR–Lipid is a new pass-through cleanup product implemented in a convenient SPE cartridge or 96-well plate format. The use of Captiva EMR–Lipid products provides > 99 % phospholipids removal and clogging-free, easy elution for in-situ protein precipitation. The 96-well Captiva EMR–Lipid plate was evaluated for the quantitative determination of representative drug compounds in human serum by LC/MS/MS. The results demonstrated that the established protocol using in-situ PPT followed by Captiva EMR–Lipid cleanup provides significant improvements for the reliable quantitative determination of drug compounds in biological matrices.

Experimental

Instrument condition

The study was run on an Agilent 1290 Infinity UHPLC system coupled to an Agilent G6490 Triple Quadrupole MS system.

LC/MS/MS conditions

- Agilent InfinityLab Poroshell 120 LC column, EC-C18, 150 x 2.1 mm, 2.7 µm (p/n 699775-902),
- Mobile phase: A) 5 mM ammonium acetate buffer with 0.1 % FA in water, B) 0.1 % FA in Acetonitrile
- Gradient:

Time (min)	%B	Flow rate (mL/min)
0	6	0.3
2.5	40	0.3
7.0	90	0.3
7.01	100	0.3
8.0	Stop	0.3

- Data acquisition:
  Precursor scan of m/z 184, product ion mode for PPLs removal evaluation; and dMRM mode for quantitation evaluation (refer ref 1&2 for more method detail)

Sample preparation

Phospholipids removal efficiency evaluation was conducted with various biological matrices, while the quantitative bioanalysis of representative drugs was conducted using human serum.

Steps	Operation parameters
Aliquot each sample into 1 mL 96-well collection plate	100 µL
Add IS working solution to each sample except control blank, or 50:50 ACN/water to control blank	10 µL
Cover with plate cover and vortex at 2500 rpm	1 min
Add ACN with 1 % FA to Captiva EMR–Lipid plate sitting (on a 1 mL collection plate)	300 µL
Using 96 liquid handler to transfer the entire sample mixture to Captiva EMR-Lipid plate	110 µL
Mixing the sample mixture in EMR-Lipid plate by pipetting	3–5 times
Insert CapiVac collar between EMR-Lipid plate and collection plate	
Add make up solution 80:20 ACN/water to each sample	300 µL
Apply appropriate vacuum for gradual and steady elution	2–4 inch Hg
At the end, apply higher vacuum to drain the cartridge bed	8–10 inch Hg
Remove the collection plate, and evaporate to dryness with CentriVap	40 °C
Reconstitute with 10:90 ACN / 5 mM ammonium acetate buffer	100 µL
Vortex at 2500 rpm, sonicate, and cap with plate matt	2 min + 5 min

Results and Discussion – Pass Through Cleanup and PPLs Removal

Simplified Addition of Captiva EMR-Lipids Cleanup after Protein Precipitation

Add crashing solvent to cartridge or 96-well plate (96-WP)

↓

Add biological sample: plasma, serum etc.

↓

Elute with vacuum or positive pressure or low speed centrifugation (only for 96-WP)

↓

Transfer eluent for Analysis or Further Treatment

- ✓ Unique frit design assures clogging-free elution
- ✓ Non-dripping feature allows in-situ protein precipitation
- ✓ Easy elution with low vacuum/pressure
- ✓ Smooth elution and efficient filtration assures clear eluent
- ✓ 96-well plate elution can be conducted by low-speed centrifugation

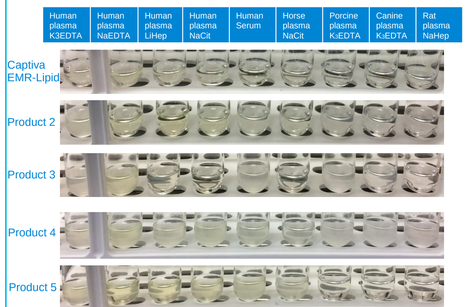

Figure 1. Comparison of sample eluent clarity collected by in-situ PPT.

Highly Selective and Efficient Lipids Removal

The use of Captiva EMR-Lipids cleanup after PPT provides >99% of phospholipids removal.

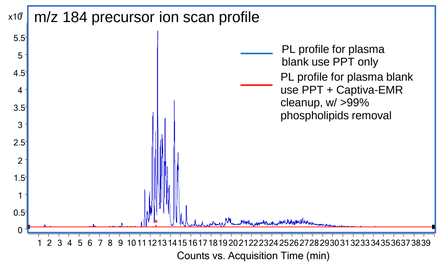

Figure 2. Overlapped chromatograms for phospholipids profile by monitoring precursor ion scan for 184.

- ✓ >99% PPLs removal demonstrated in various biological matrices
  - Various matrices and resources
  - Various anti-coagulants
- ✓ Superior to or equivalent to other cleanup products PPLs removal performance

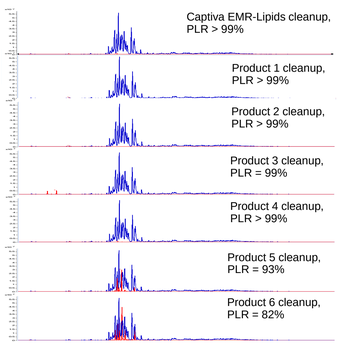

Figure 3. Phospholipids removal efficiency comparison among various cleanup methods after PPT of human plasma Na Heparin.

Results and Discussion – Quantitation of Representative Drug Compounds

Representative Drug Compounds for Quantitative Bioanalysis in Human Serum

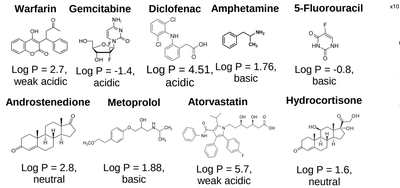

Figure 4. Chemical structures and properties of the representative drug compounds.

Captiva EMR-Lipid cleanup improves quantitative results

Sample Prepared by PPT only

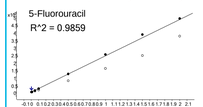

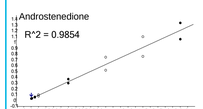

Sample Prepared by PPT + EMR-Lipid CL

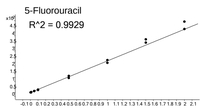

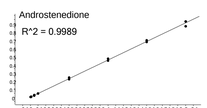

Figure 5. Duplicated calibration curves linearity comparison for sample using PPT only and PPT followed by EMR-Lipid cleanup. 0.5 – 200 ng/mL in human serum

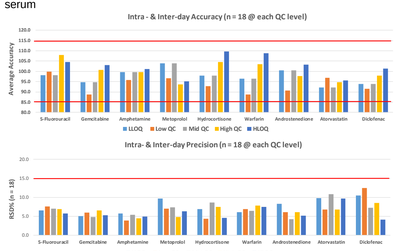

Figure 6. Method verification inter-day accuracy and precision results summary.

Captiva EMR-Lipid cleanup significantly reduces matrix ion suppression

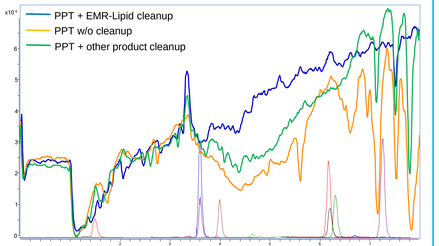

Figure 7. Standard post-column infusion profiles comparison and demonstration of matrix ion suppression effect on target analytes.

Conclusions

The use of Captiva EMR-Lipid products for bioanalysis provides

- ✓ Easy accommodation to traditional in-situ or offline protein precipitation work flow;
- ✓ Frits optimized to resist clogging and provide easy elution.
- ✓ Highly selective and efficient lipids removal (>99%), and thus significantly reduced matrix ion suppression;
- ✓ Exceptional quantitative results for easy method validation under standard criteria;
- ✓ Overall improved productivity by reducing instrument downtime and prolonging column lifetime.

References

1. L. Zhao, D. Lucas. Efficiency of Biological Fluid Matrix Removal using Captiva EMR-Lipid Cleanup. Agilent Technologies Application Note, publication number 5991-8006EN, 2017.
2. L. Zhao, D. Lucas. Quantitative LC/MS/MS Analysis of Drugs in Human Serum With Agilent Captiva EMR-Lipid Cleanup. Agilent Technologies Application Note, publication number 5991-8007EN, 2017.
3. US Food and Drug Administration, Guidance for Industry Bioanalytical Method Validation, 2001.

A metabolomics study on crtEBI recombinant saccharomyces cerevisiae with UHPLC tandem quadrupole-time of flight mass spectrometry

Wei Du, Tao Bo

Agilent Technologies, No. 3, Wang Jing Bei Lu, Chao Yang District, 100102, Beijing, CHINA

ASMS 2017
TP - 526

Agilent
Trusted Answers

Introduction

Lycopene is an effective antioxidant. Saccharomyces cerevisiae is a main organism for lycopene biosynthesis since it is easy to express crtE, crtB, and crtI genes, which encode three carotenogenic enzymes, geranylgeranyl diphosphate synthase, phytoene synthase and phytoene desaturase relating to lycopene biosynthesis. In this study, a metabolome profiling of crtEBI recombinant S. cerevisiae was conducted using an untargeted metabolomics platform based on ultra-high performance liquid chromatograph coupled to high resolution tandem quadrupole-time of flight mass spectrometry, in order to better understand the detailed mechanism of lycopene biosynthesis for generation of high-production Saccharomyces cerevisiae strain by future genetic manipulation. The metabolomics workflow used in this study was given below (Figure 1).

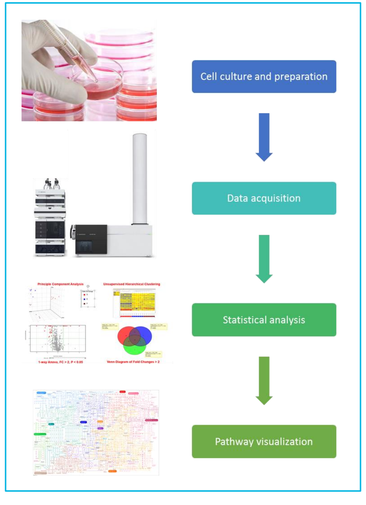

Figure 1 metabolomics Workflow

Experimental

Method

The fermentation broth was quenched and extracted by chilled methanol. The metabolites were analyzed using an UHPLC system coupled to tandem quadrupole-time of flight mass spectrometer (Agilent 6545) equipped with Jet Stream dual electrospray source. The UHPLC and Q-TOF parameters were shown in tables below. Statistical and pathway analysis was performed using Mass Profiler Professional (MPP). Compound identification was performed using Agilent-METLIN Metabolite Database and MassHunter Molecular Structural Correlator (MSC) software was used to facilitate structure elucidation.

Agilent UHPLC 1290 System	
Column	BEH Amide column 2.1×100mmm, 1.7μm
Mobile phase	A: H2O(25mM ammonium acetate and 25mM ammonium hydroxide); B: ACN Gradient Elution from 95 to 40 % B in 20 minutes
Flow rate	0.3 mL /min
Oven Temperature	40 °C
Injection	2 μL

Agilent 6545 LC/Q-TOF Mass Spectrometer	
Ion source	AJS
Polarity	Positive/Negative
Ion spray voltage	3500V(Pos) /3000V(Neg)
Dry gas temperature	300°C
Dry gas	6 L/min (N2)
Nebulizer pressure	35 psi (N2)
Sheath Gas Flow	11 L/min (N2)
Sheath Gas Temp	350°C
Acquisition Rate	4Hz MS, 4Hz MS/MS
Collision Energy	10, 20, 40 eV

Results and Discussion

Data Processing

In this study, the extracts of crtEBI recombinant and wild-type Saccharomyces cerevisiae were analyzed on both positive and negative modes. Over 5100 features in positive ion mode and 4200 features in negative ion mode were extracted from each data set (Figure 2).

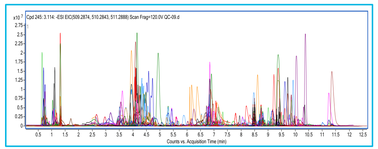

Figure 2 Overlaid chromatogram of molecular feather extraction in negative ion mode

PCA and clustering analysis showed that the crtEBI recombinant and wild-type samples clustered in the separated groups, which suggests differences between two groups (Figure 3 & Figure 4).

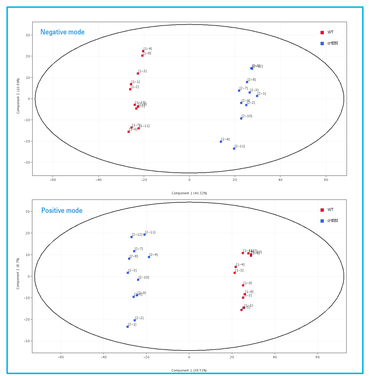

Figure 3 PCA score plot

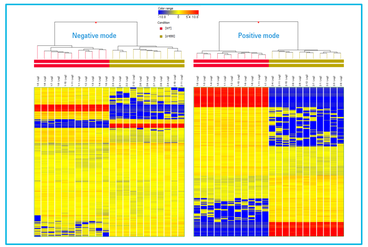

Figure 4 Clustering analysis

A differential list of 25 metabolites were obtained by significant test (Moderated t-test, p<0.01 and fold change>2) and identified by Metlin Database with MS/MS fragment confirmation, including organic acid, amino acid, nucleotide, saccharide and coenzyme. (Figure 5)

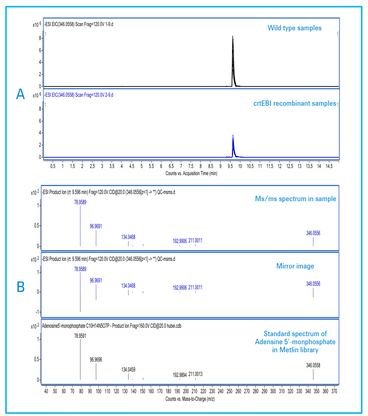

Figure 5 Compound Identification (Adensine 5'-monphosphate as an example)
EIC in crtEBI recombinant and wild-type samples(A) and MS/MS spectral match(B)

Results and Discussion

Pathway Analysis

The identified metabolites were used for significant pathway analysis in MPP, which shows metabolite enrichment using Saccharomyces cerevisiae Pathway Database from Biocyc, Wikipathway and KEGG. Tricarboxylic acid cycle, glycolysis, pyruvate metabolism and Pentose and glucuronate interconversions pathway were regulated significantly(Figure 6 & Figure 7), which suggested that crtEBI recombinant will induce regulation of energy metabolism and accelerate the consumption of Acetyl CoA, the major precursor for biosynthesis of lycopene.

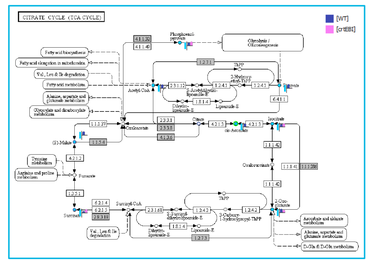

Figure 6 TCA cycle pathway (Heatstrips show the relative difference between WT and crtEBI groups)

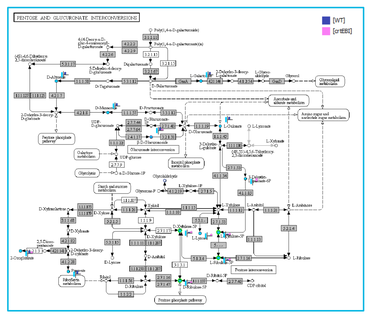

Figure 7 Pentose and glucuronate interconversions (Heatstrips show the relative difference between WT and crtEBI groups)

NLP Network

An interaction network of differential metabolites was created using Natural Language Processing (NLP) algorithm in MPP software (Figure 8), which helps to understand correlation of pathways and the mechanism of lycopene biosynthesis.

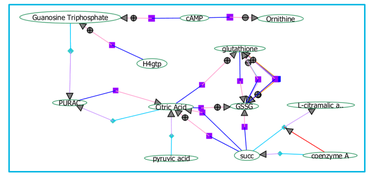

Figure 8 The NLP network of differential metabolites

Conclusions

A high-throughput metabolomics study on crtEBI recombinant saccharomyces cerevisiae using UHPLC-Q-TOF and statistical analysis revealed a significant regulation in their metabolites and pathway relative to lycopene biosynthesis.

- 25 differential metabolites were Identified using Agilent-METLIN Metabolite Database and Library.
- Pathway analysis suggested that crtEBI recombinant will induce the regulation of Tricarboxylic acid cycle, glycolysis, pyruvate metabolism and Pentose and glucuronate interconversions pathway in Saccharomyces cerevisiae.
- NLP network help to understand the detailed mechanism of lycopene biosynthesis

.

References

1. Ahmed Bahieldin, Plasmid, 72 (2014) 18–28
2. J.M.Arava-Garay, Appl Microbiol Biotechnol 93(2012) 2483-2492

Workflows for the Identification and Relative Quantitation of Glycan Variants

Stephen Madden, Aaron Boice, Aditi Koul and Caroline S. Chu

Agilent Technologies, Santa Clara, CA

ASMS 2017
TP - 316

Agilent
Trusted Answers

Introduction

Glycosylation is a common post-translational modification (PTM) found on monoclonal antibodies (mAbs). Glycans play an important role in determining the protein structure, solubility, half-life, and antigenicity of the biomolecule. The heterogeneity of glycosylation makes it a challenging modification to characterize given the diversity in their composition, sequence, and site of glycosylation. N-glycans are the most commonly found glycans on mAbs.

We have developed a workflow to both identify released N-glycans based on their accurate mass and confirm the presence of glycan isoforms on intact proteins using LC/MS. Using a predefined (or user defined) list of PTMs, users can now easily update information to add glycans and PTMs to search against their intact or digested LC/Q-TOF data.

Experimental

Sample Preparation

Samples were prepared using an Agilent AssayMAP Bravo liquid handling system (Figure 1). Multiple workflows were used with automated sample preparation including purification of the intact mAb to the release and labelling of the N-glycans off a mAb.[1]

Figure 1 Agilent AssayMAP Bravo

Experimental

Instrumental Analysis

Released glycan samples were analyzed by an Agilent 6545XT AdvanceBio LC/Q-TOF (Figure 2) using an autotune leveraging a particle swarm optimization algorithm to provide best analytical sensitivity and resolution in the mass range of glycans. Intact protein samples were acquired using a variation of this tuning algorithm to optimize on large molecule performance for improved transmission and detection of a mAb.

The Dual Agilent Jet Stream ion source was used for both the intact protein and released glycan experiments.

For intact protein, separation was achieved using an Agilent 1290 Infinity II UHPLC system and an Agilent PLRP-S 1000Å (2.1 × 50 mm, 5 µm) column. Approximately 0.5 µg of mAb sample was injected for each analysis, and separated across a four minute gradient.[2]

For released glycans an Agilent 1290 Infinity UHPLC system and an Agilent AdvanceBio Glycan Mapping (1.8 µm 2.1 x 15 cm) column was used for separation. Each analysis injected the released N-glycans from 0.5 µg of protein, and separated across a 30-minute gradient.

Data analysis was performed using a prerelease version of MassHunter BioConfirm B.09.00.

Figure 2 Agilent 6545XT AdvanceBio LC/Q-TOF.

Results and Discussion

Identification and Relative Quantitation of Glycoforms

Figure 3 shows the workflow for the data analysis of mAb glycoforms in intact protein data. The user first chooses the sequence of the mAb (in this case, 500 ng of NISTmAb RM 8671[3]) and defines its linkages and PTMs including glycans in the MassHunter BioConfirm software's Sequence Manager (Figure 4).

The BioConfirm software then extracts averaged spectra across chromatographic peaks and applies the Maximum Entropy deconvolution algorithm to construct a zero-charge deconvoluted spectrum. The mass peaks in the spectrum are matched against the protein sequence with linkages and PTMs and labeled (Figure 5).

PTMs for which there is a match are automatically quantitated against the total abundance of all matched PTMs and listed in a table (Figure 6).

The user is able to choose which PTMs to use for relative quantitative analysis by Height or Area, then the BioConfirm software will generate a report.

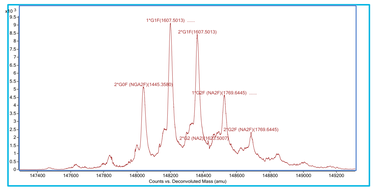

Figure 5 Deconvoluted spectrum of NISTmAb

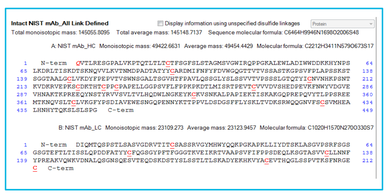

Figure 4 Protein sequence in Sequence Manager

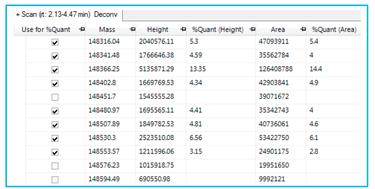

Figure 6 Columns to choose PTMs for relative quant.

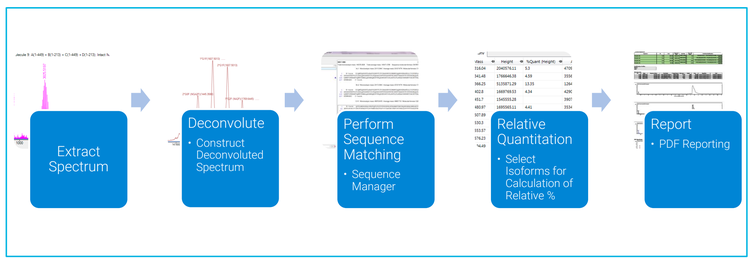

Figure 3 Workflow for the data analysis of glycoforms in intact protein data.

Results and Discussion

Identification of Released Glycans

Figure 7 shows the workflow for the data analysis of released glycans from mAb data.. The user chooses a tag in the BioConfirm software based on the sample preparation technique. A feature finding algorithm is run which will find all glycans which have formulas in a provided database with optional filtering by retention times. The scoring of matches is based on the monoisotopic mass, the isotope distribution, and the isotope spacing (Figure 8). A list of glycans that have been found is displayed with a score that indicates the confidence in the match (Figure 9). The BioConfirm software will generate a report with the identifications.

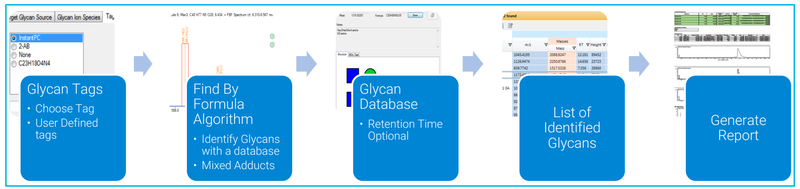

Figure 7 Workflow for data analysis of released glycans

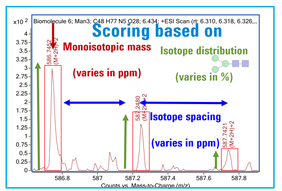

Figure 8 Scoring by feature finding algorithm

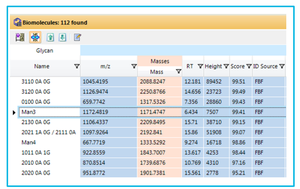

Figure 9 List of identified glycans

Conclusions

We have developed two workflows to characterize glycan variants that provide:

- High productivity through automation of sample preparation, acquisition and data analysis
- Fast optimization of the instrument using the SWARM autotune
- Superior high resolution data that can be deconvoluted to accurately reveal mAb glycoforms in intact protein data
- Fast identification of released glycans with an option of multiple tags using the same database of native structures

References

[1] ProZyme Technical Note: "Development of an Instant Glycan Labeling Dye for High Throughput Analysis by Mass Spectrometry" (Bulletin 2003 Rev. B)

[2] Agilent Application Note: "Precise Characterization of Intact Monoclonal Antibodies by the Agilent 6545XT AdvanceBio LC/Q-TOF" (P/N 5991-7813EN)

[3] Dong, Q.; Yan, X.; Liang, Y.; and Stein, S.E. In-depth Characterization and Spectral Library Building of Glycopeptides in the Tryptic Digest of a Monoclonal Antibody Using 1D and 2D LC-MS/MS, J Proteome Res. 2016 May 6;15(5):1472-86. (NISTmAb characterization article)

Intelligent algorithm using Particle Swarm Optimization (SWARM) with enhanced limit of detection for large molecule applications

Huy Bui, Christian Klein, Alex Zhu, Alex Mordehai, Gregor Overney

Agilent Technologies, Santa Clara CA

ASMS 2017
WP - 049

Agilent
Trusted Answers

Introduction

What is SWARM algorithm?

SWARM algorithm[1], which mimics the learning behavior of a flock of birds, was successfully proven to be useful in performance optimization of sophisticated instruments[2, 3]. SWARM is a proprietary algorithm combination between Particle Swarm Optimization with Simplex[4] along with mass spectrometer constraint. Traditionally, system Autotune optimizes instruments to their best performance for general purpose applications using a 3200 *m/z* mass range.

There is a natural trade off between resolution and sensitivity. The "one-size-fit-all" Autotune does not provide the sufficiently optimized sensitivity required for large molecule applications, and produces resolution performance that is more than needed for the application.

Why do we need large molecule SWARM Autotune?

The current commercial Q-TOF Autotune is tuned for general purpose applications from small to large molecules. We demonstrated the benefits of the dedicated small molecule tunes [5]; we then continued to further develop this algorithm for large molecules, and use intact monoclonal antibodies (mAb) as a mean to evaluate our algorithm. The algorithm runs for 20 minutes starting from default values, similar to the small molecules SWARM Autotune concept.

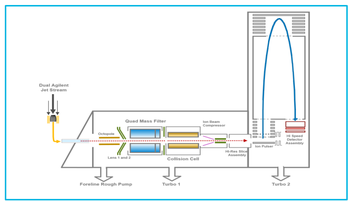

Figure 1: Schematic view of the 6545XT AdvanceBio LC/MS-QTOF used for large molecule SWARM Autotune.

Removing the constraint for producing a perfect parallel ion beam in the ion pulser region shows a significant improvement in signal abundance. The previously developed SWARM Tune for small molecules has already shown a substantial benefit in small molecule analyte abundance[5] .

Experimental

Instrumentation

A commercial 6545XT AdvanceBio LC/Q-TOF is used in the study with SWARM large molecule tune. All large molecule tune data were acquired using a 6545XT, where some data with System Tune were previously collected using a 6550 iFunnel LC/Q-TOF.

The SWARM algorithm accepts a variety of instrument optimum criteria; transmission mass range, target resolution, fragility of analytes. For large molecule optimization, the instrument is switching between extended mass range (10000 *m/z*) and standard mass range (3200 *m/z*) to capture the signal improvement in dual gain mode. The robustness and consistency of SWARM algorithm were rigorously investigated.

Algorithm strategies

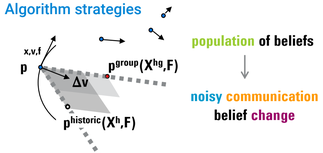

$$v' = \omega v + c_1 rand_1 (X^h - x) + c_2 rand_2 (X^{hg} - x)$$
$$x' = x + v$$

In case of no multiple maxima, SWARM switches to the simplex (Nelder-Mead) [4] optimizer for faster convergence. All optimized parameters then go through a validation given by mass spectrometer physics constraints

Reagents for algorithm

Unless otherwise noted, for most experiments we used the Agilent ESI-TOF Calibrant Mix for algorithm development.

Evaluation method using intact mAb

For consistency, the ion source settings were optimized and adjusted the same way in protein declustering and desolvation. Additionally, the optimized ion source settings remain the same for consistency.

The ion source optimized settings are then evaluated based on the qualitative and quantitative performance of intact mAb Herceptin, 145531.5 Da. Signal-to-noise ratio, peak shape, and mass accuracy are examined and compared with the same methods acquired by currently commercially available solutions.

Results and Discussion

What are the unique features of large molecule tune?

The large molecules tune removes the constraint to produce a parallel ion beam and just focuses on optimizing the beam through the center of the slits in the ion beam compressor unit before ions enter the high resolution slicer assembly. Focusing ions through the slits was the main objective of this algorithm. Parallel ion beams are a critical criterion to achieve more than 50K resolution. The focused beam does not produce the same resolution but maximizes ion transmission.

Evaluation of calibrant signal response

With our newly developed large molecule tune procedure, we routinely observe a 4X improvement in peak height and a 5X increase in peak area when compared to results from standard mass range System Tune, running back to back.

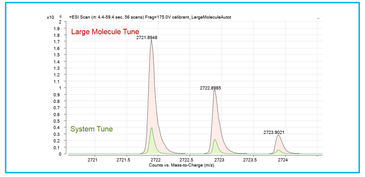

Figure 2: Overlay the signals of the highest calibrant mass in Agilent Tune mix, the signals from the large molecule tune shows a more than 4x improvement. Data was collected with the same Agilent Q-TOF G6545XT.

Evaluation of intact mAb chromatographic response

We compare the mAb chromatogram signals response by using tune files generated with two different Autotunes on the same instrument.

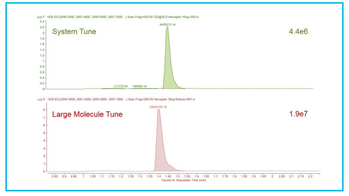

Figure 3: Comparison chromatogram signal response of a 10 ng of Herceptin (intact mAb) injection. System Tune data was collected using Agilent Q-TOF G6550A

Evaluation of intact mAb mass spectral response

The previous collected data files were then overlaid with their mass spectrum obtained with System Tune for direct comparison.

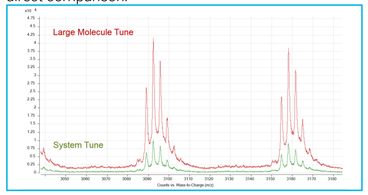

Figure 4: Comparison absolute mass spectra signal response of 10 ng Herceptin injection

Evaluation of low concentration signals

LOD determination is beyond this study. However, we were able to demonstrate the deconvolution of intact mAb with 0.1 ng injection acquired after large molecule tune.

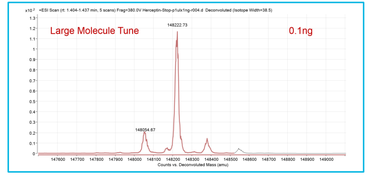

Figure 5: Deconvolute 0.1 ng of Herceptin, after large molecule tune.

Evaluation of large molecule mass accuracy

The deconvoluted glycoforms are identified with a mass deviation of less than 10 ppm. The highest glycoform peak has mass accuracy of 2.25 ppm.

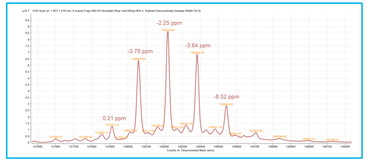

Figure 6: Deconvoluted mass accuracy

Results and Discussion

Evaluation of spectral quality

First results show a 2X improvement in protein signal above the valley between glycoforms with large molecule Autotune. Signal-to-noise proved to be the most important criterion for large molecule deconvolution.

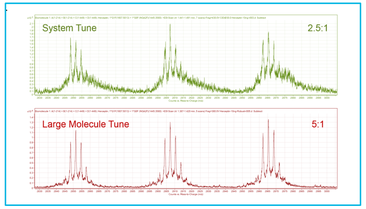

Figure 7: Comparison Signal-to-noise ratio, the System Tune data was collect with G6550A.

Evaluation of deconvoluted spectral quality

The higher deconvoluted spectrum quality directly improves the confidence for structural identification. The data clearly demonstrates that the deconvoluted spectrum quality is directly related to sensitivity and not resolution.

The System Tune settings produces higher mass resolution, but 4X less sensitivity than large molecule tune. The high sensitivity spectrum produces higher Signal-to-noise ratio and a cleaner and higher quality spectrum.

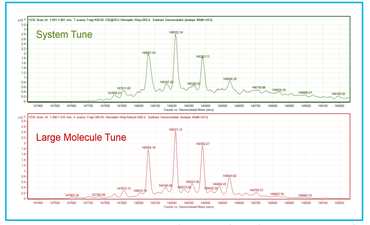

Figure 8: Comparison deconvoluted spectra with standard System Tune and large molecule tune

Application Autotune

The addition of large molecule SWARM Autotune algorithm to the QTOF application tune portfolio opens a new chapter of a powerful "Application Autotune" where the QTOF instrument will be optimized in order to provide best performance based on application demands.

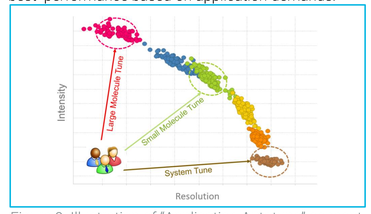

Figure 9. Illustration of "Application Autotune" concept. Data was collected using modified G6530A instrumentation and the scales are not linear.

Conclusions

The analysis of intact proteins is of great importance to the biopharmaceutical industry.

- Higher sensitivity mass spectrum produces higher quality deconvoluted spectrum.
- Large molecule SWARM Autotune produce 4X higher sensitivity than standard System Autotune.
- SWARM Tune can optimize a QTOF instrument based on application needs.

References

[1]Kennedy J, et al (1995). Proceedings of IEEE Int. Conference on Neural Networks IV. pp. 1942–1948.

[2] Bieler A, et al. J Mass Spectrom. 2011 Nov;46(11):1143-51,.

[3] Bui, H, et al. (2014) ASMS Poster WP-681

[4] Nelder, John A, et al (1965). Comp. Jour. 7: 308–313

[5] Bui, H, et al. (2015) ASMS Oral TOA am 10:10

Racial Disparity in Bladder Cancer and Identification of Altered Metabolism in African American Compared to European Bladder Cancer

Sri Ramya Donepudi[1]; Venkatrao Vantaku[1]; Tiffany Dorsey[2]; Vasanta Putluri[3]; Suman Maity[3]; Wei Tang[2]; Feng Jin[3]; Danthasinghe Waduge Badrajee Piyarathna[3]; Kimal Rajapakshe[3]; MeghaShyam Kavuri[3]; Vadiraja Bhat[4]; Seth Lerner[5]; Yair Lotan[5]; Wei Liu[6]; Cristian Coarfa[3]; Arun Sreekumar[3]; Stephan Ambs[2]; Nagireddy Putluri[3]

[1]Baylor College of Medicine, Houston, TX; [2]NIH, Bethesda, MD; [3]Baylor College of Medicine, Houston, TX; [4]Agilent, Santa Clara, CA; [5]UT Southwestern, Dallas, TX; [6]Agios Pharmaceuticals, Boston, MA

ASMS 2017
WP-480

Introduction

Bladder cancer (BCa) incidence and mortality rates vary substantially among racial and ethnic groups. Most notably, European-Americans (EA) have a higher incidence of the disease, while African-Americans (AA) experience higher mortality rates and poorer survival. To date, a metabolomic analyses aimed at understanding of bladder cancer health disparity has not been reported. We have used an Agilent LC/TQ 6495 instrument to do the metabolic measurements and also used Biocrates, a targeted quantitative metabolomics kit p180. The LC-MS/MS based AbsoluteIDQ® p180 Kit is an easy-to-use research assay for quantifying up to 188 endogenous metabolites from 5 different compound classes (i.e. acylcarnitines, amino acids, hexoses, phospho- and sphingolipids and biogenic amines). The assay requires very small sample amounts (10 µL) and shows excellent reproducibility. Our results using AA and EA BCa tissues have confirmed elevated expression of enzymes involved in the metabolism of mitochondrial metabolites and lipids, specifically in AA BCa.

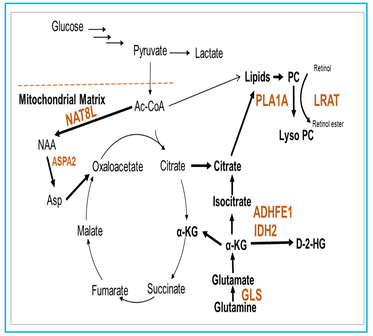

Figure 1. Altered pathways in AA BCa and formations of 2-HG, NAA and lipids.

Experimental

Targeted metabolomics was performed using 6460 Triple Quadrupole LC/MS system. The experiments were carried out in both positive and negative ionization modes. Data normalization was achieved by using isotopically labelled compounds. Quantitative data analysis was conducted using Agilent MassHunter software. J82 (EA) and Scaber(AA) cell lines were maintained and grown as per ATCC's instructions. Western Blot and qPCR experiments were performed on these cell lines and patient tissues to confirm expression of GLS1, IDH2, ADHFE1,NAT8L and ASPA

Figure2:Agilent 6495 LC/TQ instrument

Results and Discussion

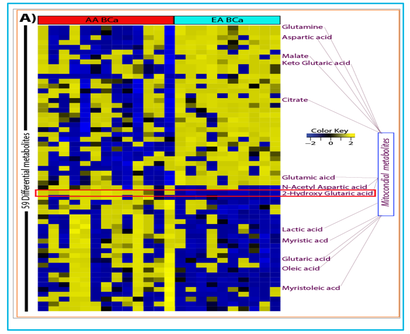

Figure 3A: Heat map showing altered mitochondrial metabolites in A) AA from EA BCa tissues- highlighted in red are 2-HG.

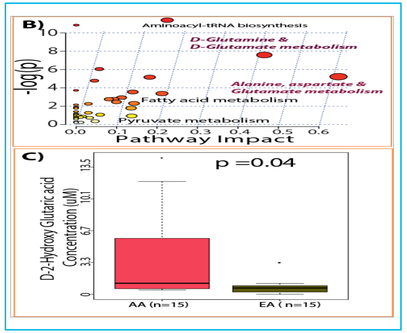

Figure 3: B) Altered Pathways in AA and EA BCa patients C) Box plot showing D-2HG in AA from EA BCa tissues and AA BCa patients having higher levels (uM) of D-2HG.

.

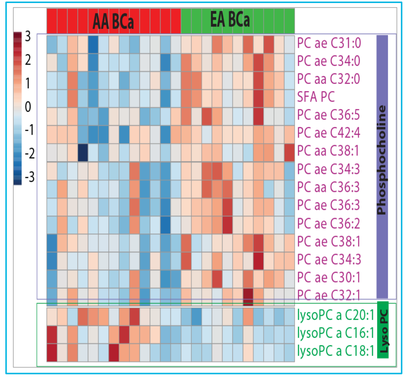

Figure 4: Heat map showing altered lipids in AA from EA BCa tissues

African American BCa – Lower PC

African American BCa – High lyso PC

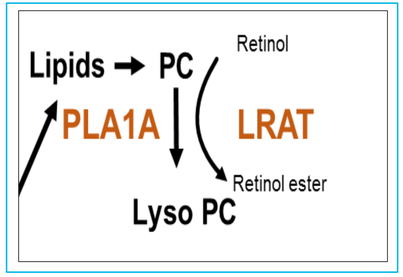

Figure 5:. Enzymes involved in conversion of PC to Lyso PC

Results and Discussion

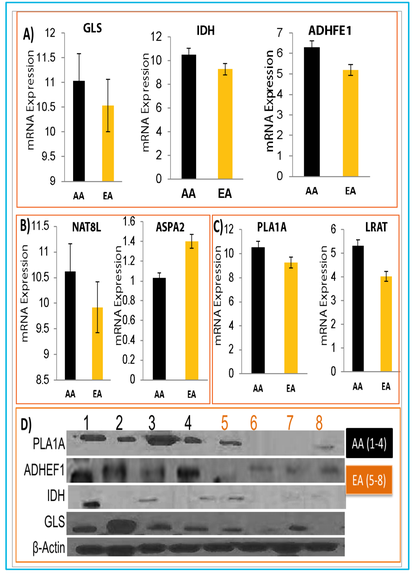

Figure 6: A-C) Bar graphs showing higher expression of IDH2, GLS, ADHFE1, NAT8L, PLA1A, and LRAT in AA from EA BCa tissues and lower levels of ASPA2. D) Western blots showing higher expression of PLA1, ADHFE1, PHGDH, IDH2 and GLS in AA from EA BCa tissues.

.

Conclusions

We conducted a metabolomics study on 15 AA, and 20 EA BCa. Using a targeted LC/MS approach we were able to measure the >200 metabolites. Among the metabolites elevated in AA BCa tumors compared to EA BCa tumors were intermediates of mitochondrial metabolism namely Glutamine, 2-hydroxyglutarate (2HG), N-acetyl aspartate .We performed Western blot and qPCR experimennts to estimate the enzymes involved in the D-2HG synthesis and NAA synthesis. It was observed that Glutaminase 1 (GLS1), isocitrate dehydrogenase 2 (IDH2), and iron-containing alcohol dehydrogenase 1 (ADHFE1), three enzymes involved in D-2HG synthesis, were significantly elevated at mRNA and protein levels in AA BCa compared with EA BCa tissues. N-Acetyltransferase 8-Like Protein (NAT8L), which is required for synthesis of NAA, was higher in AA BCa, but ASPA, which is needed for NAA breakdown, was significantly lower in AA BCa tissues.

Altered lipid metabolism between AA BCa from EA BCa show, Phospholipase A1 (PLA1A), Lecithin retinol acyltransferase (LRAT), two key enzymes required for conversion of (PC) into LPC were significantly elevated in AA BCa tissues. Consistent with this finding, global levels of PC were significantly lower in AA BCa tumors than EA BCa tissues.

In summary, these data show that mitochondrial and lipid metabolism are altered in AA BCa tissues, resulting in accumulation of key metabolites that could result in oncogenic transformation and/or disease progression.

References

- This research was supported by the following grant, CPRIT Core Facility Support Award RP120092 "Proteomic and Metabolomics Core Facility.
- NCI/ 2P30CA125123-09 Shared Resources Metabolomics core and funds from Dan L. Duncan Cancer Center (DLDCC), Baylor college of Medicine
- (ACS) award 127430-RSG-15-105-01-CNE (N.P.)
- Funds from Alkek Center for Molecular Discovery.
- Helis Foundation

For Research Use Only. Not for use in diagnostic procedures.

Tobacco-specific carcinogens induce hypermethylation, DNA adducts and DNA damage in bladder cancer

Feng Jin[1], Jose Thaiparambil[2], Sri Ramya Donepudi[1], Danthasinghe Waduge Badrajee Piyarathna[3], Venkat Rao Vantaku[3], Rashmi Krishnapuram[2], Franklin Gu4, Vasanta Putluri[1], Preeti Purwaha[3], Suman Maity[1], Salil Kumar, Bhowmik[3], Chandrashekar Ambati[1], Friedrich-Carl von Rundstedt[4,5], Daniel Gödde[6], Stephan Roth[7], Stephan Störkel[8], Stephan Degener[7], George Michailidis[9], Balasubramanyam Karanam[9], Martha K.Terris[10], Shyam M Kavuri[11], Bhat, Yadi [13], Seth P. Lerner4, Cristian Coarfa[1,3], Arun Sreekumar[1,3,4], Yair Lotan[12], Randa El-Zein[2], Nagireddy Putluri[1,3]

[1]Dan L. Duncan Cancer Center, Advanced Technology Core, Alkek Center for Molecular Discovery, Baylor College of Medicine, Houston, TX, USA; [2]Department of Radiology, Houston Methodist Research Institute, Houston, TX, USA; [3]Department of Molecular and Cell Biology, 4Verna and Mars McLean Department of Biochemistry, Baylor College of Medicine, Houston, TX, USA; [4]Scott Department of Urology, Baylor College of Medicine, Houston, TX, USA; [5]Department of Urology, Jena University Hospital, Friedrich-Schiller-University, Jena, Germany, [6]Department of Pathology, [7]Department of Urology Helios Klinikum, Witten-Herdecke University, Wuppertal, Germany, [8]Department of Statistics, University of Florida, Gainesville, FL, USA; [9]Department of Biology and Center for Cancer Research, Tuskegee University, Tuskegee, AL, USA, [10]Augusta University, Augusta, GA, USA; [11]Lester and Sue Smith Breast Center, Baylor College of Medicine, Houston, TX, USA; [12]Department of Urology, University of Texas Southwestern, Dallas, TX, USA, [13] Agilent Technologies

ASMS 2017
WP-482

Baylor College of Medicine

Agilent

Introduction

Aromatic amines, such as 4-(methylnitrosamino)-1-(3-pyridyl)-1-butanone (NNK), have been strongly implied as carcinogenic for the bladder. NNK may promote tumor metastasis by regulating cell motility by generating DNA adducts and causes DNA damage. Earlier, we identified the methylation-induced enzyme suppression associated with xenobiotic metabolism in bladder tumors. However, the identification of smoke-induced BCa, metabolic signature and its downstream effects are largely understudied. In this study, we have shown higher levels of methylated polycyclic aromatic hydrocarbons, DNA adducts, as well as DNA damage in smokers with BCa. The results suggests a potential causal role of methylation in the accumulation of DNA adducts and DNA damage in carcinogen-induced Bca.

Agilent 6495 LC/TQ was used in this experiment to identify the metabolites in bladder cancer samples.

Experimental

Overview of the strategy used to profile and characterize the metabolome of bladder cancer samples from smokers (n=78) and non-smokers (n=41)

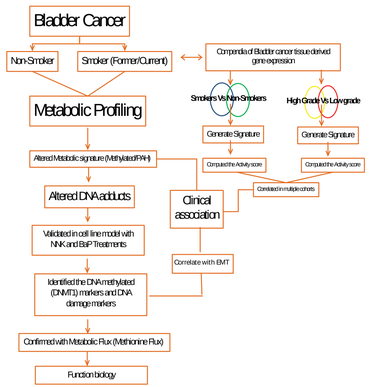

Results and Discussion

Heat map of hierarchical clustering of levels of 90 metabolites detected across 119 bladder cancer samples.

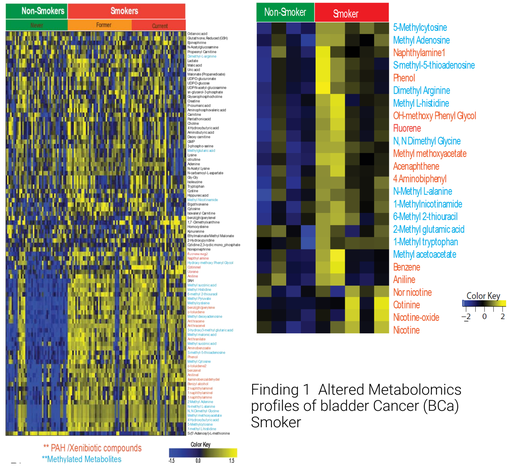

Finding 1 Altered Metabolomics profiles of bladder Cancer (BCa) Smoker

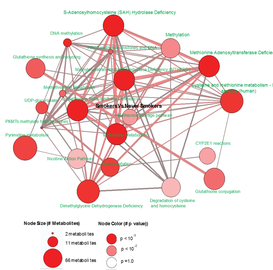

Pathway analysis of the metabolic profiles in our "BCa smoking-associated metabolic signature." The node size is proportional to the number of metabolites in the process or condition. Color represents a statistically significant enrichment (p-value)

Results and Discussion

Levels of DNA adducts, Xenobiotic enzymes, DNA damage markers in BCa between smokers and non-smokers

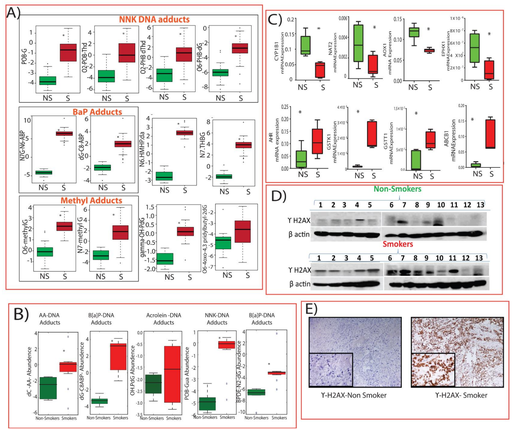

A) Box plots showing higher expression of NNK, BaP, and methyl DNA adducts in BCa from smokers (S; n=15) than in that from non-smokers (NS; n=15). *, p<0.005. B) Box plots showing higher levels of DNA adducts from the urine pellet of smokers (n=5) than non-smokers (n=5). *, p<0.005. C) Box plots showing relative transcript levels for xenobiotic enzymes obtained by real-time PCR of BCa samples from non-smokers (n=6) and smokers (n=6). *, p<0.005. D) Protein levels of Y-H2AX in non-smokers (n=13) and smokers (n=13) with BCa as determined by western blotting. E) Immunohistochemical staining for Y-H2AX expression

Results and Discussion

Tobacco-specific carcinogens induced methylation, DNA adducts, DNA damage in BCa smokers show higher DNMT1 expression than non-smokers

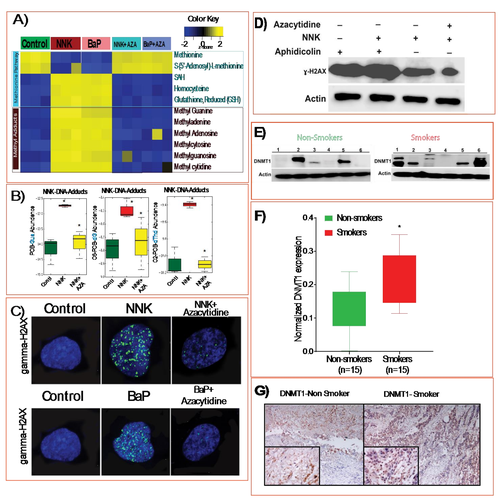

A) Box plots showing higher expression of NNK, BaP, and methyl DNA adducts in BCa from smokers (S; n=15) than in that from non-smokers (NS; n=15). *, p<0.005. B) Box plots showing higher levels of DNA adducts from the urine pellet of smokers (n=5) than non-smokers (n=5). *, p<0.005. C) Box plots showing relative transcript levels for xenobiotic enzymes obtained by real-time PCR of BCa samples from non-smokers (n=6) and smokers (n=6). *, p<0.005. D) Protein levels of Y-H2AX in non-smokers (n=13) and smokers (n=13) with BCa as determined by western blotting. E) Immunohistochemical staining for Y-H2AX expression

Results and Discussion

SNNK induce DNMT1 expression and altered methionine pathway in BCa

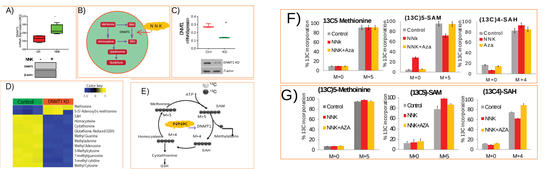

A) Box plots showing mRNA and protein expression of DNMT1, by real-time PCR and western blot, respectively, in J82 BCa cells treated with or without nitrosamine NNK. B) The role of DNMT1 in the methionine pathway. C) Confirmation of DNMT1 knockdown (KD) by mRNA and protein expression analyses in J82 cells D) Heat map of metabolites in control and shRNA knockdown (KD) of DNMT1 in J82 cells. E) 13C(U) ux in methionine pathway. F) J82 cells were pretreated with NNK or NNK+ AZA prior to the addition of 13C(U) Methionine. Cell pellets were collected after 13C(U) methionine addition and isotopomeric distribution for indicated metabolites was measured using mass spectroscopy. Individual isotopomers are graphed as a percent of the total pool for the indicated metabolite. (G) Experiments were performed in J82. Data in bar graphs are represented as means ± SEM. n=3 independent cultures for isotopomeric distributions in F and G. Statistical analysis was performed using a two-tailed Student's t-test ($p < 0.05$)

Conclusions

- Specific metabolic signature associated with BCa Smoker
- Identified DNA adducts, DNA damage in BCa Smoker
- Identified molecular mechanisms of methionine pathway alterations and DNMT1 activation using in vitro bladder cancer models.
- Results illustrate the relevance of hyper methylation, DNA adducts, DNA damage and DNMT1 overexpression in tobacco compounds induced carcinogenesis.

References

[1]Metabolomic Profiling Reveals Potential Markers and Bioprocesses Altered in Bladder Cancer Progression. Cancer Res. 2011 Dec 15;71(24):7376-86

[2]Integrative Pathway Analysis of Metabolic Signature in Bladder Cancer: A Linkage to The Cancer Genome Atlas Project and Prediction of Survival. J Urol. 2016 Jun;195(6):1911-9.

ENVIRONMENTAL

Analysis of Persistent Organic Pollutants in Atmospheric Aerosol Using a Novel Ultrasound Assisted Extraction Micro-scale Cell and a Triple Quadrupole GC/MS/MS System

Eleazar Rojas[1]; Gelasio Pérez[1], Eliana Arias-Loaiza[2], Erik Beristain-Montiel[2], Omar Amador-Muñoz[2]

[1]Agilent Technologies Inc, MEXICO, DF; [2]Centro de Ciencias de la Atmósfera, Universidad Nacional Autónoma de México

ASMS 2017
TP - 167

Introduction

Persistent Organic Pollutants (POPs) are synthesized organic compounds globally distributed in the environment. POPs include organochlorine pesticides (OCls), polychlorinated biphenyls (PCBs), polybrominated biphenyl ethers (PBDEs) and polyhalogenated dibenzo dioxins and furans (PCDDs/Fs). Atmospheric aerosol is one of the major constituents of air pollution, and was classified as carcinogenic to humans (Group 1) [1]. Selective and sensitive techniques are required to detect POPs in aerosol. This work shows POPs in atmospheric aerosol collected at several sites around the country of Mexico. Using the 7010A Triple Quadrupole GC/MS System with the new High Efficiency Source (HES) has increased the ion flux over traditional tandem GC/MS instruments by a factor of 10 to 20-fold, with a multi-fold improvement in EI detection limits.

Experimental

Sampling

Atmospheric aerosol samples were collected in Hermosillo (northern part of the country, elevation 210 masl), Mexico City (middle of the country, 2250 masl) and Altzomoni (middle of the country, 3985 masl), during 2013 and 2015. An outdoor passive air sampler housing (TE-200-PAS, Tish Environmental Inc.) was used for a duration of 80 to 110 days in each case.

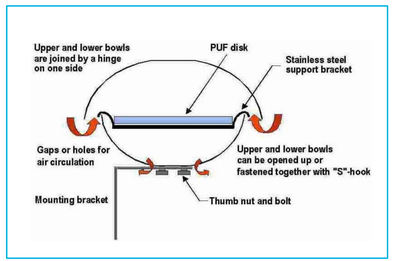

Figure 1. Passive sampler

Experimental

Sample Preparation

A novel ultrasound assisted extraction micro-scale cell (UAE-MSC), recently patented [2], was used to extract POPs from atmospheric aerosol [3].

Temperature: 50 °C
Power: 40%
Frequency: 37 kHz
Time: 40 min.

Filter and rinse using

50 ml CH_2CL_2

Concentrate to 1 ml

Filter the simple using 0.22 µm acrodisk

Figure 2. Sample preparation

Sample Analysis

Analysis was performed using the Agilent 7890A/7010A GC/MS system equipped with the High Efficiency Source(HES) operated in MRM mode. The 7890A GC was equipped with a MultiMode Inlet (MMI) and an HP-5ms UI column, 30m x 250µm x 0.25µm. Backflushing at the column midpoint was accomplished using a Purged Ultimate Union (PUU) controlled by an Aux EPC module. All of the method parameters were obtained from the Agilent G9250AA Pesticides and Environmental Pollutants database (P&EP); no further optimization was required. Three transitions were used for each compound, the most intense as the quantifier transition and the other two as qualifier transitions.

Results and Discussion

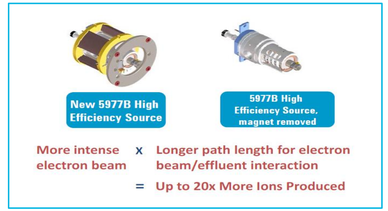

Figure 3. High Efficiency Source (HES)

UAE-MSC optimized extraction conditions reduced by 30X the solvent consumption and decreased the extraction time from several hours to ten minutes, with respect to Soxhlet extraction[4]. Atmospheric samples are extremely complex and advanced technology is required to differentiate OCls, PCBs, polycyclic aromatic hydrocarbons, PBDEs, organophosphates and other targets from organic interferences at low ppb concentrations.

The GC/MS/MS conditions (chromatographic parameters, precursor ion, collision energy, and product ions of the MRMs) were adequate to perform the quantitative analysis without further optimization.

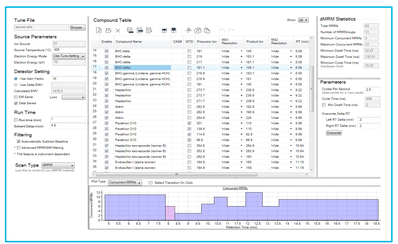

Figure 4. The G9250AA P&EP database has up to 8 transitions for each compound. This allows the user to choose alternative transitions to minimize matrix interferences and improve quantitation results.

Due to the presence of a large number of background compounds, backflushing was deemed necessary. Backflushing the GC column ensures that high-boiling compounds in the matrix are not passed through the column, thereby reducing column bleed, eliminating ghost peaks, and minimizing contamination of the mass spectrometer. Run time is also reduced because the traditional long post-run bakeout is avoided.

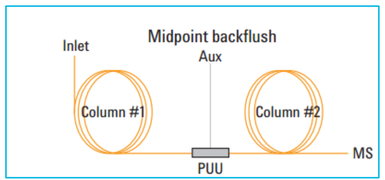

Figure 5. Diagram Midpoint Backflushing

The 7010A triple quadrupole MS was extremely sensitive to OCls (around 0.125 pg/µL) and less sensitive to some PBDEs and PCBs. High selectivity was achieved; 50 different compounds were quantitated in a single run of 20 min.

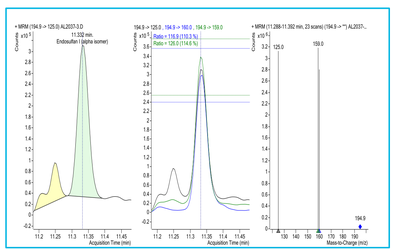

Figure 6a. Quantification and Qualifier signals for Endosulfan I for a calibration point of 5 ppb

Results and Discussion

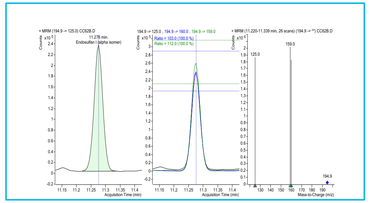

Figure 6b. Quantifier and qualifier signals for Endosulfan I for a sample with a concentration of 6.5 ppb

The linearity for most of the compounds was found to be between an r^2 of 0.902 and 0.999 in the range 0.125 to 250 pg/µL.

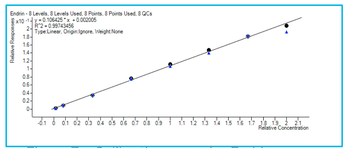

Figure 7a. Calibration curve for Endrin

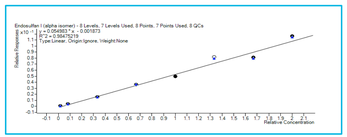

Figure 7b. Calibration curve for Endosulfan I

POPs analysis showed heptachlor, delta-HCH and p,p'-DDE in Hermosillo, Mexico City and Altzomoni. Some PCBs and PBDEs were also found in Mexico City. The highest POPs concentrations were observed in Hermosillo and Altzomoni. Since Altzomoni is located between the volcanoes Popocatepetl and Iztaccihuatl, the predominant wind trajectory suggests POPs are transported from the north to the south of the country.

Conclusions

- UAE-MSC effectively extracts pesticides from the passive sampler, using less time and solvent than Soxhlet technique.
- The 7010A GC/MS/MS system detects POPs at very low concentrations (0.125 pg/µL) in highly complex atmospheric aerosol samples.
- Use of the Agilent P&EP database parameters without additional modification allows one to detect and quantify more than 50 different POP´s in aerosol samples with an excellent linearity.
- Use of the backflushing technique helps to keep both the GC and the MS clean.
- The highest concentrations of POPs were observed in Hermosillo.
- POPs are transported from the northern part of the country to the southern part.

References

[1] IARC (2013). Outdoor air pollution a leading environmental cause of cancer deaths, WHO Press Release N° 221. 2–5.

[2] Amador-Muñoz et al. (2014). Celda de extracción a microescala, asistida por ultrasonido, con y sin reflujo, acoplada a un sistema de filtración., Mexican patent 325624.

[3] Beristain-Montiel et al. (2016). An Innovative Ultrasound Assisted Extraction Micro-Scale Cell combined with Gas Chromatography / Mass Spectrometry in Negative Chemical Ionization to Determine Persistent Organic Pollutants in Air Particulate Matter. J. Chromatogr. A, 1477, 100-107.

[4] Chen et al. (2011). Handbook on Applications of Ultrasound: Sonochemistry for Sustainability, 1st ed., CRC Press.

A Sensitive and Automated Approach Using Large Volume Injections Coupled with LC/TQ to Analyze Perfluorinated Compounds in Environmental Samples

Wen-Yen Lee[1], Ya-Nan Yang[2], Dai-Yong Huang[3], Shan-An 1

[1]Agilent Technology, Inc. Taipei, Taiwan, Taiwan

[2]Agilent Technology, Inc., Hong Kong, Hong Kong

[3]Agilent Technology, Inc., Santa Clara, CA, USA

ASMS 2017
ThP-151

Agilent
Trusted Answers

Introduction

Perfluorinated compounds (PFCs) are widely used in diverse industrial applications and consumer products due to their stability and surfactant properties. They have also been widely used in the past as a protective coating for materials such as carpets, textiles and leather, as well as in various household and industrial cleaning products. In the EU, the manufacture and use of perfluorooctane sulfonate (PFOS) is prohibited under Directive 2006/122/EC that came into force in June 2008. Perfluorooctanoic acid (PFOA) is still manufactured and is mainly used in the production of fluoropolymers, which are used in electronics, textiles and non-stick cookware. However, PFCs such as PFOS and PFOA do not decompose easily in the natural environment and can bio-accumulate or build up in certain living organisms. An automated LC/TQ method for the analysis of a mixture of PFCs comprised of 19 perfluorinated compounds has been developed using an Agilent 6495 triple quadrupole mass spectrometer. This automated method employs large volume injections to provide a faster, more sensitive, robust, and accurate solution for the analysis of PFCs without sample pre-concentration.

Experimental

Method

A eclipse plus C18 column packed with 1.8µm particles was used to achieve uHPLC analysis with symmetric peak shapes and a poroshell EC C18 trapping column to reduce background. Environmental samples were analyzed by direct large volume injection for quantification of multi-PFCs analysis.

Figure 1. Agilent 1290 II and 6495 LC/TQ

Experimental

Instrumental

A gradient elution and dMRM acquisition were employed for simultaneous identification and quantitation (optimal peak shapes and acquisition of requisite data points). The Agilent dual-needle option provides two flow paths within one autosampler by doubling the needle, the sample loops (500µL and 20 µL), and the needle-seats, along with an additional valve, it shows in Figure 2

Figure 2. Agilent 1290 II multisampler dual needle

LC system	**Agilent 1290 II**
Column	**Analytical: Agilent Eclipse plus C18 3.0x100 mm, 1.8 um** **Trap: Poroshell EC C18 3x50 mm, 2.7um**
Injection volume	**400 µL**
Mobile phase	**A: 10 mM ammonium acetate in H2O** **B: MeOH**
Column Temp	**40 C**
Gradient	**B: 2 5 50 100 100** **Time:0 4 5 18 22**
Flow rate:	**0.4 mL/min**
Post time	**3 min**
Mass system	**Agilent 6495 Triple Quadrupole**
Dry Gas Temp.	**290°C**
Dry Gas Flow	**18 L/min**
Nebulizer	**35 psi**
Sheath Gas Temp	**400°C**
Sheath Gas Flow	**12 L/min**
Nozzle Voltage	**0 (negative)**
Capillary Voltage	**4000 V (negative)**
Delta EMV	**400-600 (negative)**
Low pressure funnel	**RF: 60V (negative), V drop: 100 (negative), DC V: 15V**
High pressure funnel	**RF: 90V (negative), V drop: 110 (negative), DC V: 15V**

Results and Discussion

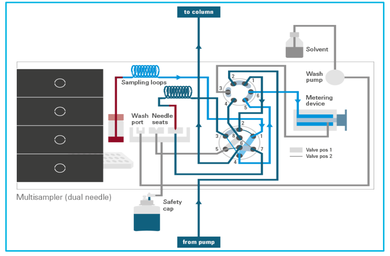

Figure 3. 1290 II multisampler dual needle valve scheme

Large-volume injection (LVI) with LC/TQ

LVI consists of the direct injection of samples with volumes ranging up to 500 µL, which is large compared to conventional injection volumes of 5-20 µL (valve scheme is shown in figure 3). LVI works on the principle of concentrating analytes onto the head of the analytical column during injection of a low-elutropic strength sample. Salts and other matrix into the stationary phase pass unretained through the column. Following analyte concentration on the analytical column, which is analogous to SPE, an increase in the elutropic strength of the mobile phase promotes elution and separation of the concentrated analytes. The major advantages of LVI include an increase in sensitivity, while maintaining accuracy and precision with minimal sample volume.

LVI was optimized and evaluated by accuracy and precision through standard addition experiments. The detection and quantification limits of the instrument and method were then determined using these optimized conditions.

Sensitivity, Linearity and Precision

The on-column sensitivity and linearity of the instrument were assessed by analyzing PFCs standards prepared in H_2O, with a calibration range of 0.1 – 1000 ng/L. A large volume injection of 400 µL was used and the linearity was evaluated using the external standard calibration approach. Excellent sensitivities were achieved through LVI. The standard mixtures for PFCs are shown in figure 4. The calibration curves for PFNA and PFOSA were generated with tap water and correlation coefficients were greater than 0.992 (shown in figure 5).

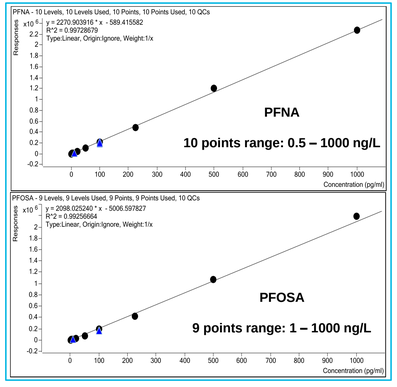

Figure 5. The calibration curves for PFNA and PFOSA

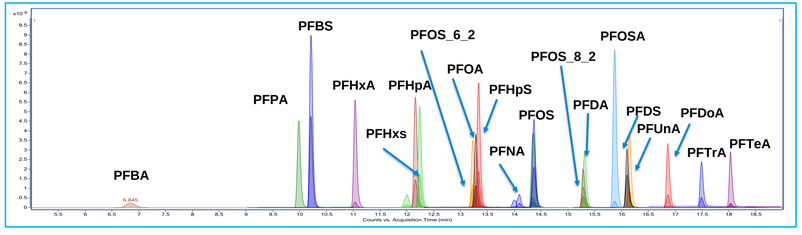

Figure 4. Standard of 19 PFCs with 100 ng/L for Large volume injection 400 uL

Results and Discussion

Compounds	Compounds Full name	Precursor Ion (charge state)	Product Ion m/z (Collision energy)	RT (min)	Limit of detection (ng/L)	Linear range (ng/L)	Calibration Curve y = ax ± b	r^2
PFOS_6_2	perfluorooctane sulfonate_6:2	427(-1)	407(25), 81(45), 80(49)	13.2	0.2	0.2 - 1000	y = 513.7* x +3757.9	0.9984
PFOS_8_2	perfluorooctane sulfonate_8:2	527(-1)	507(29), 81(29), 80(33)	15.3	0.2	0.2- 1000	y = 432.2 * x - 363.6	0.9951
PFBA	perfluorobutanoate	213(-1)	169(8)	6.80	10	25 - 1000	y = 1647.8 * x + 87659.6	0.9982
PFBS	perfluorobutane sulfonate	299(-2)	99(33), 80(40)	10.2	0.1	0.1 – 1000	y=1.41e5x-1.91e4	0.9950
PFDA	perfluorodecanoate	513(-1)	469(9), 269(17)	15.3	0.2	0.2 – 1000	y = 1380.5 * x - 238.7	0.9955
PFDoA	perfluorododecanoate	613(-1)	569(90, 319(21)	16.8	0.5	1 – 1000	y = 1137.1 * x - 5751.8	0.9921
PFDS	perfluorodecane sulfonate	599(-1)	99(50), 80(50)	16.1	0.1	0.2 – 1000	y = 561.0 * x - 587.8	0.9902
PFHpA	perfluoroheptanoate	363(-1)	319(7), 169(17)	12.1	0.1	0.2 – 1000	y = 1865.1 * x + 6317.7	0.9968
PFHpS	perfluorohexane sulfonic acid	449(-1)	99(41), 80(57)	13.3	0.1	0.1 – 1000	y= 1270.9 * x - 1044.4	0.9967
PFHxA	perfluorohexanoate	313(-1)	269(5), 119(17)	11.0	0.1	0.1 – 1000	y = 1552.8 * x + 365.0	0.9934
PFHxS	perfluorohexane sulfonate	399(-1)	99(37), 80(41)	12.3	0.1	0.1 – 1000	y = 981.3 * x - 746.0	0.9962
PFNA	perfluorononanoate	463(-1)	419(5), 219(17), 169(21)	14.3	0.25	0.5 – 1000	y = 2270.9 * x - 589.4	0.9973
PFOA	perfluorooctanoate	413(-1)	369(9), 169(15)	13.2	0.05	0.1 – 1000	y = 1648.4 * x + 2535.3	0.9972
PFOS	perfluorooctane sulfonate	499(-1)	99(53), 80(50)	14.4	0.05	0.1 – 1000	y = 898.5 * x - 171.8	0.9926
PFOSA	perfluorooctane sulfonamidoacetic acid	498(-1)	169(30), 78(45)	15.8	0.5	1 – 1000	y = 2098.0 * x - 5006.5	0.9926
PFPA	perfluoropentanoate	263(-1)	219(5), 197(8), 69(40)	10.0	1	2 – 1000	y = 1318.7 * x - 5211.1	0.9961
PFTeA	perfluorotetradecanoate	713(-1)	669(9), 269(25), 169(30)	18.0	25	25 – 1000	y = 1581.1 * x - 51796.7	0.9911
PFTrA	perfluorotridecanoate	663(-1)	619(9), 169(29)	17.5	25	25 – 1000	y = 1744.2 * x - 52794.3	0.9961
PFUnA	perfluoroundecanoate	563(-1)	519(9), 269(16)	16.2	0.5	1 – 1000	y = 1734.7* x - 3886.0	0.9918

Table 1. MRM parameters , linearity range, calibration curve and retention time information

Background reducing

The trapping column was installed in place of the JetWeaver. It was positioned after the mixing point to minimize delay volume increase and its purpose was to trap PFCs traces originating from the solvent system. Owing to this design, the trapping column was regenerated from run to run to avoid possible breakthrough of the trapped compounds over time. The introduced elution time delay between the interfering (higher RT) and target (lower RT) compounds allowed for the accurate determination of the target compounds. Tap water sample shows no carry over after injection of the QC sample. (shows in figure 6)

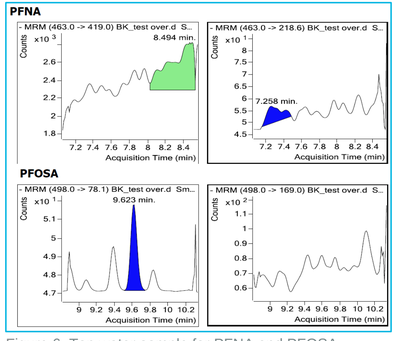

Figure 6. Tap water sample for PFNA and PFOSA

Conclusions

- Recoveries were found to be in the range of 80−120% using fortified tap water standards.
- The limit of detection (LOD) was below 0.05 ng/L for multi-PFCs analytes with standard calibration for quantitative analysis (except PFTrA and PFTeA).
- This automation method uses large volume injections and provides a faster, more sensitive, robust, and accurate solution for the analysis of PFCs without sample pre-concentration.

References

1.Trace Level Determination of PFOS, PFOA and HBCD in Drinking Water by Direct Aqueous Injection on the Agilent 6495 LC/MS/MS. Agilent 5991-5669EN.

2. TRACE LEVEL DETERMINATION OF PER- AND POLYFLUOROALKYL SUBSTANCES (PFASs) IN WATER USING THE AGILENT 6460 LC/MS/MS. Agilent 5991-5532EN.

Meet Stringent Detection Requirements for All 13 4-Nonylphenol Isomers in Water using GCMS-SIM and a High Efficiency Ion Source

Katsura Sekiguchi[1], Kamila Kalachova[2], Melissa Churley[3] and Harry Prest[3]

[1]Agilent Technologies Japan, Ltd., Tokyo, 192-8510 Japan
[2]Agilent Technologies Inc., Waldbronn, Germany
[3]Agilent Technologies Inc., Santa Clara, CA 95051 USA

ASMS 2017
WP - 129

Agilent
Trusted Answers

Introduction

Nonylphenol (NP) compounds are classified as endocrine-disruptors and listed as priority hazardous substances under the Water Framework Directive due to their potential impact upon the aquatic environment. NPs are used to manufacture nonylphenol ethoxylates (NPEs), which are nonionic surfactants found in household and industrial products such as textiles, paints and coatings, and those related to personal care and agriculture. NPEs degrade in the environment to NPs, which have been detected in surface and ground water, wastewater effluent, and food. Estrogenic effects can occur at concentrations as low as 10 µg/L and are isomer-dependent.

We describe a method for complete separation and detection of 13 isomers of 4-NP below 0.02 µg/L (or 20 ng/mL after final extraction) as regulated by the Japan Ministry of the Environment (2012).

The superior sensitivity of the HES source affords that the legislated detection limits of 20 ng/mL at injection (20 ng/L in water), are exceeded by more than 10 fold for all isomers but NP12, which is exceeded by 7 fold. The improved detection limits implies that the sample size could be decreased *at least by* 5-fold (200 ml instead of 1L) which also leads to lower transport, handling, solvent and waste disposal costs.

Structure example of 4-nonylphenol: 4-(3,6-dimethylheptan-3-yl)phenol

Experimental

Platform	**7890B GC and 5977B MS with HES**
Oven	**50°C (1.0min); 8°C/min; 280°C (5min)**
Column	**HP-5MSUI, 30m x 0.25mm i.d.x 0.25µm (p/n 190915-433UI)**
Injection mode	**pulsed splitless (30 psi, 1min)**
SSL Inlet temperature	**250°C**
Injection volume	**1 µL**
Inlet liner	**Ultra Inert, Splitless, Single taper, Glass Wool (p/n 5190-2293)**
Column flow	**He 1.2mL/min (constant flow mode) (holdup time 1.2524 min)**
Run time	**20 min**
Acquisition Mode	**SIM**
Tune File	**HES tune**
Ion source	**350°C (optimized)**
Quad temperature	**150°C**
Transfer line	**280°C**
Solvent Delay	**10 min**
Gain Factor	**15 (optimized using NP11, *m/z* 135.0)**
Surrogate	**13C-labled 4-(3,6-dimethyl-3-heptyl) phenol**
ISTD	**4-n-nonylphenol-2,3,5,6 - d4**

Experimental, cont.

SIM Table

Group #	Time	Gain	Cycle /sec	Ions								
1	10.0	15	5	107	113	121	135	149	155	163	191	220
2	19.2	15	5	111	224							

High Efficiency Ion Source (HES): Generates > 10x ion intensity compared to traditional EI ion sources

High system sensitivity is required to detect 0.02 µg/L 4-NPs in water, which are "low responders" in EI mode

A high degree of instrument sensitivity is required to achieve the detection limit for 4-NPs in water of 0.02 µg/L (20 ng/mL, concentrated 1000x for injection), which was set by the Japan Ministry of the Environment in 2012. Higher sensitivity benefits laboratories in that less sample is required. In addition, it is necessary to detect the lowest responding isomer, NP12, which has 30-fold lower peak height than isomer NP11 (the tallest isomer peak).

A high level standard was run in full scan in order to optimize the GC separation of all 13 4-NP isomers, which elute from 18.1 to 19.1 minutes. Extracted ion chromatograms (EIC) for *m/z* 107, 121, 135, 149, 163, 191, and 220 were studied for optimization as they are indicative of the analytes. This optimization of mass spectral parameters included: detector gain, which was set to 15 (to achieve the best linear working range for NP11) and ion source temperature (350°C for greater response and analytical robustness).

Repeatability %RSD and Instrument Detection Limit

Repeatability RSD% (n=10) at 10 ng/mL and 100 ng/mL (1-2 µL injection)

Repeatability for 10 injections (%RSD, n=10) of 10 ng/mL and 100 ng/mL spiked 4-NP standards (concentration in vial) yielded acceptable results even at the lower concentration. For isomers NP1-NP13, area %RSDs uncorrected for the ISTD at 100 ng/mL ranged from 1.5 to 4.3. Applying the ISTD and quantitating the isomers concentration gave %RSDs ranging from 1.2 to 4.0 ng/mL. At 10 ng/mL, and using a 2 µL rather than a 1 µL injection volume, %RSDs in the concentrations range from 2.2 to 9.8, with the highest uncertainty resulting from the low responding NP12 isomer.

Cmpd.	100 ng/mL (1 µL)		10 ng/mL (2 µL)
	Area (%RSD)	Conc. (%RSD) (corrected to ISTD)	Conc. (%RSD) (corrected to ISTD)
NP1	1.5	1.2	5.1
NP2	2.2	1.8	7.3
NP3	2.1	1.8	3.9
NP4	3.1	3.1	4.7
NP5	3.4	3.0	2.2
NP6	3.9	4.0	4.1
NP7	2.1	1.9	3.9
NP8	3.2	2.1	3.5
NP9	2.2	2.0	3.8
NP10	2.5	2.5	5.7
NP11	4.1	3.6	3.9
NP12	4.3	3.5	9.8
NP13	1.9	1.2	5.1
Min	**1.5**	**1.2**	**2.2**
Max	**4.3**	**4.0**	**9.8**

Instrument Detection Limit Calculations for the 10 replicate injections of 2 µL at the 10 ng/mL concentration:

- IDL = t0.99 · SD = t0.99 · (%RSD / 100) · 10 ng/mL
- t0.99 = 2.821 for 9 degrees of freedom

*NP12 (highlighted) is the isomer with lowest response

Cmpd.	IDL (ng/mL)
NP1	1.4
NP2	2.1
NP3	1.1
NP4	1.3
NP5	0.6
NP6	1.2
NP7	1.1
NP8	1.2
NP9	1.1
NP10	1.0
NP11	1.1
NP12	1.6
NP13	1.1

Complete isomer separation with excellent sensitivity

Scan data (1000ng/mL): EIC (*m/z* 107,121,135,149,163,191,220)

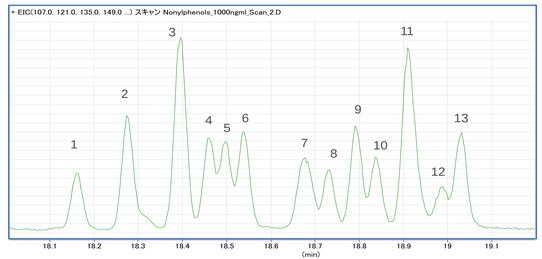

EIC for lowest responding isomer, NP12 SIM *m/z* 191.0, 10ng/mL, 2µL injection

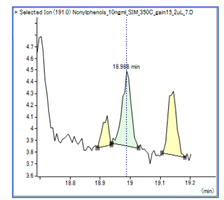

Conclusions

The legislated detection limits of 20 ng/mL at injection (20 ng/L water), are exceeded by more than 10 fold for 12 of the 13 isomers. NP12 is exceeded by 7 fold. This suggests that ***at least*** a 5-fold decrease in sample size is possible: instead of a liter of sample, only 200 mL of water need be extracted and concentrated to 1 mL. This would be a considerable savings in transport, handling, solvent and waste disposal costs. Of course, combining the HES sensitivity with large volume injection would produce further improvements.
This work demonstrates the rapid and sensitive detection of these difficult compounds and suggests upstream, bench-chemistry improvements to lower laboratory costs. The HES makes this a generally applicable approach for rethinking many existing similar analyses.

Reference

Ministry of the Environment Government of Japan (2012) *https://www.env.go.jp/en*

Analysis of Per/Polyfluoroalkyl Substances (PFASs) in Water using the Ultivo Triple Quadrupole LC/MS

Tarun Anumol[1], Theresa Sosienski[2], Craig Marvin[1], Dorothy Yang[2], Patrick Jeanville[2]

[1] Agilent Technologies Inc., Wilmington, DE, USA

[2] Agilent Technologies Inc., Santa Clara, CA, USA

ASMS 2017
ThP-174

Agilent
Trusted Answers

Introduction

Per/Polyfluoroalkyl substances (PFASs) are widely used in manufacture and industry because of their desirable properties. They find uses as surfactants, fire-retardants, non-stick cookware and other applications. Their unique properties also make them persistent and they have been detected almost ubiquitously in the environment.

The United States Environmental Protection Agency (USEPA) has issued drinking water health advisories for two PFASs, perfluorooctanoic acid (PFOA) and perfluorooctane sulfonate (PFOS) at 70 ng/L. Several US states also have public health guidelines for PFASs ranging from 20-400 ng/L in drinking water.

This study describes a method for the sensitive quantification of 17 PFASs including all 14 in the USEPAs method 537 in drinking water. The analysis is performed in a single run using the Ultivo Triple Quad LC/MS system.

Innovative technologies within Ultivo allow for reduction in its overall footprint, while conserving the comparable performance level of much larger MS systems. Ultivo's numerous innovations such as the VacShield, Cyclone Ion Guide, Vortex Collision Cell and Hyperbolic Quads, not only maximize quantitative performance in a small package, but also enhance instrument reliability and robustness in order to have greater uptime. Moreover, Ultivo reduces the need for user intervention for system maintenance, making the system operation and maintenance manageable for non-expert MS users.

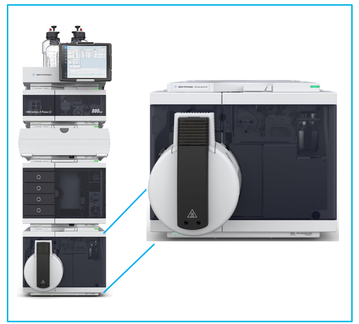

Figure 1. Ultivo Triple Quadrupole LC/MS

Experimental

Sample Preparation:

250 mL water samples were extracted using the Agilent SampliQ Weak Anion Exchange (WAX) cartridges.

Extraction conditions were similar to those in the EPA method 537 with a final extract in 96/4 (v/v) methanol (MeOH)/Water.

LC/MSMS Instrument Conditions:

Table 1. HPLC Parameters

1290 Infinity II LC Parameters	
Delay Column	Zorbax Eclipse Plus C18, 4.6x50 mm, 3.5 µm
Analytical Column	Zorbax Eclipse Plus C18, 3.0x50 mm, 1.8 µm
Injection Volume	5 µL
Column Temp.	50°C
Flowrate	0.4 mL/min
Mobile Phase	A: 5mM Ammonium Acetate in Water B: 5mM Ammonium Acetate in 95% MeOH
Runtime	19.0 min

Table 2. MRM transitions and Ret. Time for 17 PFASs

Compound	Precurs or Ion	Product Ion	RT (min)
PFBA	213	168.9	3.88
PFPeA	263	218.9	6.52
PFBS	298.9	98.9 (80)	7.06
PFHxA	313	268.9 (119)	8.52
PFHpA	362.9	319 (169)	9.9
PFHxS	398.9	99 (80)	10.07
PFOA	413	369 (169)	11.05
PFNA	463	419 (169)	11.95
PFOS	498.9	99 (80)	11.95
PFDA	513	469 (218.7)	12.71
PFUdA	563	519 (218.7)	13.37
N-MeFOSAA	570	482.9 (418.9)	13.04
N-EtFOSAA	584	525.9 (418.9)	13.38
PFDS	598.9	99 (80)	13.32
PFDoA	613	569 (268.9)	13.93
PFTrDA	663	619 (169)	14.4
PFTeDA	713	669 (169)	14.82

Table 3. LC Gradient

Time (min)	% B
0.0	10
0.5	10
2.0	30
14.0	95
14.5	100

Table 4. Ultivo Triple Quad LC/MS conditions

MS Source Parameters	
Gas Temp.	230°C
Gas Flowrate	5 L/min
Sheath Temp.	350°C
Sheath Flowrate	12 L/min
Nebulizer	15 psi
Capillary	2500 V
Nozzle	0 V
Ionization	Negative ESI

Results and Discussion

Instrument Performance:

Excellent peak shapes and sensitive detection of all PFAS in water was achieved with the Ultivo.

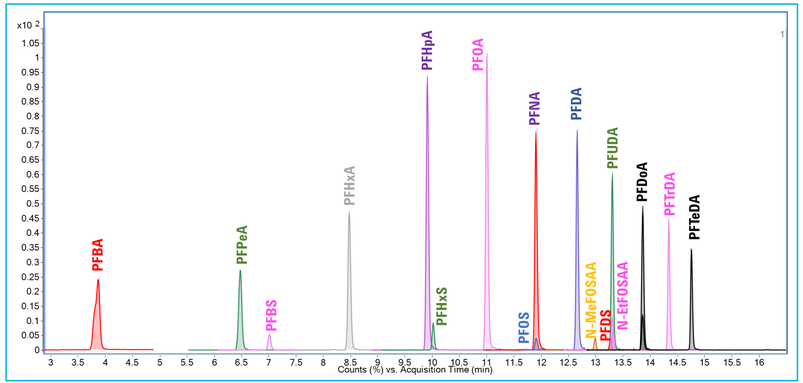

Figure 2. LC/MS/MS Chromatogram of the 17 Per/Polyfluoroalkyl substances (PFASs) analyzed at 1.0 ng/mL

Linearity and Sensitivity:

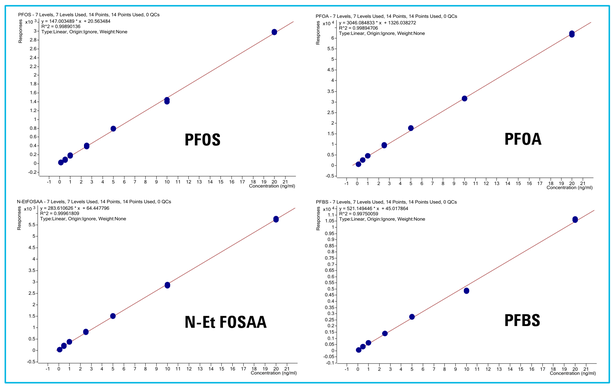

Figure 3. Calibration curves for PFOS, PFOA, N-Et FOSAA and PFBS.

All 17 PFASs ranging from 4-14 carbon-chain length had linear calibration curves with an R^2 >0.99.

Quantification using a seven point calibration curve at 0.1, 0.5, 1.0, 2.5, 5.0, 10 and 20 ng/mL were performed for all water samples.

Results and Discussion

Precision:

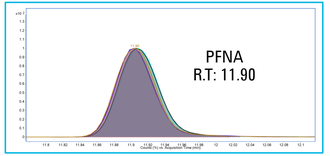

Figure 4. PFNA peak shape and retention time stability at 1 ng/mL with 5 replicate injections

Table 3. Precision expressed in RSD (%) for the 17 PFASs spiked at 1 µg/L (4 ng/L equil. In sample); n=5

Compound	RSD (%)	Compound	RSD (%)	Compound	RSD (%)
PFBA	0.28	PFOA	1.39	N-EtFOSAA	4.56
PFPeA	1.69	PFNA	0.98	PFDoA	2.43
PFBS	4.49	PFOS	5.30	PFTeDA	4.89
PFHxA	0.51	PFDA	1.62	PFTrDA	5.08
PFHpA	3.99	N-MeFOSAA	1.77	5 replicates spiked at 1 ng/mL	
PFHxS	4.72	PFUdA	2.93		

Recovery and RSD:

The recovery of the 17 PFASs were determined at 1 µg/L (4 ng/L equiv. in water) and 5 µg/L (20 ng/L equil. In water) shown in Figure 3. The overall recovery was between 70-125% for both spiking levels. Relative standard deviation was 0.3-10.8% for all compounds at both the 1 µg/L and 5 µg/L ng/mL spikes.

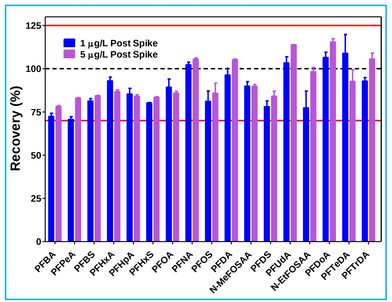

Figure 5. Recovery and RSDs for the PFASs evaluated at 1 and 5 ng/mL post-spiked into a water extract.

Analysis in Real Water Samples:

Finished drinking water samples from North-east USA and Canada were analyzed for the 17 PFASs using the extraction and analysis technique mentioned here. Figure 6 depicts the presence of PFOS and PFOA detected at low ng/L range in 2 samples along with the quantifier ion. The Ultivo was able to detect the presence of these low concentration PFASs suggesting good sensitivity and robustness for analysis of water samples.

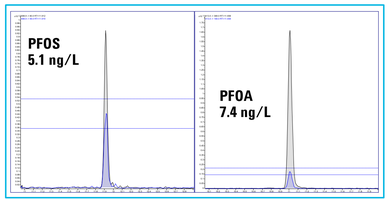

Figure 6. Overlay of qualifier and quantifier ion for PFOS and PFOA detected in finished drinking water samples at low ng/L levels using the Ultivo LC/MS/MS.

Conclusions

Ultivo Triple Quad LC/MS provides sensitive, reliable and robust quantification of PFAS in water.

- Excellent sensitivity for PFAS analysis with a reduced footprint
- Good recoveries and low RSDs achieved through innovative technologies
- Complete workflow & solution for PFAS analysis that includes the Infinity II LC, Ultivo Triple quad LC/MS and MassHunter software

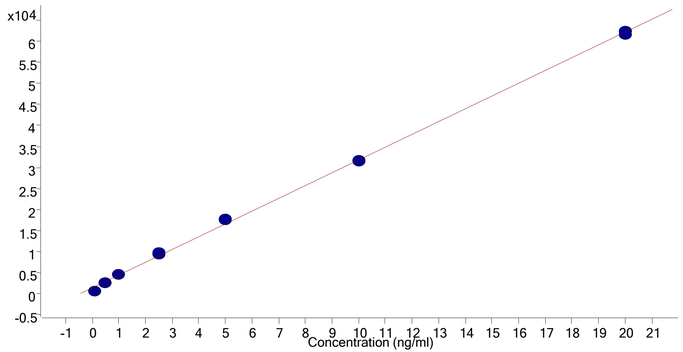
x104
6
5.5
5
4.5
4
3.5
3
2.5
2
1.5
1
0.5
0
-0.5
-1 0 1 2 3 4 5 6 7 8 9 10 11 12 13 14 15 16 17 18 19 20 21
Concentration (ng/ml)

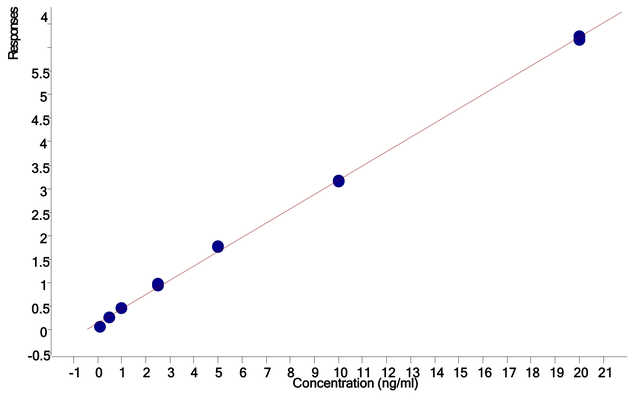
Responses
4
5.5
5
4.5
4
3.5
3
2.5
2
1.5
1
0.5
0
-0.5
-1 0 1 2 3 4 5 6 7 8 9 10 11 12 13 14 15 16 17 18 19 20 21
Concentration (ng/ml)

Automated Online SPE/Tandem-MS Analysis of Trace Organic Contaminants in Drinking Water

Patrick M. Batoon[1], Theresa Sosienski[1], Dan-Hui Dorothy Yang[1], Tarun Anumol[2], Craig Marvin[2], Shane E. Tichy[1], and Patrick Jeanville[1]

[1]Agilent Technologies Inc., Santa Clara, CA, USA
[2]Agilent Technologies Inc., Wilmington, DE, USA

ASMS 2017
TP - 178

Agilent
Trusted Answers

Introduction

A variety of organic molecules originating from pesticides, pharmaceuticals, personal care products, and industrial chemicals used in daily life can be introduced into the environment through domestic and industrial wastewater sources. These molecules are a subclass of compounds collectively known as Trace Organic Contaminants (TOrCs), commonly found in a variety of potable and non-potable water resources. Although not acutely dangerous as highly dilute individual entities, long-term synergistic exposure due to mixtures of these compounds are still to be determined.[1] While characterization for long-term and chronic toxicity are yet to be published, it is still important to monitor their presence in current water resources.[2]

Using the online SPE capabilities of the 1290 Infinity Flexible Cube with the analytical power of the Ultivo Triple Quadupole LC/MS (Figure 1), we have demonstrated a rapid and sensitive automated analysis of trace organic contaminants in drinking water without tedious offline enrichment.

Figure 1. Ultivo LC/MS Triple Quadrupole

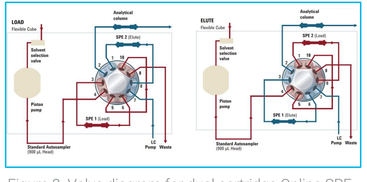

Figure 2. Valve diagram for dual cartridge Online SPE

Experimental

The Agilent 1290 Infinity Flexible Cube Online SPE dual cartridge configuration (Figure 2) allows injection volumes of up to 900 µL for sample enrichment with minimal user intervention, improving accuracy and reproducibility. The dual cartridge setup allows for enhanced sample throughput by equilibrating one cartridge as the other is cartridge is being eluted.

In the experiment presented, a selection of 31 representative TOrCs (listed in Figure 3) were analyzed in spiked water samples –from 0.5-200 ng/L (ppt) in concentration. Sample volumes of 750 µL were introduced onto the SPE cartridge for enrichment, then eluted at the 4-minute mark, triggering the start of the HPLC linear gradient. Detection of ions were carried out on the Ultivo Triple Quadrupole LC/MS using dynamic MRM for maximized sensitivity.

Online SPE, HPLC, and MS parameters

Online SPE, HPLC, and MS instrument parameters are listed in Table 1, Table 2, and Table 3, respectively

Table 1. Online SPE Conditions

SPE Cartridge	ZORBAX Extend C18, 4.6x12.5 mm, 5 µm	
FlexCube Solvents	A (Load): H_2O w/ 0.1% v/v Formic Acid B (Elute): 1:1 ACN/IPA	
Sample Volume	750µL	
SPE Elution Graduate	Time (mins) 0 - Load 4 - Elute 8 - Equilibrate	Mobile Phase 100% A 100% B 100% A

Table 2. HPLC Conditions

Column	ZORBAX RRHD Eclipse Plus C18, 3.0x50 mm, 1.8 µm	
Mobile Phase	A: H_2O w/ 0.2mM NH_4F B: ACN w/ 0.2mM NH_4F	
Flow Rate	0.350 mL/min	
HPLC Elution Gradient	Time (mins) 0 4 11 12.5	Mobile Phase 5% B 5% B 100% B 5% B
Run time	4 min (Sample enrichment) + 8.5 min (HPLC gradient) + 2.5 min (Post run) = 16 min Total	

Table 3. MS Conditions

Gas Settings	Drying Gas: Sheath Gas: Nebulizer:	11 L/min at 250 °C 12 L/min at 375 °C 45 psi
Source Voltage	Capillary Voltage: Nozzle Voltage:	4000 V(+), 3500 V(-) 500 V(+), 500 V(-)
Cycle Time	800 ms	

Results and Discussion

Detection and screening of 31 trace level TOrCs in drinking water using Online SPE

Unambiguous and confident signal response of Ultivo using 750 µL of a 10 ppt spiked water sample, illustrated in Figure 3.

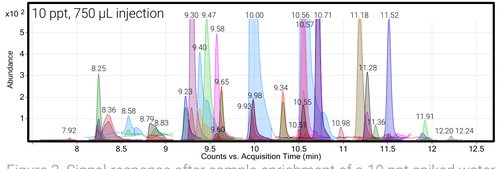

Atenolol [a]	Atrazine [b]	Benzophenone [b]
Benzotriazole [a]	Bisphenol A [b]	Caffeine [b]
Carbamazepine [b]	Clofibric Acid [a]	Diclofenac [b]
Diltiazem [b]	Diphenylhydramine [b]	Fluoxetine [b]
Gemfibrozil [a]	Hydrochlorothiazide [c]	Hydrocortizone [b]
Ibuprofen [b]	Meprobamate [b]	DEET [b]
Naproxen [b]	Norgestrel [b]	Primidone [a]
Propanolol [a]	Propylparaben [b]	Simazine [b]
Sulfamethoxazole [b]	Testosterone [a]	Triclocarban [a]
Triclosan [c]	Trimethoprim [a]	TCEP [b], TCPP [b]

Figure 3. Signal response after sample enrichment of a 10 ppt spiked water sample

Quantitative linearity over 0.5 – 200 ng/L concentration range

Highly linear calibration curves (R^2 > 0.99) for a quantitation range of 0.5, 1, 2, 5, 10, 20, 50, 100, and 200 ng/L after Online SPE sample enrichment are illustrated in Figure 5.

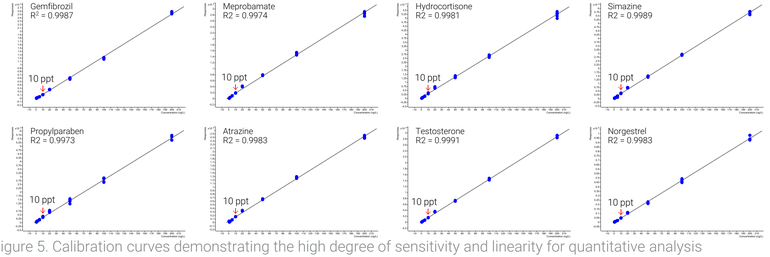

Figure 5. Calibration curves demonstrating the high degree of sensitivity and linearity for quantitative analysis

Chromatographic peak reproducibility over various concentration levels

Chromatographic peak overlays in Figure 6 demonstrate robust retention time stability and peak shape of the dual cartridge Online SPE setup over a large concentration range (0.5 – 200 ng/L) for a total of 54 injections.

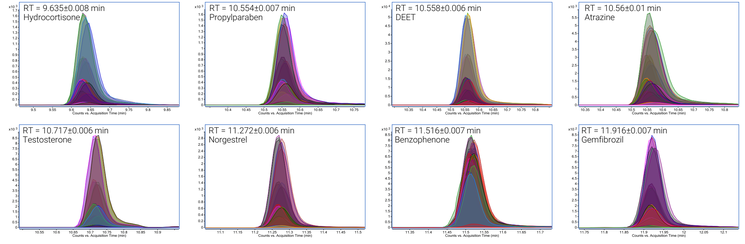

Figure 6. Chromatographic peak overlays and retention times of TOrCs over a large concentration range

Results and Discussion

Limits of Detection

Of the 31 TOrCs analyzed, 29 compounds have limits of detection that easily fall into the range of 5 ppt or less with only 750 µL of sample, illustrated in Figure 7.

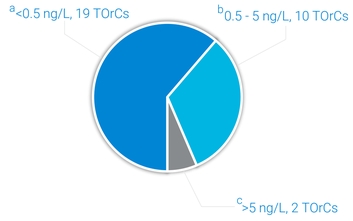

Figure 7. Distribution of the limits of detection of 31 common TOrCs found in water

Conclusions

- The 1290 Infinity Flexible Cube enables automated Online SPE sample enrichment for trace organic contaminants.
- Enhanced throughput is achieved using a dual-cartridge setup for rapid sample turnaround.
- The Ultivo Triple Quadrupole LC/MS enables enhanced trace quantitative analysis with a minimized footprint.
- Technical innovations contained in Ultivo provide optimal sensitivity and robustness without sacrificing the performance of larger instruments.

References

[1]C. G. Daughton, T. A. Terhes. "Pharmaceuticals and personal care products in the environment: agents of subtle change" *Environ. Health Perspect.* **107**, 907-938 (1999)

[2]T. Anumol, S. Snyder. "Rapid analysis of trace organic compounds in water by automated online solid-phase extraction coupled to liquid chromatography-tandem mass spectrometry" *Talanta* **132**, 77-86 (2015)

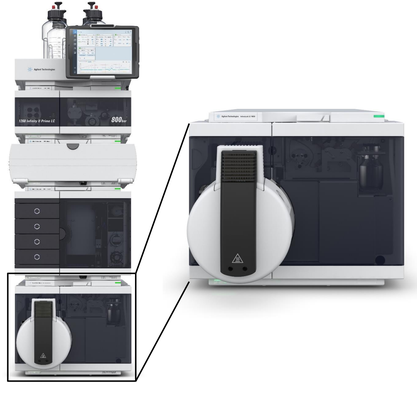

The new Agilent Ultivo Triple Quadrupole LC/MS

Ultivo is designed to address many of the challenges faced by labs performing environmental and food safety analyses. Innovative technologies housed within Ultivo allows for dramatic reduction in overall footprint, while conserving the performance found in larger MS systems.

Innovations such as the *VacShield*, *Cyclone Ion Guide*, *Vortex Collision Cell* and *Hyperbolic Quads* maximize quantitative performance in a small package. The enhanced instrument reliability and robustness results in greater instrument uptime. Ultivo reduces the need for user intervention for system maintenance, making it attractive to the non-expert to operate and maintain.

MassHunter simplifies data acquisition, method set up, data analysis and reporting. This results in the fastest acquisition-to-reporting time possible, increased lab productivity, and confidence in results.

Reduction in EI Source Cleaning Frequency: The Benefits of a Novel GC with an Inert Microfluidic Flowpath

Matthew Giardina and Rebecca Veeneman
Agilent Technologies, Inc., Wilmington, Delaware

ASMS 2017
MP-271

Agilent
Trusted Answers

Introduction

Matrix Effects in GC/MS: Flow Path Contamination

Overtime, changes in signal response may occur with the accumulation of contaminants on the ion source chamber surfaces when using GC/MS coupled with electron ionization (EI). Contamination may occur through repeated analysis of samples containing analytes or matrices of low volatility or by the accumulation of stationary phase bleed, resulting in changes in analyte response or peak skewing. When significant levels of contamination are observed, corrective action is necessary to restore initial performance. In some cases, this may require significant time associated with venting, cleaning the source, and restoring vacuum. In this paper, results indicate that the use of a novel GC with an inert microfluidic flow path reduces ion source cleaning frequency compared to traditional GC for the analysis of semivolatile organic compounds (SVOCs).[1]

Agilent Intuvo 9000 GC

The Agilent Intuvo 9000 GC is a significant advancement in the development of gas chromatographs.[2] The Intuvo includes a number of design innovations making it ideally suited for SVOC analysis particularly in high-throughput laboratory settings.

- Guard chip – easily replaceable precolumn to prevent particulate and nonvolatile contamination of the flow path, column and detector. The guard chip can be replaced as easily as an inlet liner.
- Intuvo Flow Technology (IFT) – modular microfluidic devices used to assemble the flow path from inlet to detector. The flow path is customizable to suit analysis requirements with inlet or detector splitting and mid-column or post-column backflush.
- No-trim columns – Intuvo columns are the same columns used in the Agilent 7890 wound into a planar format compatible with the Intuvo direct heating and click and run connections.
- Click and run connections – ferrules have been eliminated and replaced with direct face seal connections for easy, fast and reliable maintenance.
- Direct heating – unlike air bath ovens, the Intuvo uses direct conductive heating. This enables both fast column heating and faster cool down.

Experimental

Experimental Approach

Matrix studies were conducted concurrently on two separate instrument platforms. One system was an Agilent Intuvo 9000 GC coupled to 5977 GC/MSD and the other system was an Agilent 7890 coupled to a 5977 GC/MSD. Both MSDs were configured with an inert ion source with 6 mm drawout plate. The same instrument methods were used on both systems with the exception of the guard chip which is unique to the Intuvo 9000 GC (Table 1).

Table 1. Instrument Conditions

GC Conditions	
Injection volume	1 µL
Inlet (Split/Splitless)	Temperature 300 °C Pulsed splitless 60 psi until 0.5 min Purge 50 mL/min at 0.5 min
Liner	Agilent UI splitless single taper with glass wool (5190-2293)
Guard chip (Intuvo only)	60 °C for 2 min, 20 °C/min to 260 °C, 6 °C/min to 330 °C hold until end of run
Column	Agilent DB-5ms UI 30 m x 0.25 mm x 0.5 µm (122-5536UI-INT)
Flow	2 mL/min
Column temperature	40 °C for 2 min, 20 °C/min to 260 °C, 6 °C/min to 330 °C hold for 1.3 min
MSD Conditions	
Transferline temperature	330 °C
Ion source temperature	330 °C
Quadrupole temperature	200 °C
Scan	35 to 550 m/z
Gain factor	1
Threshold	50
A/D samples	2

Results and Discussion

Matrix Study

Figure 1 shows the scheme used to track the contamination of the system over the course of matrix study. After calibration and initial system performance check, 20 matrix injections were made. Following the matrix injection, the system performance, calibration and internal standard (ISTD) responses were reevaluated. The maintenance action level for each performance metric was based upon the limits set by USEPA Method 8270D.[1] A sequential approach to maintenance was used in order to determine the source of contamination in the instrument flowpath.

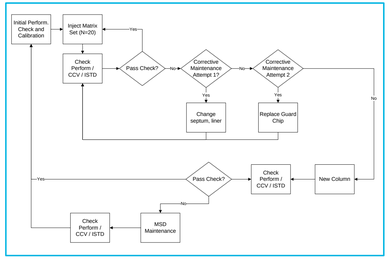

Figure 1. Scheme for tracking contamination

Soil Extracts

In order to model the worst-case soil extract typically encountered in an environmental lab, a composite soil extract in methylene chloride was donated from ESC Lab Sciences (Mt. Juliet, TN). The soil extract contained a significant level of particulate soil residue requiring liner replacement after just 20 matrix injections (Figure 2).

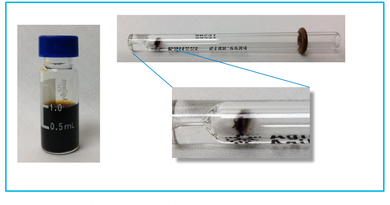

Figure 2. Soil extract and liner contamination

7890 GC/5977 MSD Internal Standard Response

In accordance with USEPA 8270D, the threshold criteria for internal standard response was set to a maximum loss of 50% peak area compared to the midpoint calibration standard in the initial calibration. Two replicate studies were carried out starting with new columns and clean sources.

The result of the first matrix study with the 7890/5977 is shown in Figure 3. Area measurements shown were taken after maintenance was performed to comply with the study scheme (Figure 1). Maintenance included liner replacement after each series of 20 matrix injections in order to restore system inertness. Inlet seal replacement and column trimming was required at certain intervals in order to restore calibration. As indicated in Figure 3, the internal area response begins to approach the 50% threshold after 240 matrix injections. Inlet maintenance and column trimming was not able to restore performance. At this point, the column was replaced and the system was retested. However, the internal standard response was not restored. Only after source cleaning did the ISTD responses return to levels close to the initial responses.

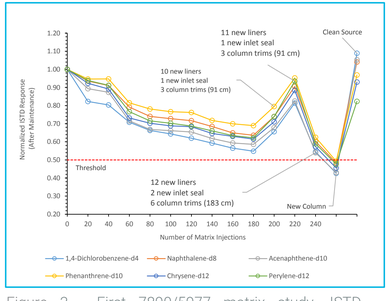

Figure 3. First 7890/5977 matrix study. ISTD response over the course of matrix injections.

The result of the second matrix study with the 7890/5977 is shown in Figure 4. After 120 matrix injections, the area response of 1,4-dichlorobenzene-d_4 dropped below the 50% threshold. Inlet maintenance, column trimming and column replacement did not return the response to the initial levels Again, source cleaning was required to return ISTD responses close to the initial levels.

Results and Discussion

7890 GC/5977 MSD Internal Standard Response

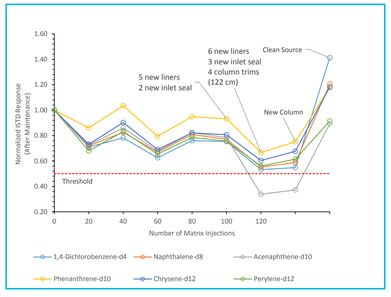

Figure 4. Second 7890/5977 matrix study. ISTD response over the course of matrix injections.

Intuvo GC/5977 MSD Internal Standard Response

The result of the matrix study on the Intuvo/5977 is shown in Figure 5. After each series of 20 matrix injections, the liner was replaced. Interestingly, the 50% response threshold was not reached over the course of 680 matrix injections. Also, it appears that the variation in ISTD response is uniform for all internal standards and not divergent as observed with the 7890/5977. This indicates that variability in response is likely due to other factors which are not related to detection (e.g. injection variability, solvent evaporation).

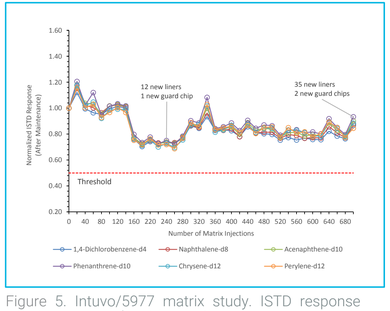

Figure 5. Intuvo/5977 matrix study. ISTD response over the course of matrix injections

Current Work

The reason for the stability of internal standard response on the Intuvo/5977 system is currently being investigated in greater detail. The first hypothesis is that the Intuvo flow path in between the distal end of the column and the source is providing some protection from column bleed. This is being tested by replicating the Intuvo flow path in the 7890 oven and measuring the internal standard response after long intervals at which the column is held at maximum temperature. Initial data indicates there is no additional protection comparing measurements with and without the Intuvo flow path in the 7890 oven.

Future Work

The second hypothesis is that the Intuvo guard chip and flow path are providing some protection of the ion source from matrix. Future studies will be carried out comparing the longevity of source response with and without the Intuvo flow path replicated in a 7890 oven for a series of matrix injections.

Conclusions

Matrix Study

In comparing results between the matrix study on the 7890/5977 and Intuvo/5977 it appears that there is a substantial increase in the number of matrix injections that can be performed on the Intuvo before source cleaning is required. Further studies are being conducted in order to verify and elucidate the exact mechanism observed in these initial studies. If verified, this would prove to be of substantial benefit in the analysis of SVOCs particularly for contract environmental laboratories.

References

[1] Analysis of Semivolatile Organic Compounds Using the Agilent Intuvo 9000 Gas Chromatograph, *Agilent Technologies*, publication number 5991-7256EN, 2016.

[2] Agilent Intuvo 9000 GC System, *Agilent Technologies*, publication number 5991-7273EN, 2016.

ANALYSIS OF DIOXINS, FURANS AND POLYCHLORINATED BIPHENYLS IN

Peter Haglund[1], Sofia Nieto[2], Nathan Eno[2]

[1] Umeå University, Umeå, Sweden; [2] Agilent Technologies, Inc., Santa Clara, CA, USA.

Overview

- The aim was to demonstrate how **high-resolution GC/Q-TOF instruments** can be used for **flexible analysis of dioxin-like compounds**
- Full spectra EI data was collected using the novel Agilent 7250 GC/Q-TOF and was queried using **target, suspect and non-target analysis workflows**
- We demonstrate **excellent accuracy in dioxin and dioxin-like PCB analyses**
- We illustrate how GC/Q-TOF instruments allow **sceening for known dioxin-like compounds** and **identification of unknown dioxin-like compounds**

Introduction

- Dioxin-like compounds bind to the Ah receptor and produces toxic effects at very low levels[1]
- Strong Ah ligands are all planar aromatic compounds and most are halogenated
- The total dioxin-like toxicity can be expressed as dioxin toxic equivalents (TEQs)[2]
- Modern GC time-of-flight MS instruments are very sensitive and provide full EI spectra
- GC/Q-TOF instruments can be used for target analysis of dioxins and dioxin-like PCBs, and for suspect and non-target screening of dioxin-like compounds

Methods

Samples and clean-up

- Baltic Sea sediment and fish: in-house reference materials (RMs)
- Sediment was Soxhlet extracted with toluene
- Fish was column extracted with acetone:hexane and hexane:ether
- Bulk matrix was removed by H_2SO_4 treatment
- Planar compounds were isolated through carbon column clean-up

GC-QTOF MS

- GC high-resolution EI-MS analysis was performed on an Agilent 7250 GC/Q-TOF
- Target compounds were detected by MassHunter (MH) Find-by-Fragments workflow
- MH Quantitative Analysis was used for quantification
- MH Qualitative Analysis was used for suspect screening of dioxin-like compounds
- MH Unknown Analysis was used for non-target screening of dioxin-like compounds

Results – Target Analysis

Table 1: Comparison of GC/Q-TOF and GC-magnetic sector high-resolution MS data (pg/g)

Congener	TEF*	Sediment			Salmon		
		QTOF HRMS	Sector HRMS	RM Average	QTOF-HRMS	Sector-HRMS	RM Average
PCB-77	0.0001	32	37	36	1125	900	910
PCB-81	0.0003	3.5	1.8	1.8	23	23	26
PCB-126	0.1	8.8	8.0	7.3	464	410	430
PCB-169	0.03	3.9	1.8	1.6	53	53	58
2,3,7,8 -TCDD	1	1.8	1.5	1.5	2.3	2.6	2.7
12378 -PeCDD	1	3.2	3.2	2.8	4.7	4.4	4.6
123478 -HxCDD	0.1	6.4	1.8	2.1	0.4	0.3	0.3
123678 -HxCDD	0.1	14	11	11	3.0	1.7	1.9
123789 -HxCDD	0.1	8.2	7.0	6.8	0.2	0.1	0.2
HpCDD	0.01	40	34	36	0.7	0.3	0.3
OCDD	0.0003	137	100	113	1.9	0.9	1.2
2378 -TCDF	0.1	13	14	17	26	23	23
12378 -PeCDF	0.03	4.7	4.1	4.2	4.2	5.4	5.0
23478 -PeCDF	0.3	11	10	9.4	29	26	25
123478 -HxCDF	0.1	7.0	7.1	9.1	1.3	0.9	0.9
123678 -HxCDF	0.1	10	5.1	4.5	2.7	1.2	1.2
234678 -HxCDF	0.1	8.5	6.1	6.1	1.5	1.0	0.9
123789 -HxCDF	0.1	3.7	1.9	2.3	ND	0.2	0.2
1234678 -HpCDF	0.01	95	76	77	0.2	0.3	0.3
1234789 -HpCDF	0.01	8.0	3.1	3.4	ND	0.1	0.1
OCDF	0.0003	130	94	105	1.6	0.2	0.3
TEQ		18	15	15	67	60	63

* TEF: World Health Organization (WHO) Toxic Equivalency Factor.

- Good agreement of planar PCB and polychlorinated dibenzo-p-dioxin and dibenzofuran (PCDD/F) concentrations from GC-QTOF-MS and GC-magnetic sector-MS (Table 1)
- The important tetra/penta-CDD/Fs, PCB-126, and TEQ are within ± 25% of the reference values
- The deviation between QTOF-MS and Sector-MS data depends on the signal quality (S/N ratio) and is less than ± 40% for all compounds with a S/N greater than 10

SEDIMENTS AND FISH USING NOVEL 7250 HIGH-RESOLUTION GC/Q-TOF

Results: Suspect screening

Suspects

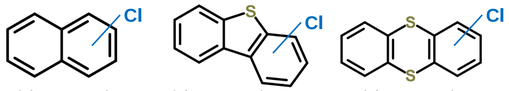

Chlorinated napthalene (PCN) | Chlorinated dibenzothiophene (PCDT) | Chlorinated Thinanthrene (PCTA)

- PCTAs were not detected
- PCDT were found in sediment at 10% of the PCDD/F levels
- **PCNs were most abundant** (**Figure 1**)
- PCN and PCDF levels were similar in sediment
- PCN levels were 100-fold higher than PCDD/F levels in salmon
- Metabolically stable PeCNs and HxCNs (wo. vicinal hydrogens) biomagnify in fish

Figure 1. PCN composition

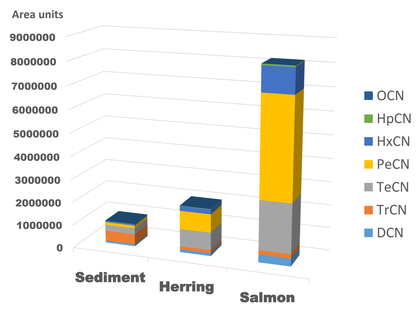

Sediment: Non-target screening

- Polycyclic aromatic compounds (PACs), incl. PAHs, dominated the dioxin fraction
- **Halogenated PAHs** was also found (**Figure 2**)
- Halo-PAHs were dominated by lower halogenated congeners (**Figure 3**)

Figure 2. Tentative identification of chloropyrene

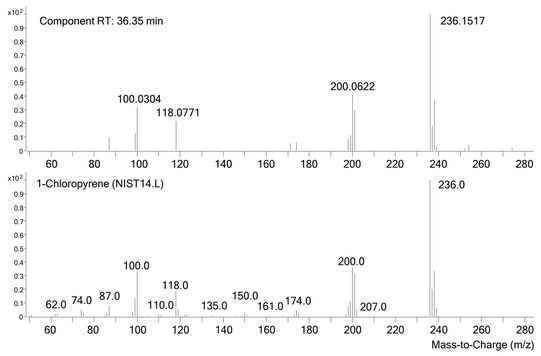

Figure 3. PAHs and halo-PAHs in sediment

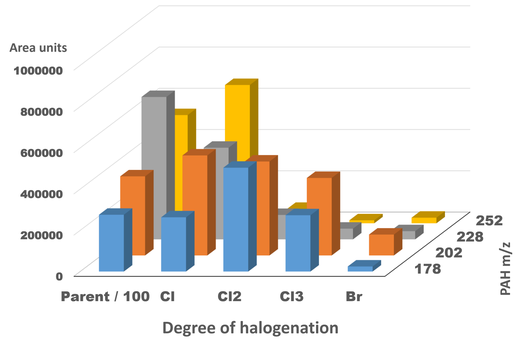

Sediment: Non-target screening

- An abundant brominated unknown with formula $C_{13}H_7NBr_4$ was found in sediment (**Figure 4**)
- A Chemspider search returned on candidate: **1,3,6,8-Tetrabromo-9-methyl-carbazole**
- $C_{13}H_7NBr_4$ unknown can be a metabolite of the natural product 1,3,6,8-Tetrabromocarbazole [1], which was also detected (**Figure 5**)
- The isotope clustering and fragmentation is supporting the proposed structure

Figure 4. EI spectrum of $C_{13}H_7NBr_4$

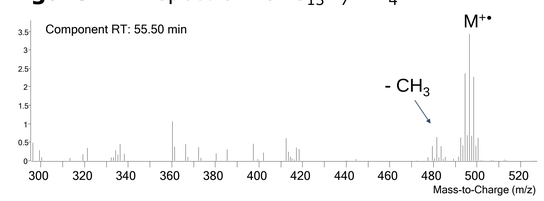

Figure 5. Isotope fidelity of $C_{13}H_7NBr_4$

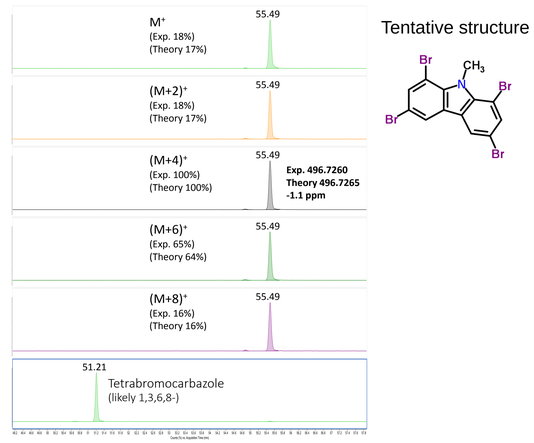

[1] Identification of Brominated Carbazoles in Sediment Cores from Lake Michigan. *Environmental Science and Technology* **39**: 9446-9451.

Summary: Sediment contaminants

- PAHs dominated the dioxin fraction (**Figure 6**)
- Halo-PAHs and brominated carbazoles and methyl carbazoles (BR-CZ/MCZ) were present at ca 100-fold lower levels
- PCNs, PCDFa and PCDDs were at comparble levels, whilst PCDTs were 10-fold lower
- Tetrahalogentated congeners dominated the bi-tricyclic planar compound groups (**Figure 7**)

Figure 6. Concentrations in sediment

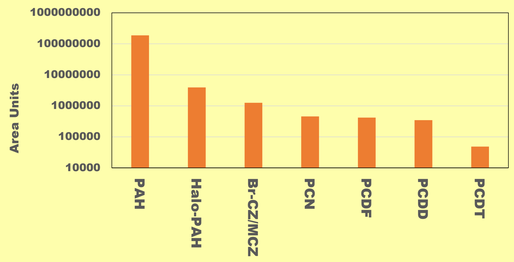

Figure 7. Congener distribution in sediment

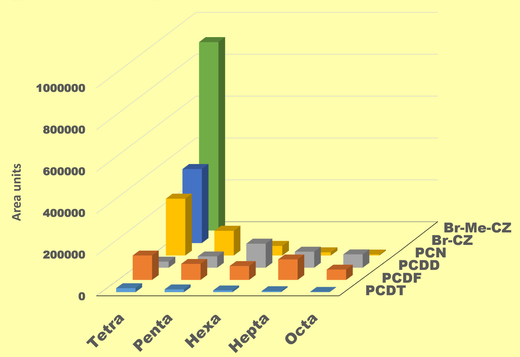

Conclusion

The new GC-QTOF system generates PCDD/F and planar-PCB concentrations comparable to those of the Golden Standard: Magnetic sector HRMS

Full spectrum data is obtained in the same run, which can be used for suspect and non-target screening of other dioxin-like compounds

UMEÅ UNIVERSITY

References

1. http://www.euro.who.int/__data/assets/pdf_file/0017/123065/AQG2ndEd_5_11PCDDPCDF.pdf?ua=1
2. https://www.epa.gov/toxics-release-inventory-tri-program/dioxin-and-dioxin-compounds-toxic-equivalency-information

FLAVORS & FRAGRANCES

Allergens in Perfume by GC/Q-TOF with a Low Energy EI Source

Matthew Curtis; Jennifer Sanderson; Tim Peck
Agilent Technologies, Santa Clara, CA

ASMS 2017
MP-273

Agilent
Trusted Answers

Introduction

The number of suspected flavor and fragrance allergens found in consumer products is driving the need to develop improved analytical methods that can be used to quantitate regulated compounds as well as screen for new and/or unreported compounds. While targeted allergens can be identified by library search, new compound identification, especially in complex matrices, can prove to be challenging. Employing a high-resolution quadrupole time of flight mass spectrometer with a new EI source capable of low energy ionization for this analysis expands the amount of unknown compounds that can be identified by molecular ion, with good resolving power to separate it from the matrix and accurate mass assignment for confidence in identification.

Presented here is a workflow that can be employed in screening, confirming and quantitating known allergens and identifying new and unknown compounds that may be allergens or have other impacts on biological systems. The creation of a user-created compound database and library for increased confidence of the identification of target analytes.

Figure 1: Agilent 7250 GC/Q-TOF

Experimental

Sample Preparation

A fragrance allergen standards kit was purchased from Restek (33105). This contained 31 components separated into three solutions by their functional groups. This solution was diluted from 400 mg L^{-1} to 1 mg L^{-1} to create a 9-point calibration curve. 1,4-dibromobenzene and 4,4'-dibromobiphenyl were used as internal standards.

11 commercially available perfumes and colognes were diluted 10:1 with MTBE prior to analysis.

Instrumentation

The new Agilent 7250 GC/Q-TOF (Figure 1) equipped with the 7890B GC was used for this analysis. A 0.5 microliter injection was made into a multi-mode inlet at 280°C, with a 200:1 split flow into the Agilent UI low-pressure drop liner with glass-wool. Separation was performed on a DB-17MS UI 20 m x 180 µm x 0.18 µm with a He carrier gas flow of 1.6 mL/min. The International Fragrance Association has an analytical procedure for the analysis of allergens; this method was utilized for the work presented here[1].

The Q-TOF system was equipped with a new high efficiency EI source heated at 280°C for 70eV and 250°C for low-eV. Operated in full scan mode, spectral data was collected at a mass range of 40-700 m/z with an acquisition rate of 5Hz. Ionization using the new Low Energy-EI source was operated at the standard electron energy (70eV) and at lower electron energy optimized for this method (12.5eV). Data analysis was performed using Agilent MassHunter Software.

Workflow/Post Data Analysis

-Build Personal Compound Database and Library (PCDL) for both ionization energies

-Use the PCDL to quickly screen the commercial perfumes for target analytes.

-Use the PCDL to create a quantitation batch of the standard compounds

-Analyze and quantitate commercial fragrances for target allergens

-Use the quantitation batch, and the NIST14 library to identify components not included in the PCDL

-Use 12.5eV to confirm high m/z ions to aid in the identification of the molecular ion

Results and Discussion

Building a Unique Screening Library with Agilent PCDL Manager

Accurate mass libraries are easily created from a MassHunter datafile. MassHunter Qualitative Analysis is used to locate the analyte, extract the spectrum and add an identification for the compound (Figure 2). The Molecular Formula Generation algorithm confirms the molecular ion and fragment ions using accurate mass, isotope ratios, and isotope spacing.

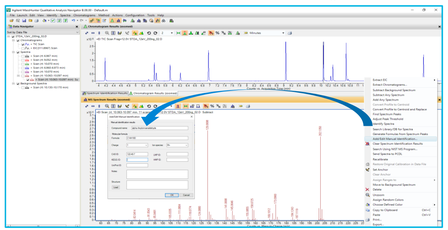

Figure 2: MassHunter Qualitative Analysis Manual Identification

After reviewing the identification, a right-click on the spectrum performs the transfer of all the compound information to the PCDL (Figure 3).

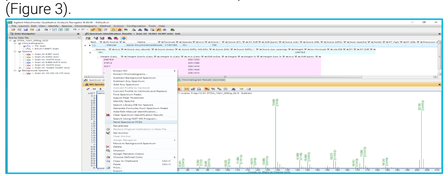

Figure 3: MassHunter Qualitative Analysis Send to PCDL

PCDL Manager includes the compound name, retention time, CAS #, molecular formula, structure, spectrum, and more (Figure 4). The PCDL can be used for screening targets or as a specific library to search prior to a general library (NIST).

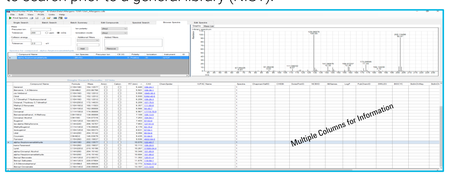

Figure 4: MassHunter Allergen PCDL

Utility of a User-Created PCDL

PCDL uses the accurate mass, isotope ratios, fragment ions, coelution graphs, and RT to confirm the identification of the target.

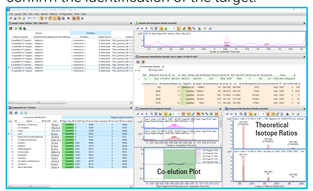

Figure 5: MassHunter Qualitative Analysis Screening

Deconvolution followed by a library search can also be performed in MassHunter Qualitative Analysis. Even when a unit mass library is used, the exact mass is calculated from the molecular formula and compared to the spectrum. This provides additional confirmation (Figure 6).

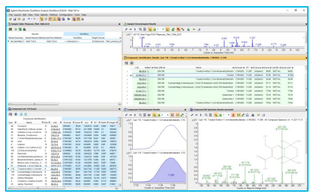

Figure 6: MassHunter Qualitative Analysis Unknown Identification (NIST14)

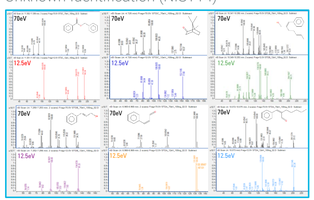

Figure 7: Comparison of 70eV and 12.5 eV of several allergens

Results and Discussion

Table 1: Quantitation of Target Analytes from 7 of the commercial products (10x due to dilution).

Compound Name	Sample 1				Sample 2				Sample 3				Sample 4				Sample 5				Sample 6				Sample 7			
	RT (min)	MZ	Mass Accuracy (mmu)	Final Conc. (µg/L)	MZ	Mass Accuracy (mmu)	Final Conc. (µg/L)		MZ	Mass Accuracy (mmu)	Final Conc. (µg/L)		MZ	Mass Accuracy (mmu)	Final Conc. (µg/L)		MZ	Mass Accuracy (mmu)	Final Conc. (µg/L)		MZ	Mass Accuracy (mmu)	Final Conc. (µg/L)		MZ	Mass Accuracy (mmu)	Final Conc. (µg/L)	
D-Limonene	3.013	94.0777	0.1	20.1	94.0776	-0.1	1830.6		94.0776	0	50.4	94.0787	1	16.6	94.0775	-0.1	55.8	94.0778	0.2	26.4	94.0775	-0.1	592.4					
Eucalyptol	3.18				154.1357	0.6	11.6		154.1358	0.7	42.0	154.1353	0	77.2	154.1354	0.1	163.2	154.135	-0.1	10.3								
Camphor	4.8								152.12	0.5	43.2	152.1192	-0.3	103.6	152.1195	0	65.9											
Estragole	5.316	148.0888	0.6	19.2					148.0881	-0.1	19.1	148.0881	-0.1	23.4														
methyl 2-nonynoate	6.36	100.0517	-0.2	30.6																								
Safrole	6.57	162.0685	-1	19.4	162.0675	0	18.6		162.0676	0.1	21.0	162.0677	0.2	19.8	162.0679	0.4	21.0								162.0673	-0.2	19.3
iso-alpha-methylionone	7.952	150.104	0.2	1103.1					150.1041	0.3	881.5	150.1037	0	3252.6	150.1039	0.1	1526.8	150.1039	0.1	873.4	150.1037	0	5624.5					
Coumarin	9.434	146.0363	0.2	3010.0	146.0367	0.6	20.3		146.0363	0.2	141.3	146.0361	0	272.4	146.0363	0.2	74.3	146.0361	0	152.3	146.0358	-0.3	19.0					
Benzyl Benzoate	11.353	212.0833	0.1	222.7	212.0832	0	412.5		212.084	0.8	22.2	212.0829	-0.3	58.0	212.0836	0.3	102.2	212.0832	-0.1	134.5	212.0827	-0.6	20.7					
Benzoic acid, 2-hydroxy-, phenylmethyl ester	11.877	91.0544	0.2	127.7	91.0541	0	8268.4		91.054	-0.1	20.7	91.0552	1.1	20.5	91.0542	0.1	37.1	91.0543	0.2	95.0	91.054	-0.1	3213.5					
Benzyl cinnamate	13.158	192.0936	0.3	16.7	192.0936	0.2	21.6								192.0923	-1.1	15.2											
methyl 2-octynoate	5.263																											
Phenylacetaldehyde	4.191				92.0621	0.1	22.7																					
Citral	5.94	123.1168	-1.9	31.1					123.1172	0.5	37.6	123.1162	-0.5	109.1	123.1169	0.3	333.8	123.1175	0.8	38.2	123.1162	-0.5	166.6					
Octanal, 7-hydroxy-3,7-dimethyl-	6.207	96.0934	0.2	517.8	96.0933	0	255.9		96.0936	0.3	62.5	96.0919	-1.3	70.2	96.0935	0.3	58.0	96.0933	0.1	2177.1	96.0924	-0.8	706.0					
Cinnamal	6.974											132.0565	-0.3	18.5	132.0573	0.6	19.7											
Lilial	9.057				189.1273				189.1275	0.3	310.3	189.1272	-0.1	591.4	189.1275	0.2	431.0	189.1276	0.3	17.8	189.1273	0	5085.2					
alpha-Amylcinnamaldehyde	10.071	202.1351	0.1	79.6	202.1341	-0.8	18.8		202.1362	1.2	16.3				202.1352	0.3	20.9				202.1345	-0.7	17.5					
Lyral	10.325				136.0882	0.1	241.4		136.0882	0.2	267.9	136.0882	0.1	465.9							136.0885	0.4	18.2					
alpha-Hexylcinnamaldehyde	10.685	216.1531	2.6	18.5	216.1505	0	3427.5		216.1474	-3.1	39.4							216.1507	0.2	1105.2	216.15	-0.5	24.3					
Linalool	3.684	93.0699	-0.1	3623.3	93.0699	-0.1	1662.6		93.0698	-0.2	5914.4	93.0698	-0.2	11771.7	93.0699	-0.1	879.7	93.0698	-0.2	502.9	93.0698	-0.2	138.0					
Benzyl alcohol	3.987	108.0569	-0.3	184.0	108.0568	-0.4	36.4		108.0571	-0.1	30.1	108.0567	-0.4	63.5	108.0566	-0.6	19.6	108.0567	-0.5	104.4	108.057	-0.2	47.4					
Citronellol	4.965	81.0699	0	305.8	81.0698	-0.1	668.3								81.0698	-0.1	555.8	81.0699	0	1679.4	81.0698	-0.1	2078.3					
Geraniol	5.442	69.0699	-0.1	454.2	69.07	0	2251.0								69.0699	-0.1	321.1	69.0699	-0.1	41.2	69.0697	-0.3	1806.7					
Benzenemethanol, 4-methoxy-	7.028																											
Cinnamyl Alcohol	7.251	134.0726	0	369.1																								
Eugenol	7.405	164.0834	0.1	529.1																								
Methyleugenol	8.176	178.0989	0	21.6																								
Isoeugenol	8.626				164.0831	-0.1	25.0																					
Farnesol	10.118	136.1248	0.1	78.7	136.1206	-4.1	754.9		136.1229	-1.9	653.9	136.1241	-0.7	759.7														
alpha-amylcinnamic alcohol	10.405	130.0734	-4.2	23.1					130.0775	-0.2	22.9																	

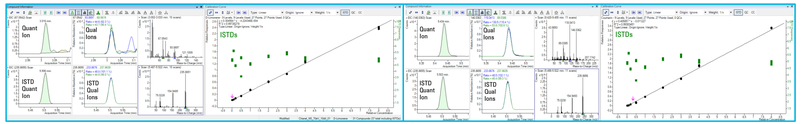

Figure 8: Calibration curve and qualifier ratios for D-Limonene (left) and Courmarin (right).

Unknowns Analysis with Accurate Mass and High Resolution

To identify additional components beyond the target list, MassHunter Unknowns Analysis was used to verify the target hits while separating other hits from the NIST14 library.

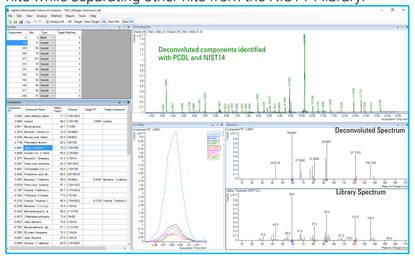

Figure 9: Unknowns Analysis for Known-Unknown identification

Conclusions

The Agilent 7250 GC/Q-TOF successfully analyzed allergens in fragrance products

- High mass accuracy, accurate isotope ratios provided high confidence of identification
- An accurate mass library was created for target quantitation and screening of allergens
- Low energy EI provided confidence in the identification of the molecular ion cluster and possible structural identification
- 31 allergen components were quantitated in 11 commercially available perfumes

References

[1]GC/MS Quantitation of Potential Fragrance Allergens in Fragrance Compounds. *International Fragrance Association*. V3, 2007

FOOD

Analysis of Sulfur Containing Compounds in Heavy Matrices using Low Energy Electron Ionization

Matthew Curtis; Jennifer Sanderson
Agilent Technologies, Santa Clara, CA

ASMS 2017
MP-274

Agilent
Trusted Answers

Introduction

Sales of craft beer has been on a steady increase, with a 6.2% increase last year. The number of breweries in the United States grew 16.2% from 2015 to 2016 and is expected to grow even more this year. The popularity of more flavorful and unique beer has created the need for the analysis of beer hops for optimal flavoring. There are about 80 commercial varieties of hops available to brewers, but similar to wine, the terroir can affect the chemical composition of the hop cone. Polyfunctional thiols are significant in defining the hop's character, but difficult to identify in hops due to their low concentration compared to terpenes and other aroma components. Two forms of hops (whole cone and pellets) of several varietals used by brewers were analyzed to identify possible differences between forms. This work discusses the utility of low energy ionization on the novel Agilent 7250 GC/Q-TOF as a possible solution to the fragmentation of the polyfunctional thiols as well as suppressing the hydrocarbon rich background.

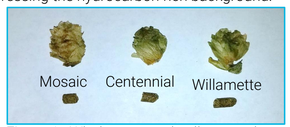

Figure 1: Whole cone and pellet samples

Figure 2: Agilent 7250 GC/Q-TOF

Experimental

Sample Preparation:

Neat standards for several different polyfunctional thiols, headspace grade water and absolute ethanol were purchased from Sigma Aldrich (St. Louis, MO). The hop whole cone and hop pellet samples (figure 1) were purchased from More Beer (Los Altos, CA). These included Centennial, Mosaic, Willamette, and Magnum hop varietals. For sampling, 3g of hops were placed in 300mL of a 5% ethanol solution (by volume) to create a "hop tea." The suspension was set in the refrigerator overnight, filtered, and 10mL was added to a 20mL amber headspace vial. 3g of NaCl was added along with 2-bromo-3-methylthiophene (ISTD).

SPME Sampling:

The samples were prepared for injection using the Gerstel MPS Autosampler, utilizing Maestro.

The vials were incubated for 2 mins at 40°C prior to a 50 mins extraction using the Supelco DVB/CAR/PDMS 23 ga fiber. The fiber was injected into the Agilent MMI with the Merlin MicroSeal, for 10 mins. The GC parameters can be found in table 1.

Each sample was prepped in triplicate and the sample injection sequence was randomized to minimize replicate sample variances.

Table 1: Agilent 7250 GC/Q-TOF; 7890B GC Parameters

GC and MS Conditions:		
Column	DB-35ms UI, 30 m, 0.25 mm ID, 0.25 µm film	
Injection	Gerstel MPS SPME (pink)	0.75mm straight liner
Split	5:1 split	
Inlet temperature	270 °C	
Oven temperature program	40 °C for 1 min 20 °C/min to 50 °C 5 °C/min to 220 °C 220 °C hold for 5 min	
Carrier gas	Helium at 1.4 mL/min constant flow	
Transfer line temperature	250 °C	
Source temperature	250°C	
Quadrupole temperature	150°C	
Spectral range	35 to 500 m/z	
Spectral acquisition rate	5 Hz, both centroid and profile	
Emission	0.8µA	
Ionization parameters used in the method		
12.5 eV low energy ionization (after optimization)		

Results and Discussion

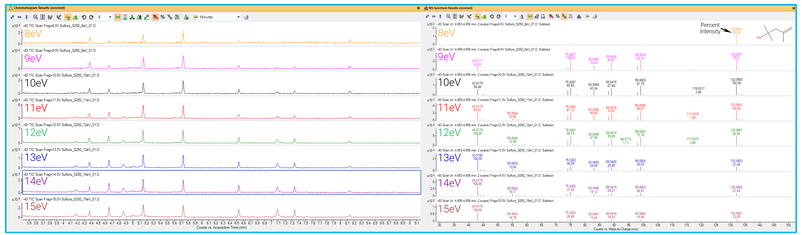

Figure 3: Sulfur standard eV survey to identify the optimal ionization energy.

Figure 4: Comparison of 70eV and 12.5eV for a co-eluting component.

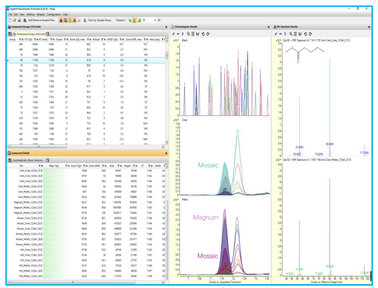

Figure 5: Component detection of analytes by grouping samples.

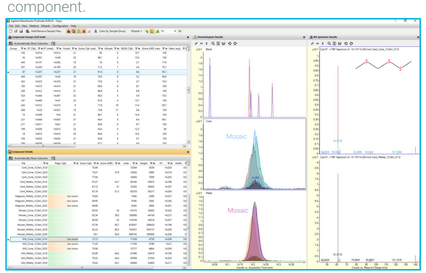

Figure 6: Component detection of analytes by grouping samples illustrating differences in varietals.

Discussion of figures.

Multiple injections were performed to vary the ionization energy and select an energy where the spectrum was tilted towards the high *m/z* range without a significant loss in sensitivity (Figure 3). After optimization, it was observed that one of the analytes was not detected due to the high degree of fragmentation and low concentration. The low energy eV analysis provided a molecular ion and isotope for confirmation (Figure 4). Figure 5 and 6 were produced from Agilent's Profinder B.08 using Molecular Feature Extraction to detect components within a chromatogram. The samples were grouped based on the type of hop form (cone vs pellet). Each varietal is overlaid with the group to illustrate the difference in intensity and a quick identification of significant components.

Results and Discussion

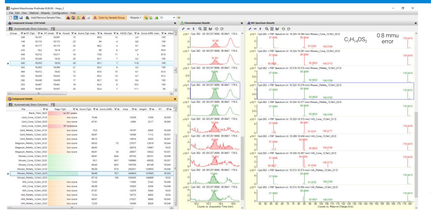

Figure 7: Molecular ion information for two isomers of $C_7H_{14}OS_2$ only observed in low energy ionization.

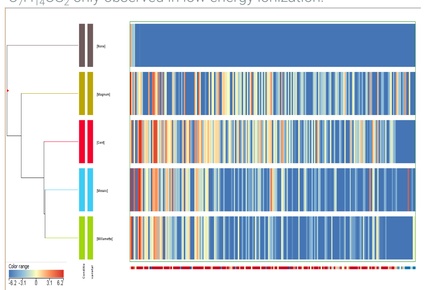

Figure 9: Clustering heat map illustrating the entities with an increased intensity when compared to the pellet.

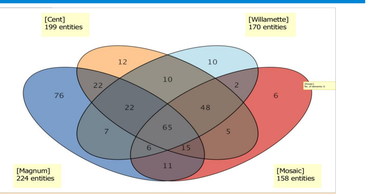

Figure 8: Venn diagram using entities with a >2 fold change.

Discussion of figures.

Figure 7 demonstrates the identification of two isomers of a di-sulfur component with molecular ion information retained. The following images were created in Agilent's Mass Profiler Professional after the analysis of all samples with Profinder. All of the samples were normalized to the ISTD (Bromo-thiophene) prior to statistical significance analysis. The Venn diagram (Figure 8) was produced using a >2 fold change requirement to show the diversity of the different varietals, 65 entities were found in all four samples. The last image was produced by averaging the three replicates for each sample and comparing the differences in intensity of entities with respect to the whole cone and the pellet forms (Figure 9). The more "red" a bar in the heat map a higher intensity was observed in the whole cone for each varietal.

Future Work.

Continue to optimize the extraction with SPME fiber selection and extraction parameters. Purchase additional standards to create a low eV RT-Locked high resolution spectral library to increase the confidence of identification.

Conclusions

Low energy ionization provided an additional level of information for these samples.

- Simplified chromatogram minimizing signals from hydrocarbon matrix
- Identification of co-eluting components not observed in the 70eV analysis
- High mass accuracy and precision provided confidence for statically significance interpretations
- The pellet formation process does change the volatile component composition.

References

[1]Lermusieau, G., and S. Collin. 2003. Volatile Sulfur Compounds in Hops and Residual Concentrations in Beer – A Review. J Am Soc Brew Chem 61:109-113.

[2] Occurrence of Odorant Polyfunctional Thiols in Beers Hopped with Different Cultivars. First Evidence of an S-Cysteine Conjugate in Hop (Humulus lupulus L.) Jacques Gros, Florence Peeters, and Sonia Collin Journal of Agricultural and Food Chemistry 2012 60 (32), 7805-7816

[3]Determination of Volatile Compounds in Different Hop Varieties by Headspace-Trap GC/MS—In Comparison with Conventional Hop Essential Oil Analysis Anita Aberl and Mehmet Coelhan Journal of Agricultural and Food Chemistry 2012 60 (11), 2785-2792

Quantitative B vitamin analysis via Liquid chromatography-mass spectrometry with a multimode ionization source

Sue D'Antonio[1]; Rita Steed[2]; Tina Chambers[2]; Joan Stevens[2]
[1]Agilent Technologies Inc., Santa Clara, CA; [2]Agilent Technologies, Inc., Wilmington, DE

ASMS 2017
WP - 189

Agilent
Trusted Answers

Introduction

Due to increasing concern about our food supply, more food and beverage companies are looking for lower detection limits and more confidence in their results. For these reasons, mass spectrometry has become an increasing popular approach, as detection limits are lower than traditional LC detectors. With the advent of reliable, sensitive and low cost single quadrupole mass selective detectors (MSD), quality control labs are adding liquid chromatography-mass spectrometry (LC/MS). The simplicity of the single quadrupole mass detector positions it well for the quality control environment in the food lab. QuEChERs extraction with EMR-Lipid cleanup for sample cleanup is used to simplify the matrix. In this work, quantitation and confirmation of B vitamins is demonstrated using unit mass technology. In this series of experiments we quanititate five B vitamins in vitamin drink, using the Multimode Source. The Multimode Source performs simultaneous ESI and APCI. This source enables both quantitation for target compounds and simultaneously screening for impurities, in a single analytical run.

Experimental

Initial concentration was 1.0 mg/ml. The samples where diluted using the injector programing capabilities of the Agilent autosampler

Cerilliant certified reference standards were used for calibration

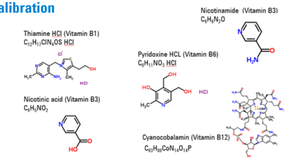

QuEChERS Enhanced Matrix Removal (EMR) technology was used for sample preparation. . Sample preparation was performed with a customized version of the EMR protocol as follows. Experiments were run on the Agilent LC/MSD XT. Samples were run in both SIM and scan mode with the Multimode Source using APCI and ESI ionization. Calibration curves were produced and samples were quantitated against these curves with N=6 replicates. Results were automatically reported and confirmed with both quantifier

Experimental

Several key vitamins were quantified using Agilent LC/MS system including the Agilent LC/MSD XT single quadrupole with the 1260 Infinity LC. The LC/MSD XT with the extended mass range to 3000 m/z made it a good choice for this application. Following the individual analysis of vitamin standards, analysis of several vitamin supplemented drinks were performed to identify the presence or absence of these vitamins as well as their level.

We chose the multi-mode source for these experiments

LC MS CONDITIONS

Mode	Positive ESI
Nebulizer	30 psi
Drying Gas Flow	5 L/min
Drying Gas Temperature	350 degrees C
V Cap	1850 V

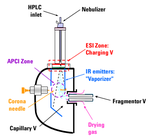

LC Conditions

Column	Agilent Poroshell SB Aq< 3.0 mm x 100 mm part number
Column Temperature	35 degrees C
Mobile Phase A	20 mM Ammonium formate and 0.1% formic acid in H20
Mobile Phase B	Methanol
Flow rate	0.5 ml/min
Injection volume	10 ul with a 20 second needle wash of 75 % MeOH & 25 % H20

Gradient	%A	%B
Time 00	90	10
Time 8.0	10	90
Stop Time10.0	10	90
Post time 2.0	90	10

Results and Discussion

Figure 1 is a breakout showing the extracted ions for the 5 vitamins studied. In addition, we show the spectra on the right side of the figure. The spectra is important because in addition to retention time mass, it also gives us isotopic spacing and pattern for compound confirmation

Results and Discussion

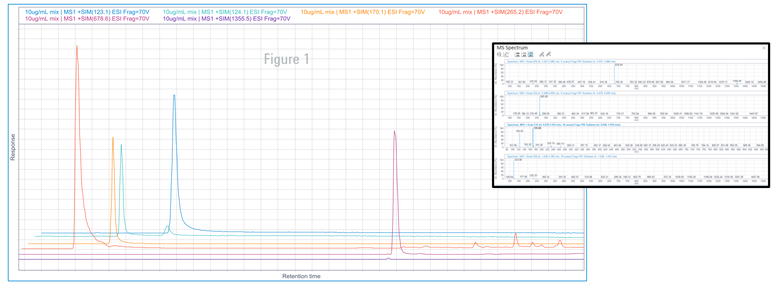

We looked at the individual vitamins and the results for Vitamin B12 are shown in figures 2 and 3 .Cyanocobalamin (Vitamin B12) is important to the body and a key result from its deficiency is anemia. Early symptoms of deficiency may include weakness, tiredness, shortness of breath, as well as many others.

B12 is a large molecule and is capable of picking up multiple charges (figure 2A). At different charges the isotope spacing will be different, e.g. with the second charge it will be ½. Instead of one Dalton for singly charged, doubly charged will be 0.5, triply 0.33, etc.

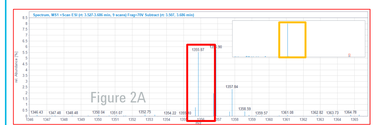

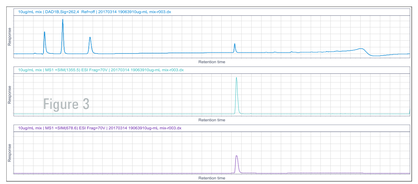

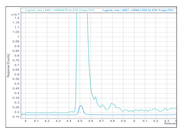

From the total ion chromatogram in figure we did extracted ion chromatograms, reran everything and ran a SIM (single ion monitoring) on 678 which is typically used for B12 We wanted a qualifier ion like you get with a QQQ (triple quadrapole) so we were able to SIM on the second ion. When we overlay the SIMS we have the same retention time and the mass is what we expect which confirms we have B12.

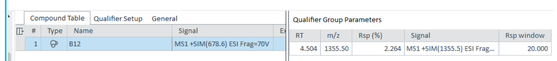

Results and Discussion

RSD of Levels and LOQ of Standards

	Vitamin	M/z	RSD of Replicates	LOQ	Correlation
B 12	Cyanocobalamin	678.6	0.9	5 ppb	0.998
B 6	Pyridoxine	170.1	1.2	10 ppb	0.999
B3	Nicotinic acid	124.1	1.0	10 ppb	0.999
B3	Nicotinamide	123.1	0.8	10 ppb	0.999
B 1	Thiamine	265.2	1.6	10 ppb	0.999

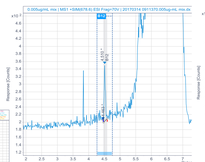

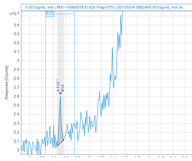

Drink ID	B1 Thiamine 265	B6 (170) Pyridoxine	B3 Nicotinic Acid (124)	B3 Nicotinamide (123)	B12 Cyanocobalamin (768)
a	12	44	103	13	71
b	nd	24	32	nd	30
c	nd	88	123	nd	20
d	nd	20	28	nd	20
e	136	18	366	38	71
f	10	263	106	48	48
g	9	249	99	nd	45
h	33	12	412	nd	nd
i	1	nd	228	nd.	84
j	12	27	51	nd	160
k	40	nd	168	8	nd
l	9	26	97	nd	46
m	12	42	136	17	31
n	96	nd	nd	nd	nd
o	nd	11	184	nd	25
				results in ug/ml	

Representative chromatographic results of the sports drinks we analyzed are shown in Figure 5

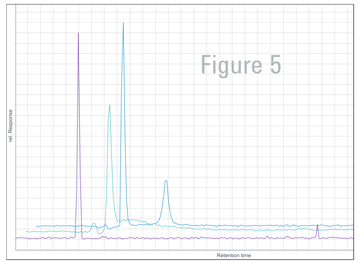

Conclusions

The MSD has shown to be a robust and reliable system for the analysis of B vitamins. We are able to calibrate linearly over more than four orders of magnitude with excellent correlation coefficients. The use of EMR has allowed us to test for vitamin B in dairy type matrices. The addition of the qualifying ion adds an extra order of certainty to our compound identification. The MSD can be used easily in a quality assurance lab for accurate measurements.

References

Sheher Moshin, Michael Zumwaldt, & Indarpal Singh, "Quantitative Analysis of Water-Soluble B-Vitamins in Cereal Using Rapid Resolution LC/MS/MS", Agilent Technologies Publication 5898-7084EN

Chemometric Methods for Analysis of Graftage-related Black Tea Aroma Variation by Solid Phase Mirco-extraction and Gas Chromatography-Mass Spectrometry

Wei Chen[1]; Wenwen Wang[2]; Chengying Ma[1]; Junxi Cao[1]; Aiqing Miao[1]; Shi Pang[1]

[1] Tea Research Institute, Guangdong Academy of Agricultural Sciences, Guangdong, China

[2] Agilent Technologies Company. Ltd., Beijing, China

ASMS 2017
TP - 270

Introduction

As one of the key indicators of sensory quality, tea (Camellia sinensis) aroma is the representation of volatile components. Possible changes of the volatile components may occur after graftage due to potential secondary metabolite variation in the scion resulting from rootstock replacement. Gas chromatography-mass spectrometry (GC-MS) coupled with chemometrics is an efficient technique to investigate and reveal variations in the complex mixtures of volatile and semi-volatile compounds among tea samples. In this study, solid phase mirco-extraction (SPME) combined with GC-MS and chemometrics was applied to extract and analyze the volatile components of black tea samples prepared from non-grafted and grafted "YingHong No.9", a popular tea variety in Guangdong province, China, to show the aroma profile difference induced by graftage.

Method

The graftage-related black tea samples were analyzed by solid-phase micro-extraction and a triple quadrupole GC/MS/MS operated in MS scan mode. Masshunter Profinder software was applied to extract the compound information and export data in compound exchanged files (.cef). Mass Profiler Professional (MPP), a software for bioinformatics data mining and chemometric analysis, was used for sample alignment and data filtering to obtain a data matrix of characteristic volatile compounds with good reproducibility. The resulting compounds were subjected to univariate analysis, principle component analysis and hierarchical clustering analysis to reveal the differences among samples.

Experimental

Tea Sample

Five groups of cut-tear-curl black tea samples including six biological replicates were prepared from the non-grafted YingHong No.9 (CK) and the grafted YingHong No.9 on rootstocks of four different tea varieties including BaiMao No.2 (BM), HeiYe ShuiXian (HY), HuangZhiXiang DanCong (HZX) as well as WuLingHong (WLH).

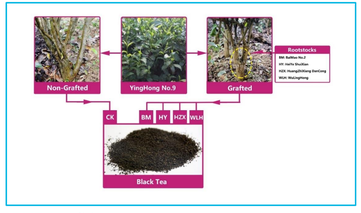

SPME Conditions

3.5 g black tea sample was weighed in a glass vial and 10 mL boiling water was infused, followed by 10.0 μL ethyl decanoate (0.2 μg/μL in ethyl ether) as an internal standard. The vial was sealed and transferred into the 60 ℃ water bath and kept for 5 min. The extraction was carried out at 60 ℃ for 40 min with a DVB/CAR/PDMS-50/30μm SPME fiber. The SPME fiber was desorbed for 4.5 min at 270 ℃.

Instrument Conditions

GC and MS Conditions	Value
GC system	Agilent 7890A
Column	DB-5MS (60 m×0.32 mm×0.25 μm)
Oven program	50 °C hold 3 min , at 5 °C /min to 250 °C hold 5 min
Carrier gas	Helium
Flow rate	1.0 mL/min
Injection mode	Manual, SPME Fiber
Injection port temperature	270 °C
Interface temperature	280 °C
MS system	Agilent 7000D
Ion source	EI, 70 eV
Ion source temperature	230°C
Quadrupole temperature	150 °C
Spectral Acquisition	Full scan, 35-500 m/z

Results and Discussion

Data Extraction

The total ion chromatograms of different graftage-related black tea samples are shown in Fig.1. Masshunter Profinder software is a productivity tool for processing multiple samples in profiling analyses, allowing the user to visualize, review, and edit results by compound across many samples. Higher quality results can be obtained based on cross-sample processing. Chromatographic peak extraction was done using the Profinder software (version B. 08) by molecular feature extraction features (MFE) (Fig. 2). Cef files of each sample were obtained by Profinder software and imported to MPP software for analysis.

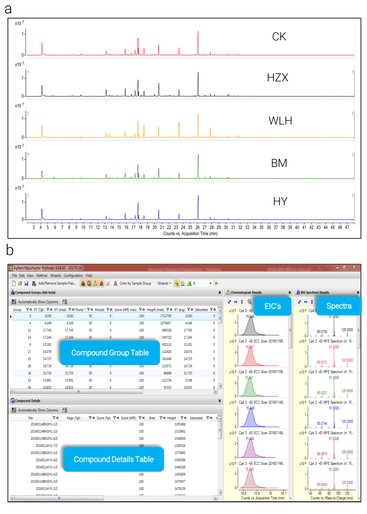

Fig.1 (a) The total ion chromatograms of five groups of black tea samples;

(b) The main view of the MassHunter Profinder software.

Mass Profiler Professional (MPP)

Data filtering and chemometric analyses were carried out via MPP software (version B. 14.5, Agilent Technologies). All the collected cef files were subjected to data filtering. The identified compounds underwent the chemometric analyses of principal component analysis and hierarchical clustering analysis for sample classification.

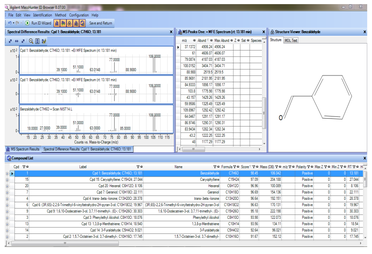

Fig.2 ID Browser function in MPP for compound identification

Data Filtering

A total of 584 entities were obtained through data alignment across five sample groups. Step-wise data filtering was carried out based on filters of frequency of occurrence, sample variability and one-way analysis of variance (one-way ANOVA). 102 entities, which consistently existed within at least one sample group ("frequency of occurrence" filter) and demonstrated good reproducibility (coefficient of variation < 25%, "sample variability" filter) were obtained. Then, 44 entities were selected through one-way ANOVA with a p-value cutoff of 0.05 and a fold change threshold of 1.5 (FC >= 1.5) in reference to the CK (non-grafted group). Finally, 34 compounds were identified by ID Browser according to the library searching based on NIST14 standard database (Fig.2). The 34 identified tea volatile compounds mainly consisted of alcohols, ketones, organic acids, esters and etc.

Results and Discussion

Principle Component Analysis (PCA)

PCA is a commonly used unsupervised statistical method to reduce the dimensionality of large data sets to reveal the differences among samples. The 34 identified compounds were subjected to PCA. The first 3 principle components explained approximately 90% of the variance in the original data. The 3-D score plot presented clear separation among CK and the four grafted sample groups indicating that the selected compounds were characteristic for non-grafted and grafted sample discrimination (Fig. 3). 47.6% of the variance was explained in PC1; separation of HZX, BM and the rest of the groups was achieved along this coordinate. PC2 explained 25.4% of the variance; samples of CK, HY and WLH were separated from each other along this coordinate.

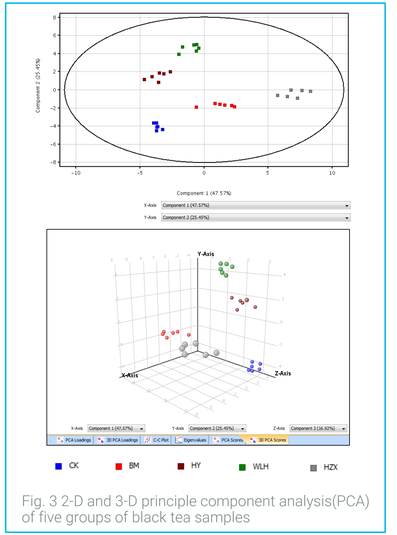

Fig. 3 2-D and 3-D principle component analysis(PCA) of five groups of black tea samples

Hierarchical Clustering Analysis (HCA)

HCA is a powerful method to uncover subgroups within a dataset. The method allows observations with similar abundance profiles to merge into clusters. The HCA was conducted with the 34 identified compounds. The result is displayed as a dendrogram (Fig. 4). Tea samples were classified into five clusters in accordance with their graftage treatment. Samples from grafted groups of BM shared high similarity of compound abundance with those from CK., while the abundance profile of HZX was distinctive toward both CK and the rest of grafted groups.

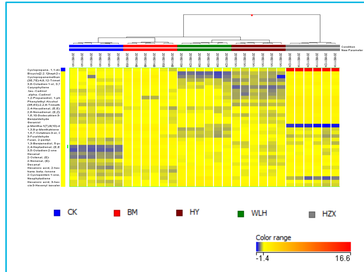

Fig. 4 Hierarchical clustering analysis (HCA) heat map for association of compounds detected in various black tea samples.

Conclusions

- A SPME and GC-MS method for profiling of black tea samples prepared from non-grafted and grafted "YingHong No.9" has been developed;
- 34 volatile compounds with significant variation among non-grafted and grafted sample groups were identified;
- Clear separation was achieved among the 5 groups with PCA and HCA based on the 34 identified compounds via MPP;
- The finding is potentially beneficial for guidance of rootstock selection in tea propagation.

Determination of Pesticide Residues for Quality Control of Tobacco Products by LC/TQ

[1]Prasanth Joseph, [2]Samir Vyas

[1]Agilent Technologies India Pvt. Ltd, Bangalore, Karnataka, India

[2]Agilent Technologies India Pvt. Ltd, Manesar, Haryana, India

ASMS 2017
TP-172

Agilent
Trusted Answers

Introduction

Pesticides applied during cultivation can remain in the tobacco leaves at harvest and extend to post-harvest processing treatments, finally appearing in the finished products. Global concern by the public and in industry about pesticide residues being taken into the body through the consumption of various tobacco products has risen dramatically.

Multi-pesticide residue analysis in tobacco is a challenge in both sample preparation and instrumental detection. Multiple Reaction Monitoring (MRM) based LC/TQ methods have been employed increasingly in detection and quantification of multiple pesticide residues in agriculture products. SANTE regulations specify that a minimum of two product ions are required for the identification of pesticides. Moreover, ion ratio's should be within 30% of the average of calibration standards from the same sequence.

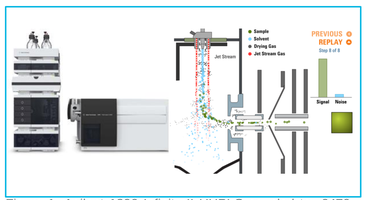

Figure 1: Agilent 1290 Infinity II UHPLC coupled to 6470 LC/TQ installed with Agilent Jet Stream ion source

Because of the sensitivity of 6470 LC/TQ system, sample extracts can be diluted to reduce matrix effects; which is an attractive feature for many routine testing labs as the requirement for clean-up can be avoided. QuEChERS is used for extraction of pesticides from tobacco products. An aliquot of the extract was diluted 10-fold followed by filtration and the sample was ready for LC/TQ analysis. By diluting the extracted sample, the amount of matrix injected into the LC/TQ system is limited, resulting in less matrix interference, increased robustness of the analytical method and minimization of instrument contamination.

Experimental

Sample preparation:

- **Sample weighing:** Approx. 1.0 g of tobacco was accurately weighed in a 50 mL polypropylene tube. 10 mL of water was added to the tobacco sample and kept for 30 min.
- **Extraction ACN:** 10 mL of Acetonitrile was added as extraction solvent. The mixture was thoroughly shaken for 1 min and stored for 10 minutes at -18 °C.
- **Extraction QuEChERS:** Agilent Bond Elut QuEChERS Extraction Kit *(P/N: 5982-5650)* was then added to the above mixture.
- **Centrifuge:** The tube was closed tightly and shaken for 1 minute. Samples were centrifuged for 5 min at 5000 rpm.
- **Filtration:** 1 mL of the clear supernatant was diluted 10x using the diluent. Diluted extract was then filtered through a 0.45 µm PTFE syringe filter.

Instrumentation: This study was performed on an Agilent 1290 infinity II coupled to an Agilent 6470 LC/TQ with Agilent Jet Stream ion source operated in positive ionization mode. Gradient elution was employed on Agilent Rapid Resolution High Definition (RRHD) Eclipse plus C18 (2.1 mm X 100 mm, 1.8 um) stationary phase for separation of targeted analytes. The mobile phase consisted of A: 5 mM ammonium formate and 0.01% formic acid in water and B: 5 mM ammonium formate and 0.01% formic acid in Water: Acetonitrile (5:95). Injection volume used was 2 µL.

MRM transitions were imported from a tMRM database and a LCMS acquisition of 100 ng/mL standard was performed. Dynamic MRM (dMRM) creates more powerful quantitative methods by grouping MRMs in retention time windows instead of time segments. On the basis of the generated MRM chromatogram, the method was converted to a dMRM method.

Agilent MassHunter acquisition software version B.08.00 was used for acquisition, MassHunter Qual version B.07.00 was used for data processing and MassHunter Quant software version B.07.01 was used for quantification of the pesticides in real and recovery samples.

Results and Discussion

Limit of Quantitation (LOQ): LOQ of the standards was calculated using the formula LOQ = (t* RSD* concentration)/100 (t for 99% confidence level, n-1 degree of freedom) by considering % RSD of 9 replicate injections of 0.05 ng/mL. For all the tested compounds, calculated LOQs were ≈ 0.03 ng/mL. Noise was calculated using the auto RMS algorithm available in the MassHunter qualitative software. All samples were effectively diluted 100-fold (1 g sample in 10 mL acetonitrile followed by 10X dilution) and the Method Detection Limit (MDL) was determined to be 10 ng/g. However, for most of the pesticides, lower LOQs and MDLs may be achieved when considering the minimum signal to noise ratio of 10:1 required to calculate the LOQ.

Linearity range: Three orders of linear dynamic range, from 0.05 ng/mL to 100 ng/mL was established with 8 concentration levels in both solvent and matrix matched standards. Concentration levels required for matrix matched calibration curves were prepared by post-spiking the diluted extracted matrix. For example, a matrix-matched concentration level of 0.05 ng/mL was prepared by diluting 100 µl of 5 ng/mL to 900 µl of the extracted tobacco matrix, followed by a 10X dilution. Six replicate injections at each level were used to plot the calibration curve. The linearity of all pesticides in study had regression coefficient of: (r^2) > 0.9950

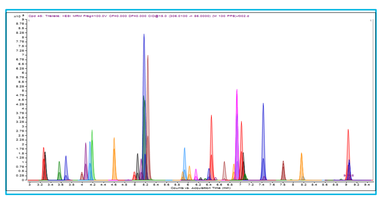

Figure 2: Representative chromatogram of pesticides involved in this study

Recovery: Recovery studies were conducted at three different fortification levels; 10 ng/g, 100 ng/g and at 200 ng/g. Blank tobacco samples were pre-spiked with pesticide working solutions in order to prepare the recovery samples.

The pre-spiked samples were then extracted with 10 mL of acetonitrile followed by QuEChERS extraction kit, then diluted ten times. Recovery samples prepared in this way were then compared against the matrix-matched calibration graphs. Matrix matched calibration curves from 0.05-100 ng/mL were prepared by post-spiking pesticide standards in the diluted matrix. As per SANTE 11945/ 2015, residue data adjustment is not required when the mean recovery ranges between 70-120%. All 40 pesticides in this study had recovery percentages between 75-120% and therefore, recovery correction was not required.

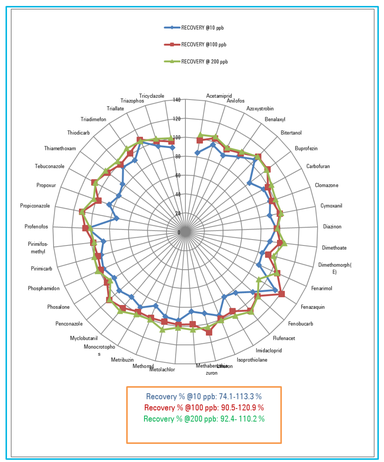

Figure 3: Radar plot of recovery of various pesticides

Sample analysis: Five commercially available branded tobacco samples were collected from various locations of southern India and analysed in triplicates. Out of the forty pesticides, most of them were below LOQ level in all the tobacco samples. Carbendazim was found at ppm levels in two of the samples. Azoxystrobin was detected at 0.9 ppm in sample #5. Imidacloprid, Pendimethalin, Triadimefon and Tebuconazole were detected above 200 ng/g in many samples.

Results and Discussion

Pesticides detected above 10 ng/g	Conc. in Sample 1 (ppb)	Conc. in Sample 2 (ppb)	Conc. in Sample 3 (ppb)	Conc. in Sample 4 (ppb)	Conc. in Sample 5 (ppb)
Carbendazim		1098	4681		385.0
Imidacloprid		270.7	348.0		121.7
Pendimethalin	130.9	205.7	252.0		
Triadimefon	201.1			39.22	
Tebuconazole		329.5	129.5		199.2
Azoxystrobin	63.20	306.6	315.4		903.6
Methomyl	19.11				
Tricyclazole			11.33		
Propoxur					22.42
Acetamiprid		89.72	28.11		39.31
Thiamethoxam					28.54
Dimethomorph	52.34			32.71	

Table 1: pesticides detected in five tobacco samples

Ion ratio's of the MRM transitions helps in identification and elimination of false positives. A major challenge for this study was to obtain blank tobacco matrix. Several samples were tested and the sample that is free from pesticides was chosen for spike recovery study. Also, analytes detected in blank matrix were excluded from this study. Blanks Tobacco samples were pre-spiked with pesticide working solutions. Prepared recovery samples are then analysed against the matrix-matched calibration graphs. Matrix matched calibration curves were prepared by post spiking pesticide standards in the diluted matrix.

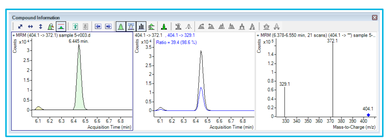

Figure 4: Chromatogram and ion ratio for Azoxystrobin detected in sample 5

Matrix Suppression/Enhancement study: Post column infusion study was conducted in order to evaluate the suppression/ enhancement in the signal of pesticides in presence of matrix interferences. A matrix suppression region was observed at around 0.5 minutes. The result of this study proved that there is no matrix suppression of signal for all 40 analytes at the retention time (3 - 9.5 minutes) in the developed method.

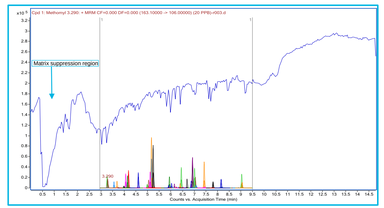

Figure 5: Post column infusion study for the identification of matrix suppression /Enhancement

Conclusions

The developed method allows the user to screen and quantify 40 pesticides in tobacco samples employing an Agilent 6470 LC/TQ system. Our method involves a simple sample preparation, resulting in less contamination of the instrument. Post column infusion study revealed that all analytes in this study are free from matrix suppression in their ionization. This method can be easily implemented for routine quality control of tobacco samples.

References

[1] Fei Yang et. al 'Analysis of 118 Pesticides in Tobacco after Extraction With the Modified QuEChERS Method by LC–MS-MS' Journal of Chromatographic Science 2013;1–5 doi:10.1093/chromsci/bmt112

[2] Agilent application note "Analysis of multi-pesticide residues in tobacco" http://www.agilent.com/cs/library/applications/5991-5763EN.pdf

.

Development of Compounds Identification by Using Various Chromatography and Multiple Mass Spectrometry in Food Adulteration

Chun-Ye Sun[1],Shao-Zhen Wang[1],Heng-Tao Dong[1],Shu-Chin Yang[2]

[1]Agilent Technology, Inc. Shanghai, China

[2]Department of Health, New Taipei City Government, New Taipei, Taiwan

ASMS 2017

TP - 215

Introduction

Although more and more evidence in recent years indicates that the abuse of food adulteration may harm health and cause disease[1], various kinds of food adulteration are still widely used because of their low price, easy availability and high effectiveness.

Food adulteration is a common in the Chinese market at present, especially for dietary supplements, weight-loss products, and erectile dysfunction supplements. However, China has not yet released relevant official testing standards and methods, therefore developing effective test methods of the food fraud product is necessary and urgent.

In this study, combining powerful database (NIST Library and Agilent PCDL), a feasible workflow based on various chromatography, spectrum and multiple mass spectrometry techniques (TLC, UV, GC/MS, LC/QQQ and LC/QTOF) was introduced for the food adulteration. The solution can help to realize reliable confirmation and accurate quantitative analysis for the sample of the food adulteration.

Experimental

Instruments and Conditions:

Camag automatic TLC sampler system

Separation mobile phase:

1. Butanol/H2O/Acetic acid=7/2/1 (v/v/v)
2. Ethyl acetate/Ethyl ether=4/1 (v/v)
3. Chloroform/Ethanol=9/1 (v/v)
4. Ethyl acetate/Methanol/NH4OH=8/1/1 (v/v/v)

Agilent 7890/5977 GC/MS system

Column: Agilent DB-5ms 30 m × 0.25 mm, 0.25 µm

Carrier gas: He, Flow:1.65 mL/min, Split ratio 99:1

Oven program: Gradient program 60 mins (not shown)

MSD transfer line: 280°C

Source temperature: 230°C

Quadrupole temperature: 150°C

Ionization mode: EI, 70 eV

Acquisition mode: SIM & Scan (m/z 35-550).

Experimental

Agilent 1290 Infinity II UHPLC system

The mobile phases are 0.1% formic acid in water and Acetonitrile, column temperature is 35 °C, injection volume is 2µL, gradient run time is 30 min (not shown) with the flow rate of 0.5 mL/min.

Agilent 6460 LC/TQ & 6545 QTOF System

MS Conditions	6460 QQQ	6545 QTOF
Ion source	AJS ESI	AJS ESI,Dual spray
Gas Temp(°C)	325	325
Drying Gas(L/min)	9	9
Nebulizer Gas(psi)	40	40
Sheath Gas Temp(°C)	350	350
Sheath Flow(L/min)	11	11
Capillary Voltage(V)	3500(+)/3500(-)	4000(+)/4000(-)
Nozzle Voltage(V)	500(+)/1500(-)	250(+)/1500(-)
Acquisition mode	Triggered MRM (tMRM)	All Ion MS/MS (AIM)
Scan range(m/z)	N/A	50-1500

Table 1. 6460 & 6545 acquisition conditions.

Results and Discussion

Sample preparation and TLC & UV-VIS scan

Weigh 3.00g powder sample, then sonicate for 30 min with ethanol as extraction solvent and centrifuge for 5 min at 3500rpm. After filtration of the supernatant with 0.2µm membrane, process TLC separation and scrape off suspicious spot for UV-VIS analysis.

Results of target screening

Target screening is applied to GC/MS and LC/TQ. GC/MS uses target deconvolution (TD) and LC/TQ uses triggered MRM (tMRM).

TD uses deconvoluted full mass spectra and reference retention time lock (RTL) library spectra matching to have high confidence in target identification beyond retention time and ion ratio measurement.

The tMRM acquisition combines primary and secondary MRMs to generate a product ion spectrum and confirm the analyte structure by comparing with reference library. The secondary MRMs are acquired when primary MRMs exceed predefined thresholds so that tMRM provides sufficient data points for quantitation with extra product ions for confirmation.

Results and Discussion

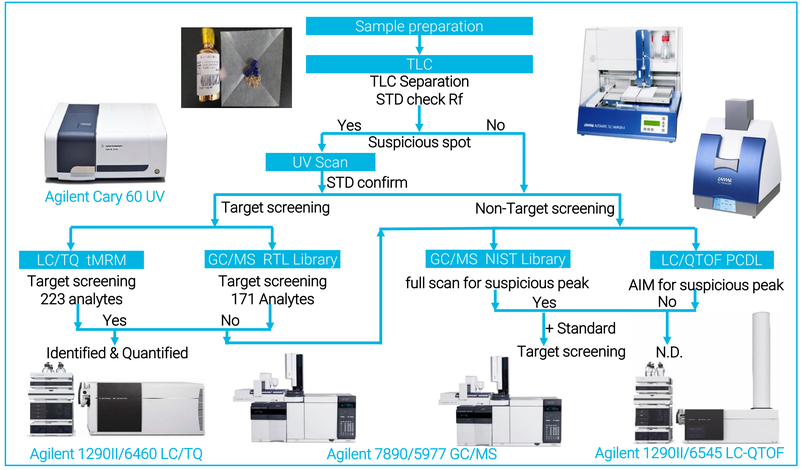

Figure 1. The workflow of analysis and confirmation for food adulteration sample.

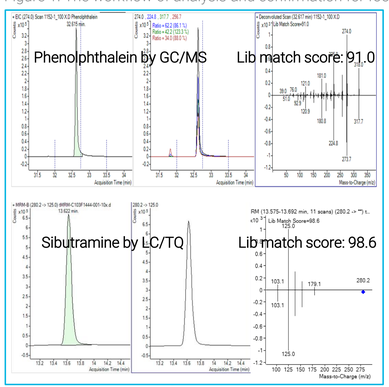

Figure 2. The screening of target by GC/MS and LC/TQ

Results of non-target screening and confirmation

We use an array of instruments for unknown compounds identification. Agilent LC/QTOF All Ions MS/MS (AIM) acquisition and PCDL search provide confident identification of analytes with molecular formula generation and structure confirmation by fragment ions. The self-created adulteration PCDL contains accurate masses and MS/MS spectra for thousands of compounds.

The AIM provides another features for unknown targets with "average fragment spectrum". This function can get possible fragment ions into check list with co-eluting calculation, even no library spectra are established in PCDL. The suspicious compound is determined as Moroxydine with confidence as shown in Figure 3.

For further unmistakable confirmation, the standard of suspicious compound is purchased and compared with the sample by GC/MS or LC-MS. For example, in Figure 4, the retention time and fragment ions of the suspicious compound are the same as the Moroxydine standard, thus confirming the suspicious compound being Moroxydine with 100% confidence.

Results and Discussion

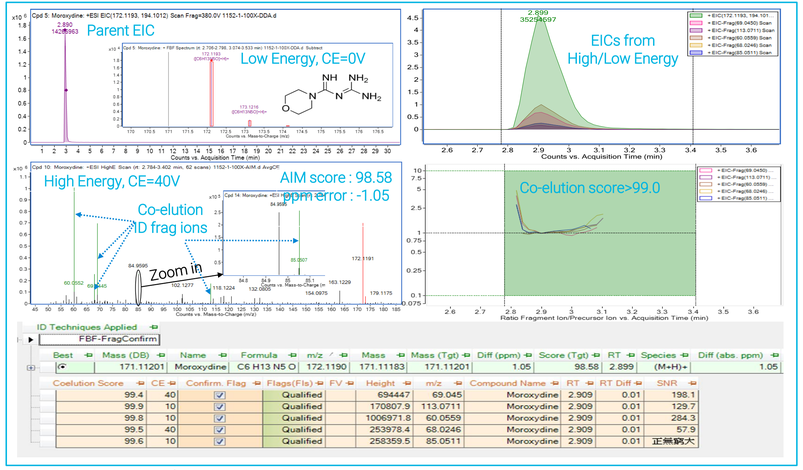

Figure 3. The screening of Non-target by LC/QTOF with AIM mode.

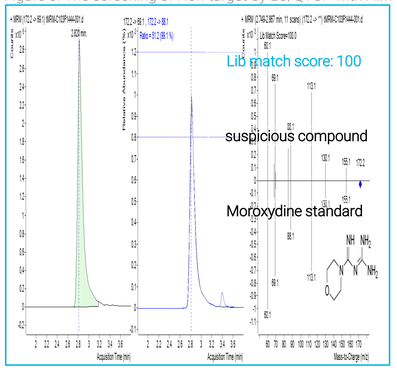

Figure 4. The confirmation of the suspicious compound by tMRM with standard.

Conclusions

This study demonstrates an important application in food adulteration. Our solution is to use various chromatography, spectrum and mass spectrometry techniques complementary to each other for compound identification with high confidence. The suspicious compounds can be ultimately confirmed with standard material.

References

1. Srivastava, Shakuntala. "Food adulteration affecting the nutrition and health of human beings." Journal of Biological Sciences and Medicine 1.1 (2016): 65-70.
2. Triggered MRM: Simultaneous Quantitation and Confirmation Using Agilent Triple Quadrupole LC/MS Systems-Agilent Technologies, Inc., 2013
3. All Ions MS/MS: Targeted Screening and Quantitation Using Agilent TOF and Q-TOF LC/MS Systems-Agilent Technologies, Inc., 2013

Study on triacylglycerides in edible vegetable oils by ultra-high performance liquid chromatography tandem quadrupole-time of flight mass spectrometry

Jianzhong Li; Yao Xiao;Xin Ma;Qilei Guo;Tao Bo

Agilent Technologies, No.3, Wang Jing Bei Lu, Chao Yang District, Beijing, 100102, China

ASMS 2017
TP - 466

Agilent
Trusted Answers

Introduction

Edible vegetable oils constitute an important class of food products, widely used throughout the world. For the food chemist, the determination of the triglyceride(TAG) composition in edible oils provides information that complements that of the fatty acid composition. Knowledge of the distribution of the fatty acids within the glyceride molecules is used for nutritional purposes.

In principle, either GC or HPLC can be used to determine the triglyceride profile of fats and oils. GC analysis using robust columns with high temperature limits can quickly provide the carbon numbers of the triglycerides. However, HPLC analysis provides better resolution between triglycerides of the same carbon number. GC methods have problems with the complexity of sample preprocessing, which requires saponification. Triglycerides are known to be difficult compounds to analyze by HPLC using traditional detectors as the applicability of UV detectors for triglyceride analysis is limited. If the purpose of the analysis is to gain a better knowledge of the fatty acid composition of each triglyceride, LC coupled with MS detection is recommended. In this study, UHPLC-HRMS with positive mode electrospray ionization(ESI+) were used to realize the analysis and identification of triglyceride in edible vegetable oils.

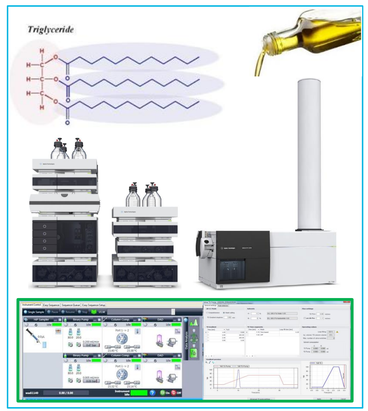

Experimental

Sample preparation

Edible vegetable oils were purchased at local supermarkets. 100mg (±0.1mg) of oil was transferred to a 10mL volumetric and dissolved with 10mL of isopropanol(IPA). The dilutions were vigorously shaken, and 1mL of extract was transferred into an autosampler vial for UHPLC/HRMS analysis.

Instrumentation

UHPLC-QTOF system consists of the Agilent 1290 Infinity II ,binary pump, autosampler, TCC, and 6545 LC/Q-TOF with Agilent Jet Stream. The UHPLC-Q-TOF experimental conditions are summarized in Table1. The chemical formulae were calculated based on accuracy mass and isotope ratio calculation by MassHunter Qualitative Analysis software.

Table 1 UHPLC-QTOF Conditions

Column	Poroshell 120 EC-C18, 2.1x100 mm , 2.7 µm	
Mobile phase	A=2mM acetonitrile containing 10% 10mM ammonium formate and 0.2% formic acid B=Isopropanol containing 2% water and 0.2% formic acid	
Flow rate	0.3mL/min	
Column temperature	40°C	
Injection volume	1µL	
Gradient Program	Time(min)	B(%)
	0.00	25
	3.00	25
	20.0	80
	23.0	80
	23.1	25
Post Time	3 min	
AJS Dual ESI source	-Ion mode: positive -Capillary voltage: 4000V -Nozzle voltage: 500V -Drying gas: 7L/min@300°C -Sheath gas: 11L/min@350°C -Nebulizer: 35psi -Fragmentor: 170V -MS scan:100-1500 m/z	

Results and Discussion

Intact triglycerides generally have very low water solubility and as such are commonly separated by normal phase chromatography, which separates species largely based on differences in polar functional groups. This chromatography approach has challenges when trying to apply it to routine analysis for triglycerides in edible vegetable oils. Reverse phase chromatography operating in a non-aqueous mode of separation, which has more selectivity for small differences on carbon character such as chain length or degree of saturation, and is easier to use for routine analysis. A typical gradient separation TIC of triglycerides from peanut oil using acetonitrile/IPA gradient is shown in Figure 1.

Most of the LC-MS methods used atmospheric pressure chemical ionization(APCI) as ionization mode for triglycerides. However, its stability is lower than that of ESI ionization mode, due to the problem of corona needle carbonization. By adding a small amount of water and ammonium formate in the mobile phase, formation of $[M+NH_4]^+$ ammonium adduct ions was promoted, which are more suitable for ESI analysis.

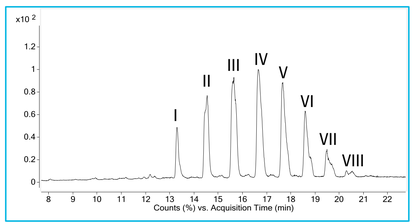

Figure 1.TIC of TAGs from peanut oil

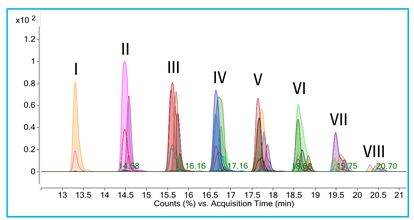

Figure 2. EIC of TAGs from peanut oil

Through the optimization of chromatographic separation and LC/MS source conditions for ionization, 28 kinds of triglyceride in peanut oil were identified. EICs of triglycerides from peanut oil is shown in Figure 2. The 8 groups (I-VIII) of triglyceride clusters are clearly separated from each other. Each group contains triglycerides similar to carbon chain length or unsaturation. The vast majority of triglycerides ionize the peak of $[M+NH_4]^+$, but also contain $[M+Na]^+$ mass spectrum peak. Typical spectral pattern (from group II) is shown in Figure 3.

Triglycerides in plants are made up predominantly of fatty acids with even numbers of carbons (C_{14},C_{16},C_{18}, etc.) and either 0,1, or 2 double bonds per acid. The main fatty acids include; **M**, myristic acid (14:0); **P**, palmitic acid (16:0); **S**, stearic acid (18:0); **O**, oleic acid (18:1); **L**, linoleic acid (18:2); **Ln**, linolenic acid (18:3); **E**, Eicosanoic acid

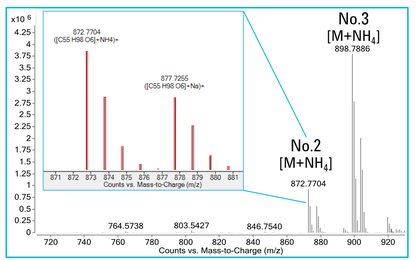

Figure 3. Mass spectrum of a mixed TAGs from group II

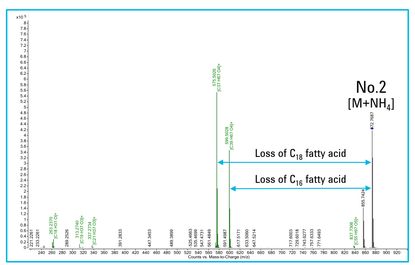

Figure 4. Fragment mass spectrum of typical TAG (LLP)

Results and Discussion

(20:0); **Ee**, Eicosenoic acid (20:1); **De**, Docosenoic acid (22:1); **Lg**, Lignoceric acid (24:0); **N**, Nervonic acid (24:1).

The information (types of fatty acids and their positions) is important for nutritional purposes, the identification and characterization of fatty acids of triglycerides can be satisfied by MS/MS mode with collision induced dissociation (CID).The No.2 triglyceride of group II of MS/MS confirmation can be obtained using CID, this is shown in Figure 4. The kinds of fatty acids can be identified by MS/MS fragmentation information of loss of fatty acid. The main ion fragments *m/z* 575.5026 and *m/z* 599.5028 respectively correspond to linoleic acid (2) and palmitic acid (1) , the fatty acid composition (LLP) of the No.2 peak from group II can be identified by MS and MS/MS information. The 8 groups of triglyceride and fatty acid composition of peanut oil were successfully identified by UHPLC-HRMS with ESI+ mode. Detailed information in Table 2.

Table 2. Composition of TAGs from peanut oil

Group	No.	Formula	Fatty acid composition	RT	$[M+NH_4]^+$
I	1	C57H98O6	LLL	13.4	896.7699
II	2	C55H98O6	LLP	14.5	872.7701
	3	C57H100O6	LLO	14.5	898.7856
III	4	C53H98O6	LPP	15.6	848.7696
	5	C55H100O6	LOP	15.6	874.7855
	6	C57H102O6	LLS	15.6	900.8009
	7	C59H104O6	LLEe	15.6	926.8166
IV	8	C53H100O6	POP	16.6	850.7856
	9	C55H102O6	POO	16.6	876.8009
	10	C57H104O6	PLEe	16.6	902.8166
	11	C59H106O6	OLEe	16.6	928.8327
	12	C61H108O6	LLDe	16.6	954.8486
V	13	C55H104O6	SOP	17.6	878.8169
	14	C57H106O6	POEe	17.6	904.8326
	15	C59H108O6	PLDe	17.6	930.8482
	16	C61H110O6	OLDe	17.6	956.8637
	17	C63H112O6	LLN	17.6	982.8794
VI	18	C57H108O6	POE	18.6	906.8477
	19	C59H110O6	PODe	18.6	932.8639
	20	C61H112O6	PON	18.6	958.8794
	21	C63H114O6	LEeDe	18.6	984.8952
VII	22	C61H114O6	PODe	19.5	960.8954
	23	C63H116O6	OON	19.5	986.9106
	24	C65H118O6	LEeN	19.5	1012.9263
VIII	25	C59H114O6	PPLg	20.3	936.8946
	26	C61H116O6	POLg	20.3	962.9106
	27	C63H118O6	OOLg	20.3	988.9263
	28	C65H120O6	OEeN	20.3	1014.9422

Because of the complex molecular species and isomers in fatty acids, the use of a single liquid phase system will be difficult for the separation of triglycerides in natural oils, as a result of interference caused by superposition, which led to the accuracy of fatty acid identification. For the separation of complex samples, it is very effective to use the two dimensional liquid chromatography (2D-LC).This separation mode have more selectivity for triglycerides on carbon character such as chain length or unsaturation, shown in Figure 5.

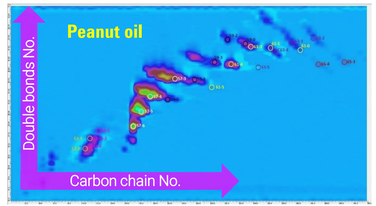

Figure 5. Chromatography of 2D-LC system

Conclusions

-A fast UHPLC-HRMS with positive mode electrospray ionization(ESI+) method with a minimum of sample preparation was used to detect the triglycerides of edible vegetable oils.

-Optimized reverse phase chromatography coupled to high resolution LC/MS/MS provided a highly effective method to characterize the fatty acid composition of nutritional glyceride in edible oil.

-A more detailed analysis of the triglycerides in edible vegetable oils by 2D-LC provided even greater separation of complex families of triglycerides is being pursued in further research.

References

[1] Hiroki Kumagai,Agilent Technologies publication 5988-4235EN.

[2] Michael Woodman,Agilent Technologies publication 5990-4292EN.

[3] Doug McIntyre, Agilent Technologies publication 5989-8441EN.

[4] Wm.Craig Byrdwell,Lipids,Vol.31,No.9(1996),919-934

Cannabinoid Profiling and Quantitation in Hemp Extracts using the Agilent 1290 Infinity II / 6230B LC/TOF system

Mike Adams[1], A. Roth[1], Karen Kaikaris[1], Joan Stevens[2], Anthony Macherone[2] & Sue D'Antonio[2]
[1]CWC Labs, Cedar Creek, TX
[2]Agilent Technologies, Inc. Wilmington, DE

ASMS 2017
WP-184

Introduction

Hemp, a fibrous variety of *Cannabis sativa* with a low psychoactive component concentration, is a commodity used in many commercial industries. Although all *C. sativa* species contain psychoactive Δ-9-tetrahydrocannabinol (THC), they also contain non-psychoactive cannabinoids including cannabidiol, (CBD) cannabinolic acid (CBNA), cannabinol (CBN), cannabigerol (CBG), cannabidiolic acid (CBDA) and many others. The United States Drug Enforcement Agency differentiates hemp from Schedule I THC-containing marijuana based on the intended or anticipated use of the product e.g., whether the product causes THC to enter the body. If using the product does not cause THC to enter the body, it can be legally sold and possessed in the United States.

Due to recent changes in legislation at the state level in the United States, analysis of hemp extracts has recently become an area of scientific interest. Some of these extracts include CBD, CDBA, CBN and CBG that occur in relatively high to moderate concentrations, and THC, which occurs in very low concentrations (<0.3% wt/wt) in hemp products. Traditional methods for profiling and quantification of cannabinoids in *C. sativa* products include Thin Layer Chromatography, GC-FID, GC-MS, and HPLC-UV. Unfortunately, none of these traditional methods offer the dynamic range necessary to analyze the major cannabinoid components of hemp in a single analytical run. Some methodologies also degrade CBDA, yielding results which do not accurately represent the composition of the sample. Furthermore, some of these methodologies require extensive sample preparation which can result in the loss of time and analyte[1].

The method presented here allows for the simultaneous profiling and quantification of high concentrations of CBD and related components as well as low THC levels within a single analysis using a liquid chromatography-time of flight mass spectrometer (LC-TOF) system. The method automatically creates standards using dilution functions of the Agilent autosampler and enables a total cycle of 20 minutes. Shorter run times (<10 min) may be achieved with more extensive sample preparation. he use of a custom Personal Compound Database and Library (PDCL) allows the analyst to verify compound identity by matching accurate mass spectra and retention times while avoiding the errors introduced by co-elution of analytes. Additional screening for toxic contaminants can be accomplished by comparison of the acquired data to the PCDL.

Experimental

HPLC Conditions

Agilent 1290 Infinity II UHPLC series Quaternary Pump, Multisampler with wash, Multi Column Thermostat, DAD

Column:	Zorbax Bonus RP 2.1 x 100 mm, 1.8 µm
Column temp.:	50°C
Injection volume:	0.05 µL
Autosampler temp:	23 °C
Needle wash:	3.5 s Flush Port (25:25:50) (H_2O:IPA:MeOH)
DAD-UV	254 nm
Mobile phase:	A = Water
	B= Methanol
	C= 0.1% CH_2O_2 + 2.2mL 5M NH_4HCO_2

Flow rate: 0.5 mL/min

Gradient:	Time (min)	%B	%C
	0.0	72	5
	12.5	95	5

Stop time:	15.0 min.
Post time:	5.0 min.
Overall run time	20.0 minutes (incl. re-equilibration)

Note the sample prep consists dilution of the CBD oil. This requires a longer time for the oil to elute from the column. Allowing a longer run time ensures reproducible retention times and lower carryover.

MS: Agilent 6230B Time-of-Flight Mass Spectrometer

MS Parameters

Ion Mode:	Dual ESI, Positive
Mass Range:	100-1700 m/z
Scan Rate (spectra/sec):	1.00

Source Parameters

Drying Gas Flow:	10 L/min
Drying Gas Temperature:	350 °C
Nebulizer Pressure:	40 PSI

Scan Source Parameters

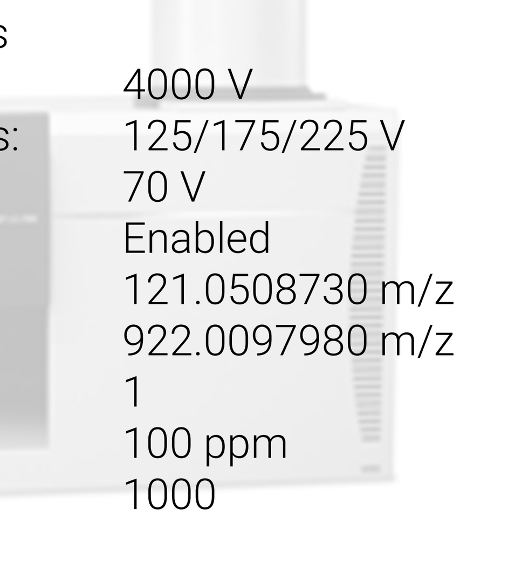

Capillary Voltage:	4000 V
Fragmentor Voltages:	125/175/225 V
Skimmer Voltage:	70 V
Reference Mass:	Enabled
Reference Masses:	121.0508730 m/z
	922.0097980 m/z
Average scan:	1
Detection window:	100 ppm
Min Height :	1000

Results and Discussion

Quantitation for THC and CBD

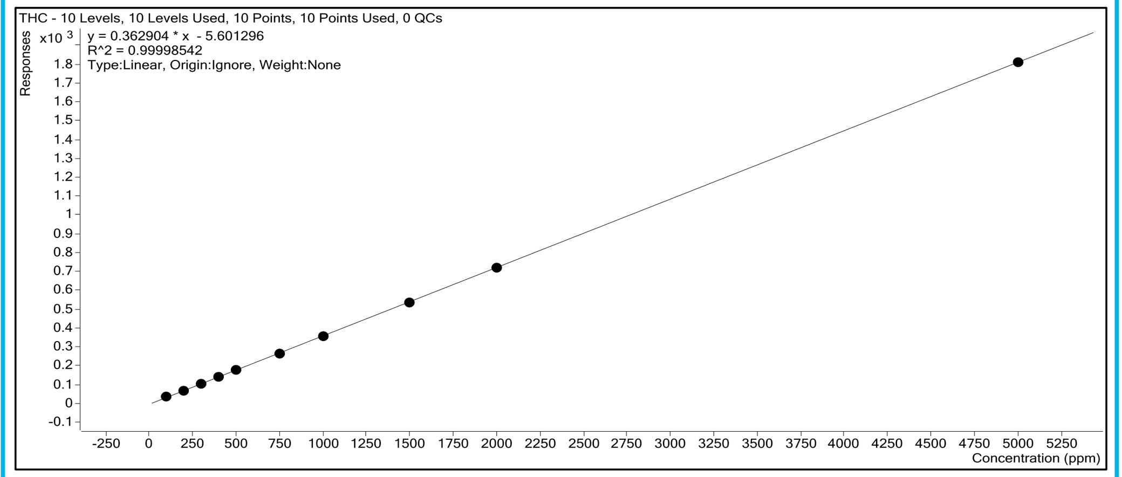

	Name	Data File	Type	Level	Exp. Conc.	RT	Resp.	Calc. Conc.	Final Conc.	Accuracy
	9 peak mix	level 1.d	Cal	1	100.0000	8.408	35	110.7183	110.7183	110.7
	9 peak mix	level 2.d	Cal	2	200.0000	8.422	68	203.0966	203.0966	101.5
	9 peak mix	level 3.d	Cal	3	300.0000	8.427	103	299.8599	299.8599	100.0
	9 peak mix	level 4.d	Cal	4	400.0000	8.427	138	396.4041	396.4041	99.1
	9 peak mix	level 5.d	Cal	5	500.0000	8.435	177	503.9937	503.9937	100.8
	9 peak mix	level 6.d	Cal	6	750.0000	8.446	266	747.4100	747.4100	99.7
	9 peak mix	level 7.d	Cal	7	1000.0000	8.437	356	996.0243	996.0243	99.6
	9 peak mix	level 8.d	Cal	8	1500.0000	8.438	536	1491.6483	1491.64...	99.4
	9 peak mix	level 9.d	Cal	9	2000.0000	8.445	719	1995.9952	1995.99...	99.8
	9 peak mix	level 10.d	Cal	10	5000.0000	8.436	1811	5004.8495	5004.84...	100.1
	9 peak mix	level 5 with all ions.d	Sample			8.429	176	501.2125	501.2125	
	Sample14	F1 sample.d	Sample			8.444	110	319.1457	319.1457	
	Sample15	F2 sample d.d	Sample			8.450	61	184.1997	184.1997	
	Sample16	blend.d	Sample			8.458	2	21.9074	21.9074	
	Sample17	hemp hri.d	Sample			8.449	374	1045.9793	1045.97...	

Figure 1: Quantitation of THC from 100 to 5000 ppm

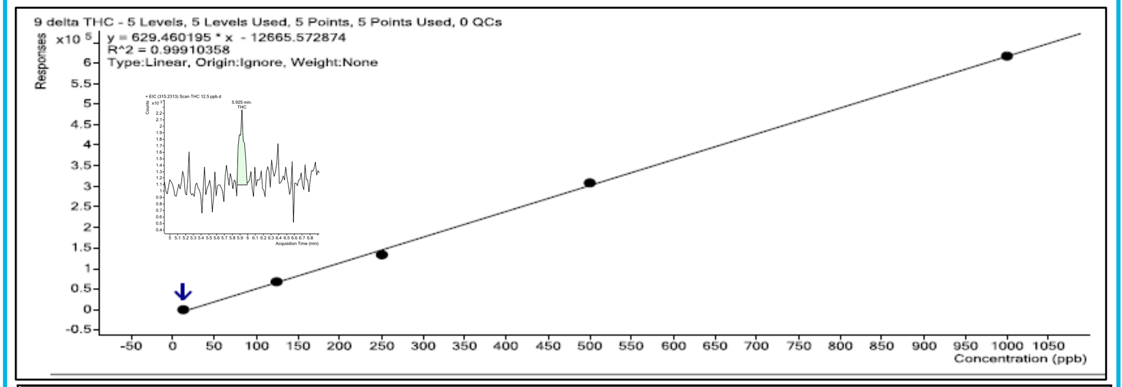

	Name	Data File	Type	Level	Acq. Date-Time	Exp. Conc.	RT	Resp.	Calc. Conc.	Final Conc.
	thc	THC 12.5 ppb.d	Cal	1	8/9/2016 3:20 AM	12.5000	5.925	4703	17.9468	17.9468
	tox standard	THC 125 ppb.d	Cal	2	8/9/2016 3:40 AM	125.0000	5.910	68067	118.1281	118.1281
	tox standard	THC 1000 ppb...	Cal	5	8/9/2016 4:42 AM	1000.0000	5.922	626243	1000.6274	1000.62...
	tox standard	THC 500 ppb.d	Cal	4	8/9/2016 4:21 AM	500.0000	5.920	316156	510.3682	510.3682
	tox standard	THC 250 ppb.d	Cal	3	8/9/2016 4:01 AM	250.0000	5.923	138773	229.9177	229.9177

Figure 2: Quantitation of THC from 12.5 ppb to 1000 ppb

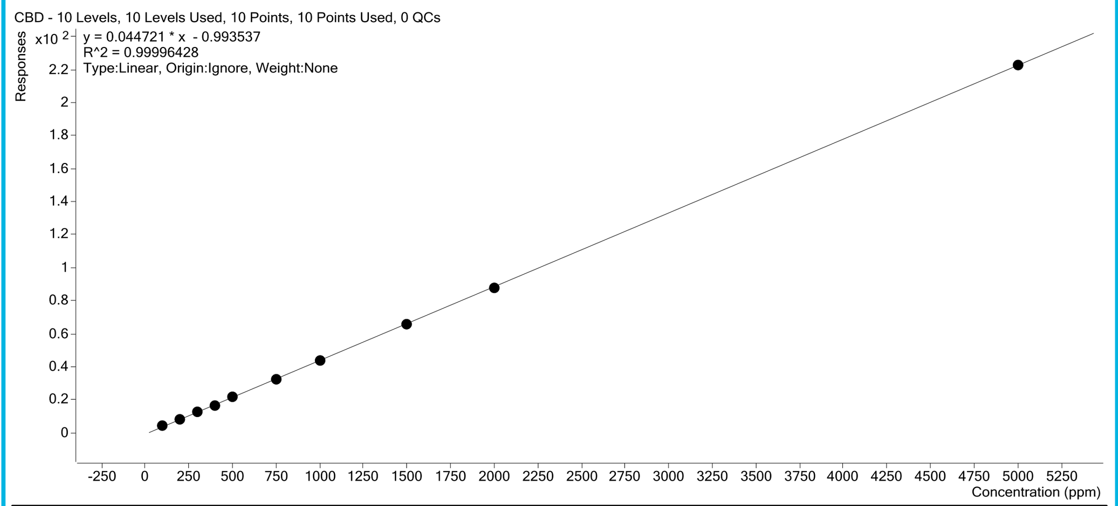

Data File	Type	Level	Exp. Conc.	RT	Resp.	Calc. Conc.	Final Conc.	Accuracy
level 1.d	Cal	1	100.0000	7.549	4	114.6761	114.6761	114.7
level 2.d	Cal	2	200.0000	7.566	8	203.0707	203.0707	101.5
level 3.d	Cal	3	300.0000	7.567	12	299.8328	299.8328	99.9
level 4.d	Cal	4	400.0000	7.568	17	393.2657	393.2657	98.3
level 5.d	Cal	5	500.0000	7.576	21	502.1863	502.1863	100.4
level 6.d	Cal	6	750.0000	7.585	32	745.9138	745.9138	99.5
level 7.d	Cal	7	1000.0000	7.578	44	1006.1116	1006.11...	100.6
level 8.d	Cal	8	1500.0000	7.581	66	1493.4677	1493.46...	99.6
level 9.d	Cal	9	2000.0000	7.587	88	1983.6854	1983.68...	99.2
level 10.d	Cal	10	5000.0000	7.577	223	5007.7899	5007.78...	100.2

Figure 3: Quantitation of CBD from 100 ppm to 5000 ppm

Compound EICs and Levels

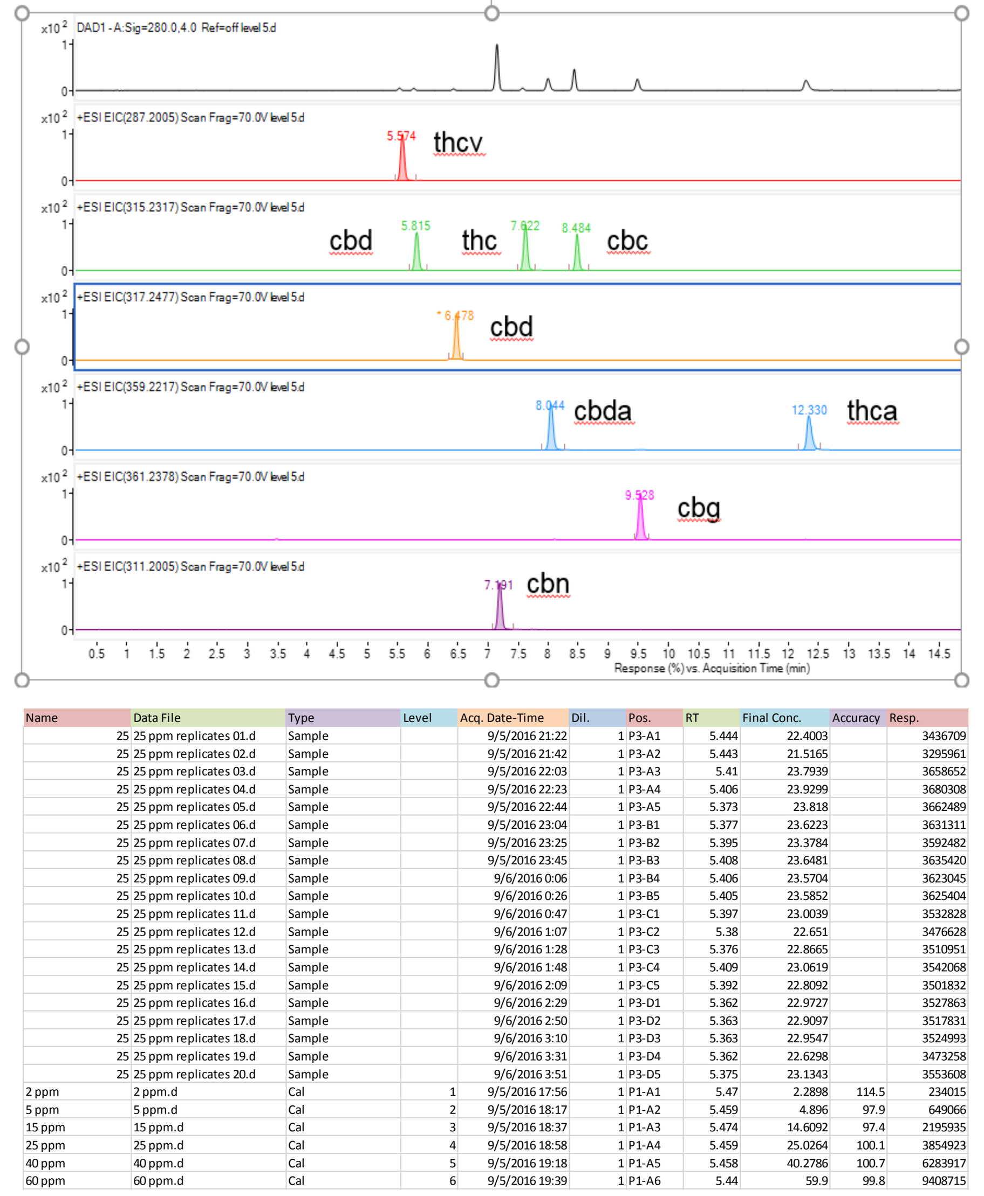

Figure 4: THC and CBD EICs and Concentrations

High Resolution Spectral Library and Tools

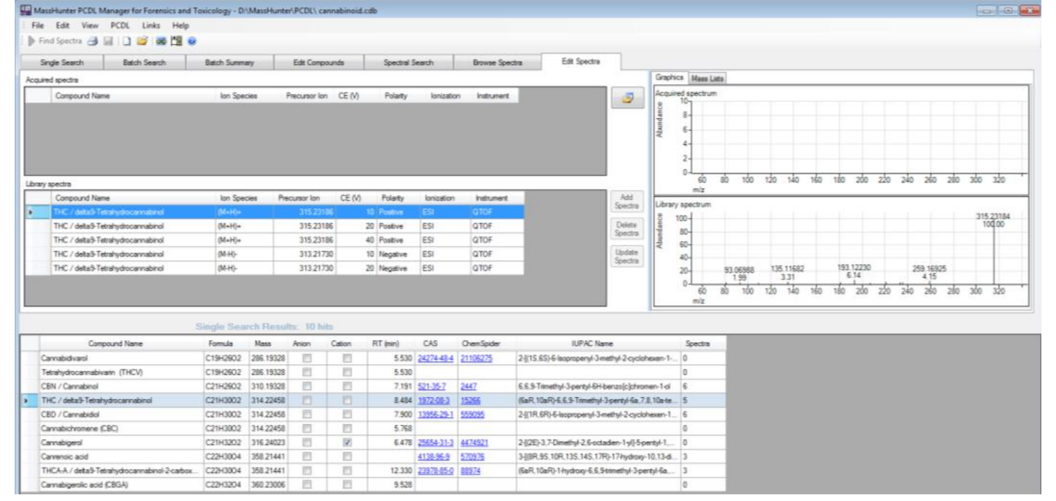

Figure 5: Personal Compound Database and Library (PCDL) for THC and CBDs

Extended Dynamic Range in a single injection

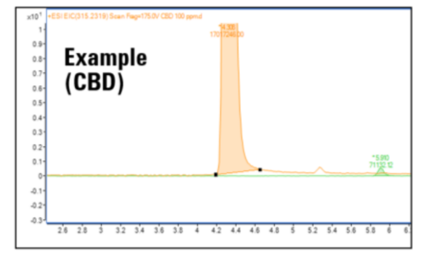

Extended Dynamic Range usable for Quantitation
CBD concentration at 100 ppm
THC concentration at 12.5

Quantification across a suitable dynamic range is achieved. Quantitative accuracy is maintained by establishing a linear calibration curve greater than the expected concentration levels for target analytes.

Results and Discussion

Screening for pesticides in a commercial CBD candy bar using subset PCDL of targeted pesticides

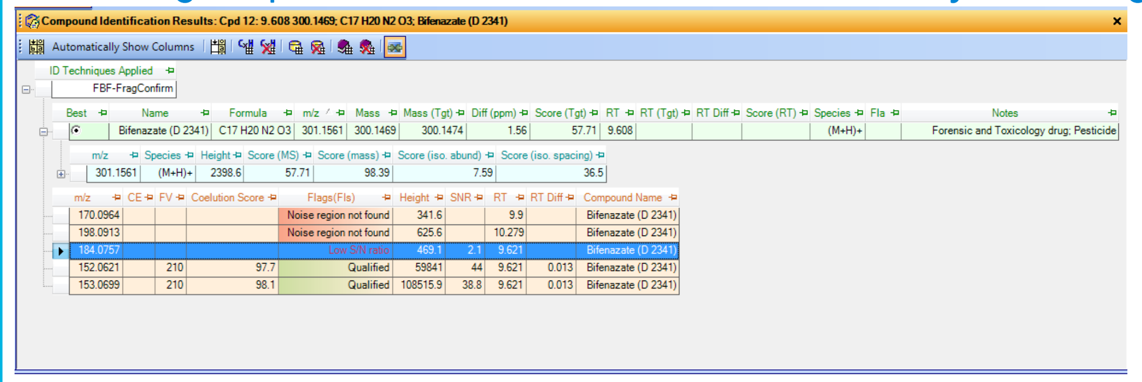

Figure 8: Compound Identification with PCDL

A commercially available CBD candy bar was processed by a QuEChERS extraction/partitioning and EMR (enhanced matrix removal) Lipid dispersive SPE clean-up and dSPE. HPLC conditions are identical to the CBD assay with only a different column introduced via column switching valve. Figure 8 shows the results with the PCDL subset of the targeted compounds with fragmentation confirmation.

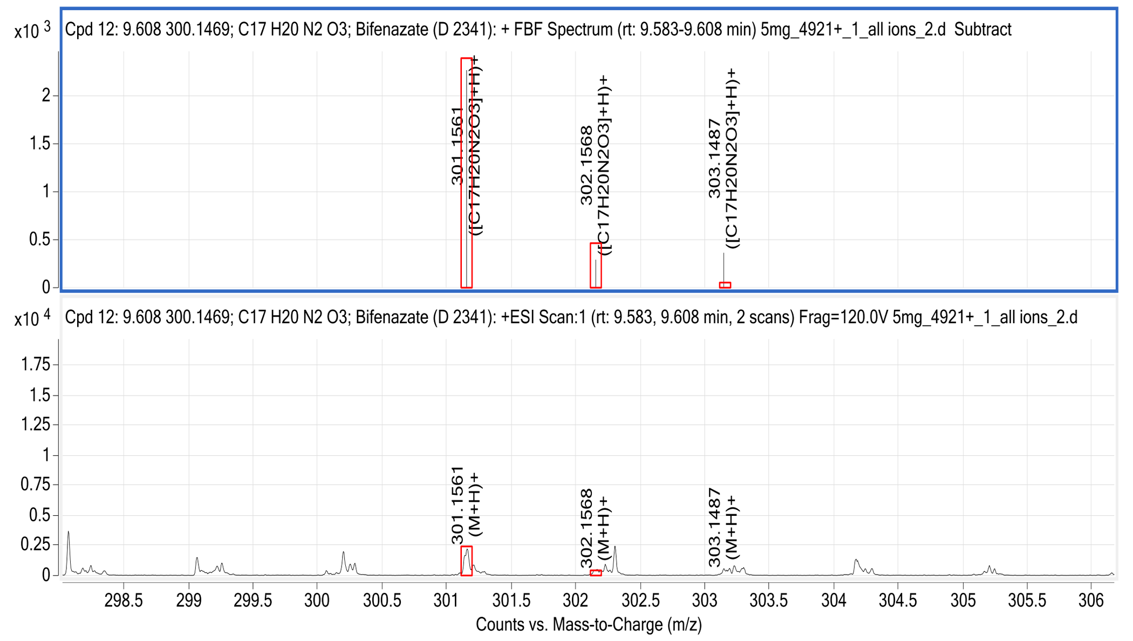

Figure 6: **Mass Spectra for suspect compounds.** All of the spectra from the extracted ions are compared with the product ion spectra from the PCDL

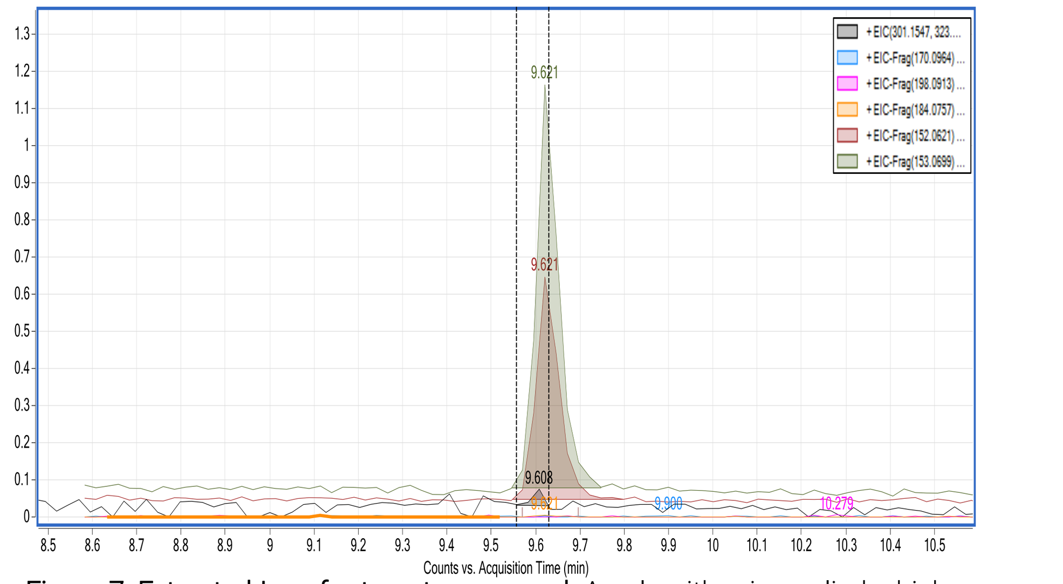

Figure 7: **Extracted ions for target compound.** An algorithm is applied which takes into account retention times of the EICs this data is then searched against the unique PCDL.

Screening for Drugs of Abuse

A standard of 99 drugs of abuse was spiked into natural hemp oil. The sample was then run on the TOF using the All Ions technique. Figure 9 shows 99 drugs found from the PCDL screening with mass and spectral fragment confirmation.

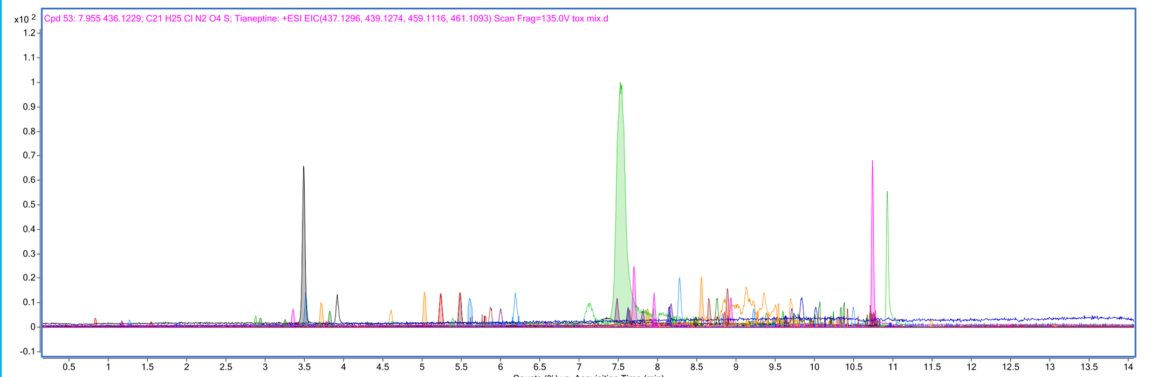

Figure 9: **Spiked Analytes in Hemp Oil matrix.** Screening for various compound classes is enabled on the same data set using available PCDLs

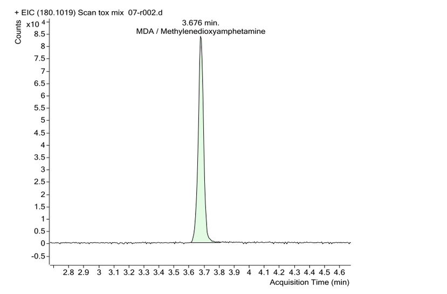

Figure 10: Example Spiked Compound EIC

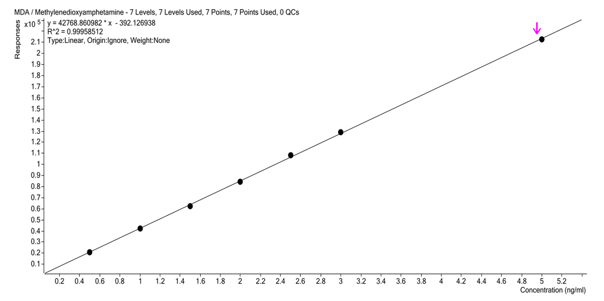

Figure 11: Example Calibration Curve for spiked compound

All of the 96 compounds had calibration curves created with correlation coefficients of 0.995 to 0.999, figure 11 is an example of a curve. The randomly spiked sample was quantitated against this calibration curve. The methodology used has the same mobile phases as the potency assay only a different column

Conclusions

We are able to use the LC/TOF for both qualitative and quantitative work with high resolution accurate mass spectral information and fit-for-purpose linear dynamic range. With the All Ions methodology, we have the ability to have MS/MS like spectral confirmation for screening of suspect compounds against a high resolution spectral library.

References

[1]The United States Drug Enforcement Agency. (October 9, 2001). *DEA Clarifies Status of Hemp in the Federal Register*. Retrieved from https://www.dea.gov/pubs/pressrel/pr100901.html.

Screening of pesticides and other contaminants in food matrices using a novel high resolution GC/Q-TOF with low-energy capable EI source

Kai Chen and Jennifer Sanderson

Agilent Technologies, Inc., Santa Clara, California

ASMS 2017
MP-196

Agilent
Trusted Answers

Introduction

The increasing demand on screening for contaminants in food requires an efficient and sensitive technique [1]. High resolution GC/Q-TOF has emerged as a tool to fit this purpose for GC-amenable compounds. The same full-spectrum accurate mass data enables both confident identification of compounds in the sample and quantitation capability to address the stringent requirements on maximum residue levels (MRLs). The addition of low energy electron impact (EI) ionization enhances the possibility to preserve or confirm molecular ions on EI mass spectra, aiding in the study of unknowns. In this work, a novel high resolution, low-energy EI capable GC/Q-TOF was used to screen pesticides and other contaminants in food matrices.

Experimental

Sample Preparation

Homogenized food commodities were extracted using QuEChERS (EN) kit. The cleanup of Avocado extract used EMR-Lipid dSPE and drying pouches. Broccoli extract was cleaned up by dSPE for pigment matrix, and others by dSPE for fruits/vegetables. A mixture of 140+ pesticides was spiked in the organic matrices to evaluate the method. Screening of contaminants was performed on non-organic food extracts.

Figure 1. 7250 GC/Q-TOF system

Experimental

Instrument Analysis

A retention time locked method was set up to acquire data using an Agilent 7250 GC/Q-TOF system (figure 1) configured with a mid-column backflushing system (figure 2). Table 2 lists the operational parameters.

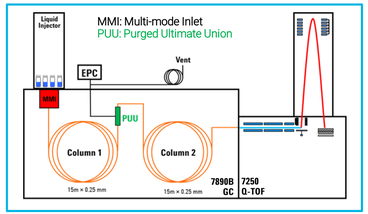

Figure 2. Mid-column back flushing system

Table 1. GC/Q-TOF Operational Conditions.

GC and MS Conditions	Value
Columns (2 ea.)	HP-5 MS UI, 15 m, 0.25 mm ID, 0.25 µm film
Inlet	MMI, 4-mm UI liner single taper w wool
Injection	2 uL, cold splitless
Carrier gas	Helium
Inlet flow (column 1)	~1 mL/min (Chlorpyrifos-methyl locked at 9.143 min)
PUU flow (column 2)	column 1 flow + 0.2 mL/min
Oven program	60 °C for 1 min 40 °C/min to 170 °C, 0 min 10°C/min to 310 °C, 3 min
Backflushing conditions	5 min (Post-run), 310 °C (Oven) 50 psi (Aux EPC), 2 psi (Inlet)
Transfer line temperature	280 °C
Ion source	EI, 70 eV, 15 eV
Source temperature	280 °C (70eV), 250 °C (15 eV)
Quadrupole temperature	180 °C
Spectral Acquisition	45 to 650 m/z, 5 spectra/sec (70 eV)

Data Analysis

- The data processing used Agilent MassHunter Data Analysis Software B.08.00, including SureMass.
- The targeted screening of pesticides (a combined quantitative and qualitative workflow) was based on a commercial GC/Q-TOF pesticides library [2] which contains accurate mass spectra and retention times for 850+ compounds.
- The untargeted screening of other contaminants relied on the NIST GC/MS library.

Results and Discussion

Food Matrix and Pesticides

The diversity of food matrix complexity in this study is reflected by TICs in figure 3. The pesticides spiked for method evaluation represent OCs, OPs, carbamates, triazoles and pyrethroids, etc.

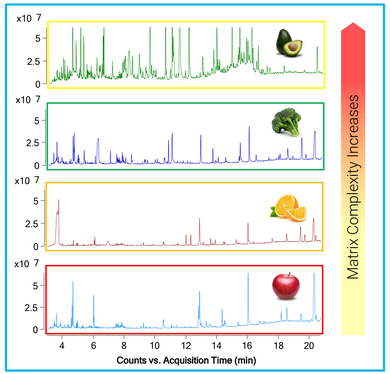

Figure 3. Total ion chromatograms of organic food matrices spiked with 10 ng/mL each pesticide.

Method Repeatability

The repeatability (six replicates) of retention time and response are shown in figure 4 and 5 for all of the identified compounds spiked at 10 ng/mL.

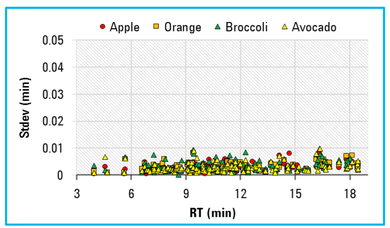

Figure 4. Retention time repeatability (SD ≤ 0.01 min).

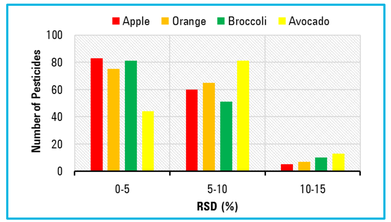

Figure 5. Total ion chromatograms of food matrices.

Matrix Matched Calibration

With SureMass used for quantitation, the multiple-level matrix matched calibration in avocado (triplicates at each level) yielded over 85% of the target pesticides achieving a linear calibration curve with $R^2 \geq 0.99$ in the range of 5-500 ng/mL. The majority of remaining pesticides yielded $R^2 \geq 0.985$ for the same concentration range. Figure 6 displays the examples from various pesticide groups.

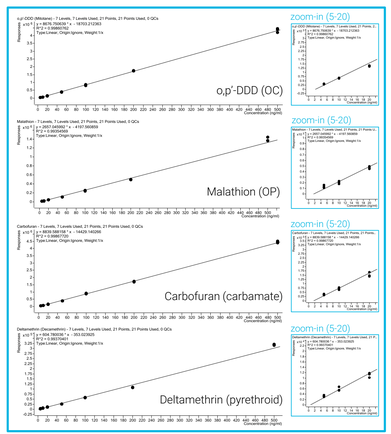

Figure 6. Calibration curves from 5 to 500 ng/mL.

Results and Discussion

Mass Accuracy

Figure 7 shows the mass accuracy of example pesticides over a wide concentration range. At spiking level of 10 ng/mL, all the detected pesticides in each food matrix have been measured with mass accuracy < 5 ppm.

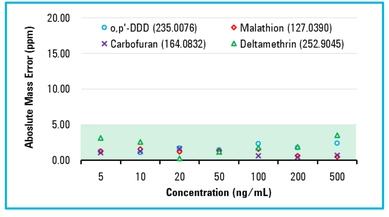

Figure 7. Mass accuracy of example pesticides from 5 to 500 ng/mL in avocado matrix.

Targeted Screening (Quant and Qual Combined)

Targeted screening of pesticides in non-organic food used the accurate mass pesticides library (Table 2).

Table 2. Targeted Screening Results of non-organic food

Matrix	Pesticide Identified *	Amount (ppb)
	Boscalid (Nicobifen)	qual only
	Fludioxonil	qual only
	Pyraclostrobin	qual only
	Pyrimethanil	qual only
	TBZ / Thiabendazole	qual only
	Carbaryl	6.5
	Propiconazole (I & II)	qual only
	Pyrimethanil	qual only
	TBZ / Thiabendazole	qual only
	(1R)-cis-Permethrin	30.7
	(1R)-trans-Permethrin	30.6
	Azoxystrobin	878 (>500)
	Boscalid (Nicobifen)	qual only
	Dimethomorph (E)	535 (>500)
	Fludioxonil	qual only
	Pentachlorobenzonitrile	qual only
	Pyraclostrobin	qual only
	TBP / Tributylphosphate	qual only
	λ-Cyhalothrin	43.0

* Identification criteria: mass error < 5 ppm (≥ two ions), RT ≤ 0.1 min, S/N ≥ 3
qual only = qualitative screening only, standard not available for calibration

Untargeted Screening

Untargeted screening of other contaminants was performed by matching NIST library after SureMass peak detection. Low energy EI spectrum helped to confirm molecular ion (figure 8).

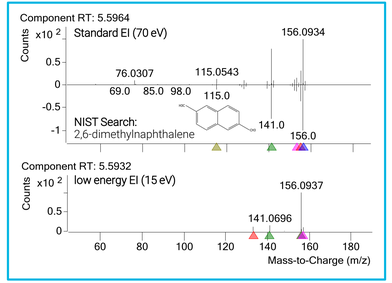

Figure 8. Example result of untargeted screening from non-organic broccoli extract.

Conclusions

- A new GC/Q-TOF has been used to successfully screen pesticides in various food matrices.
- The confidence in results is enhanced by stable RT, repeatable response and good mass accuracy.
- A wide linear response range has been achieved for matrix matched calibration.
- Low energy EI facilitates untargeted screening.

References

[1] Belmonte-Valles, N., et al; Analysis of pesticides residues in fruits and vegetables using gas chromatography-high resolution time of flight mass spectrometry. *Anal. Methods* 7, 2162-2171 (2015).

[2] Chen, K., Nieto, S., Stevens, J.; GC/Q-TOF Surveillance of Pesticides in Food, *Agilent Technologies Application Note*, 5991-7691EN (2016).

Analysis of Pesticides and Environmental Pollutants in Essential Oils Using Multi-Platform GC/MSD, GC/TQ and GC/Q-TOF

Vivian Xianyu Chen[1], Bruce Quimby[2] and Kai Chen[3]

[1]Agilent Technologies Co., Ltd., Shanghai, China
[2]Agilent Technologies, Inc., Wilmington, Delaware
[3]Agilent Technologies, Inc., Santa Clara

ASMS 2017
MP-270

Agilent
Trusted Answers

Introduction

Essential oils are concentrated liquids containing volatile aroma compounds from various plants and are widely used in flavors and fragrances. Traces of pesticides are sometimes present in these oils, resulting in the need to screen them. This analysis is challenging due to the intense matrix background interference presented by oils, therefore traditional GC/MS is limited in capacity to perform the task. This work demonstrates the use of enhanced techniques for pesticide screening in essential oils.

The enhanced techniques are:

- **GC/MSD:** Use of a retention time locked (RTL) spectral library of 950+ compounds and screening based on match scores of deconvoluted spectra.
- **GC/TQ:** Initial screening of samples using scan mode (as above) with subsequent MRM analysis for trace level identity confirmation and quantitation.
- **GC/Q-TOF:** Use of a RTL library containing accurate mass spectra for 850+ compounds and screen using six principle accurate mass ions, fragment ratios and RT matching.

This multi-platform GC/MSD, GC/TQ and GC/Q-TOF approach also offers a streamlined workflow utilizing different platforms offering enhanced qualitative and quantitative capabilities.

Experimental

Sample Preparation

Eight essential oils were diluted 10:1, 50:1 and 100:1 by volume in ethyl acetate for direct injection on GC/MSD, GC/Q-TOF and GC/TQ, respectively. A mixture of 150+ pesticides standards was spiked in Lavender oil (100:1 dilution) at 0.02–200 ng/mL (two calibration sets, low & high concentrations) for matrix matched calibration on GC/TQ.

Instrumental Analysis

The samples were analyzed in EI mode by:

- Agilent 7890B GC and 7250 high resolution accurate mass GC/Q-TOF
- Agilent 7890B GC and 5977B GC/MSD
- Agilent 7890B GC and Agilent 7010 GC/TQ

All three systems were configured with a mid-column backflush setup (Figure 1). A 20 minute constant flow RTL method (chlorpyrifos-methyl locked at 9.143 min) has been used for chromatographic separation, with parameters listed in Table 1.

Experimental

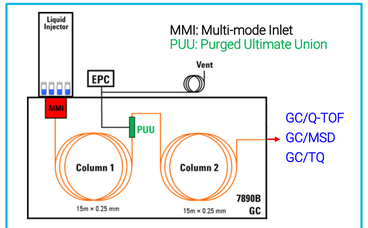

Figure 1. Mid-column backflush system

Table 1. GC and MS operational conditions

GC and MS Conditions	Value
Columns (2 ea.)	Agilent J&W HP-5ms UI 15 m × 0.25 mm × 0.25 µm (P/N: 19091S-431 UI)
Inlet	MMI, 4-mm UI liner with wool
Injection	1 or 2 µL cold splitless
Carrier gas	Helium
Inlet flow (column 1)	~ 1 mL/min
PUU flow (column 2)	column 1 flow + 0.2 mL/min
Oven program	60°C for 1 min 40°C/min to 170°C for 0 min 10°C/min to 310°C for 3 min (Total Run Time 20.75 min)
Backflush Conditions	5 min (Post-run). 310 °C (Oven). 50 psi (Aux EPC pressure). 2 psi (Inlet pressure)
Transfer line temperature	280 °C
Ion source temperature	280 °C
Quadrupole temperature	150 °C

Data Analysis

The Agilent Pesticides and Endocrine Disruptors mass spectral library/database [1] was modified with the retention times for the constant flow 20 minute method utilized in the MSD, TQ and Q-TOF systems. This unit mass library with 950+ compounds was then used on GC/MSD, GC/TQ and GC/Q-TOF for compound identification through MassHunter Unknowns Analysis B.08.00. In addition, an accurate mass pesticides library (PCDL) with 850+ compounds was employed for compound identification on GC/Q-TOF via Find by Fragments in MassHunter Qualitative Analysis [2]. The GC/TQ used MRMs from the database supplied with the Pesticides & Environmental Pollutants Analyzer (M7412AA) [3].

Results and Discussion

Compound Identification on MSD, Q-TOF and TQ

Eight essential oils were analyzed. Nothing of interest was detected in eucalyptus oil, rosemary oil or lavender oil. Multiple pesticides were detected in grapefruit oil, lemon oil, neroli oil, orange oil (Brazil origin) and orange oil (California origin). Grapefruit oil (Figure 2) is one of the most challenging of the 8 matrices and is used as an example in this work.

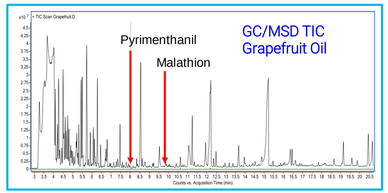

Figure 2. TIC Chromatograms of Grapefruit Oil

Pyrimenthanil was identified on all three platforms. The raw MSD spectrum where pyrimenthanil elutes is shown in Figure 3. With the help of deconvolution, a clean spectrum of pyrimenthanil on MSD was obtained with a library spectrum match score of 90 (Figure 4).

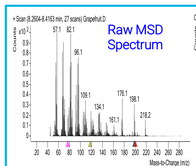

Figure 3. Raw MSD Spectrum

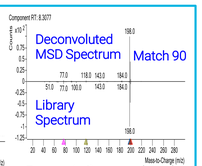

Figure 4. Deconvoluted and Library MSD Spectra

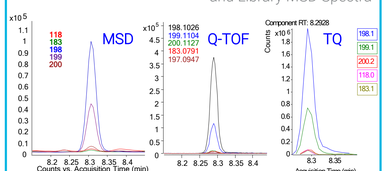

Figure 5. EICs of Pyrimenthanil on Three Platforms

On TQ, the library match score is 87.8 for MS1 full scan and 88 for MS2 full scan.). On Q-TOF, the Frag Ratio Score is 98.05 and the mass error (ppm) is 3.68. The EICs of pyrimenthanil from all platforms are shown in Figure 5.

Screening Power of Q-TOF

All three platforms perform well in the identification of pyrimenthanil, whose quantitation result by GC/TQ is 29.4 ng/mL (100:1 dilution). However, malathion was initially not found in the MSD and TQ deconvolution scan mode screens. The red arrow in Figure 6 shows where malathion should have been detected.

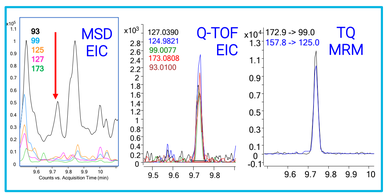

Figure 6. Chromatograms of Malathion on 3 Platforms

The Q-TOF screen, however, had a high confidence identification of malathion with small RT difference, good fragment ratio score and mass accuracy (Table 2). The TQ MRM mode then confirmed the presence of malathion, with an amount of only 1.26 ng/mL quantified. At this trace level, malathion cannot be identified by using scan mode on the MSD and TQ in heavy matrix. This illustrates that for low level screening in complex matrices, the Q-TOF screen is highly desirable due to its high selectivity over matrix interferences.

Workflow

GC/Q-TOF, GC/MSD and GC/TQ can all provide screening capability which relies on deconvolution to process full spectrum acquisition data (GC/Q-TOF) or full scan data (GC/MSD or GC/TQ). The initial identification was achieved by searching deconvoluted compound spectra against a unit mass library. The accurate mass data from GC/Q-TOF can also be used for suspect screening. This process consists of selecting principle ions of each compound from an accurate mass PCDL for screening, with the identified hits verified via mass accuracy, fragment ratio and RT match. Positive hits are then sent to TQ (MRM) for further confirmation and quantification. This provides a detailed comprehensive multi-platform screening and quantification workflow (Figure 7).

Results and Discussion

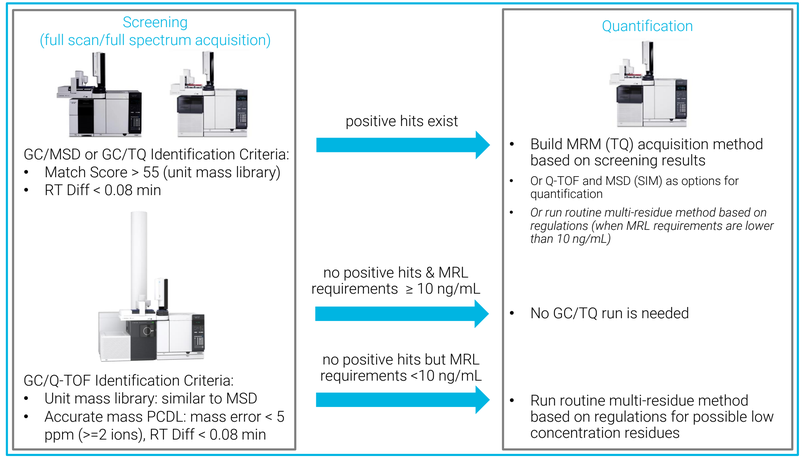

Figure 7. Workflow of Compound Screening and Quantification using GC/MSD, GC/TQ and GC/Q-TOF

The example results of this comprehensive workflow is shown in Table 2.

Table 2. Identification and Quantification Results from Grapefruit Oil by Multiple Platforms

Compound Name	GC/MSD		GC/Q-TOF			GC/TQ (MRM)	
	Match Score	RT Diff (min)	Frag ratio Score	RT Diff (min)	mass diff (ppm)	RT Diff (min)	Conc. (ng/mL)
Aniline	68	0.068	rejected after review			*n.d.*	*n.d.*
Pyrimethanil	96	0.023	98.05	0.015	3.68	0.012	29.41
Chlorpyrifos Methyl	79	0.000	99.92	0.005	1	0.006	3.33
Chlorpyrifos	93	-0.002	95.33	0.006	0.42	0.009	30.69
Imazalil	57	0.047	95.99	0.048	0.88	0.019	25.20
Pyriproxyfen	81	0.020	85.83	0.019	1.55	0.016	10.86
Malathion	*n.d.*	*n.d.*	82.15	0.014	0.17	0.011	1.26
*Primiphos-methyl **	*n.d.*	*n.d.*	*n.d.*	*n.d.*	*n.d.*	*0.011*	*0.22*
*Oxadixyl **	*n.d.*	*n.d.*	*n.d.*	*n.d.*	*n.d.*	*0.021*	*0.36*
*Methidathion **	*n.d.*	*n.d.*	*n.d.*	*n.d.*	*n.d.*	*0.004*	*0.54*

* quantified by the routine multi-residue method on TQ
n.d. = not detected or identified

Conclusions

- This work demonstrates a comprehensive multi-platform untargeted and targeted analysis workflow with examples in complex matrix.
- For untargeted screening, Q-TOF > MSD > TQ.
- TQ can quantify analytes at low concentration which may not be identified by MSD or Q-TOF screening.

Reference

[1] Wylie, P.L.; Screening for 926 Pesticides and Endocrine Disruptors by GC/MS with Deconvolution Reporting Software and a New Pesticide Library. *Agilent Technologies Application Note*, 5989-5076EN (2006).

[2] Chen, K., Stevens, J., Nieto, S.; GC/Q-TOF Screening of Pesticides in Food, *Agilent Technologies Application Note*, 5991-6884EN (2016).

[3] Westland, J., Stevens, J.; An Optimal Method for the Analysis of Pesticides in a Variety of Matrices. *Agilent Technologies Application Note*, 5991-7303EN (2017).

Improving Gas Chromatograph-Mass Spectrometer System Longevity for Multi-Residue Pesticide Methods with Heavy Matrix Through Inert Microfluidic Retention Gap Technology

Rebecca A. Veeneman and Matthew Giardiana
Agilent Technologies, Wilmington, DE USA

ASMS 2017
MP-193

Agilent
Trusted Answers

Introduction

Analysis of pesticides in food

The analysis of pesticides in food is known to be complex. With increasing target compound and commodity lists, decreasing detection limit requirements, and the need for a wide linear dynamic range, pesticide analysis is demanding. Tandem mass spectrometry (MS/MS) is incredibly useful in screening, confirming, and quantifying a wide range of pesticides especially with its ability to minimize matrix interferences. However, despite these advantages and advances in sample preparation like QuEChERS, matrix can still contaminate the inlet liner, analytical column(s), ion source, etc., leading to peak tailing, loss of response, and even ion enhancement. Users often default to regular liner replacements, column trimming, and source maintenance. By employing an inert, microfluidic retention gap, system maintenance can be reduced and system longevity improved.

Agilent 9000 Intuvo Gas Chromatograph

A redesigned modular flow path featuring an inert, microfluidic retention gap (guard chip) protects the analytical column(s) and ion source from matrix and eliminates the need to trim the column. It also offers these additional advantages over conventional gas chromatographic systems:

- Simplified maintenance
- Improved inertness
- Smaller footprint

Experimental

Instrumentation

The analysis was conducted on an Agilent Intuvo 9000 Gas Chromatograph coupled with an Agilent 7000C Triple Quadrupole Mass Spectrometer. The system was configured with a split/splitless inlet equipped with an ultra-inert liner with wool and a single HP5-ms UI column (15m x 0.25mm x 0.25µm). Target pesticides were evaluated in seven different food commodities (honey, rice, orange, olive oil, black tea, cucumber, and onion). Calibration curves for the pesticides ranged from 1-1000 ng/mL and the 50 ng/mL standard was evaluated over the course of 60 matrix injections for accuracy. Column lifetime and required system maintenance comparison studies were also evaluated by spinach extract injections on both the Intuvo GC/MS/MS and 7890B GC/MS/MS systems. Instrument conditions are show below.

Parameter	Value
Agilent 9000 Intuvo GC & 7890B GC	
Inert flow path configuration	Simple MS
Sandwich injection	3-layer sandwich L1 (matrix) 1µL L2 (analyte protectant) 0.5µL L3 (sample) 1µL
Inlet	SSL; pulsed SL 280°C
Injection pulse pressure	30psi until 0.5min
Intuvo guard chip	Track oven
Intuvo bus temperature	290°C (default)
Column	HP5-ms UI 15m x 250µm x 0.250µm
Column flow	1.4mL/min
Column temperature program	60°C (1.5min) then 50°C/min to 160°C then 8°C/min to 240°C then 50°C/min to 280°C (2.5min) then 100°C/min to 290°C (1.1min)
Agilent 7000C GC/MS/MS	
Transfer line	280°C
Source temperature	280°C
Quad temperature	150°C

Results and Discussion

Calibration

A calibration curve consisting of eight levels run in triplicate was determined for each matrix. A subset of a larger list of pesticides typically analyzed was used throughout this study to allow for more rigorous examination of calibration coefficients and chromatographic performance. Deuterated polyaromatic hydrocarbons were used as internal standards.

Excellent linearity for concentrations ranging from 1ng/mL to 1000ng/mL was found. Correlation coefficients ranged from 0.972 to 0.998.

1. 1,4-dichlorobenzne-d4
2. Naphthalene-d8
3. Methacrifos
4. Acenaphthene-d10
5. Ethalfluralin
6. Sulfotep
7. Demeton-S
8. Simazine
9. Lindane
10. Phenanthrene-d10
11. Chlorpyrifos methyl
12. Fenitrothion
13. Aldrin
14. Pendimethalin
15. Tolyfluanid
16. Dieldrin
17. Buprimate
18. Triazophos
19. Chrysene-d12
20. Iprodione
21. EPN
22. Phosalone
23. Mirex
24. Coumaphos
25. Perylene-d12
26. Pyraclostrobin
27. Deltamethrin

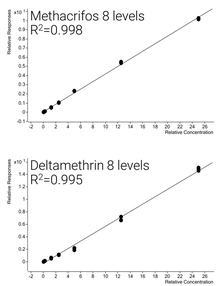

Figure 1. Calibration curves for methacrifos and deltamethrin in honey are representative of the 21 analytes evaluated in seven different matrices.

Accuracy and Chromatographic Consistency

After calibrating with the matrix of interest, 60 additional sandwich injections were evaluated for continuing calibration accuracy. Figure 2 shows the average accuracy of the 60 injections for each matrix and analyte.

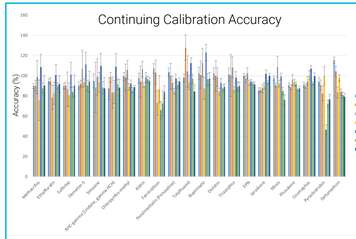

Figure 2. Continuing calibration accuracy for 21 analytes and seven matrices demonstrates consistent responses over 60 injections.

When examining Figure 2 there are a few analyte/matrix pairs that show a higher degree of variability (wider error bars) or a lower degree of accuracy. However, the majority of the analyte/matrix pairs demonstrate continuing calibration accuracy between 70% and 120% for an average of 60 matrix injections. These results indicate a high degree of consistency among the data with limited cases of response loss, peak distortion, or ion issues.

Overlaid chromatograms highlighting the start of the experiment, after batch completion, and after performing a guard chip replacement are shown in Figure 3.

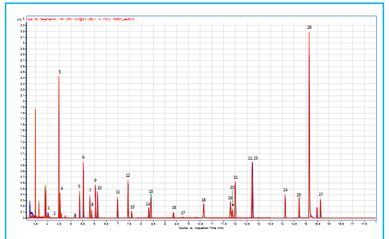

Figure 3. Overlaid chromatograms demonstrate the chromatographic consistency after calibration (blue), after completing an additional 60 matrix injections with black tea (red), and after guard chip replacement on the Intuvo system (green).

Results and Discussion

Comparison to Conventional Gas Chromatographs

To demonstrate further the added longevity afforded by the guard chip as part of the Intuvo inert flow path, a side-by-side comparison was done with a 7890B GC/MS/MS system. Spinach, a high pigment matrix, was used for this comparison study. Sandwich injections were used to introduce matrix, analyte protectants, and a 50ng/mL standard each injection. The accuracy of the 50ng/mL standard, compared to the calibration curve, was monitored and maintenance on either system was performed if the calibration accuracy fell outside of the 70-120% window.

In the previous study, the Intuvo system routinely completed nearly 100 injections in a given batch without suffering from analyte tailing or response loss. However, in conventional GC/MS/MS systems, where retention gaps are not typically used, peak shape degradation can be seen in as few as 30 matrix injections (Figure 4).

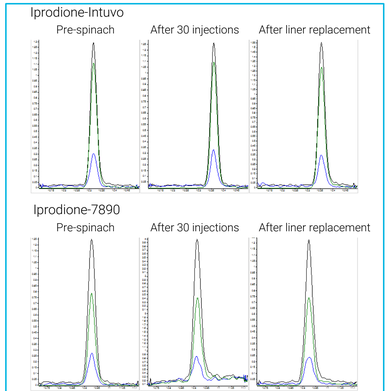

Figure 4. Multiple reaction monitoring target and qualifying ions are overlaid for iprodione. The peak shape differences between the two systems pre-matrix, after 30 injections, and after liner replacement highlight the benefit of including a retention gap.

With a single 15m column configuration, the Intuvo/7000C GC/MS/MS was able to withstand over 300 injections with liner or guard chip replacements. The system did not require retention time re-locking to maintain accurate time segments. In the case of the 7890B/7000C GC/MS/MS, less than 200 injections were completed. While liner replacements often improved performance on the 7890B/7000C GC/MS/MS system, column trimming was also required through the course of the experiment in order to maintain calibration accuracy within the 70-120% range. This shortened the column length to a point that a retention time locked chromatogram could no longer be achieved.

Conclusions

Improved chromatographic consistency and longevity

A calibration and matrix evaluation was performed on an Agilent Intuvo 9000 GC and an Agilent 7000C Triple Quadrupole Mass Spectrometer configured with an Intuvo HP5-ms UI column. Twenty-one pesticides were evaluated with seven matrices to represent a range of commodities, with varying levels of difficulty. The instrument showed excellent calibration linearity and continuing calibration accuracy. With the implementation of the Intuvo guard chip, the following was observed:

- The need to trim the column to maintain peak shape was eliminated
- The ion source did not require maintenance for the duration of the experiment
- Excellent peak shape and calibration accuracy was maintained on a simple, single column configuration

In this evaluation, calibration curve coefficients were usually 0.995 or better, regardless of matrix complexity. The average calibration accuracy for a 50ng/mL standard across 60 matrix injections was ~100% for the seven food commodities evaluated. Consistent peak shape and response was also observed through the experiment.

When comparing to conventional GC/MS/MS systems, the Intuvo guard chip preserves chromatographic fidelity for a greater number of injections while eliminating the need to trim the column. This resulted in a 50% increase in column longevity since the column length was maintained.

With regular maintenance of the liner and guard chip, Intuvo GC/MS/MS systems could last 500 injections without column or ion source maintenance.

Evaluation of Matrix Interferences on Multiresidue Pesticide Analysis in Different Commodities Using LC/TQ

Mondragon Olguin Victor Manuel
Agilent Technologies, Mexico City, Mexico

ASMS 2017
TP-181

Agilent
Trusted Answers

Introduction

The current occurrence of pesticide residues in food and environmental samples has intensified the development of new analytical methods for the analysis of these compounds. During method validation, special attention should be paid to matrix interferences. When matrix compounds and analytes enter the ion source at the same time, the ionization efficiency of the analyte can be reduced in a significant way. In many studies, it is reported that the presence of matrix components can affect the quantification procedures based on electrospray ionization (ESI) in LC/MS methods. To avoid these drawbacks and increase the productivity of routine laboratories, modifications to multiresidue methods have been adopted (clean-up after extraction, adjustment of chromatographic conditions in LC, extract dilution and use of appropriate calibration techniques) to determine as many pesticides as possible in one single run.

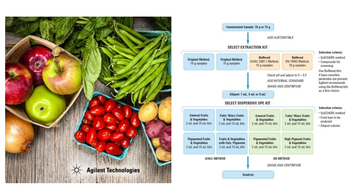

Figure 1. QuEChERS general workflow.

The objective of this work is explore the diversity of QuEChERS sample preparation techniques, where some of them have as a purpose to improve the practical efficiency for a given analyte or matrix removal and some others are used only for personal preferences. Due to this diversity and the number of compounds that usually are involved in this kind of analysis, the decision to choose the best sample preparation technique could be complicated or biased for some compounds. Additionally, sample dilution is studied as a means of reducing matrix effects during the quantification process.

Experimental

A 1290 HPLC system was interfaced with an Agilent 6470 Triple Quadrupole LC/MS system equipped with an ESI ionization source. Pear samples were prepared using three different QuEChERS sample preparation procedures (two AOAC procedures and European method, each with their respective sample clean-up procedure). The samples were spiked with 160 pesticides and pesticides metabolites (20 ng/g). In order to reduce the matrix interferences, the final extract was diluted 1:10 (sample: water). The acquisition method was setup using the Pesticide Triggered MRM Database (tMRM) from Agilent Technologies using 2 transitions for each compound. Data analysis was conducted using MassHunter Qual/Quant software. In order to assess which extraction method produces best performance, quantification was performed by external standard

Figure 2. LC 1290 and 6470 LC/TQ.

Table 1. Instrument Conditions

LC		
Column: Zorbax Eclipse Plus C18 (2.1x50mm 1.8-Micron)		
Flow: 0.3 mL/min		
Injection volume: 10 µL		
Column Temperature: 30 °C		
Mobile Phase: A (Water - 0.1 % Formic Acid), B (Methanol).		
Time (minutes)	**% A**	**% B**
1.0	80.0	20.0
3.0	50.0	50.0
5.0	10.0	90.0
10.0	10.0	90.0
10.1	80.0	20.0
13.0	80.0	20.0
MS		
Gas Temp: 300 °C		
Gas Flow: 5 L/min		
Nebulizer: 45 psi		
Sheath Gas Heater: 300 °C		
Sheath Gas Flow: 11 L/min		
Capillary: 3500 V		

Results and Discussion

The conditions (Precursor ion, Fragments, Collision Energy, Fragmentor Voltage and Capillary Voltage) from the tMRM database were adequate to perform the quantitative analysis without further optimization and a Dynamic MRM (dMRM) method was used to obtain the maximum sensitivity from the instrument. The r^2 values obtained were higher than 0.990 for all measured compounds , over the calibration range from 1.0 ng/mL to 50 ng/mL.

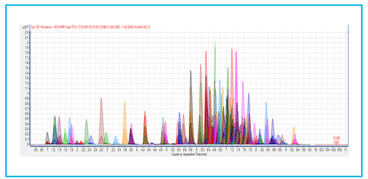

Figure 3. Chromatogram for 160 pesticides using dMRM method

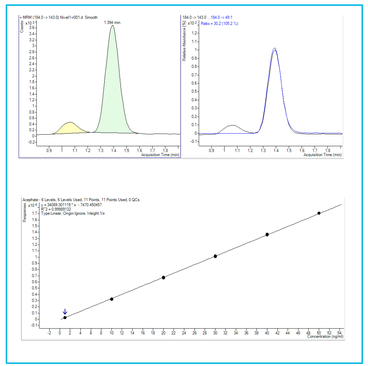

Figure 3. Chromatographic data and Calibration Curve for Acephate

In order to optimize the extraction and reduce matrix interferences, different QuECHERS methods and SPE cleanup kits were investigated. Table 2 contains the information about which QuEChERS Method and SPE gave the best results for each matrix.

Table 2. Sample preparation Kits for each matrix

SAMPLE TYPE	QuEChERS METHOD	SPE CLEAN UP
Apple	AOAC (5982-5755)	AOAC (5982-5021)
Orange	EN 15662 (5982-5650)	AOAC (5982-5021)
Guava	AOAC (5982-5755)	5982-5258
Mango	AOAC (5982-5755)	AOAC (5982-5021)
Tamarind	AOAC (5982-5755)	5982-5258

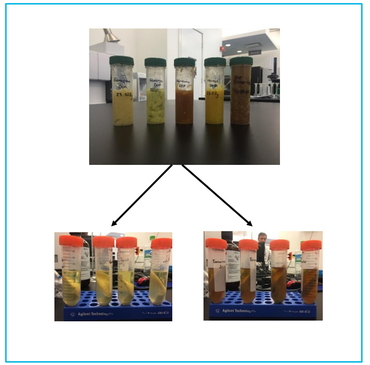

Figure 4. Sample Homogenization and Extraction.

In addition, as a strategy to reduce matrix interferences and in the case of polar pesticides which are marginally retained on the C18 column, a 1:10 dilution of the final extract produces improved chromatographic shapes.

Results and Discussion

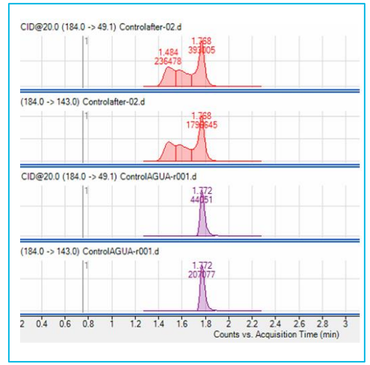

Figure 5. Chromatographic peak shape improvement with water dilution.

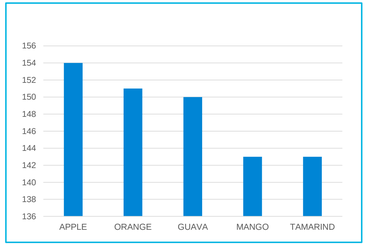

Figure 6. Number of pesticides with recovery between 70 – 120 %.

Conclusions

Three different procedures based on the QuEChERS method were compared for the determination of 160 pesticides including herbicides, fungicides and insecticides widely used in different matrices.

Most of the pesticides have recoveries in the range 70 – 120 % and precision (%RSD < 20), meeting the EU guidelines for method performance criteria.

Regarding the co-extraction of matrix components, this method provides cleaner chromatograms, better chromatographic shape for polar pesticides and less matrix interferences. In the case of pesticides with low recoveries, this methodology could be used as a screening method.

References

- L. Pareja et al., Talanta 83 (2011).
- I. Machado et al., Food Chemistry 227 (2017).
- SANTE/11945/2015.

Analysis of Mycotoxins in Food Matrices using the Innovative Ultivo Triple Quad LC/MS

Theresa Sosienski[1]; Dan-Hui Dorothy Yang[1]; Joan Stevens[2]; Christian Hegmanns[3]

[1]Agilent Technologies Inc., Santa Clara, CA; [2]Agilent Technologies Inc., Wilmington, DE; [3]Agilent Technologies Sales & Services GmbH & Co. KG, Waldbronn, BW

ASMS 2017
TP-197

Agilent
Trusted Answers

Introduction

Mycotoxins are compounds produced by fungi which grow on various crops ranging from grains to fruits, vegetables, nuts and spices. Mycotoxins can be harmful to humans and livestock through consumption of contaminated crops; therefore, mycotoxin levels are monitored in foods to minimize the risk of ingestion.[1] Regulatory agencies around the globe set Maximum Residue Limits (MRLs), which range from <10 to >500ppb to ensure harmful levels of mycotoxins do not enter the food supply. It is important to have the ability to detect and accurately quantify the mycotoxin contents at low levels across various food matrices, as each matrix composition poses different challenges in detection.

In this study, we demonstrate the accurate and sensitive quantification of up to 12 regulated mycotoxin compounds in three commonly regulated foods using the novel Ultivo triple quad LC/MS. (Figure 1)

Agilent Ultivo Triple Quad LC/MS

Figure 1: Ultivo Integrated into LC Stack

Ultivo is designed to address many of the challenges faced by labs performing environmental and food safety analyses.

Innovative technologies housed within Ultivo allowed us to achieve a reduced overall footprint, while conserving the performance found in many larger MS systems.

Innovations such as VacShield, Cyclone Ion Guide, Vortex Collision Cell and the Hyperbolic Quads maximize quantitative performance in a small package, enhancing instrument reliability and robustness resulting in greater uptime.

Ultivo reduces the need for user intervention for system maintenance, making it attractive to the non-expert MS user to operate and maintain.

MassHunter simplifies data acquisition, method setup, data analysis and reporting. This results in the fastest acquisition-to-reporting time possible, increasing lab productivity and confidence in results

Experimental

Sample Preparation

Corn, peanut, and black pepper were chosen as commonly regulated food crops of diverse matrix components for mycotoxins. 12 mycotoxins in corn and peanut matrices, and 5 mycotoxins in black pepper matrix were quantified using dynamic MRM in a 9 minute LC/MS/MS method. Mycotoxin standards were spiked into matrix extracts for analysis.

5g corn flour, 5g peanuts, or 2g black pepper were extracted with 10 mL of ACN, 10 mL H_2O and EN Extraction Salts (5982-5650). Dispersive SPE for fruits and vegetables (5982-5058) was used on corn, and a universal dispersive SPE kit (5982-0029) was used for black pepper. A novel modified lipid removal sorbent in flow through cartridge format was used on each matrix as a final clean-up step. Spiked black pepper extracts were diluted 30:70 extract/water prior to analysis.

Instrument Parameters

1290 Infinity II LC Parameters		
Column	Eclipse Plus C18 3.0 x 150 mm, 1.8µm	
Column temp	45°C	
Injection volume	2 µL Corn,Peanut; 10 µL Black Pepper	
Mobile phase	A: Water, 0.5mM NH_4F +5 mM NH_4 formate+ 0.1% Formic Acid B: MeOH, 0.5mM NH_4F +5mM NH_4 formate+ 0.1% Formic Acid	
Flow rate	0.450 mL/min	
Gradient	Time	B%
	0	30
	0.5	30
	7.5	100
	9.0	100
	9.1	30

Ultivo Triple Quad MS Parameters	
Drying gas temp	250 °C
Drying gas flow	8 L/min
Sheath gas temp	350 °C
Sheath gas flow	12 L/min
Nebulizer pressure	30 psi
Capillary voltage	3300 V(+); 2800 V(-)
Nozzle voltage	0 V(+); 0 V(-)
Cycle Time	500 ms

Table 1: LC and MS Parameters

Results and Discussion

Mycotoxin Signal Response

Excellent precision and sensitivity was attained for mycotoxins in various food matrices due to a combination of sample preparation techniques, LC separation, and the innovative technology in the Ultivo triple quadrupole mass spectrometer.

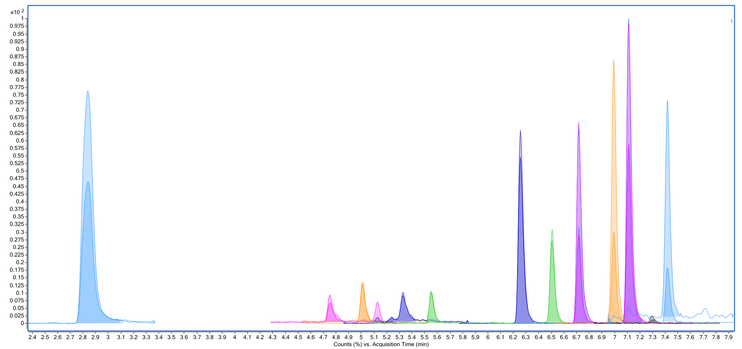

Figure 2: Excellent detection of mycotoxins in corn matrix at 1/10 assigned Maximum Residue Limit (MRL).

Mycotoxin Maximum Residue Limits and Sensitivity

Outstanding sensitivity was achieved, with the majority of the mycotoxin compounds in each matrix studied reaching a limit of quantitation (LOQ) at 1/20 the Assigned Maximum Residue Limit (MRL).

	European Union MRL for Mycotoxins. [2,3]			Assigned MRL level used for this study.	
Mycotoxin	Corn	Peanut	Black Pepper	Corn and Peanut	Black Pepper
Aflatoxin B1	2 ppb	2 ppb	5 ppb[a]	2 ppb	5 ppb
Aflatoxin B2	Sum of Aflatoxins: 4 ppb	Sum of Aflatoxins: 4 ppb	Sum of Aflatoxins: 10 ppb	2 ppb	5 ppb
Aflatoxin G1				2 ppb	5 ppb
Aflatoxin G2				2 ppb	5 ppb
Ochratoxin A	3 ppb	n/a	15 ppb[b]	3 ppb	15 ppb
Fumonisin B1	Sum of B1 and B2: 1000 ppb	n/a	n/a	500 ppb	Not included
Fumonisin B2				500 ppb	Not included
Fumonisin B3	n/a		n/a	500 ppb	Not included
Deoxynivalenol	750 ppb	n/a	n/a	75 ppb	Not included
Zearalenone	100 ppb	n/a	n/a	100 ppb	Not included
T-2 Toxin	n/a	n/a	n/a	100 ppb	Not included
HT-2 Toxin	n/a	n/a	n/a	500 ppb	Not included

Table 2: Maximum Residue Limits (MRLs) for mycotoxins used in this study. EU reg No. 1881/2006 and 105/2010 used for reference. All assigned MRLs in this study are equal to or lower than EU MRL.

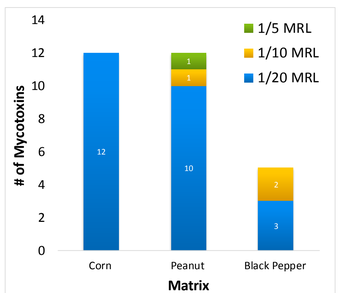

Figure 3: Quantitation limit for all mycotoxins studied in each matrix, defined as a fraction of the assigned MRL.

Results and Discussion

Precision and Linearity of Mycotoxin Compounds

Great accuracy was achieved for all compounds studied in each matrix, even in the complex black pepper matrix. Excellent linearity was achieved over each calibration range.

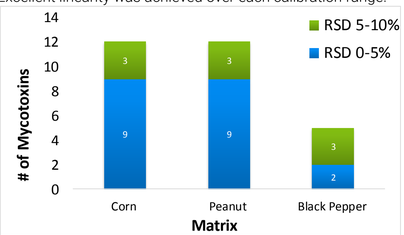

Figure 4: The mycotoxins show excellent precision in all three matrices, with all RSD<10% at LOQ.

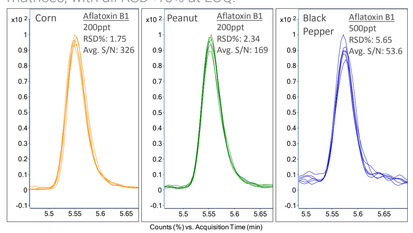

Figure 5: Excellent precision demonstrated for Aflatoxin B1 at 1/10 MRL (200 ppt or 500ppt) in all matrices.

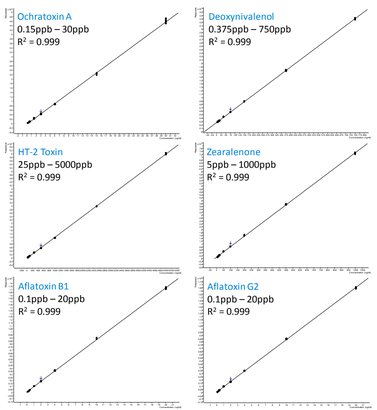

Figure 6: Exceptional linearity was demonstrated for all compounds, with R^2 values ≥0.99 for all compounds in all matrices. Pictured above, examples of excellent linearity for 6 selected compounds in corn matrix.

Conclusions

- Ultivo is an exceptionally innovative new mass spectrometer, which can minimize laboratory workspace needs, as well as reducing maintenance challenges, creating a productive work environment for high throughput laboratories.
- Ultivo is a small but powerful tool enabling the accurate and sensitive detection of commonly regulated mycotoxins in various food matrices well below set MRL levels.
- Agilent MassHunter software provides an easy to use, all-inclusive tool for managing and reporting LC/MS data.

References

[1] Bennett JW, Klich M. Mycotoxins. Clinical Microbiology Reviews. 2003;16(3):497-516. 2003.
[2] Commission Regulation (EC) No 1881/2006. Setting maximum levels for certain contaminants in foodstuffs. Official Journal of the European Union. L 364/5-24. 19 December 2006.
[3] Commission Regulation (EU) No 105/2010. Amending Regulation (EC) No 1881/2006 setting maximum levels for certain contaminants in foodstuffs as regards ochratoxin A. L 35/7-8. Official Journal of the European Union. 5 February 2010

Simultaneous determination of 16 mycotoxins in cereals using stable isotope labeled internal standards and e-Method by UHPLC-MS/MS

Jin Ye[1], Yu Wu[1], Songxue Wang[1], Qilei Guo[2], Jianzhong Li[2], Tao Bo[2]

[1]Academy of State Administration of Grain, Beijing, China;

[2]Agilent Technologies. Inc., Beijing, China

ASMS 2017
TP - 203

Introduction

Mycotoxins are toxic secondary metabolites of fungi, which can occur in various cereals, including corn, wheat, and barley. Due to the complexity of food matrices and structural diversity of mycotoxins, their simultaneous and sensitive analysis is rather challenging. In this study, a rapid UHPLC-MS/MS technique with excellent sensitivity and good repeatability for sixteen mycotoxins in cereals was developed. Matrix effects observed during electrospray ionization are compensated for by addition of stable isotope labeled mycotoxins as internal standards.

A homogenous sample is extracted by acetonitrile-water-acetic acid (70:29:1, v/v/v). After centrifugation, the extract is diluted with water, centrifuged at low temperature and filtered. The final solution is mixed with isotope-labeled internal standard solution and determined by ultra-high performance liquid chromatography and triple-quadrupole mass spectrometry.

This article describes a plug-and-play solution for international validation of mycotoxin testing. e-Methods make it easier to share methods between instruments worldwide, without the tedious process of entering all the parameters each time. It makes the LC-TQ method simpler and easier-to-use.

Experimental

Sample Preparation

Weighed 5 g of sample into a 50 mL centrifuge tube with screw cap. Added 20 mL extraction solvent, closed the tube and mixed with a vertex shaker for 1 min. Placed the sample on a rotary shaker for 30 min, followed by centrifuging @ 3,500g for 5 min. Added 0.5 mL supernatant into a 1.5 mL centrifuge tube, diluted with 0.5 mL water and placed on a vertex shaker for 1 min. Then centrifuged at 7200 g for 10 min and 4 °C. The supernatant was filtered through a 0.22 μm PTFE filter.

Transferred an 180 μL aliquot of the filtrate, blanks or standard solutions into 400 μL micro-inserts (in the sample vials) containing 20 μL of the ISTD working solution. It is critical to use the same ISTD working solution as used in the preparation of the standard curve. Capped and mixed. Injected the 2 μL into the UHPLC-MS/MS system.

Experimental

Materials and Instrumentation

All mycotoxin analytical standards were purchased from Romer Lab, in methanol, acetonitrile or water/acetonitrile (1:1, v/v). Ammonium acetate, acetic acid and formic acid were acquired from Dikma Technologies Inc. LC/MS grade methanol and acetonitrile were purchased from Merck. Purified water was obtained by a Millipore Milli-Q system. Samples were provided by the Chinese Academy of State Administration of Grain.

Agilent 1290 Infinity LC system: G4220A Binary Pump, G4226A Sampler, G1326C TCC with heat exchanger G1316-80002/3. Agilent 1290 Infinity II LC system: G7120A High speed Pump, G7167A Multisampler, G7116B MCT with heat exchanger G7116-60015. Agilent 6460/6470/6490/6495 Triple Quadrupole LC/MS system.

LC Conditions

Column	ZORBAX Eclipse Plus C18 (2.1 x 100 mm, 1.8 μm)
Flow rate	0.3 mL/min
Column Temperature	35 ℃
Injection	2 μL
Needle wash	H_2O-Methanol-Acetonitrile-IPA (1:1:1:1, with 0.1% Formic acid)
Mobile phase	A: H_2O with 0.5% Acetic Acid and 2.5 mmol/L Ammonium Acetate; B: Methanol with 0.01% Formic Acid Gradient Elution

MS Conditions

Positive and Negative ESI with Agilent Jet Stream		
Equipment	6460/6470	6490/6495
gas temperature	300 ℃	150 ℃
Gas flow	7 L/min	15 L/min
Nebulizer pressure	35 psi	35 psi
Sheath gas temperature	350 ℃	370 ℃
Sheath gas flow	11 L/min	12 L/min

Results and Discussion

Method Optimization

In the positive ionization mode, the $[M+H]^+$ species produced the most abundant precursor ion except for 15-AcON, T-2 and HT-2 toxin, which were analyzed as the $[M+NH_4]^+$ species. For ZEN, the highest sensitivity could be achieved in negative ionization mode, with $[M-H]^-$ as the precursor. The $[M+CH_3COO]^-$ moiety was chosen as the precursor ion for NIV, DON and DON-3G, when acetic acid was used in mobile phase.

MRM Transitions and Conditions

Compound	Prec. Ion	Prod. Ion	Frag. (V)	CE (V)	+/-
[^{13}C]-NIV	386	295.1	90	10	-
NIV	371	281.1/59.1	90	10/30	-
[^{13}C]-DON	370.1	279.0	90	10	-
DON	355.1	265.0/247.0	90	10/10	-
DON-3G	517.1	427.0/247.0	120	20/20	-
15-AcDON	356.1	261.0/137.0	90	15/15	+
[^{13}C]-3-AcDON	356.2	245.1	110	10	+
3-AcDON	339.2	231.1/213.1	110	10/20	+
[^{13}C]-AFB_1	330.1	301.1	160	21	+
AFB_1	313.2	285.1/241.1	160	22/38	+
[^{13}C]-AFB_2	332.2	303.0	160	21	+
AFB_2	315.2	287.1/259.1	160	24/30	+
[^{13}C]-AFG_1	346.1	257.1	150	25	+
AFG_1	329.2	311.1/243.1	150	20/25	+
[^{13}C]-AFG_2	348.1	330.1	160	23	+
AFG_2	331.2	313.1/245.1	160	23/30	+
[^{13}C]-FB_1	756.5	356.4	180	45	+
FB_1	722.4	352.3/334.3	180	45/45	+
[^{13}C]-T-2	508.3	322.1	110	10	+
T-2	484.3	305.1/185.1	110	10/20	+
[^{13}C]-HT-2	464.1	278.1	100	10	+
HT-2	442.2	263.1/215.1	100	10/10	+
[^{13}C]-FB_2	740.5	358.3	180	45	+
FB_2	706.5	336.3/318.3	180	45/45	+
[^{13}C]-OTA	424.2	250.1	120	25	+
OTA	404.1	358.0/239.0	120	10/25	+
[^{13}C]-ST	343.1	327.1	150	20	+
ST	325	310.0/281.0	150	20/36	+
[^{13}C]-ZEN	335.2	185.0	190	25	-
ZEN	317.1	175.0/130.8	190	25/33	-

A new multi-target UHPLC/MS/MS method for the screening and quantitation of mycotoxins was developed using the 1290 Infinity UHPLC System coupled to an Agilent Triple Quadrupole Mass Spectrometer. Due to the large number of analytes and the expected matrix load caused by the crude solvent extraction, a column length of 100 mm and a total runtime of 22 minutes were chosen. By having a flattened gradient in the run, a better separation of the analytes was achieved. Figure 1 shows the chromatogram of a calibration sample including all 16 mycotoxins and their internal standards. To minimize the amount of matrix going into the spray chamber, the HPLC flow was diverted to waste for the first 1.8 minutes of the analysis, then again from 18 minutes until the end of the analysis.

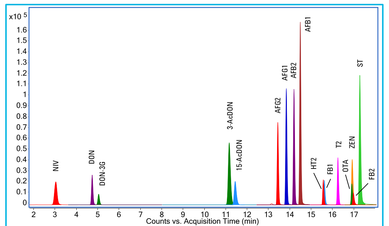

Figure 1. Separation of 16 mycotoxins under optimized UHPLC-MS/MS conditions. 12 compounds were analyzed in the positive ionization mode and the other 4 compounds were analyzed using negative ionization.

In this method, chromatographic resolution was maximized through use of a ZORBAX Eclipse Plus column. Baseline separation of 3-AcDON and 15-AcDON was achieved under the optimized conditions. It is important since they are isomers and share identical MRM transitions. Improved chromatographic resolution minimizes matrix effects, allowing for injection of 2 μL of raw extract without further dilution or cleanup.

Fast polarity-switching was used for this method, since ZEN eluted in the same time segment as OTA and FB_2. This can be done by using MRM with time segmentation, affording the measurement of each mycotoxin in a single analytical run and in the ionization mode that produces optimal sensitivity.

Results and Discussion

Method Performance Characterization

Figure 2 shows the exemplary calibration curves for the internal standard calibration of DON, AFG_1, OTA, and ZEN. The relevant concentration ranges are different for the individual mycotoxins depending on the maximum limits specified in current legislation. The method allows the reliable determination of calibration standard of AFB_1 down to 0.075 μg/kg, while for NIV, DON, Fumonisins, and ZEN, for which higher maximum limits are specified, the upper limit of quantitation is in a range of up to several hundreds of μg/kg, which allows direct analysis even beyond the regulatory limit without further dilution.

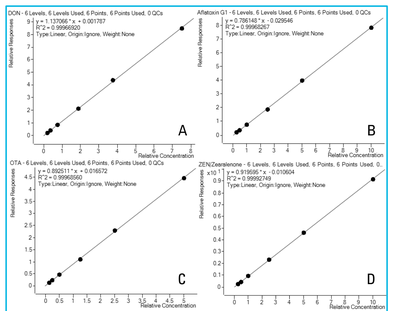

Figure 2. Example calibration curves for the internal standard calibration of DON(A), AFG_1(B), OTA(C), ZEN(D) using solvent standards, linear fits R^2≥0.9996.

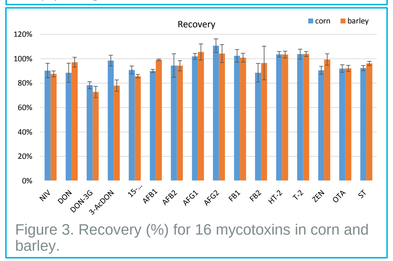

Figure 3. Recovery (%) for 16 mycotoxins in corn and barley.

Application of e-Method

Agilent provides e-Methods, a plug-and-play solution for international validation of mycotoxin testing methods. e-Methods make it easier to share methods between instruments worldwide, without the tedious process of entering all the parameters each time the method is ported. e-Method includes three parts; acquisition and quantitative methods, as well as a user guide.

The e-Method can be downloaded directly through the link in the Application Note 5991-7862CHCN from the Agilent Web site. Using the “Open Method” MassHunter Acquisition software feature, one can load the complete method; including all LC and MS set-points (the calibration table is a component of the quantitative method). The user guide is provided for the method developer to update the acquisition method and quantitative method, including updates of retention times and qualifier ratios.

e-Method can be distributed over the web, by e-mail, or on storage media. Installation takes just a minute or so. As such, it makes the LC/TQ method simpler and easier-to-use.

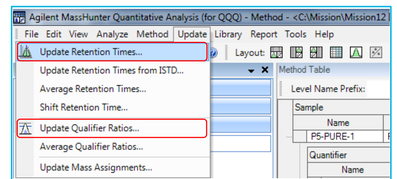

Figure 4. Update retention time and update qualifier ratios feature of MassHunter Quantitative software.

Conclusions

- A sensitive, rapid and accurate method for the determination of 16 mycotoxins was presented.
- Ion suppression was compensated for by addition of ^{13}C-labeled ISTDs after sample extraction.
- e-Method, a plug-and-play solution, benefits from the sensitivity and robustness of the Agilent Triple Quadrupole LC/MS system and from the powerful functionality of Agilent MassHunter Software.

For Research Use Only. Not for use in diagnostic procedures.

Multi-Residue Pesticide Analysis in Food Matrices Using Ultivo Triple Quad LC/MS

Dan-Hui Dorothy Yang[1], Theresa Sosienski[1], Joan Stevens[2], Patrick Batoon[1]

[1]Agilent Technologies, Inc., Santa Clara, CA; [2]Agilent Technologies, Inc., Wilmington, DE

ASMS 2017
TP-208

Agilent
Trusted Answers

Introduction

Pesticides are vital to the success of crop production. Regulatory agencies have set maximum residue levels (MRLs) for hundreds of pesticides and their metabolites in foods. Most MRLs are set at low ppb levels, posing significant challenges to screen and quantify hundreds of analytes in complex food matrices simultaneously.

In this presentation, we demonstrate the screening and quantitation for 246 pesticides and metabolites using Ultivo Triple Quad LC/MS (Figure 1).

Ultivo is designed to address many challenges faced by routine production labs, especially in the environmental and food safety arenas. Innovative technologies within Ultivo allowed us to reduce its overall footprint, while conserving the comparable performance level of much larger MS systems. Innovations, such as VacShield, Cyclone Ion Guide, Vortex Collision Cell and the Hyperbolic Quads, not only maximize quantitative performance in a small package, but also enhance instrument reliability and robustness, which promote greater uptime. Moreover, Ultivo reduces the need for user intervention for system maintenance, making the system operation and maintenance manageable for non-expert MS users. MassHunter Software simplifies data acquisition, method set up, data analysis and reporting, which results in the fastest possible acquisition-to-reporting time, increasing lab productivity.

Figure 1. Ultivo Triple Quad LC/MS

Experimental

Sample Preparation

246 pesticides are detected in matrices using a dynamic MRM (dMRM) method. Orange, avocado, and black tea were chosen to represent most fruits, vegetables, and dried herbs. 10 grams of organic orange/avocado and 2 grams of organic black tea were extracted with 10 mL of ACN and EN Extraction Salts (5982-5650). Dispersive SPE for high pigment (5982-5356CH) was used on black tea; modified EMR-Lipid was used on avocado and PSA containing kit was used on orange (5982-5058).

LC and Mass Spectrometer parameters

The LC and MS parameters are listed in Table 1 and 2.

Table 1. LC Conditions

Column	Eclipse Plus C18 3.0 x 150 mm, 1.8µm	
Column temp	45°C	
Injection volume	2 µL	
Mobile phase	A: Water, 0.5mM NH_4F +4.5mM NH_4 formate+ 0.1% Formic Acid B: MeOH, 0.5mM NH4F +4.5mM NH4 formate+ 0.1% Formic Acid	
Flow rate	0.45 mL/min	
Gradient	Time	B%
	0	2
	0.5	2
	1	50
	4	65
	16	100
	18	100
	18.1	2
Stop Time	20min, Post Time 1.5min	

Table 2. MS Parameters

Drying gas temp	250 °C
Drying gas flow	11 L/min
Sheath gas temp	350 °C
Sheath gas flow	12 L/min
Nebulizer pressure	40 psi
Capillary voltage	3500 V(+); 3500 V(-)
Nozzle voltage	300 V(+); 1000 V(-)
Delta EMV	200 V(+); 200 V(-)
Cycle Time	800 ms

Results and Discussion

Instrument Performance

The signal response of Ultivo was outstanding due to the technological innovations as illustrated in Figure 1 and 2.

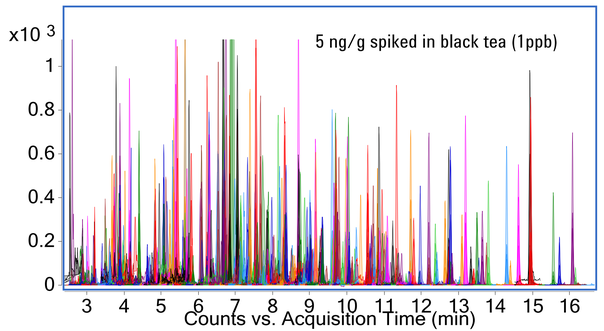

Figure 2. Outstanding signal response of 5 ng/g spike in Black Tea matrix (1ppb)

Sensitivity and Precision

Most of the compounds could be detected far below MRL with accuracy of 80-120% for at least 4 out of 6 replicates. The precision was excellent, with %RSD less than 10% for most of the compounds at the LOQ as shown in Figure 3, 4.

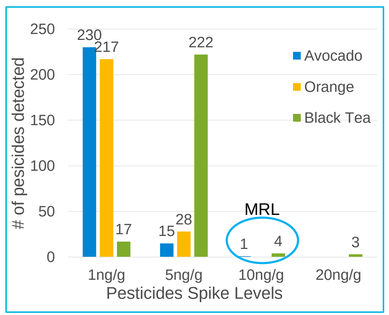

Figure 3. Outstanding sensitivity: Most of compounds could be accurately detected far below MRL (one compound was not detected in orange due to matrix interference).

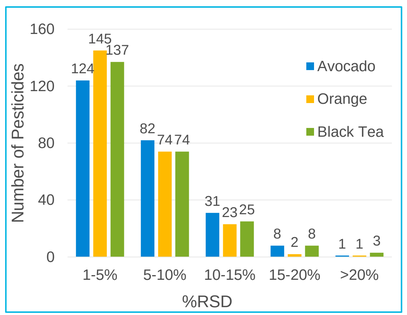

Figure 4. Excellent precision: most of compounds had %RSD less than 10% at the lowest quantitation level (n=6) without any outlier rejection.

Results and Discussion

Real World Samples Analysis: Non-Organic Orange and Avocado

Non-organic orange and avocado were acquired from a local market and processed as organic matrices. Most of the calibration curves had R^2 > 0.99, allowing accurate quantitation of samples. No pesticides could be detected in non-organic avocado, while 3 pesticides were detected in non-organic orange above MRL (Figure 5).

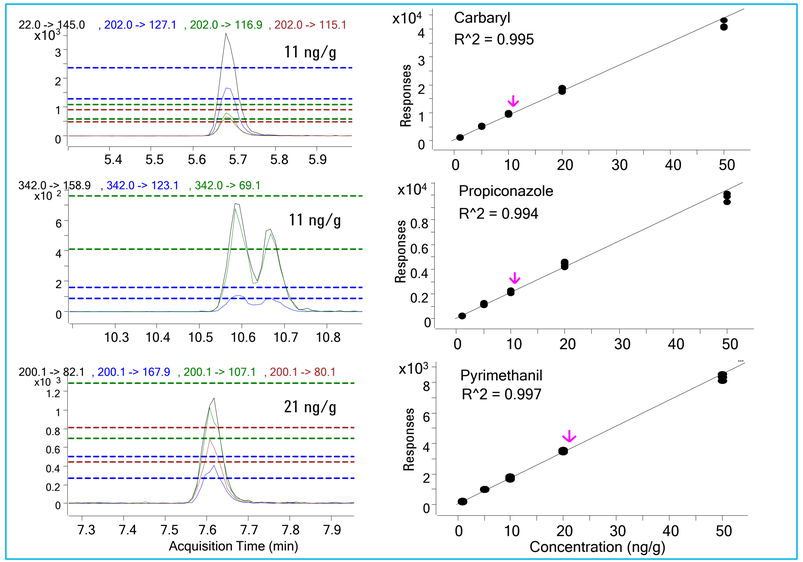

Figure 5. Pesticides detected above MRL in non-organic orange

Conclusions

- Ultivo Triple Quad LC/MS delivers the ultimate performance of an analytical instrument with a minimized footprint.
- Technological innovations within Ultivo afford optimal sensitivity, robust detection and easy maintenance; thereby improving productivity and confidence in results.
- Ultivo provides significant advantages in routine production testing laboratories with enhanced capabilities for non-expert LC/MS users.
- Agilent total workflow solutions that include sample preparation, databases, methods and reporting facilitate fast method development and validation in food safety and environmental analyses.

FORENSIC TOXICOLOGY

Development of Succinylcholine Chloride in Biologic Extracts Using Liquid Chromatography Triple Quadrupole Mass Spectrometry

Dai-Yong Huang[1], Jun-Gang Lu[2], Cai-Yong Lin[2], Zhi-Quan Yuan[2], Shan-An, Chan[3]
[1]Agilent Technologies, Inc. Hong Kong, China; [2]Agilent Technologies, Inc. Guangzhou, China;
[3]Agilent Technologies, Inc, Taipei, Taiwan

ASMS 2017
TP-241

Agilent
Trusted Answers

Introduction

Succinylcholine chloride is a medication used as part of general anesthesia for short-term paralysis, to help with tracheal intubation or electroconvulsive therapy. Since it is quickly degraded by plasma butyrylcholinesterase and the duration of the therapeutic effect is usually in the range of a few minutes, it has been described as a "perfect poison" for murder and has been used by criminals for this purpose. As a result, a highly sensitive and reliable method must be developed for its detection and that where LC/TQ provides a perfect solution. Since succinylcholine is highly polar (refer to the structure shown below), hydrophilic interaction (HILIC) liquid chromatography is used for the separation of succinylcholine from the plasma matrix.

Another important point concerning forensic analysis is that, a blank sample is required in legal cases as it contributes to clarification of the method reliability. Since succinylcholine chloride is a quaternary ammonium salt, it can easily attach to the surface of stainless steel. When a sample or standard sample containing succinylcholine chloride is injected into an LC system, it may take hours or even days for clean-up. In our study, a background check has been processed and a special wash method is implemented, reducing the duration of clean-up significantly.

Moreover, the stability of succinylcholine has been studied as additional information.

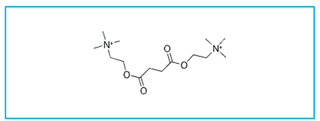

Figure 1. Structure of Succinylcholine

Experimental

Sample Preparation

Add 100 µL sample on to
Captiva ND^{Lipids} Filter Cartridge
↓
Add 300 µL acetonitrile and mix
↓
Precipitation and Filtration
↓
Injection into LCMSMS

Equipment and conditions

LC conditions

HPLC system	1290 II Binary Pump UHPLC
LC column	Xbridge BEH Amide (2.1×100 mm, 3.5 µm)
Mobile phase	Phase A: 0.2% Formic Acid and 40 mM Ammonia Formate in H2O. Phase B: Acetonitrile
Gradient program	0 min, 95% B; 1 min, 95% B; 5 min, 45% B; 10 min, 45% B
Injection volume	1 µL
Flow rate	0.5 mL/min

MS conditions

Mass system	Agilent 6470 LC/TQ
Ion source & Polarity	ESI with AJS, Positive mode
Parent Ion	145.1
Quant. / Quali Ions	115.5 / 93.6
Nebulizer gas	N2 @ 45 psi
Drying gas	N2 @ 10 L/min @ 250 ºC
Sheath gas	N2 @ 11 L/min @ 200 ºC
Capillary voltage	3500 V
Nozzle voltage	300 V

Results and Discussion

Column and mobile phase selection

As succinylcholine is highly polar, it cannot be retained by common C18 packing columns. In this study, one amide column is selected, and a hydrophilic interaction (HILIC) separation mode is used. And usage of a high concentration of ammonium salt is applied to elute succinylcholine from the column, as well as to modify peak shape. With the LC method modification, succinylcholine can be retained more than 4 minutes, which means a good separation of matrix to minimize matrix effects. The resulting peak width at half height of succinylcholine is 3.96 seconds and the peak tailing factor is only 1.2. The chromatogram of succinylcholine is shown below.

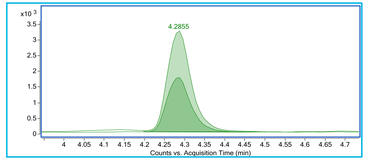

Figure 2. MRM Chromatogram of Succinylcholine

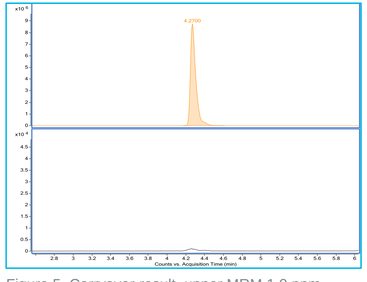

Figure 5. Carryover result, upper MRM 1.0 ppm Succinylcholine standard. The lower pane is a blank injection immediately after the 1.0 ppm Succinylcholine standard injection.

Sensitivity

A high analytical sensitivity method is critical for succinylcholine detection, since it may be required if a murder has occurred, and the compound is quickly degraded by plasma butyrylcholinesterase. After method development and with the analytical power afforded by the Agilent 6470 LC/TQ system, the detection limit of succinylcholine was determined to be 0.2 ng/mL with a 1 µL injection; that is 0.2 fg on column, and the calculated signal to noise ratio (peak-to-peak) is 54. The result is shown as in Figure 3.

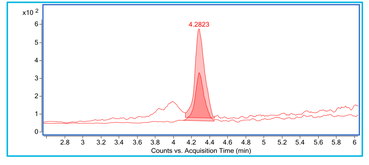

Figure 3. Performance of 0.2 ng/mL standard

Quantitation

For all forensic analysis, quantitation is as important as qualitative analysis. In this study, 9 calibration levels ranging from 0.2 ng/mL to 100 ng/mL, with 3 replicates for each level, was constructed. The correlation coefficient r^2 was 0.997 and the relative standard deviation (%RSD) range is from 0.28% to 2.41%. The calibration curve with standard deviation bars is shown as below:

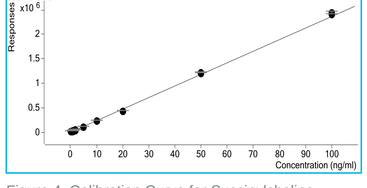

Figure 4. Calibration Curve for Succinylcholine

Results and Discussion

Clean-up Process for LC system

In the field of forensic analysis, a complete set of validated data must be provided as evidence in court. The data set must include: blank samples, standards, QC samples, carryover checks and case samples. The failure to provide reliable data will led to the failure of sentencing, which has occurred in China. The case commonly known as "Nian Bin Case", in which the lawyer challenged the forensic analysis data because it lacked a reliable blank sample. In this instance, a positive result was obtained due to the contamination of the sample during analysis.

As structure shown in Fig. 1, succinylcholine is a quaternary ammonium salt and it easily adheres to stainless surfaces in LC system. Once succinylcholine is injected into the LC system, false positives may appear for subsequent samples. So a powerful clean-up method is essential for succinylcholine detection.

In order to solve the carryover problem, first the source of contamination must be identified. First-pass, we suspect the source to be either the needle, or needle seat in auto-sampler. The rationale is that they directly contact the samples containing succinylcholine and may contaminate other samples. To solve the problem, an add-on kit called "Multi-Wash" is installed on the auto-sampler; this kit is designed to eliminate carryover. Also, we can either reduce the carryover by washing the outer needle surface with the choice of three different wash solvents, or backflush the needle seat and the rotor seal with the appropriate solvents or both. In this case, the three solvents used are Agilent HPLC flushing solvent, organic solvent mix and a high concentration buffer.

With the use of Multi-Wash, carryover can be significantly lowered, but trace carryover still persisted. After investigation, we suspect that it may arise from the stainless material used in injector valve. So an injection program is integrated into the analysis method. The program includes switching the injector valve several times and performing multiple injections of high concentration buffer solution. The resulting chromatogram is shown in Fig 5. The upper MRM chromatogram is the quantitation ion from a 1.0 ppm standard. The pane below is analysis of a blank sample immediately following analysis of the 1.0 ppm standard injection to check for carryover.

Further Confirmation by tMRM

For forensic analysis, positive confirmation is as important as elimination of false positives. As per the EU Directive 2002/657/EC, two MRMs data displaying proper ratio criteria is acceptable. In real cases, matrix effects may cause complications, which affect MRM ratios. In these cases, further confirmation can be provided by tMRM function, shown as follows:

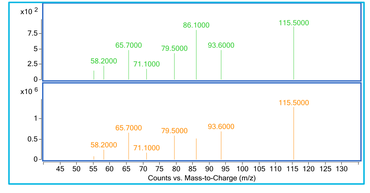

Figure 6. MRM spectra from 1 ng/mL and 100 ng/mL

Conclusions

In this study, a comprehensive solution for succinylcholine detection is provided, taking into the consideration of the compound property and the facing problem in real-life criminal investigation. And it can be summarized like this:

- HILIC chromatography mode can provide a better separation of succinylcholine from matrix components with symmetrical peak shape.
- The calibration range for succinylcholine is 0.2 fg to 100 fg on-column.
- The combination of "Multi-Wash" and a injection program as part of the analysis method can remarkably decrease the carryover of succinylcholine.
- tMRM can increase confidence in the analytical results.

INSTRUMENTATION

Improving Quadrupole Performance with a Thin DC Only Quadrupole Prefilter: Achieving High Performance in Tandem Mass Spectrometers with Reduced Size

Laura L. Pollum, Haopeng Wang, Kenneth R. Newton, James L. Bertsch, Shane E. Tichy

Agilent Technologies, Santa Clara, CA

ASMS 2017
ThP-380

Agilent
Trusted Answers

Introduction

Prefilters enhance quadrupole sensitivity

Ion transmission efficiency at unit resolution can be enhanced by augmenting the fringe field region of a quadrupole mass filter. A conventional RF-only Brubaker prefilter modifies this fringe field region by applying the filtering RF to four quadrupole rods placed adjacent to the filtering quadrupole to create a delayed DC ramp. Alternatively, a similar enhancement of ion transmission efficiency can be achieved by partially cancelling the quadrupole DC field in the fringe field region, see Ref 1. This can be achieved by applying cancelling DC voltages (±W) to a thin quadrupole lens positioned directly before the filtering quadrupole, as shown in Figure 1.

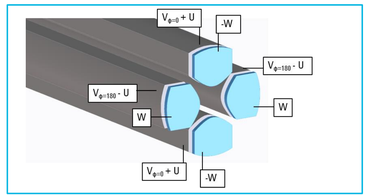

Figure 1. DC prefilter (blue) adjacent to a quadrupole. V and U are the filtering RF and DC voltages, respectively, applied to the quadrupole.

Here, we report the characterization of our thin DC-only prefilter, which is a key component in Agilent Technologies new reduced size triple quadrupole LC/MS system, the Ultivo (Figure 2). The size reduction between Brubaker prefilters and thin DC-only prefilters enables high performance within a compact instrument footprint.

Figure 2. Agilent's Ultivo triple quadrupole LC/MS.

Instrumentation

The DC prefilter is a key part of Agilent's Ultivo.

After ions are created in an atmospheric pressure ion source, they pass through a sampling capillary and skimmer before reaching a novel multipole ion guide called the Cyclone, as shown in Figures 3 and 5.

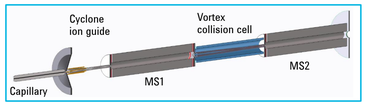

Figure 3. Simplified ion optics of Agilent Technologies Ultivo triple quadrupole LC/MS. DC pre- and postfilters shown in red. ±10 kV HED and electron multiplier not shown (right hand side).

The Cyclone ion guide compresses and collimates the ion beam using two superimposed twisted and tapered hexapoles that pass through several vacuum stages. The inner hexapole receives two out of phase (φ = 0° and 180°) RF voltages at 9 MHz, which allow transmission of low mass ions. One phase of 1 MHz RF voltage is applied to the short outer hexapole, which improves high mass transmission at the Cyclone entrance. The taper causes compression of the ion beam, and the twist enables a greater pressure drop over a shorter length by allowing smaller openings between the vacuum stages. A DC bias along the inner rods gently pulls the ions through the device. See Refs 2 and 3.

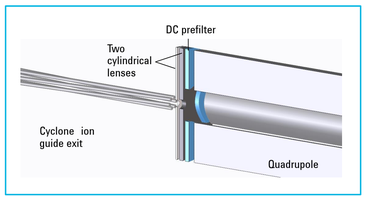

Figure 4. DC prefilter positioned between ion guide exit and quadrupole entrance

Upon exiting the Cyclone ion guide, the ions pass through two cylindrical lenses before reaching a DC prefilter (also called a Virtual prefilter) and entering the first quadrupole, as shown in Figure 4.

Instrumentation

A DC postfilter follows the first quadrupole. Two cylindrical lenses follow the MS1 postfilter and enable efficient ion injection into the Vortex collision cell shown in Figures 3 and 5.

The Vortex collision cell is made of a tapered and twisted hexapole surrounded by a shroud to contain nitrogen, the collision gas. The taper enables ion beam compression, and the twist reduces the gas flow out of the cell while maintaining a large opening to collect ions exiting MS1. A DC bias along the rods gently pulls the ions toward the second quadrupole. Two cylindrical lenses follow the vortex collision cell.

Figure 5. Cyclone ion guide (left) and Vortex collision cell with rods shown in blue.

The second filtering quadrupole is preceded by a DC prefilter. After MS2, the ions reach a detector assembly made of a cylindrical lens followed by a ± 10 kV high energy dynode and an electron multiplier.

Method

The DC prefilter was characterized using ion trajectory modelling and experiments.

Ion trajectory modelling was also used to characterize the performance of the DC pre- and postfilters. 3D models of MS1 were created in Simion test release version 8.1 in early access mode to enable multi-core parallel computations, see Ref 4. Simulated ions were generated in the low pressure exit of the Cyclone ion guide, where they were thermalized with a low pressure background gas. The ions passed through two cylindrical lenses before reaching the DC prefilter, the filtering quadrupole, a DC postfilter, two more cylindrical lenses, and finally a simulated ion detector (in place of the Vortex collision cell). The simulated quadrupole was tuned to yield approximately unit resolution (0.7 m/z FWHM), and the resulting simulated abundance and peak width were recorded during mass scans 3 m/z wide centered at 118, 622, 1222 Th. The percent of ions transmitted through the MS1 optics (abundance analogue) and peak width were recorded as a function of the two DC voltages applied simultaneously to both the pre- and postfilter.

Method

To experimentally characterize the DC pre- and postfilters, opposing elements of the DC prefilter were shorted together, and the resulting electrode pairs were connected to two ± 600 V DC voltage supplies. Resulting ion abundances and peak widths for Agilent Technologies ESI-L tuning mix ions (approx. m/z/: 118, 322, 622, 922, 1222) ionized using an Agilent JetStream ion source were recorded at various combinations of voltages applied to the DC prefilter. Performance of the MS1 DC prefilter, MS1 DC postfilter, and MS2 DC prefilter were investigated.

Results and Discussion

Ion trajectory modelling and experiments show ion transmission enhancement when cancelling DC voltages are applied to the DC-only prefilter.

The results of ion trajectory modelling through a simulated MS1 assembly with DC pre- and postfilters are shown in Figure 6.

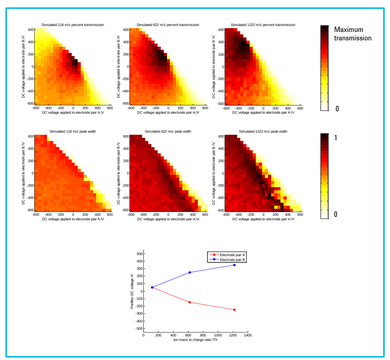

Figure 6. Simulated MS1 normalized percent ion transmission (upper) and peak FWHM (middle) as a function of two DC voltages applied simultaneously to the pre- and postfilter for ions of increasing m/z. The inset plot shows the voltages required to achieve maximum ion transmission for each m/z.

Results and Discussion

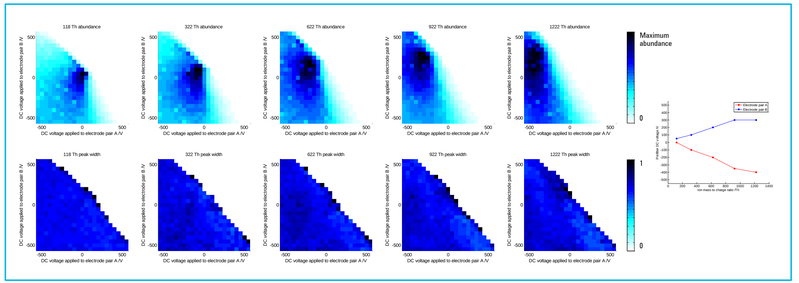

Figure 7. Experimental MS2 abundance (upper) and peak FWHM as a function of two DC prefilter voltages for ions of increasing m/z. The inset plot shows the voltages required to achieve maximum ion transmission for each m/z.

Maximum ion transmission is achieved when the DC applied to each prefilter element is the opposite polarity of the filtering DC applied to the quadrupole rod. Additionally, increasingly large DC voltages are required to maximize ion transmission as the ion m/z increases, as is shown in the inset plot. Minimal effect on peak width is observed as the pre- and postfilter voltages are changed indicating that the DC prefilter enhances the ion transmission efficiency without loss of resolution.

Figure 7 shows experimental results for the MS2 prefilter. These experimental results are similar to what was observed in the in the MS1 pre- and postfilter ion trajectory modelling shown in Figure 6. Maximum ion transmission is achieved when the DC applied to each prefilter element is opposite in polarity to the filtering DC applied to the quadrupole rod. Additionally, increasingly large DC voltages are required to maximize ion transmission as the ion m/z increases. Minimal effect on peak width is observed as the prefilter voltages are changed indicating that the DC prefilter enhances the ion transmission efficiency without loss of resolution.

Similar data were recorded for the MS1 prefilter and MS1 postfilter. The data are not presented here, but their performance shows similar trends to those presented.

Conclusions

Data presented here demonstrate that DC (Virtual) prefilters can be used to enhance ion transmission efficiency at unit resolution in a quadrupole mass filter by partially cancelling the DC field in the fringe field region. A primary advantage of the DC-only prefilters is their small size when compared to traditional Brubaker RF-only prefilters, which makes them an ideal component for miniaturized and small footprint instruments. These DC-only pre- and postfilters are a key component of Agilent's new reduced size yet high performance Ultivo triple quadrupole LC/MS.

References

[1] Brubaker WM. Proc. 6th Internl. Vacuum Congr. 1974 Japan J. Appl. Phys. Suppl. 2, Pt 1, 1974

[2] Bertsch JL, Newton KR, Howard L. US Patent No. 9,449,804 B2. Sep. 20, 2016.

[3] Wang H, Pollum LL, Newton KR, Bertsch JL, Tichy SE. ASMS Annual Conference 2017. TOG am 08:30

[4] http://simion.com

Use of Methylamine PICI for Qualitative Analysis by GC/Q-TOF

Ryo Ogasawara, Sadao Nakamura
Agilent Technologies Japan, Hachioji-shi, Tokyo

ASMS 2017
MP-272

Agilent
Trusted Answers

Introduction

The demand for comprehensive qualitative analysis by GC/MS is increasing in all fields. In general, EI mass spectrum libraries are used for qualitative analyses by GC/MS, but there are many compounds that do not provide a hit in commercially available libraries.

GC/Q-TOF, with high resolution and MS/MS capabilities, has excellent qualitative abilities for such unknown compounds by utilizing positive ion chemical ionization (PICI). An ideal PICI trait is that protonated molecule and/or cationized molecules can appear and be identified in many compounds. The outline of a typical qualitative workflow by GC/Q-TOF is shown in Figure 1.

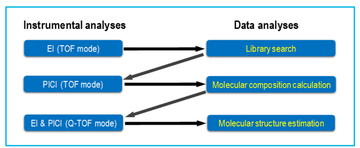

Figure 1. GC/Q-TOF qualitative workflow.

Methane, isobutane and ammonia are generally used as reagent gas, but protonated molecule and cationized molecules can not necessarily be obtained. Although it is known that amines have the possibility of being a very soft PICI reagent gas at the research level[1)], it is not very practical. We confirmed that 2% methylamine (MA) in methane is easy to obtain cationized molecules even in compounds that are difficult with other reagent gases[2)].

In this study, 2% MA in methane as well as pure methane were applied to commercially available insecticide, and many qualitative compound aspects could be obtained.

Experimental

Spray-type liquid household insecticide (0.5 mL) was collected in a sample vial. Acetone was added to make 1mL to use as the analytical sample.

Analysis was performed by Agilent 7200B GC/Q-TOF combined with Agilent 7890B GC. The analytical conditions are described in Table1.

Experimental

Gases in the cylinder were purchased and used as reagent gas (Takachiho Chemical Industrial, Tokyo, Japan). The flow rate of 2% MA in methane is the value optimized in the preliminary experiment, the flow rate of pure methane is the recommended value of Agilent.

Table 1. GC/Q-TOF operational conditions.

Instrument	
GC	Agilent 7890B
Autosampler	Agilent PAL2
MS	Agilent 7200B GC/Q-TOF
GC Conditions	
Column	DB-5ms, 30 meter, 0.25 mm ID, 0.25 µm film
Injection volume	1 µL
Split mode and ratio	Split 100:1-10:1 (Demands on measurement mode)
Split/Splitless inlet temperature	250 °C
Oven temperature program	100 °C
	15 °C/min to 325 °C, 2.0 min hold
Carrier gas	Helium at 1.2mL/min constant flow
Transfer line temperature	300 °C
MS Conditions	
Ionization mode	EI and PICI
PICI reagent gas	Methane at 20% flow
	2% MA in Methane at 10% flow
Source temperature	250°C for EI
	180°C for PICI
Quadrupole temperature	150°C

Results and Discussion

Peak Identification by library search

A total of 50 or more components were obtained by deconvolution. In this presentation, we will cover nine peaks with the largest area as shown in Figure 2. Seven of them were identified by library search of EI mass spectra using NIST database. They are listed in Table2. However, the other two (No.2 and No.8) did not hit.

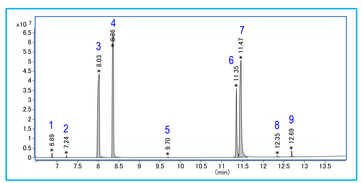

Figure 2. Total ion current chromatogram obtained by EI.

Results and Discussion

Table 2. Compounds identified by library search.

No.	R.T.	Compound	CAS	Molecular fomula	M.W.	DBE
1	6.89	Isopropyl laurate	10233-13-3	C15H30O2	242.2246	1
2	7.23					
3	7.98	Metoxadiazone	60589-06-2	C10H10N2O4	222.0641	7
4	8.34	Isopropyl myristate	110-27-0	C17H34O2	270.2559	1
5	9.69	Isopropyl palmitate	142-91-6	C19H38O2	298.2872	1
6	11.33	Imiprothrin (isomer1)	72963-72-5	C17H22N2O4	318.1580	8
7	11.42	Imiprothrin (isomer2)	72963-72-5	C17H22N2O4	318.1580	8
8	12.34					
9	12.69	DEHP	117-81-7	C24H38O4	390.2770	6

Molecular composition determination of unknowns

Each mass spectrum of peak No.2 (unknown1) is shown in Figure 3. Although protonated molecule and cationized molecules could not be identified by methane PICI, the ion *m/z 290* obtained by 2% MA could be identified as $[M+CH_3NH_3]^+$. The evidence of Identification is the description of methylammonium ($[CH_3NH_3]^+$) from $[M+CH_3NH_3]^+$ by MS/MS (Figure 4).

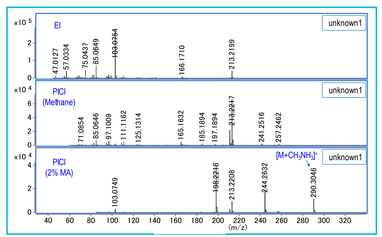

Figure 3. Each mass spectrum of unknown1.

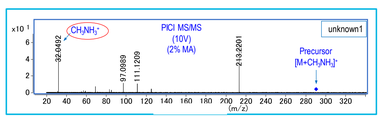

Figure 4. Product ion spectrum of unknown1 obtained by MS/MS of $[M+CH_3NH_3]^+$.

For peak No.8 (unknown2), the ion *m/z 380* could be identified to $[M+CH_3NH_3]^+$ in the same way as unknown1. The mass spectra are shown in Figure 5 and the product ion spectrum is shown in Figure 6, respectively.

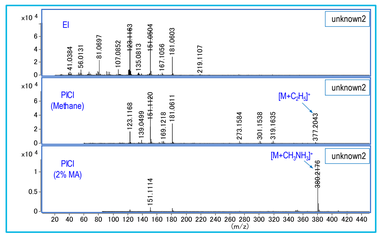

Figure 5. Each mass spectrum of unknown2.

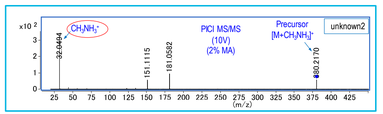

Figure 6. Product ion spectrum of unknown2 obtained by MS/MS of $[M+CH_3NH_3]^+$.

The molecular composition of unknown 1 and unknown2 was calculated to $C_{16}H_{34}O_2$ and $C_{18}H_{24}N_2O_5$ (Table3). The mass error was 2.6ppm and 1.1ppm respectively.

Table 3. Molecular composition of unknown1 and unknown2 calculated from $[M+CH_3NH_3]^+$.

No.	R.T.	Compound	CAS	Molecular fomula	M.W.	DBE
2	7.23	unknown1		C16H34O2	258.2559	0
8	12.34	unknown2		C18H24N2O5	348.1685	8

Molecular structure estimation of unknowns

The molecular structure of unknown1 could be easily estimated from EI mass spectrum to which the fragment ions were assigned (Figure 7).

Results and Discussion

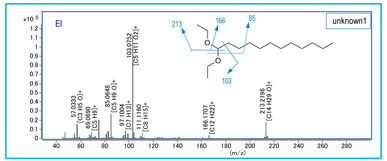

Figure 7. EI mass spectrum of unknown1 and estimated structure.

Unknown2 had a molecular composition close to Imiprothrin. The difference is only CH_2O. The mass spectra had many same fragment ions with Imiprothrin especially on the methane PICI spectrum. The common ions are indicated by blue arrows (Figure 8). The ion *m/z 181* ($[C_8H_9N_2O_3]^+$ indicated by a red arrow is characteristic for unknown2.

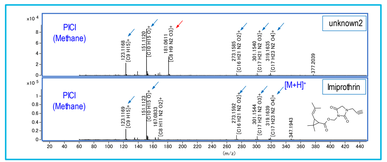

Figure 8. Methane PICI mass spectrum of unknown2 and Imiprothrin.

The product ion spectrum of *m/z 319* obtained from unknown2 was almost perfectly matched with that obtained from $[M+H]^+$ of Imiprothrin (Figure 9). This indicates the structure of unknown2 is partially identical to Imiprothrin.

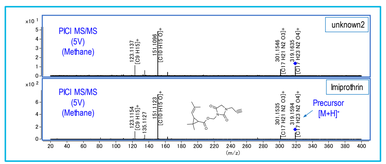

Figure 9. Product ion spectrum of *m/z 319* obtained from unkonwn2 and Imiprothrin.

As shown in Figure 10, the desorption of CH_2O from the ion *m/z 181* ($[C_8H_9N_2O_3]^+$) gives information on the presence of methoxy group and its bonding position. One of the possible structures of unknown2 is shown together in Figure 10.

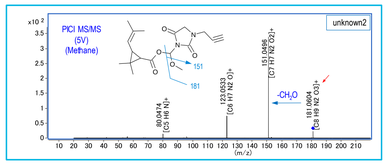

Figure 10. Product ion spectrum of *m/z 181* obtained from unkonwn2.

Conclusions

- As a result of qualitative analysis of insecticide using GC/Q-TOF, seven components out of the nine major components could be identified by library search..
- The molecular composition of the remaining unknown two components was determined by MA PICI and the structure could be estimated using MS/MS.
- Excellent performance of GC/Q-TOF in qualitative analysis was shown

References

1) J.L.Little and A.S.Howard., J. Am. Soc. Mass Spectrom., 24, 1913-1918 (2013)
2) R.Ogasawara and S.Nakamura., The 62th Annual Conference on Mass Spectrometry, Osaka, Japan, (2014)

The Application of Dual Channel High Speed Oscilloscope Analog-to Digital Converters to Time-of-Flight Mass Spectrometry

August Hidalgo, Jennifer Sanderson, Kai Chen
Agilent Technologies, Inc., Santa Clara, California

ASMS 2017
ThP-382

Agilent
Trusted Answers

Introduction

Summary Statement: An improved sample rate TOF data acquisition system that has enhanced resolution and dynamic range modes, which run simultaneously.

In TOFMS, the digitization rate of the detector signal has a direct effect on the resolution of the system. Commercially available ADCs have a sample rate which limits resolution and/or a bit depth, which limits dynamic range. Having access to high sample rate ADCs developed for oscilloscopes, a Dual Channel 20GSa/s TOF data system has been developed, resulting in an increase in resolution and in dynamic range. The architecture allows for numerous novel signal processing techniques, thereby allowing optimization to different detector speeds, accommodating decreases in detector pulse width and greatly reducing the detector's pulse width as a contribution to degrading resolution. These resolution enhancements can run simultaneously with an extended dynamic range mode.

Experimental

Component Description and Data System Block Diagram

The TOFMS data acquisition system starts with two DC-8GHz bandwidth pre-amps. The pre-amps gain and bandwidth are programmable, which allows for different detector gains and pulse widths, and to accommodate multiple operating modes. A dual channel 20 GSa/s, 8-bit ADC (analog to digital converter) is configurable to run one channel at 20GSa/s or 2 channels at 10GSa/s, this speed and flexibility will accommodate future decreases in detector pulse width. The digitized signal(s) are read into an FPGA (field programmable gate array). The FPGA's parallel processing power allows for real time signal processing at the full sample rate.

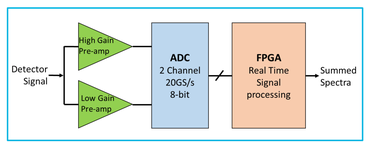

Figure 1. Block Diagram

Experimental

Extended Dynamic Range Mode

The analog signal from the detector is split and routed to two pre-amps, each with different gains. These two signals are digitized at 10GSa/s. This data can be down sampled and filtered in real time. The high gain signal and the low gain signal are combined, which also increases the bit depth to 11bits and greater.

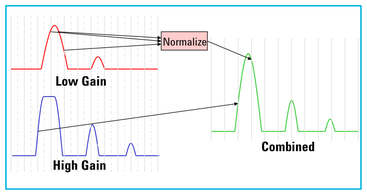

Figure 2. Extended Dynamic Range Mode

High Resolution Mode

In standard operation all digitized points are passed to the summing function. The width of the resultant peak is a combination of the pulse width of the detector and the transient to transient variation in arrival time. In resolution enhancement mode only the digitized data points associated with a peak apex are significant. This data containing both signal response and accurate arrival time is passed to the summing function.

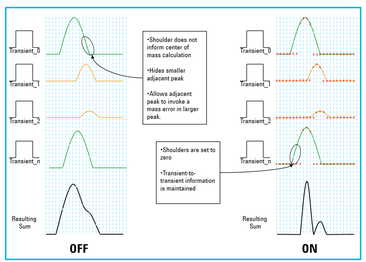

Figure 3. High Resolution Mode

Results and Discussion

System Configuration

The data was taken with the Agilent 7250A GC/Q-TOF. The data system was configured for simultaneous "Extended Dynamic Range Mode" and "High Resolution Mode". These two signals are digitized at 10GSa/s, processed and down sampled to 5GSa/s, increasing the bit depth.

Figure 4. Agilent 7250A GC/Q-TOF

Extended Dynamic Range with High Resolution

Polycyclic Aromatic Sulfur Heterocycles (PASH) compounds were spiked into gasoil matrix and a calibration curve from 100fg/µL to 1,000pg/µL was performed to determine the linear dynamic range in high resolution mode. 4 orders of magnitude were achieved with analytes 2-Methylthiophene, Dibenzothiophene and 4,6-Dimethyl Dibenzothiophene

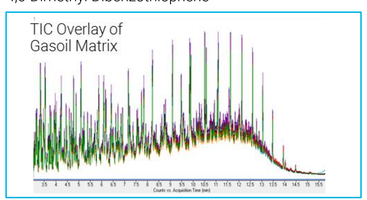

Figure 5. Total Ion Chromatogram (TIC) of gasoil matrix spiked with PASHs.

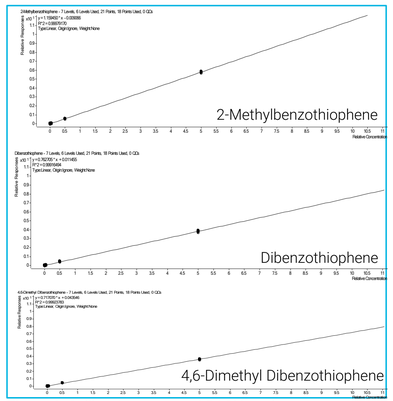

Figure 6. Calibration curves of PASH analytes

At the lowest concentration of the calibration curve, high resolution is maintained for the quantitation ion. Concentrations at or near the saturation point have excellent resolution as well, as can be seen below in Figure 7 and 8.

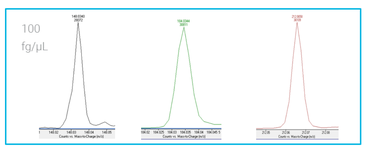

Figure 7. Quantitation ion 100fg/µL: PASH analytes

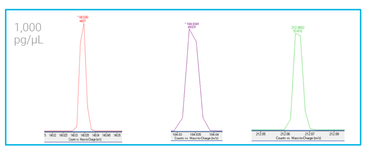

Figure 8. Quantitation ions 1000pg/µL: PASH analytes

Results and Discussion

Detectability Comparison Example

Thiamethoxam, spiked at 5ppb in avocado matrix, have two qualifier ions that are not well resolved and have mass errors of more than 20ppm when measured on prior instrument platforms. The new data system resolves the ions from the matrix interference, resulting in sub-ppm mass error.

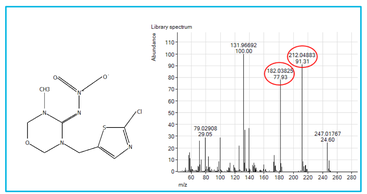

Figure 9. Thiamethoxam in Avocado (5 ppb)

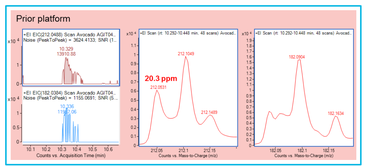

Figure 10. Prior platform result.

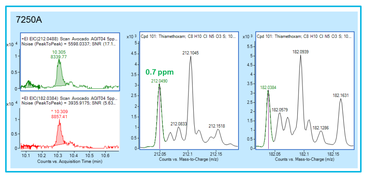

Figure 11. 7250A result.

In-Spectrum Dynamic Range Example

Demonstrated with essential oil an increase from ~3.8 orders of magnitude to ~4.9 with the 7250A

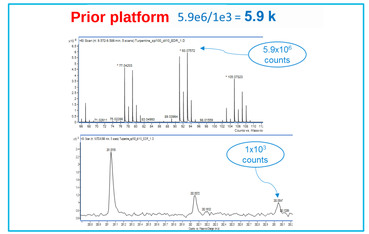

Figure 12. 7200B Ratio of largest to smallest peak with a single spectrum

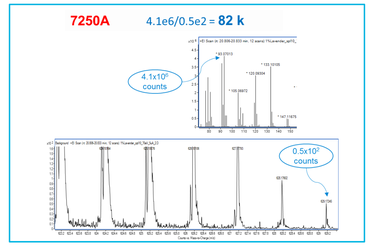

Figure 13. 7250A Ratio of largest to smallest peak with a single spectrum

Conclusions

Highest sample rate and bandwidth TOFMS data acquisition system, allowing for increase in dynamic range without compromising resolution.

Previous limitations to ultimate TOF performance can be significantly eliminated by the use of ultra high speed ADC sampling system combined with real time processing.

Increased resolution improves the detection of trace levels of pesticides in a complex matrix.

The Implications of Detector Performance in GC/MS and LC/MS Analysis – Detectors Make the Difference!

Nathan C. Contino, Jeff Kernan, Harry Prest, Bjorn Flatt, Bill Russ
Agilent Technologies, Inc., Santa Clara, CA

ASMS 2017
ThP-358

Agilent
Trusted Answers

Introduction

Detector performance is critical to the success of any given chemical analysis. Two criteria by which to judge detectors are: 1) linear dynamic range, and 2) lifetime, which represent instantaneous performance and long term stability, respectively.

Linear dynamic range is determined by two competing effects, saturation and superlinearity. As analyte concentration increases, a saturation point is reached where the actual signal is lower than the expected linear response. Superlinearity is an observed effect which leads to a signal that appears larger than expected (Fig. 1). A long lifetime provides consistent detector response, minimizing the need to frequently retune the instrument. Several detector types are compared to showcase these effects.

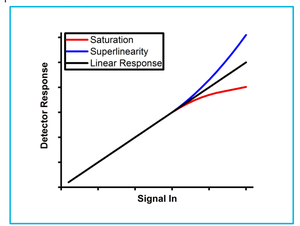

Figure 1. Saturation vs. superlinearity.

Experimental

All detectors tested were of the channel electron multiplier (CEM) style (Fig. 2). Three types of detectors were compared for GC/MS linearity, the Agilent Triple Axis Detector 1 (TAD 1; used in the 5975 and the 5977A), Agilent TAD 2 (used in the 5977B), and a third-party OEM detector meant to replace the TAD 1. For lifetime tests, the Agilent TAD 2 was used for GC/MS and the LC/MS CEM detector was used for LC/MS.

Figure 2. Agilent GC/MSD TAD 1 Electron Multiplier.

Experimental

GC/MS experiments were performed on an Agilent 5977B GC/MSD (Fig. 3). LC/MS experiments were performed on an Agilent 6470A LC/TQ (Fig. 4). Linearity results (GC/MS only) were obtained by monitoring the ratios of PFTBA calibrant ions and their ^{13}C isotopes as the detector gain was increased. Because the true isotopic ratio is known, any deviation from this value arises from either saturation or superlinearity.

Data was collected in SIM mode for lifetime tests, so that a controlled duty cycle could be created by observing an ion of interest alongside a "dummy" mass which shows no signal. The signal was monitored and the detector gain was adjusted as necessary to maintain an output above a desired threshold. Argon was introduced into the system through a mass flow controller for GC/MS measurements. LC/MS lifetime tests were performed by continual introduction of Agilent tune mix via an isocratic pump.

Figure 3. 5977B GC/MSD System.

Figure 4. 6470A LC/TQ System.

Results and Discussion – Linearity

GC/MS Linearity Results – Agilent TAD 1 vs. Agilent TAD 2

Figure 5 shows the compiled results of 14 different compounds using the Agilent TAD 1 detector. The relative response factor (RRF) should be flat across the linear dynamic range until the saturation point is reached. However, this detector is showing a compound independent superlinear response, beginning at fairly low response (concentration/signal).

We claim that the superlinear response is due to the voltage drop across the detector changing as a function of output current. As the output current increases, so too does the local voltage. This in turn leads to an undesired increase in gain and manifests as superlinearity.

Applying a bias voltage to the anode end of the Agilent TAD 2 detector clamps the back end to a fixed voltage, thereby mitigating the superlinear effect. This is highlighted in Figure 6, which shows a superlinear response from the TAD 1 detector, while the TAD 2 detector shows only saturation. These two effects, saturation and superlinearity, were always at play in the TAD 1 detector. After eliminating superlinearity, only saturation dominates at high output currents.

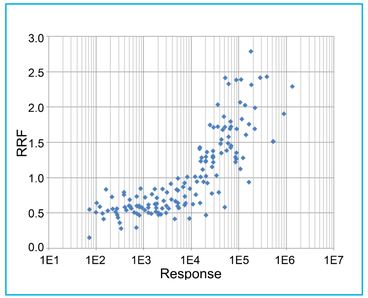

Figure 5. Superlinear response of 14 different compounds with Agilent TAD 1.

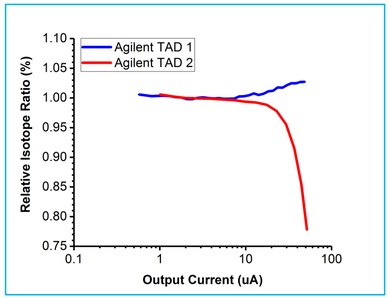

Figure 6. PFTBA mass 219/220 relative isotope ratio.

GC/MS Linearity Results – Agilent TAD 1 vs. OEM

The Agilent TAD 1 detector was compared to a third-party OEM detector (Fig. 7). The relative isotope ratio of PFTBA mass 219/220 should be unity over the detector's linear dynamic range. Two identical OEM detectors were tested. The first was never linear, showing an isotopic ratio drop from the very beginning, while the second was linear up to ~2-3µA. The Agilent TAD 1 detector, on the other hand, showed linearity up to ~50µA with <5% deviation.

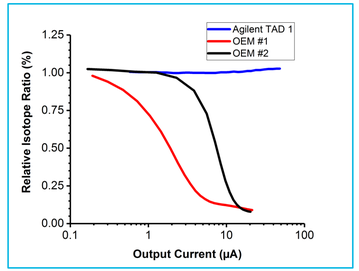

Figure 7. PFTBA mass 219/220 relative isotope ratio.

Results and Discussion – Lifetime

Detector Burn-in

It was observed that CEM detectors require a burn-in time of ~7-10 hours before stable signal can be achieved (Fig. 8). We posit that this is due to surface effects of adsorbed water on the detector which increases the observed gain. As the water is "ion scrubbed" away, the gain drops and signal stabilizes.

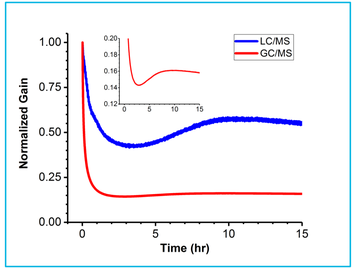

Figure 8. CEM detector burn-in period.

GC/MS Lifetime Results

Once the detector has been burned-in, signal is stable for extended periods of time. Over a period of 108 hours (4.5 days) of constant sample introduction, the signal only dropped by ~3%, while outputting almost an entire Coulomb of charge (Fig. 9).

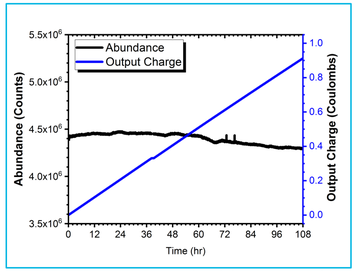

Figure 9. 5977B GC/MSD signal stability & output charge over 108 hours.

LC/MS Lifetime Results

After adequate burn-in was achieved, the LC/MS detector was also very stable, showing a signal drop of only ~8% over 108 hours (4.5 days) of constant sample introduction (Fig. 10). During this time, well over half a Coulomb of charge was output.

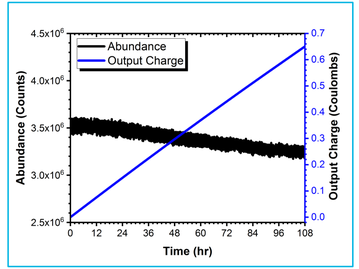

Figure 10. 6470A LC/TQ signal stability & output charge over 108 hours.

Lifetime Extrapolation

The full detector lifetime can be extrapolated based on the CEM applied voltage and the output charge at a given voltage. When the signal decayed below a pre-determined threshold, the voltage was increased and the experiment was repeated. After several measurements, an extrapolated lifetime of >20 Coulombs was calculated for both GC/MS and LC/MS detectors.

Conclusions

Linearity

- Superlinearity can be eliminated by applying a bias voltage to the anode end of the detector.
- Linear dynamic range is limited by saturation effects.
- Agilent detectors show greater linear dynamic range than aftermarket third party OEM detectors.

Lifetime

- Burn-in is required in order to obtain stable signal.
- Signal is stable for extended periods of time, and extrapolated lifetime charge output is >20 Coulombs.

Ion Mobility Support in a Novel Compound-centric Database and Accurate Mass Spectral Library

Emma E. Rennie, Kristina L. Milkovich, Norton Kitagawa, Mahsan Miladi, Sarah M. Stow, Crystal K. Cody, Stephen Madden, Nagapadmini Pavuluri, and John C. Fjeldsted

Agilent Technologies Inc., Santa Clara

ASMS 2017
MP-369

Agilent
Trusted Answers

Introduction

Ion mobility mass spectrometry (IM-MS) is a very useful analytical technique:

- for separation, identification and characterization
- which can reveal analytical detail in complex samples
- with the ability to quickly acquire and process complex data samples

With IM-MS, a compound can be identified using:

- molecular formula
- retention time (RT)
- fragmentation rich accurate mass spectra
- collision cross section (CCS)

There is a lack of easily accessible compound databases (DBs) that combine CCS values with chemical identifiers, for **quick**, **selective** and **accurate identification**.

A DB is needed which can combine all MS related identification criteria for use with a data analysis software which has meaningful scoring algorithms. The ability to easily create, manipulate and edit the DB and/or spectral library is crucial.

We have developed a novel compound-centric IM-MS DB comprised of three data repositories:

1. a compound DB for chemical identifiers and RTs
2. a spectral library for mass spectra
3. an IM DB for CCS values

MassHunter Personal Compound Database and Library (PCDL) features:

- Browse compounds, spectra, structure and IM information all at the same time.
- Easy data curation with advanced search/edit functionality for Compounds, Spectra or IM tabs.
- Easy DB subset creation for screening workflows.
- Easy import for compounds, RT's, and CCS values.
- Traceability for MS and CCS Chemical Standards.
- GC/MS or MS/MS spectra can be exported directly from MassHunter Qualitative Analysis software.
- CAS, KEGG, HMP, LMP, METLIN IDs in data analysis results for pathway analysis.
- Structure and chemical identifiers in each PCDL are displayed in data analysis to aid visual review.

Experimental

All data was acquired on an Agilent 6560 Ion Mobility Q-TOF LC/MS, a uniform field drift tube ion mobility-mass spectrometer. IM and MS information for the DBs were obtained from infusion data acquired with a stepped field method per Agilent IM protocols[1] in support of producing standardized CCS values.

Time Seg.	Time (min)	Drift Tube Entr. (V)	Drift Tube Exit (V)	Rear Funnel Entr. (V)	Rear Funnel Exit (V)
1	0.0 – 0.5	1074	224	217.5	45
2	0.5 – 1.0	1174	224	217.5	45
3	1.0 – 1.5	1274	224	217.5	45
4	1.5 – 2.0	1374	224	217.5	45
5	2.0 – 2.5	1474	224	217.5	45
6	2.5 – 3.0	1574	224	217.5	45
7	3.0 – 3.5	1674	224	217.5	45

Table 1: Standardized stepped field method voltages[1]

Two new IM-MS DB's (IM-PCDLs) were created using MassHunter PCDL Manager B.08 software (a metabolite IM-PCDL and a sulfa drugs IM-PCDL).

DB entries with compound information and spectra were transferred from existing PCDLs where possible, all additional data was curated per standard Agilent protocols.

All new compound, RT and IM data was imported using the Import compounds, Import RTs and Import CCS functions and template csv files.

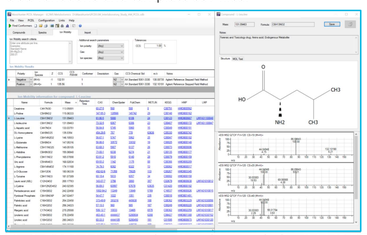

Fig 1: PCDL Manager showing the metabolite IM-MS DB

The fruit tea and metabolite infusion data was acquired with the single field method[1]. Fruit tea was spiked with sulfa drugs at two concentrations (1:1000 and 1:10000), with four replicates acquired.

MassHunter software was used for all data analysis.

- IM-MS Browser B.08 to produce a single field calibration from Agilent tune mix ions.
- Mass Profiler B.08 to find IM-MS features.
- ID Browser B.08 to identify features.

Results and Discussion

Metabolite single field infusion data identification with DB search on the metabolite IM-PCDL

Single field data drift times were translated into CCS values in IM-MS Browser B.08 with a calibration created using tune mix ions (Fig 2). This calibration was saved to the single field data files.

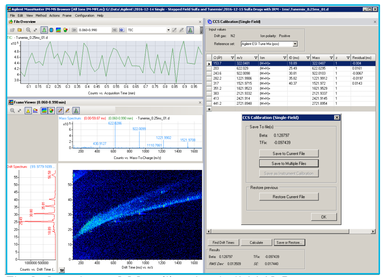

Fig 2: Creating a CCS calibration in IM-MS Browser

Features were found in single field infusion data using Mass Profiler B.08, based on m/z, isotope patterns and CCS values. These features were then identified using ID Browser B.08 with a DB search (with a CCS 1% tolerance).

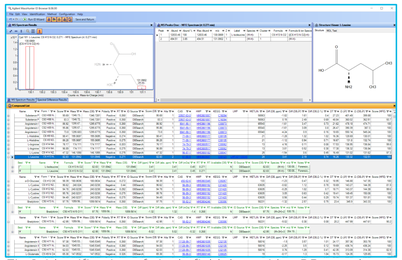

Fig 3: Identification of single field data with a DB search requiring CCS values in ID Browser

Measurements were made at three independent partner laboratories, along with an Agilent site, as part of an intra- and interlaboratory study[1] to evaluate the:

- Precision and reproducibility of CCS values.
- Single field method for integration of IM into LC/MS or MS/MS workflows.

Reproducibility

- CCS values for the metabolites standards across the three partner labs averaged a 0.29% RSD.

Ability to interface on the chromatographic timescale

- Single field CCS values compared to stepped field CCS values resulted in an average error of 0.27%

Identification scores (Fig 3 and Table 2) show excellent agreement between the stepped field CCS values, used to create the IM-MS DB, and the fast single field data .

Compounds	Mass	CCS	DB CCS	Score
Uric Acid $[M-H]^-$	168.0283	125.49	126.93	97.73
Lauric Acid $[M-H]^-$	200.1776	154.37	154.82	99.14
Pyridoxal Phosphate $[M-H]^-$	247.0246	149.28	150.80	83.55
Cortisol $[M+H]^+$	362.2093	189.13	189.27	99.13
Bradykinin $[M+2H]^{2+}$	1059.5614	345.90	343.33	97.75
Angiotensin I $[M+3H]^{3+}$	1295.6775	478.18	474.71	86.92
Ubiquitin $[M+9H]^{9+}$	8559.6167	2077.96	2052.43	78.74

Table 2: Selected results showing typical DB scores

LC/IM-MS screening workflow: drugs in a complex matrix

Fast screening methods for contaminants in complex food matrices are among some of the most demanding analytical LC/MS applications. Adding IM to LC/MS applications introduces an additional orthogonal degree of separation which can substantially reduce matrix interference. To evaluate the new single field CCS measurement approach for interfacing IM-MS with LC separations, we looked at fruit tea spiked with four sulfa drugs (see table below).

Compounds	Formula	Mass	RT	CCS
Sulfamethizole	$C_9H_{10}N_4O_2S_2$	270.0245	10.47	158.8
Sulfachloropyridazine	$C_{10}H_9ClN_4O_2S$	284.0134	11.16	161.8
Sulfamethazine	$C_{12}H_{14}N_4O_2S$	278.0837	10.44	163.4
Sulfadimethoxine	$C_{12}H_{14}N_4O_4S$	310.0735	13.53	169.6

Table 3: Sulfa drugs IM-MS data

Results and Discussion

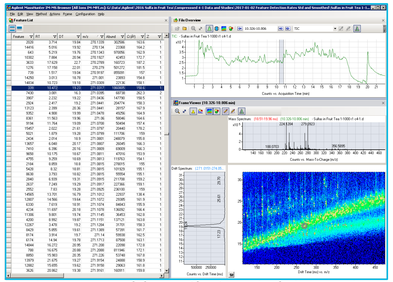

Fig 4: Features of four sulfa drugs in fruit tea using a screening workflow in IM-MS Browser

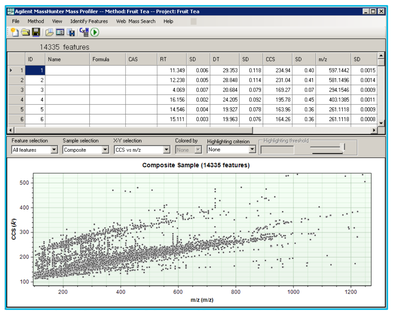

Fig 5: Identification of four sulfa drugs in fruit tea using a screening workflow in Mass Profiler

LC/IM-MS screening workflow: drugs in a complex matrix

Fig 4 shows IM-MS Browser with the TIC highlighting a high abundance feature with an m/z of 271.0317 ($[M+H]^+$ ion) and a RT of 10.472 mins. The heat map shows drift time vs *m/z* for this feature (sulfamethizole).
In ID Browser B.08 a DB search restricted to RT and CCS on the target PCDL (sulfa drugs IM-PCDL) identified the four compounds with excellent RSDs (Table 4 and Fig 5).
The DB search tolerances were 5 ppm + 2 mDa for mass, 0.1 mins for RT and 1% for CCS.

Compounds	CCS_{obs} ($Å^2$)	CCS_{DB} ($Å^2$)	Diff ($Å^2$)	Diff (%)
Sulfamethizole	158.4	158.8	0.4	0.25
Sulfachloropyridazine	161.87	161.8	0.07	0.04
Sulfamethazine	164.33	163.4	0.93	0.57
Sulfadimethoxine	170.36	169.6	0.76	0.45
Average			0.54	0.33

Table 4: Detailed CCS results for the sulfa drugs

Conclusions

- PCDL Manager can easily create and manipulate IM-MS data, in new DB's or adding IM data to current DBs.
- PCDLs interface with data analysis software integrating CCS values into standard LC/MS/MS analytical workflows, including pathway analysis.
- The Agilent 6560 IM Q-TOF LC/MS has excellent intra- and interlaboratory precision and reproducibility for CCS values.

References

[1] *An Interlaboratory Evaluation of Drift Tube Ion Mobility Collision Cross Section Measurements*, S. M. Stow, T. J. Causon, X. Zheng, R. T. Kurulugama, T. Mairinger, J. C. May, E. E. Rennie, E. Baker, R. Smith, J. A. McLean, S. Hann and J. C. Fjeldsted, Anal. Chem. Submitted.

NATURAL PRODUCTS

Qualitative and Quantitative determination of Cannabinoid Profiles and Potency in CBD Hemp Oil using LC-UV-MSD

Mike Adams[1], Annette Roth[1], Sue D'Antonio[2], Guannan Li[2], John Palmer[2], Jamie Dougherty[2], Anthony Macherone[2]

[1]CWC Labs Cedar Creek, TX, [2]Agilent Technologies, Inc. Santa Clara, CA USA.

ASMS 2017
WP-531

Agilent
Trusted Answers

Introduction

With respect to recent legislation in 37 U.S. States legalizing the use of recreational and/or medicinal marijuana (Cannabis sativa), there has been an exponential growth in the need for analytical services that determine the quality and potency of the retail product. Traditional methodologies used in agricultural and food testing such as testing for pesticide residues, residual solvents, toxic metals and others have been migrated to analyze this new matrix. Herein, we describe a LC-UV-MS method developed for the analysis of ten cannabinoids common to C. sativa that includes delta 9-tetrahydrocannabinol for potency determination and quality profiling.

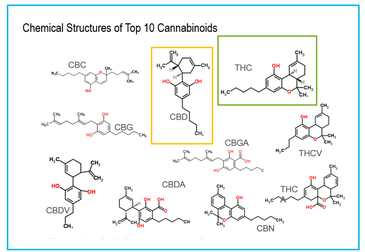

Samples of commercially available CBD oil were purchased and run in replicate (n = 6) to demonstrate statistical reproducibility. Samples were prepared via rugged and reliable automated dilution. Among the 10 analytes, there is a diversity in the chemical structure. We characterized and quantified the cannabinoids in CBD oils using the Agilent LC/MSD single quadruple system. Mass information was included to provide unambiguous confirmation of the cannabinoids. We compared the quantitative results across the various modes of detection: UV, ESI and ACPI.

part number	compound	M/z	formula
C-045	Cannabidiol (CBD)	315.2	C21H30O2
C-046	Cannabinol (CBN)	311.2	C21H26O2
C-140	Cannabidivarian (CBDV)	287.2	C19H26O2
C-141	Cannbigerolic acid (CBG)	317,2	C21H32O2
C-143	Cannabichromene (CBC)	315.2	C21H30O2
C-144	Cannabidiolic acid (CBDA)	359.2	C22H30O4
T-094	Tetrahydrocannabivarin (THCV),	287.2	C19H26O2
T-005	(-)-Δ9-THC	315.2	C21H30O2
T-093	Δ9-Tetrahydrocannabinolic acid A (THCA-A)	359.2	C22H30O4
C-152	Cannabidivarinic Acid (CBDA)	359.2	C22H30O4
T-032	(-)-Δ8-THC	315.2	C21H30O2

Cerilliant standard part numbers

Experimental

LC Conditions

Agilent 1290 Infinity II UHPLC System. Quaternary Pump, Multisampler with wash, Multi Column Themostat, DAD

Column: Zorbax Poroshell Bonus RP, 3.0.1 x 50mm, 2.7. µm

Column temperature: 50°C
Injection volume: 0.5 µL
Autosampler temp: 25°C
Needle wash: 3.5 s Flush Port (25:25:50) (H_2O:IPA:MeOH)
DAD-UV 230 nm
Mobile phase: A = Water
B= Methanol
C= 1 liter of H_2O + 1ML of CH_2O_2 + 2.2 ml of 5M NH_4HCO_2
Flow rate: 1.0 mL/min
Gradient:

Time (min)	%B	%C
0.0	60	5
6.25	95	5

Stop time: 6.25.
Post time: 2.0 min.
Overall run time:
8.2 minutes (incl. re-equilibration)
For binary systems only, A mobile phase with modifier, the final column cleanup must be 100 % pure Methanol.

LC/MSD Conditions

The Agilent LC/MSD single quadrupole system was used with the multimode ionization source.

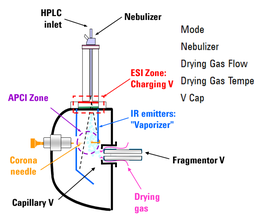

Mode	Positive ESI
Nebulizer	30 psi
Drying Gas Flow	5 L/min
Drying Gas Temperature	350 degrees C
V Cap	1850 V

Dwell	70
Fragmentor	70
M/Z SIM	315,287,311,359,317,361
M/Z SCAN	150-700

Results and Discussion

UV DAD Results

All Curves were 0.999 for the UV DAD responses, confirmed with spectra, and purity

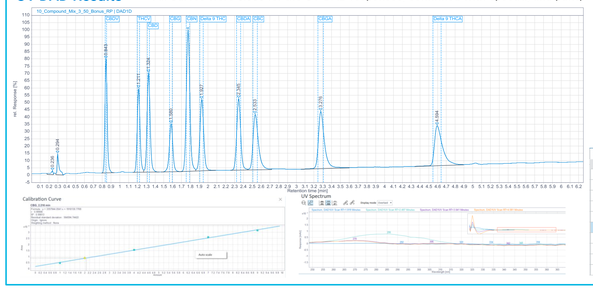

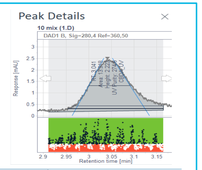

#	Type	Name	Signal	Exp. RT
1		CBDV	DAD1D	0.843
2		THCV	DAD1D	1.211
3		CBD	DAD1D	1.324
4		CBG	DAD1D	1.580
5		CBN	DAD1D	1.772
6		Delta 9 THC	DAD1D	1.927
7		CBDA	DAD1D	2.345
8		CBC	DAD1D	2.533
9		CBGA	DAD1D	3.276
10		Delta 9 THCA	DAD1D	4.594

MSD Standards Results

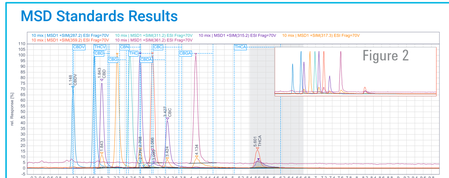

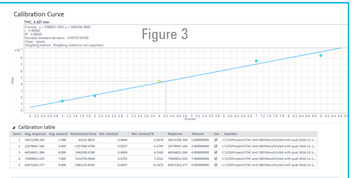

Figure 2 is an overlay of the 10 compound mix. You see the different colors for different M/Z SIMS (selected ion monitoring). You can see with so many isobaric compounds, the chromatography gives assurance of separation. Figure 3 is the calibration curve for the MSD EIC signal for THC. The precision for all 10 Compounds were at least 0.995 most were 0.999. Figure 5 shows the EIC at 315.2 m/z for CBD, THC and CBC. However, we saw a small peak in our samples which we investigated further.

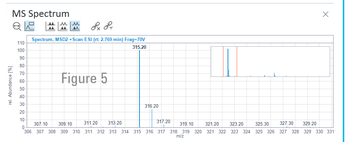

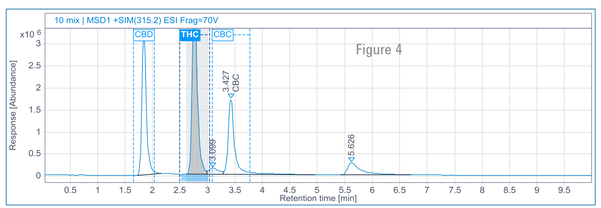

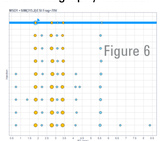

Figure 5. Spectral integrity and isotopic pattern of the THC compound. This adds extra confirmation to the chromatography method.

Results and Discussion

MSD INVESTIGATIVE RESULTS

The small peak was investigated and found to be delta 8 THC. A standard was obtained and analyzed with the same retention time as our unknown peak. We created a standard curve and appended that compound to our method for sample quantitation. In addition we added this peak to a cannabinoid NIST library which allows searching. Figure 7 shows the match results.

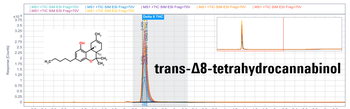

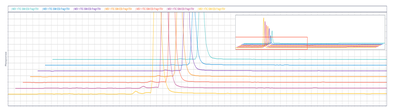

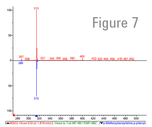

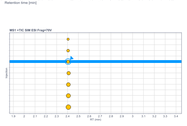

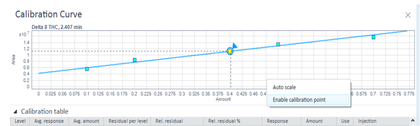

Below is a table showing the results of our testing, we did not expect to find all of the cannabinoids in any sample. These where sample of CBD oils. We also sampled natural Hemp as our control blank. In addition we spiked a sample of natural oil with the now 11 compound mix. We found all 11 compound in our mix

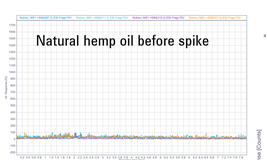

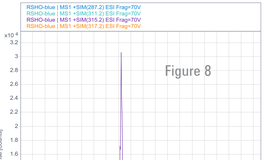

Sample	CBD	CBN	8 THC	9 THC	CBC	CBDV	CBDA	THCA	THCV	CBG	CBN
natural hemp	nd	nd	nd	nd	nd	nd	nd	nd	nd	nd	nd
sample 1	25	nd	nd	0.06	nd	nd	1.5	nd	nd	6	nd
sample 2	24,9	nd	nd	0.06	nd	nd	1.5	nd	nd	5	nd
sample 3	16	nd	nd	0.12	nd	nd	3	nd	nd	nd	nd
sampler 4	8	nd	nd	0.04	nd	nd	4	nd	nd	nd	nd
sample 5	8	nd	nd	0.04	nd	nd	4	nd	nd	nd	nd
sample 6	17	nd	nd	0.07	nd	nd	2,7	nd	nd	nd	nd

Figure 8 is a typical sample of the CBD oil. It shows high quantities of CBD, some THCA and low concentrations of delta 9 THC.

Conclusions

With mass spectrometry, using the Agilent LC/MSD system, CBD oils were characterized and individual cannabinoids were quantitated to access the quality and potency of the CBD oils from commercially available source. The Agilent LC/MSD single quadruple system combined with OpenLAB CDS software makes this analysis robust, simple and fast. The mass spectrometry data adds additional confidence to the analysis compared to optical detection using LC/UV alone.

Valve Based 2D-UHPLC/QTOF MS Solution for Exploring Natural Products

Guoqiang Liu[1]; Yue Song[1]; Bo Chen[1]; Shan-An Chan[2]

1. Agilent Technology, Inc., Shanghai, China; 2. Agilent Technology, Inc., Taipei, Taiwan

ASMS 2017
WP-525

Agilent
Trusted Answers

Introduction

Natural products are chemical compounds extracted from the microorganisms, plants and animals. Nowadays, LC/MS has been helped to obtain the chemical and structural information of natural products.

However, the commonly used LC/MS solution for qualifying the natural products still exists several challenges: 1. High resolution mass spectrometer alone cannot resolve co-eluted isomers or interfering compounds with similar molecular weights. 2. The complex crude extract usually shows matrix signal suppression effects for the analysis of natural products. 3. Low abundance compounds could be misidentified due to analytical sensitivity limitations.

In this study, a new valve based 2D-UHPLC/Q-TOF solution was introduced for exploring natural products, which helps to address the LC-MS challenges during natural products analysis.

Experimental

Chemicals and materials

Acetonitrile, methanol, and water (LCMS grade) were purchased from Merck (Darmstadt, Germany). Formic acid (purity 99.9%) was purchased from Dikma (California, USA). Ammonium acetate was purchased from Sigma Chemical Company (St. Louis, MO, USA).

Two-dimensional-liquid chromatography conditions

Agilent series 1290 HPLC instrument equipped with two binary pumps, two diode-array detectors, an auto-sampler, and two column compartments were used for 2D-LC analysis.

A 2-position/6-port valve was used to perform the heart-cutting (HC) analysis (Figure 1). When the targeted peak was eluted in the first LC, it was transferred to the second dimensional column for separating it from the matrix or co-eluted interference with similar molecular weight.

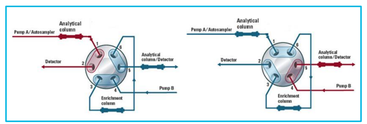

Figure 1. Schematic of heart-cutting interface with a 2-position/6-port valve.

Experimental

Two 6-pos/14-port select valves connected to a 2-position/4-port-duo valve were used to perform the multiple heart-cutting (MHC) analysis (Figure 2). The interested area in the first LC was cut multiple times and then trapped in the discrete loop positions. Then the elution trapped in the loops was sequentially transferred to the second dimensional column for further separating and identification.

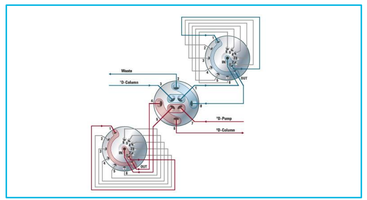

Figure 2. Schematic of multiple heart-cutting interface with 2-pos/4-port duo valve and two parking decks with a total of 12 sampling

Mass spectrometry conditions

An Agilent 6530 Accurate-Mass Q-TOF mass spectrometer was connected to 2D-LC instrument via an AJS ESI or APCI ion source. Positive and negative ion mode were used for analysis, the operating parameters for MS analysis were as follows: dry gas (N2) flow rate 10 L/min, nebulizer pressure 40 psi, sheath gas flow rate 12 L/min, dry gas temperature 300°C, sheath gas temperature 350°C, Vcap 3500, fragmentor voltage 150 V and nozzle voltage 500 V.

Software

The software included an Agilent MassHunter Workstation (B.06.00) for data acquisition, MassHunter Qualitative Analysis software (B.07.00) for data analysis, and MassHunter MetaboliteID (B.04.00) and MassHunter MSC software (B.07.00) to facilitate the elucidation of compound structures. OpenLAB ChemStation with 2DLC (1.7) was used for data acquisition and analysis for MHC experiment.

Results and Discussion

Heart-cutting 2D-UHPLC Q-TOF MS system employed for resolving two co-eluted compounds with similar molecular weights

Osthole metabolites in rat liver microsomes have been studied by LC Q-TOF system. It was noted that the metabolites $C_{15}H_{14}O_3$ and $C_{15}H_{16}O_3$ were coeluted at 11.7 min. Because the ^{14}C and ^{18}O isotope of metabolite $C_{15}H_{14}O_3$ interfered with the monoisotopic ion of the metabolite $C_{15}H_{16}O_3$, it cannot acquire pure MS/MS spectrum to elucidate the structure of metabolite $C_{15}H_{16}O_3$ (Figure 3).

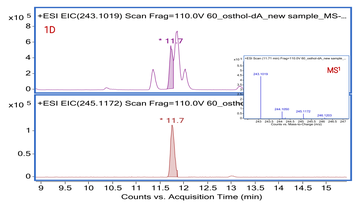

Figure 3. The MS^1 and EIC of coeluted metabolites $C_{15}H_{14}O_3$ and $C_{15}H_{16}O_3$ on the first dimension.

So the coelution at 11.7 min was transferred into the second LC dimension via a 2-position/6-port switching valve, and separated with different column and mobile phase. It was found that the coeluted metabolites can be separated on the second LC dimension and get pure MS^1 spectra at 16.5 and 16.7 min, respectively (Figure 4).

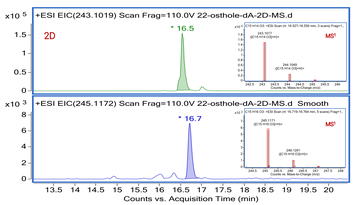

Figure 4. The MS^1 and EIC of coeluted metabolites $C_{15}H_{14}O_3$ and $C_{15}H_{16}O_3$ on the second dimension.

Heart-cutting 2D-UHPLC Q-TOF MS system employed for solving matrix effect and interference

In the present study, heart-cutting 2D-UHPLC Q-TOF system was employed for addressing LC-MS matrix signal suppression effects. The targeted peak in grape extract eluted at 9.51 min on 1D LC was tentatively identified as $C_{29}H_{40}O_4$ or $C_{29}H_{48}O_{14}$ using UHPLC-Q-TOF (Figure 5). However, $C_{29}H_{40}O_4$ with one degree of unsaturation and $C_{29}H_{48}O_{14}$ with elution time at 9.74 min of EIC do not match the information of 480 nm absorption and elution time at 9.51min on 1D LC, respectively. In this context, the two compounds identified by UHPLC-Q-TOF could be matrix background, which suppresses the signal of target for detection and identification.

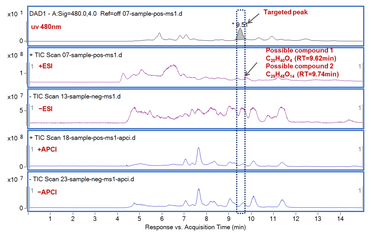

Figure 5. The UV and ±TIC chromatography obtained on the first dimension.

So the elution at 9.51 min on 1D LC was transferred to the second dimensional column for separating the co-eluted targeted compound from the matrix. It was interesting that the targeted peak can be separated on the second LC dimension at 19.76 min, and it was further identified as $C_{40}H_{54}O_5$ based on heart-cutting 2D-UHPLC/QTOF system (Figure 6).

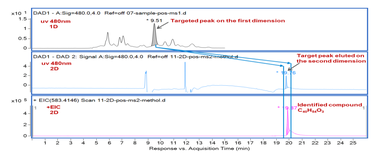

Figure 6. Separating results using heart-cutting 2D-UHPLC/QTOF .

Results and Discussion

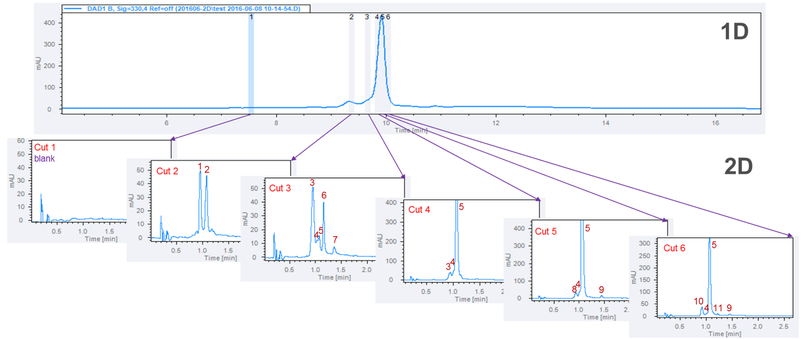

Figure 6. The separated peaks obtained on the second dimension by the multiple heart-cutting 2D-LC analysis.

Multiple heart-cutting 2D-UHPLC Q-TOF MS system employed for enhancing low level detection with LC/MS instruments

The multiple heart-cutting (MHC) UHPLC-Q-TOF system was used for finding and identifying low abundance compounds buried in the main peaks from plant extract sample. Two peaks were detected at 9.34 and 9.92 min at 330 nm on 1D LC, respectively. The interested area on the first LC between 9.34 and 9.92 min was cut five times and then was transferred to the second dimensional column for further separating and identification. It is interesting find that 11 peaks were further detected and identified on the second dimensional LC (Figure 6). In conclusion, there are 2 compounds buried at 9.34 min and 9 compounds buried at 9.92 min, respectively. The identified results were shown in the Table 1.

Table 1. The identified peaks by the multiple heart-cutting 2D-LC Q-TOF MS analysis

No.	Cut No.	Formula	m/z [M+H] or [M+NH4]+	Error (ppm)
1	2	C26H28O14	565.1549	0.55
2	2	C21H20O11	449.1076	0.77
3	3, 4	C27H30O16	611.1604	0.46
4	3, 4, 5, 6	C26H28O15	581.1500	0.26
5	3, 4, 5, 6	C22H22O11	463.1233	0.42
6	3	C29H34O17	655.1866	0.54
7	4	C25H32O10	510.2328	0.96
8	5	C21H20O11	449.1077	0.59
9	5, 6	C26H54O14	591.3581	0.55
10	6	C27H30O15	595.1655	0.52
11	6	C27H30O15	595.1654	0.8

Conclusions

In this study, a new valve based 2D-UHPLC/Q-TOF solution was introduced for resolving two co-eluted osthole metabolites with similar molecular weights, identifying the co-eluted targeted compound in grape extract from the interfering matrix, and exploring low abundance compounds buried in the main peaks from plant extract sample. Our study corroborated that 2D-LC MS system can help to address the LC-MS challenges during natural products analysis.

BIOPHARMA/PHARMA

Sensitive and robust quantitation of intact monoclonal antibody using a newly developed Q-TOF instrument

Alex Zhu[1], David Wong[2], Aaron Boice[2]
[1]Agilent Technologies, Wilmington, DE; [2]Agilent Technologies, Santa Clara, CA

ASMS 2017
WP-637

Agilent
Trusted Answers

Introduction

Bioanalytical LC/MS protein quantitation analysis is traditionally performed by monitoring signature peptides from enzymatically digested samples based on targeted multiple reaction monitoring (MRM) techniques. While this technique does offer the highest level of sensitivity, it has two significant limitations: inability to observe unexpected molecular species as well as possible artifacts introduced through sample handling. Quantifying at the intact protein level avoids these limitations, but faces separate challenges of sensitivity and reproducibility. Using the latest developments in chromatography and the high performance 6545XT AdvanceBio LC/Q-TOF, this study establishes a highly sensitive and reproducible quantitative method that spans an impressive linear dynamic range, which allows for the development of reliable bioanalytical methods for therapeutic proteins and its biotransformation products.

Experimental

Reagent and chemicals

Formulated Trastuzumab monoclonal antibody (mAb) standard was sourced from Genentech (So. San Francisco, California, USA). Bovine serum albumin (BSA) and formic acid (FA) were sourced from Sigma-Aldrich.

Sample preparation

Stock 24 µg/µL concentration of glycosylated Trastuzumab was diluted in DI water containing 0.01 % BSA (w/v) and 0.1 % FA to cover a range from 0.01 ng/µL to 100 ng/µL. The dilution ratio was constant at 1:3.162, the square root of 10, resulting in a half order of dynamic range per dilution level.

Software

Agilent MassHunter Acquisition (B.08.01) workstation software with large molecule SWARM autotune feature was used to acquire data. Agilent MassHunter BioConfirm (B.08.00) and Agilent MassHunter Quantitative Analysis (B.08.00) were used for data analysis.

Experimental

LC Conditions

Agilent 1290 Infinity II UHPLC with an Agilent Zorbax 300 Diphenyl RRHD column (1.8µm, 2.1×50mm, 857750-944).

LC Parameters	
Mobile phase A	0.1% formic acid in water
Mobile phase B	90/10 Acetonitrile/H_2O with 0.1% formic acid
Gradient	0.0 min → 34.6 % B 0.1-1.0 min → Stop flow 2.0 min → 34.6 % B 3.0 min → 90% B
Stop time	4.0 min
Post time	1.5 min
Column Temperature	80°C
Flow rate	0.5 mL/min
Flow rate	30 sec of 90/10 ACN/H_2O, then 10 sec of starting condition

MS Conditions

Agilent 6545XT Q-TOF System with Agilent Jet Stream ion source.

MS parameters	
Ion mode	Positive ion mode (Centroid)
Drying gas temperature	290 °C
Drying gas flow	13 L/min (nitrogen)
Nebulizer	45 psi
Sheath gas temperature	380 °C
Sheath gas flow	112/min
Capillary voltage	5500 V
Nozzle voltage	2000 V
Fragmentor	380 V
Mass Range	600-5000
CE	0
Quad AMU	350
Acq Rate	2 spec/s

Results and Discussion

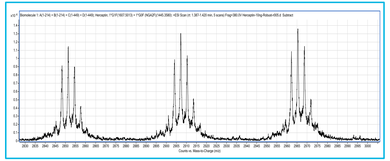

Figure 1. Zoom in of raw spectrum for TrastuzumAb with 10 ng on-column injection

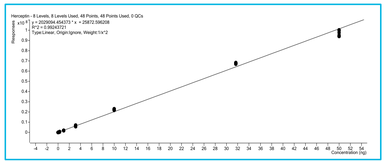

Figure 2. Calibration curve of TrastuzumAb in neat solutions from 0.0316 ng to 50 ng (on-column)

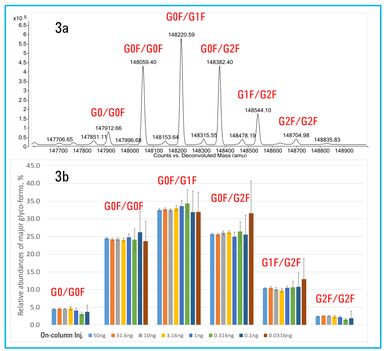

Figure 3. a) Deconvoluted spectrum of TrastuzumAb; b) Relative abundances of major glyco-forms at different levels from 50ng down to 31.6 pg on-column with error bars from 6 replicates at each level.

Analytical sensitivity and linear dynamic range

An example raw spectrum from 10 ng on-column injection of TrastuzumAb is shown in Figure 1. Notice the excellent spectral quality and low spectral background.

For quantitative analysis, extracted ion chromatograms (EICs) were generated that summed a total of the 12 most intense glycoform peaks over three charge states, with an extraction window of ± 2 m/z for each peak.

As shown in the calibration curve in figure 2, this workflow was able to detect injections down to a quantity of 0.0316 ng of intact mAb on-column. It has been reported that linear response of intact protein analysis by LC/MS has more limitations than that of traditional small molecule analysis[1]. With this method, linear response was maintained from 0.0316 ng on-column up to 50 ng on-column. This represents a linear dynamic range of 3.2 orders, which is greater than anything currently published.

The excellent intact protein sensitivity of the 6545XT AdvanceBio LC/Q-TOF can be attributed to a variety of design attributes in optics, vacuum, and heater systems that are fully realized when paired with the SWARM autotune feature to optimize for large molecules.

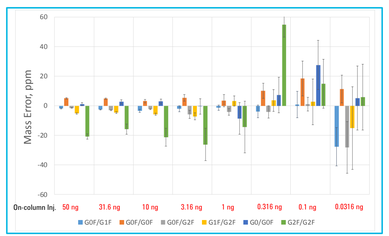

Figure 4. Mass accuracy of 6 major glyco-forms at different levels across the linear range.

Spectral fidelity and mass accuracy

As shown in figure 3 & 4, the relative abundances of the glyco-forms are highly consistent across the linear range including the LLOQ level, and the low ppm mass accuracy even with sub-ng on-column injections allows for confident identification of the mAbs at extremely low levels.

Results and Discussion

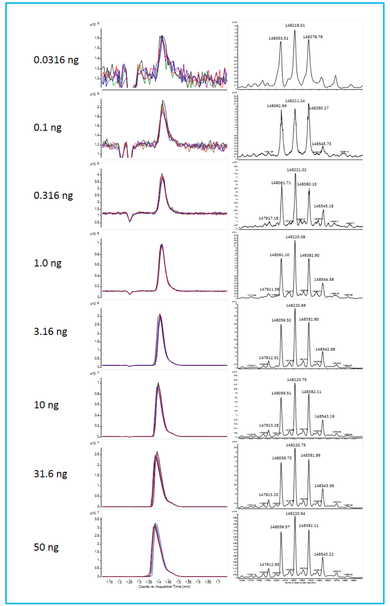

Figure 5. Overlaid EICs of six replicate injections for each dilution level, with representative deconvoluted spectra for each level

Reproducibility of response and mass accuracy

As shown in figure 5-7, mAb abundances and mass accuracies are extremely reproducible across the entire linear dynamic range, with the major glyco-forms clearly detected at the LLOQ level (31.6 pg on-column).

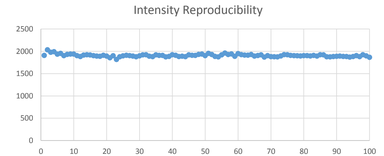

Figure 6. Intensity reproducibility over 100 injections of 10-ng TrastuzumAb on-column

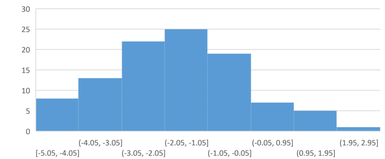

Figure 7. Histogram of mass accuracy measurements for the most abundant glyco-forms from 100 injections of 10-ng on-column

Conclusions

For intact analysis of large molecule such as monoclonal antibodies, 6545XT AdvanceBio LC/Q-TOF provides:

- Sub-ng limit of quantitation.
- >3 orders of linear dynamic range.
- Extremely reproducible LCMS responses and mass accuracy across the entire linear range

References

[1]van den Broek, I.; van Dongen, W. D. LC-MS-based quantification of intact proteins: perspective for clinical and bioanalytical applications. *Bioanalysis* 2015, 7.15, 1943-1958

Antibody Drug Conjugate Analysis using automated affinity purification and sensitive intact protein based LC/Q-TOF analysis

Shuai Wu[1]; Alex Zhu[2]; Jing Chen[3]; Zach Van Den Heuvel[3]; Steve Murphy[3]; Maryann Shen[1]

1. Agilent Technologies Inc., Santa Clara, CA
2. Agilent Technologies Inc., Wilmington, DE
3. Agilent Technologies Inc., Madison, WI

ASMS 2017
MP-132

Agilent
Trusted Answers

Introduction

Quantitation of proteins in biological systems is traditionally performed either by ligand binding assays (LBA) or multiple reaction monitoring (MRM). LBAs can be highly sensitive but do not provide information about the physical state of the biomolecules (i.e. mass) and can be affected by non-specific binding. MRM assays are sensitive, but surrogate peptides represent only a portion of the total protein. Both LBA and MRM assays may miss unexpected changes to biomolecules that can alter the efficacy and immunogenicity. We developed a workflow using automated affinity purification of antibody-drug conjugates (ADCs) from serum with streptavidin cartridges, followed by UHPLC separation coupled to a newly developed 6545XT AdvanceBio LC/Q-TOF providing a reproducible, sensitive and accurate quantitation method for bioanalytical analysis of intact proteins.

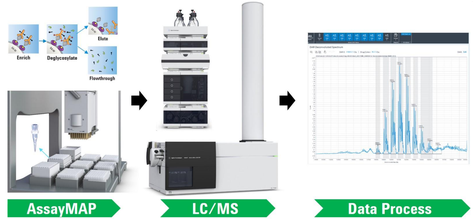

Figure 1. A complete workflow for ADC quantitation

Experimental

Immobilization

- Her2 extracellular domain (ECD) was biotinylated using EZ-Link™ Sulfo-NHS-LC biotin kit.
- 2 µg of biotinylated Her2 ECD was immobilized on each streptavidin (SA-W) cartridge using AssayMAP Bravo.

Affinity Purification and On-Cartridge Deglycosylation using AssayMAP Bravo

- Commercially obtained ADC (T-DM1) was diluted with water from 10 mg/mL to 1 mg/mL.
- Rat serum was centrifuged at > 14,000g for 5 min. The supernatant was diluted 1:1 with HEPES buffer (10 mM HEPES, 150 mM NaCl, pH=7.4). ADC was spiked into diluted rat serum to make 10, 3.2, 1, 0.32, 0.1 ng/µL samples.
- 100 µL ADC samples (n=6) were loaded on SA-W cartridge at 3 µL/min, followed by 150 µl HEPES buffer wash, and 50 µl deglycosylation buffer (20 mM Tris, pH=8.0) wash at 10 µl/min.
- 6 µl of Rapid PNGase F at 37 ^{0}C or a buffer control was aspirated onto each cartridge containing ADC and heated for 30 minutes. 10 µl of deglycosylation buffer was aspirated through the cartridge to remove the released glycan and enzyme after the reaction.
- Each cartridge was washed with 50 µl 1 M NaCl in HEPES buffer, and 50 µl 0.003% formic acid at 10 µl/min.
- The purified ADC was eluted with 15 µl of 1% formic acid into sample plate containing 15 µl 0.5% ammonium hydroxide to neutralize the purified ADC samples.

LC/MS Analysis

- Samples were analyzed using Agilent 1290 Infinity II UHPLC system with a PLRP-S column (PL1912-3802) coupled to an Agilent 6545XT AdvanceBio LC/Q-TOF with a Dual Agilent Jet Stream ESI source.

Deconvolution and DAR calculation

- Spectra were extracted, averaged and deconvoluted using MassHunter BioConfirm. Drug-to-antibody (DAR) of ADC were determined using the MassHunter DAR Calculator. Peak area integrated in DAR calculator was used to generate the quantitation curve.

DAR Determination of T-DM1 Purified from Serum

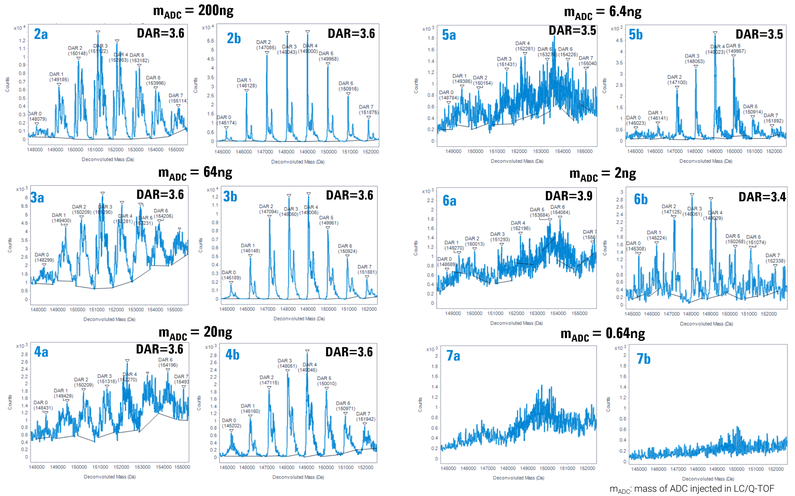

Figure 2-7. Deconvoluted spectra and DAR of (a) glycosylated and (b) deglycosylated T-DM1 purified from rat serum

ADC samples in serum were simultaneously processed on the AssayMAP Bravo system. The steps taken include: 1) all ADC samples were purified with streptavidin affinity purification cartridge 2) Half of the sample were treated with buffer control and half were treated with on-cartridge PNGase F digestion. 6 µL of final processed ADC samples were injected into LC/Q-TOF in triplicate. The injection amounts were 200, 64, 20, 6.4, 2 and 0.64 ng. DAR values were compared between (a) glycosylated and (b) deglycosylated ADCs at each injection amount (Fig. 2-7). The lowest injection amount where DAR values can be reliably determined were 6.4 ng for glycosylated T-DM1 and 2 ng for deglycosylated T-DM1.

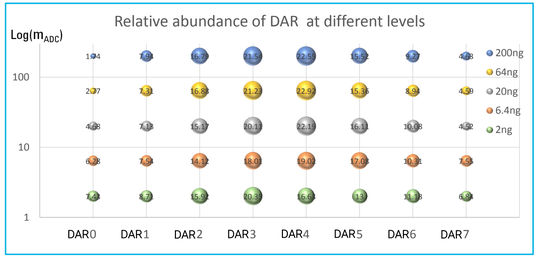

Figure 8. Relative abundance of different DAR species at different levels

The relative abundance of different DAR species (D0-D7) were compared for deglycosylated T-DM1 across different samples. (Fig. 8). The relative abundance (represented by the size of the bubbles) for each DAR species was consistent with D3, D4 being the most abundant and D0, D7 being the least abundant. The relative abundance of D0 and D7 increased when at very low sample amounts potentially due to interference of the background.

T-DM1 Quantitation Curve

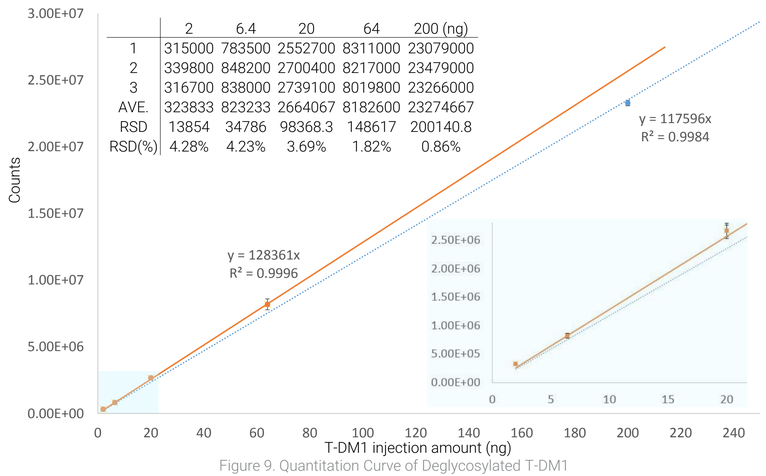

	2	6.4	20	64	200 (ng)
1	315000	783500	2552700	8311000	23079000
2	339800	848200	2700400	8217000	23479000
3	316700	838000	2739100	8019800	23266000
AVE.	323833	823233	2664067	8182600	23274667
RSD	13854	34786	98368.3	148617	200140.8
RSD(%)	4.28%	4.23%	3.69%	1.82%	0.86%

Figure 9. Quantitation Curve of Deglycosylated T-DM1

The peaks in deconvoluted spectra were integrated using the DAR calculator. The total peak area was calculated from D0 to D8. The average of the total peak area were calculated from triplicate injections and plotted against T-DM1 on-column injection amount. As shown in Figure 9, for deglycosylated T-DM1, a linear response from the detection limit of 2ng up to an injection of 200ng was achieved.

Conclusions

A complete workflow for ADC quantitation was implemented that integrates automated affinity purification, on-cartridge deglycosylation, LC/MS analysis, deconvolution and quantitation with DAR calculation.

- AssayMAP Bravo enables wide range of automated protein sample preparation applications, such as affinity purification and on-cartridge deglycosylation.
- 6545XT AdvanceBio Q-TOF provides high resolution and high analytical sensitivity for ADC sample analysis with 2 ng on-column limit of detection.
- MassHunter DAR calculator delivers fast and reliable peak integration and DAR values even at low detection levels.

References

[1] Beck, A.; et al. Cutting-edge mass spectrometry methods for the multi-level structural characterization of antibody-drug conjugates. Expert Reviews of Proteomics 2016, 13:2, 157-183.

A Complete Data Integrity Solution for Quality Control Laboratories using Mass Spectrometry

Leo Wang and Hua Dong

Software and Informatics Division, Agilent Technologies

ASMS 2017
ThP - 352

Agilent
Trusted Answers

Introduction

Data integrity regulatory enforcement has evolved dramatically since 2013. Both technical and procedural controls are required to meet current regulatory guidelines. Compared with procedural control, technical controls are preferred to maintain data integrity.

Residual solvent analysis (RSA) is a common quality control activity in a pharmaceutical QC laboratory to evaluate the content of residual organic volatile chemicals in pharmaceutical products. Adding mass spectrometry for RSA greatly improves the method sensitivity and provides the capability to screen more than 50 solvents in a single run.

Here we present a complete data integrity solution for mass spectrometric applications using OpenLAB CDS with advanced technical control features to facilitate the generation and management of regulated records, and to reduce the burden on extensive procedural control measures, while improving laboratory productivity.

Experimental

Residual solvent analysis (RSA) is performed using an Agilent GC/MS with a headspace sampler. Data is acquired and processed by OpenLAB CDS software.

Samples containing residual chemicals with concentrations higher than the USP<467> limits (and confirmation with mass spectrometry) are flagged and reported.

Unknowns found are searched against a spectral library for identity confirmation based on acquired MS signals. Reporting for Unknown Analysis and MS Library Search can be easily performed with pre-defined report templates with optional customization.

Once identity is confirmed, a residual chemical analyte with a concentration above the threshold is calculated using the embedded Custom Calculator.

All electronic records, including raw data, sequence/result set, acquisition methods, processing methods, processed results, reports, along with audit trails can be reviewed and approved electronically with e-Signatures.

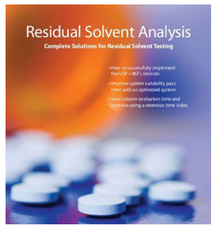

Figure 1. OpenLAB CDS provides a compliance solution for data integrity in pharmaceutical QC labs using mass spectrometry

Results and Discussion

Workflow Automation

Figure 2 illustrates a typical GC/MS chromatogram for residual solvent analysis, where organic solvent analytes were separated by gas chromatography and detected with both FID and MS detectors.

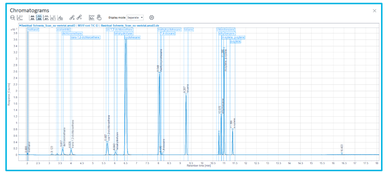

Figure 2. Example Chromatogram for residual solvent analysis with GC/MS

In high throughput laboratories, the complete sample analysis can be performed in an unattended manner where data acquisition, analysis and reporting are completed automatically.

User, User Group and Privilege Management

In a regulated environment, the user role and privilege control is a critical part of the compliance technical control features.

OpenLAB CDS provides comprehensive yet flexible management of users, user groups and user privileges. User privileges and access can be segregated and defined to specific instruments, specific projects, specific type of data sets and specific activities.

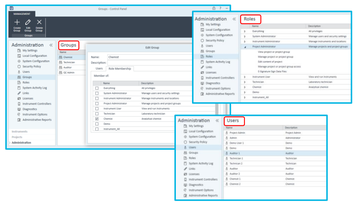

Figure 3. OpenLAB CDS provides central and flexible management for user, user group, user role and privileges

Activity Log and Audit Trail

Another key requirement for technical control features for a regulated laboratory is the capability to record and track all activities and changes that happened in the system. In OpenLAB CDS, System Activity Log records all activities per system, and comprehensive audit trails keep track of generation, transfer, process, modification and other changes for regulated records..

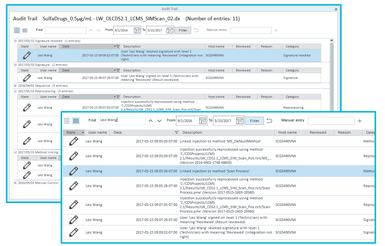

Figure 4. Audit Trail Review

Audit trail entries can be viewed by categories or list, search and filter functions are also available to quickly identify entries of interest.

Electronic Signature (e-Signature)

OpenLAB CDS supports e-Signature workflows. Privileges of applying or revoking e-Signatures can be assigned to specific user(s) or user group(s) that belong to different authorization levels, e.g. technician, supervisor or manager. Meanings of the e-signature can also be defined or customized per regulatory and procedural requirements.

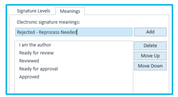

Figure 5. OpenLAB CDS supports e-Signature workflow with e-Signature management

Results and Discussion

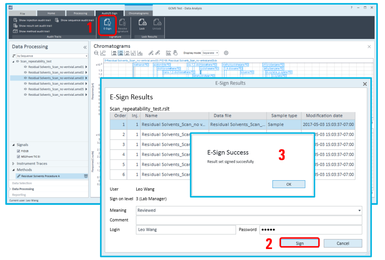

Figure 6. Use of e-Signatures to approve result set

Figure 6 above demonstrates 3 easy steps to approve a result set with e-Signature by authorized users, with the meaning of the signature and review comments. Similarly, e-Signature can be revoked to allow further editing or reprocessing of the data.

Revision Control

OpenLAB CDS tracks the versions of regulated records when audit trail is activated (audit trail for result is activated by default).

For example, Figure 7 below demonstrates the version history of a processing method.

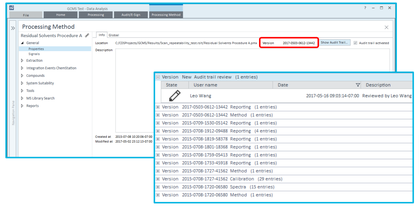

Figure 7. OpenLAB CDS version control

OpenLAB CDS not only tracks the versions of regulated records, but also can provide access to all saved previous versions.

For example, Figure 7 illustrates the versions of a result set from data acquisition, unattended data processing, saving, data review and reprocessing.

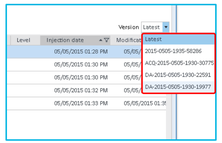

Figure 8. Version control with OpenLAB CDS and OpenLAB Server content management

Conclusions

OpenLAB CDS provides a complete data integrity solution for mass spectrometry applications in quality control laboratories via advanced technical control features:

- Secure centralized data storage
- User, user group and privilege control and management
- Comprehensive activity log and audit trails
- Electronic Signatures
- Revision control and access

References

- Support for Title 21 CFR Part 11 and Annex 11 compliance: Agilent OpenLAB CDS version 2.1, Whitepaper, 5991-6492EN, Agilent Technologies;
- Data Integrity and Compliance with CGMP, Guide for Industry (https://www.fda.gov/downloads/drugs/guidances/ucm495891.pdf, accessed May, 2017)

Versatile Strategies for Analysis of Sulfonate Ester Related Genotoxic Impurities Based on High Performance Chromatography Combined with Mass Spectrometry

Zhengxiang Zhang, Tao Bo

Agilent Technologies (China), No.3 Wang Jing Bei Lu, Chao Yang District, 100102, Beijing, P.R. China

ASMS 2017
TP-709

Agilent
Trusted Answers

Introduction

Genotoxic impurity (GTI) has attracted worldwide attention due to its adverse toxic effect, stemming from accumulation in the human body. Sulfonate ester (Figure 1), like genotoxic impurities are subject of high interest and concern. As such, their strict control in drug substances, as well as drug product is required. The European Pharmacopoeia has introduced a GC-MS based approach to monitor four methanesulfonates in two matrices. Direct injection is suitable for methanesulfonic acid matrix, whereas derivatization with sodium iodide is required for solid matrices. In this work, we have further developed more versatile strategies using different separation tools (GC, LC, 2D-LC), different ionization sources, and different mass analyzers (low resolution and high resolution) to provide multiple choices for real applications.

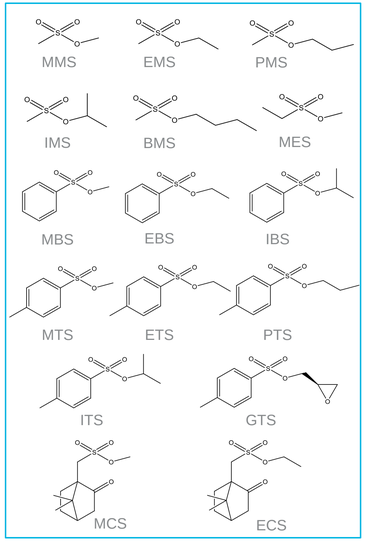

Figure 1. Chemical structures of the investigated targets.

Experimental

Profiling strategy based on LC/TQ for sixteen sulfonate ester like impurities

UHPLC conditions
Injection volume: 10 µL
Column Temp.: 40 ºC
Column: C18 (3.0 x 100 mm, 1.8 µm)
Pump Flow: 0.8 mL/min
Mobile Phase:
A = Water (10 mM ammonium formate); B = MeOH
Gradient elution:
0 min, 15% B; 3 min, 25% B; 9 min, 85% B; 9.1 min, 98% B; 12 min, 98% B.

LC/TQ conditions
Ionization Mode & Polarity: APCI (-)
Gas Temp.: 350 ºC
Gas Flow: 5 L/min
Nebulizer Pressure: 50 psi
Vaporizer: 500 ºC
Capillary HV: 4000 V
MRM Table:

Name	Precursor	Product	Fragmentor (V)	Collision Energy (V)
XTS	171	107	110	21
XTS	171	80	110	33
XBS	157	93	90	17
XBS	157	80	90	33
MES	109	80	90	20
XMS	95	80	110	20
XMS	95	64	110	50
XCS	231	80	100	38

Derivatization strategy based on UHPLC-SQ and GC-SQ for five methanesulfonate ester like impurities

GC-SQ conditions
Refer to EUROPEAN PHARMACOPOEIA 8.0

UHPLC-SQ conditions
Derivatization reagent: 10% (V/V) trimethylamine and 10% (V/V) triethylamine

Experimental

UHPLC conditions
Injection volume: 5 µL
Column Temp.: 40 ºC
Column: Hilic Plus (2.1 x 50 mm, 1.8 µm)
Pump Flow: 0.3 mL/min
Mobile Phase:
A =Water (50 mM ammonium formate & 0.1% FA)
B =ACN
Gradient elution:
0 min, 95% B; 5 min, 85% B; 13 min, 5% B; 15 min, 5% B; 15.1 min, 95% B.

SQ conditions
Ionization Mode & Polarity: AJS-ESI (+)
Gas Temp.: 325 ºC
Gas Flow: 5 L/min
Nebulizer Pressure: 50 psi
Sheath Gas Temp.: 350 ºC
Sheath Gas Flow: 11 L/min
Capillary HV: 3500 V
SIM ions @ m/z 88, 102,116

Fast analysis of ten non-methanesulfonate ester impurities based on LC/TQ

UHPLC conditions
Injection volume: 20 µL
Column Temp.: 40 ºC
Column: C18 (3.0 x 100 mm, 1.8 µm)
Pump Flow: 0.4 mL/min
Mobile Phase:
A =Water (5 mM ammonium formate & 0.1% FA)
B =MeOH
Gradient elution:
0 min, 20% B; 1 min, 20% B; 7 min, 85% B; 8 min, 98% B; 10 min, 98% B; 10.1 min, 20% B.

LC/TQ conditions
Ionization Mode & Polarity: AJS-ESI (+)
Gas Temp.: 325 ºC
Gas Flow: 5 L/min
Nebulizer Pressure: 50 psi
Sheath Gas Temp.: 350 ºC
Sheath Gas Flow: 11 L/min
Capillary HV: 3500 V

Results and Discussion

Overall hardware and software

Below combined platforms were used in this study: GC coupled to single quadrupole (SQ) and Q-TOF mass spectrometers with EI source, and LC coupled to triple-quadrupole (LC/TQ) mass spectrometer with both ESI and APCI sources. Various data acquisition modes including full scan, selected ion monitoring (SIM), and multiple reaction monitoring (MRM) were utilized to collect desired data. Both derivatization and non-derivatization sample pretreatment workflows were employed. Qualitative and quantitative data mining and process work were implemented on dedicated software.

Comprehensive screening

As shown in Figure 2, sixteen sulfonate ester like impurities covering five kinds of structural features, are well resolved under the proposed separation condition and can be quantitatively determined, respectively. This approach is intended to monitor above mentioned compounds in formulation without sulfonate salt and sulfonic acid.

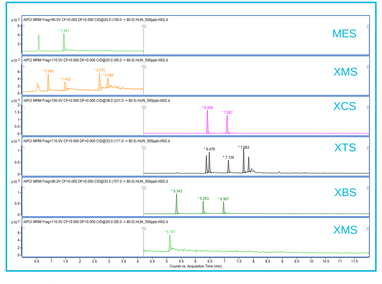

Figure 2. Typical chromatogram of sixteen targets.

Analysis for five methanesulfonate ester based on LC/SQ

Figure 3 displays typical chromatogram of five methanesulfonate ester after derivatization with trimethylamine and triethylamine. LOQ of 0.1 to 1 ng/mL has been achieved to meet the requirement of real application. Even though GC-SQ is recommended by regulatory agency in Europe, this work can become an alternative approach and provide more choices for end-user.

Results and Discussion

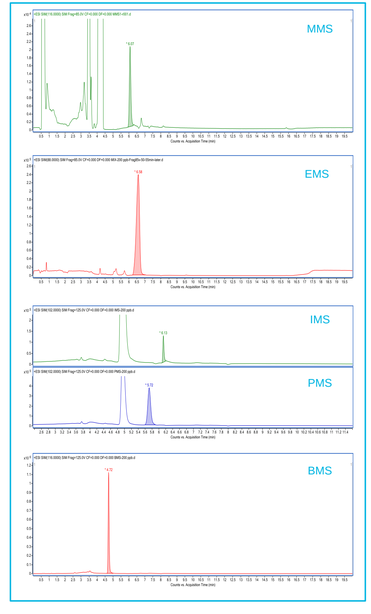

Figure 3. Typical chromatogram of five methane-sulfonate ester.

Highly sensitive detection of ten non-methanesulfonate ester without derivatization

A dedicated method for ten non-methanesulfonate esters without derivatization has been successfully established. As displayed in Figure 4, satisfactory separation and peak shape are provided, especially for structural isomers PTS and ITS. Sub-ng/ml sensitivity can be achieved regardless of the formulation form. Since derivatization is not required, it is easy to test for routine QA/QC and regulatory checks.

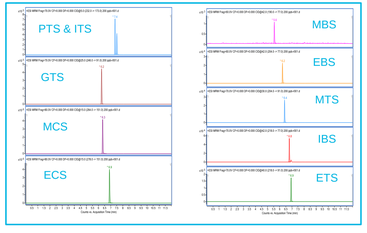

Figure 4. Typical chromatogram of ten non-methane-sulfonate ester.

Conclusions

Seven analytical methods have been successfully developed and validated to monitor GTIs with sulfonate ester structure feature. Each strategy focuses on its corresponding applicability. Strategy one based on an LC/TQ platform supports high-throughput, and comprehensive screening of sixteen GTIs with acceptable analytical sensitivity. Strategy two and three mainly focus on five methanesulfonate esters. Derivatization is performed for better selectivity prior to LC/SQ and GC-SQ analysis in SIM mode. Strategy four provides highly efficient and sensitive detection of ten targets on LC/TQ without derivatization. Strategy five and six are intended to qualitatively and quantitatively investigate benzenesulfonate esters in solid preparations (not shown in this poster). In strategy seven, 2D-LC is utilized to eliminate matrix interferences for accurate determination (not shown in this poster). In summary, the most sulfonate ester related GTIs are covered in current study. It will facilitate drug development and drug product quality control.

References

[1]EUROPEAN PHARMACOPOEIA 8.0

[2]JG An, MJ Sun, L Bai, T Chen, DQ Liu, J. Pharm. Biomed. Anal. 48 (2008) 1006–1010.

Revealing hidden Impurities in Bio-Pharmaceuticals by Multi-Dimensional Chromatography preceding ESI-MS

Buckenmaier Stephan[1], Stoll Dwight[2], Petersson Patrik[3]

[1]Agilent Technologies R&D & Marketing GmbH & Co KG, Waldbronn, Germany

[2]Gustavus Adolphus College, Department of Chemistry, St. Peter, USA.

[3]Novo Nordisk A/S, Global Research, Denmark.

ASMS 2017
ThP-439

Introduction

Impurities in bio-pharmaceuticals are often determined using reversed-phase (U)HPLC with salt gradients. Addition of salts to the mobile phase improves chromatographic performance, but lacks MS-compatibility. Peak tracking in method development is often based on peak areas and experience. MS-characterization requires offline fraction collection, which suffers from time consumption, poor recovery, or impurity degradation.

This work addresses these problems. Degradants of heat-treated bovine insulin were analysed using multiple heart-cutting (MHC) two-dimensional liquid chromatography (2D-LC) coupled to ESI-MS, which allowed acquisition of real time MS-data for low level impurities despite high amounts of salt used in the primary chromatographic method.

Further data demonstrate how Active Solvent Modulation (ASM) improves resolution in 2D-LC and sensitivity.

Experimental

2D LC/MS Setup

Fig. 1: Data acquisition used an Agilent 1290 Infinity II 2D-LC system with multiple heart-cutting operated with OpenLAB CDS Edition C.01.07.

First dimension (^{1}D, blue path):

- Binary pump (0.30 mL/min), MCT (40°C), DAD (215 nm, 20 Hz).
- Column: Poroshell HPH C18 150 x 2.1 mm, 2.7 µm.
- Mobile phase: A = 40 mM $(NH_4)_2HPO_4$ + 60 mM Na_2SO_4 (pH 2.2), B = ACN/water 80:20 v/v.
- Gradient: 29 – 43 %B in 28 min.
- ASM experiments used 0.1% TFA as additive, other conditions similar.

Second dimension (^{2}D, red path):

- Binary pump (0.4 mL/min), MCT (40°C), DAD (215 nm, 40 Hz) and 6550 QTOF MS.
- Column: Poroshell HPH C18 50 x 2.1 mm, 2.7 µm.
- Mobile phase: A = water (0.1% FA), B = ACN/water 80:20 v/v (0.09% FA)
- ^{2}D-gradient: 6.25 %B at 0 min, (to 23% B at 0.1 min, 32 %B at 2.1 min), 90 %B at 2.2 min, held until 2.3 min, 6.25 %B at 2.4 min; cycle time: 4 min.

Experimental

ASM experiments used an isocratic hold at 6.25 %B for for 1 min; cycle time: 5 min.

Multiple heart-cutting (MHC) interface

- 2D-LC Duo Valve connected to two parking decks (A + B) holding twelve 40 µL sampling loops.
- Switch of the 2D-LC valve places decks in sampling or ^{2}D-analysis position.
- Switch of selector valves provides access to discrete loop positions.
- ASM experiments used a 2D-LC Valve ASM (see Fig. 6); sampling loop volumes were 120 µL.

Fig. 1 **Multiple Heart-Cutting (MHC) Interface**

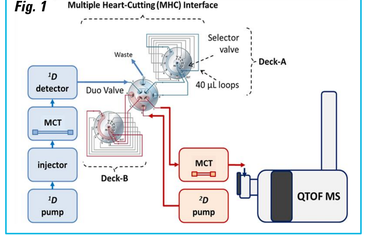

6550 iFunnel Q-TOF LC/MS

- TOF MS in positive mode.
- Mass range 100 – 3,200 m/z, 2 spectra/s.
- Dual AJS ESI source: V_{cap}: 2500 V, Nozzle: 300 V, drying gas-T: 200°C at flow: 15 L/min, nebulizer gas: 35 psi, sheat gas-T: 375°C and flow: 12 L/min.
- Reference masses 121.0509 and 922.0098 m/z.
- MassHunter Qualitative Analysis B07.00 for data processing.
- 2D-chromatogram creator for MassHunter was used for MHC data evaluation.

Samples

Insulin (bovine pancreas, Sigma) was selected as model substance. Degradation was provoked by exposing to 50°C for 72 h at pH 7.4.

Results and Discussion

Salt in Reversed Phase (^{1}D) Chromatography

Fig. 2. Improvement of insulin separation due to addition of 60 mM Na_2SO_4 (A) to the mobile phase containing 40 mM $(NH_4)_2HPO_4$ buffer, pH 2.2 (A+B). 0.1% TFA (C).

- Ionic strength likely to have suppressed mass overload caused by strong electrostatic interactions.

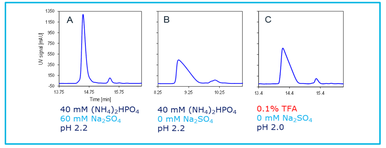

MHC 2D-LC to de-salt prior to MS detection

Fig. 3 (A) ^{1}D-separation of degraded insulin (bovine) and heart-cutting scheme.

- Samples contained higher level of impurities than typical insulin drug. In contrast to drug products, no preservatives were present.
- 13 heart-cuts made from the first dimension of which 11 (highlighted in blue) in close proximity.
- Monitor shows: Cut #8 is ^{2}D-analysed (previously sampled in loop-6 of deck B). Algorithm had parked cuts #3 to 7 into deck B and cuts #9-13 in deck A.

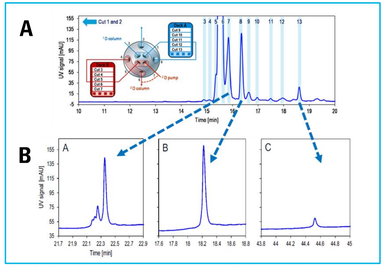

Fig. 3 (B): ^{2}D-separations for cuts #7, 8 and 13.

- Good peak shape obtained in 2D with heights similar to ^{1}D using formic acid as mobile phase additive.
- ^{2}D improved the separation. Four peaks in cut #7 despite use of similar 1D/2D-conditions (same stationary phase & org. modifier, similar pH).
- Additional selectivity in 2D-LC enabled MS detection with high ionic strength ^{1}D-mobile phases and revealed 4 isomers of singly de-amidated insulin; would not have been distinguished by LC/MS alone.
- Cut #8 also contained de-amidation product; only a single peak was observed.
- Cut #13: Likely a product corresponding to a reaction of primary amino group and formaldehyde always present at low levels in lab air.

Limit of detection

Fig. 4 Estimate of the limit of detection. (A) 1D/UV-data showing chromatograms for loads 0.03 - 0.13 area% relative to main API in 1D at a load of 5 µg abs. on column. (B) Superimposed 2D/UV-chromatograms corresponding to cut #2 in (A). (C) Extracted ion 2D-chromatogram of cut #2 from the 0.03% level. (D) Spectrum of the +5 charged molecule.

- Impurity level 0.03% was readily detected in 1D/UV (A).
- 2D-LC/UV allowed levels down to 0.05% (B).
- 2D-LC/MS gave prominent EIC peaks and high quality MS spectra for the 0.03% level (C,D).
- Spectra did not contain marked amounts of adducts and no salt clusters at elution times of insulin degradation products. Demonstrates successful de-salting by using MHC 2D-LC.
- Linear responses were obtained at these low area% levels with R^2 = 1.000 in ^{1}D and 0.9994 in 2D obtained for plots total peak area vs. %area relative to main API at injection of 5 µg abs.

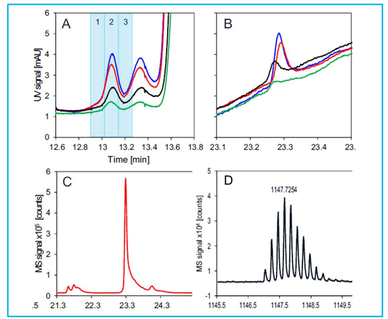

Results and Discussion

Active Solvent Modulation (ASM)

ASM addresses potential solvent incompatibility issues between ^{1}D and ^{2}D, which may occur if solvent in which the compound of interest is sampled from ^{1}D (before being transferred to ^{2}D) has high elution strength relative to the ^{2}D-column. This incompatibility can cause severe peak broadening/splitting, loss of resolution.

Fig. 5 Demonstration of solvent incompatibility issue and solution = ASM results. (A): ^{1}D-sampling scheme. 120 µL aliquots were transferred to the ^{2}D-column (void-V.:~104µL)*. (B): Representative ^{2}D results, without (left) and using ASM (right).

- ASM enabled focusing of analytes on the head of the ^{2}D column ➔ ASM process improved resolution.
- Helps to reveal insulin (bovine) impurities.

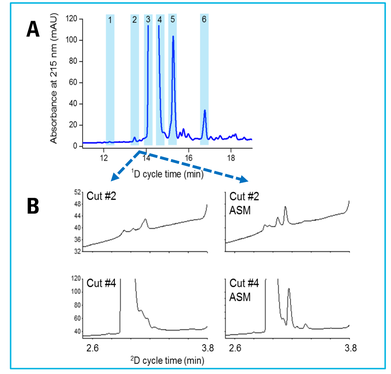

Fig. 6 (A) Description of ASM workflow (B) ^{2}D gradient.

- Pos-1: Sampling from ^{1}D in loop-2 (L-2), analysis of sample from L-1, bypass offline.
- Pos-2: Start of ^{2}D from L-2, bypass in line ➔ sample transfer, dilution with weak portion of the ^{2}D gradient (B) to cause analyte focusing on ^{2}D column.
- Pos-3: ^{2}D gradient start through loop, bypass offline.
- Pos-4: Solvent modulation position for sample in L-1.

For Research Use Only. Not for use in diagnostic procedures.

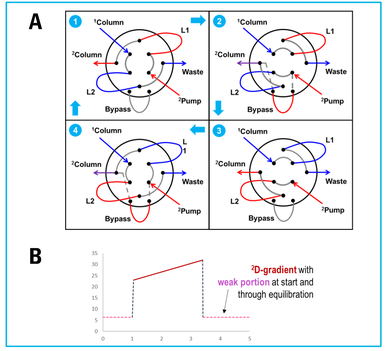

Conclusions

MHC 2D-LC was successfully applied for online de-salting of samples of insulin degradation products that were obtained from chromatography that used high salt content in the mobile phase.

Allowed employment of optimized "salty" methods for best performance in ^{1}D and almost real time MS detection in ^{2}D, which eliminates guesswork during method development for separations of related impurities in bio-pharmaceuticals.

2D-LC permitted differentiation of mass isomers, which could not have been done by LC/MS alone.

Linear response at low concentration levels was obtained allowing quantification of ≤0.05% impurity levels with 2D-LC/UV.

MS gave clean spectra, which were salt cluster and almost adduct free, enabling characterization even at very low detection limits (<<<0.03%).

Thus, MHC 2D-LC reduces the time for a current characterization workflow substantially (from days to hours), and lowers the risk for poor recovery and degradation when using offline fraction collection approaches.

Active Solvent Modulation (ASM) boosts detection capability, and sensitivity.

Understanding metabolism of an achiral Drug to chiral metabolites in biological matrices using SFC-TQ technology

Siji Joseph[1], Rajendra Prasad T[2], Prashant Kole[2], Prabhakar KR[2], Patrick Jeanville[3]

[1]Agilent Technologies, Bangalore, India,
[2]Biocon BMS R&D Center, Syngene International Ltd., Bangalore, India
[3]Agilent Technologies, Santa Clara, CA

ASMS 2017
TP-154

Introduction

Risperidone, an antipsychotic drug, is metabolized by different cytochrome P-450 enzymes, to predominantly form 9-hydroxy metabolites. The 9-hydroxylation results in the formation of a chiral carbon atom yielding two enantiomers, 9S-(+)- and 9R-(-)-hydroxyrisperidone. To a **lesser extent N-dealkylation and also another pair of 7(RS)-hydroxy stereoisomers. Thus, sensitive and selective analytical methods are required to profile these metabolite stereoisomers. To distinguish stereoisomers, and identify trace level metabolites,** baseline resolved chromatographic separation and the sensitive mass spectrometer are required.

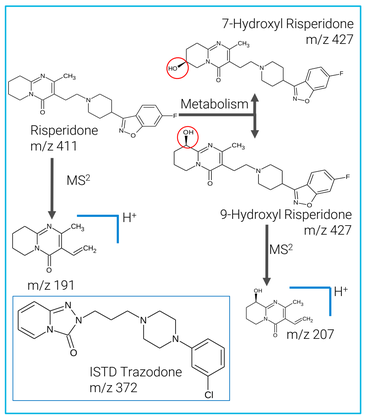

Figure 1: Structures of risperidone, hydroxy metabolites and most abundant product ions

Figure 2: SFC-TQ Instrumentation

Experimental

LC-QQQ Methodology

A robust SFC-MS/MS method was developed for quantitation of achiral risperidone and its enantiomeric hydroxy metabolites. The SFC-TQ method was fast and offered efficient separation of risperidone and the enantiomers of 7- and 9-hydroxy risperidone for sensitive quantitation. The total separation time was 6 minutes and trazodone was used as an internal standard. Protonated precursors of risperidone and its metabolites were selected for MRM based quantification. Experiments were performed to assess specificity and carry over for each analyte. The method was partially validated from 0.9 nM to 15 mm using rat liver microsomes as the matrix for risperidone and enantiomers of its major metabolite, 9-hydroxy risperidone. Samples were protein crashed with 4 volumes of methanol containing internal standard and then centrifuged at 10,000 rpm for 6 min and supernatant was used for the SFC-TQ analysis.

Table 1: Agilent 1260 Binary SFC Method Parameters		
SFC	BPR, Pressure;120 bar, Temp; 60°C	
Mobile Phases	A: CO2, B: 0.1%FA in MeOH with 40mM ammonium acetate	
Column	CHIRALPAK AD-3 (3.0x100)mm 3µm at 45°C	
Injection Vol.	Partial Loop: 3µL	
Gradient (Flow rate: 2.5mL/min)	Time (min)	%B
	0	25
	1.5	35
	6	35
Post Run	2 min	

Table 2: Agilent 6460 TQ Acquisition parameters	
Acquisition Mode	MRM, +ve Mode
Capillary Voltage	30V
Fragmentor Voltage	140V
Dwell Time	50ms
Q1 / Q2 Resolution	Wide/ Unit
AJS Source Parameters	
Gas Temperature	325°C
Gas Flow	8 L/min
Nebulizer	25 psi
Sheath Gas	375°C
Sheath Gas Flow	12 L/min
V Cap	3500 V

Results and Discussion

Elution of Target Analytes

Chiral SFC analysis using a CHIRALPAK AD-3 column was able to resolve enantiomers of both 7- and 9-hydroxy risperidone as well as parent drug and internal standard. Excellent baseline separation of all analytes was observed with good method reproducibility (Figure 3). The selectivity, accuracy, precision and linearity range were evaluated to ensure the method reproducibility. The linearity was tested from 0.9 to 15000 nM using rat liver microsomes as the matrix for risperidone and enantiomers of its major metabolite, 9-hydroxy risperidone. For the minor metabolite, 7-hydroxy risperidone, the method was found to be linear from 0.5 to 7500 nM.

Consistent reproducibility over 300 repeated injections confirmed the method repeatability (Figure 4). Precision was determined by measuring relative standard deviation (RSD) of retention time (RT) and peak area on replicate injections for six different preparations of QC samples (LQC, MQC & HQC). Excellent retention time and peak area ratio precision values for all samples were observed. The RT RSD was < 0.7 % and area ratio RSD was < 3.0 % for all three QC samples (Figures 5). Method accuracy was calculated using quality control samples and was found to be within 100+/-10%. The validated method was used to study risperidone in-vitro metabolism and in-vivo pharmacokinetic studies

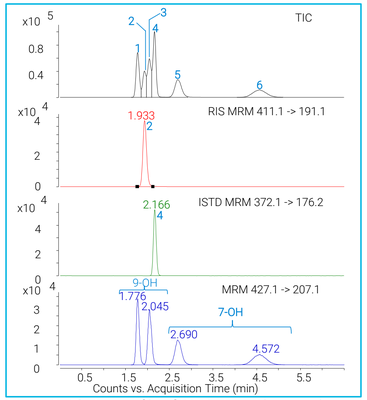

Figure 3: Elution profile of ISTD, risperidone, and hydroxy metabolites. The top trace is the total ion chromatogram (TIC) and below are individual MRM traces of each analyte

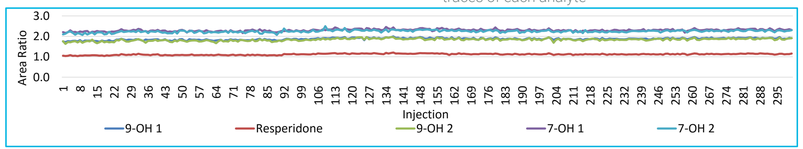

Figure 4: Area ratio reproducibility of risperidone, and hydroxy metabolites over 301 injections

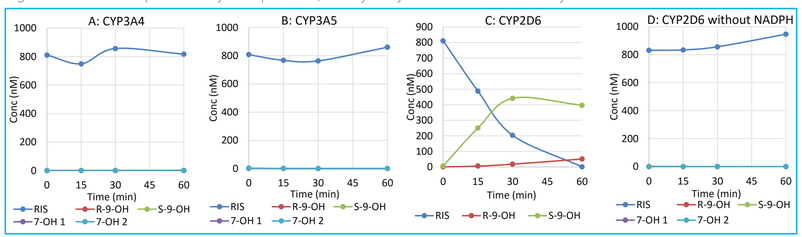

Figure 5: Metabolism of 1 µM risperidone with enzymes, A: CYP3A4, B: CYP3A5, C: CYP2D6, D: CYP2D6 without NADPH

Results and Discussion

In-vitro metabolism and in-vivo pharmacokinetics

A chiral SFC method was successfully used in-vitro metabolism and in-vivo pharmacokinetic study for clinical research purposes.

Rat Liver Microsomes (RLM) were incubated with 10µM risperidone and the formation of metabolites over 5-time points (0, 5, 10, 20, 30, and 60min) was monitored. It was observed that S-(+)-9-hydroxyrisperidone is the major enantiomer formed in rat liver microsomes (Figure 6).

A **phenotyping** reaction revealed that CYP2D6 is the major enzyme involved in the formation of 9-hydroxy metabolites, while CYP3A4 and CYP3A5 did not show any involvement in risperidone metabolism (Figure 5).

The method was used to collect PO and in-vivo pharmacokinetic profiles of risperidone in Sprague-Dawley rats. Time points: 0m,15m, 30m, 1h, 3h, 5h, 7h, 24h, 32h, 48h (Figure 7). Pharmacokinetic parameters obtained were similar to the reported values.

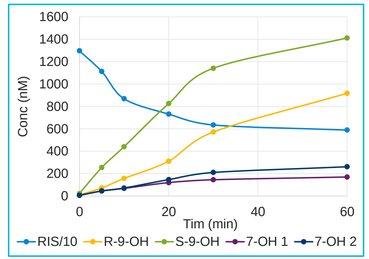

Figure 6: Representation of risperidone metabolism and formation of metabolites over one hour

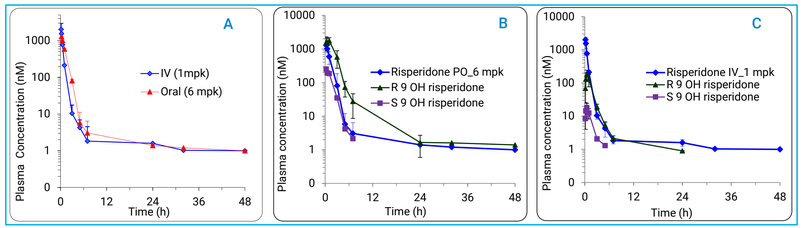

Figure 7: A: PK profile of Risperidone in SD rat. B: Profile of Risperidone and its metabolites after PO administration of risperidone in mice, C: Profile of Risperidone and its metabolites after IV administration of risperidone in mice.

Conclusions

- SFC-TQ can be an orthogonal analytical technology for the qualitative and quantitative analysis of NCEs in biological matrices
- Our method demonstrates an efficient, fast (6 min), sensitive and robust separation of achiral risperidone and its enantiomeric hydroxy metabolite in biological matrices
- The method was partially validated from 0.9 nM to 15000 nM for risperidone and enantiomers 9-hydroxy risperidone. For 7-hydroxy risperidone, the method was found to be linear from 0.5nM to 7500nM
- Intra-day precision for all analytes was ≤ 3% and the corresponding value for inter-day precision was <7%. Method accuracy was calculated using quality control samples and was found to be within 100 + 10%
- Validated method was used to study risperidone in-vitro metabolism and in-vivo pharmacokinetic studies for clinical research purposes

  For more details: Refer to Agilent Publication 5991-7708EN

2D-LC/MS analysis of fosfomycin trometamol and related substances in stress testing solvent

Nan Hu, Xialong Zuo
Agilent Technologies (China), Beijing, CHINA

ASMS 2017
ThP - 438

Agilent
Trusted Answers

Introduction

Fosfomycin is a broad-spectrum antibiotic discovered in 1969. Today, it is often dispensed as an oral formulation for a variety of infections with low toxicity. Due to the compounds characteristics (small molecule, highly hydrophilic phosphoric acid and no UV absorption at above 220nm), it is difficult to separate and detect fosfomycin trometamol and related substances. In British, Chinese and European pharmacopoeia [1-3], the related substances are analyzed by HPLC with NH_2-column, KH_2PO_4 solvent and RID detector.

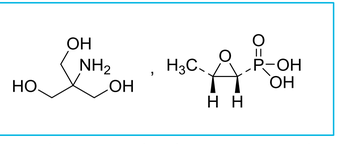

Figure 1. The Structure of Fosfomycin Trometamol.

Based on pharmacopoeia, a 2D-LC/MS methodology was developed as a more suitable assay for unknown impurities. A short SAX trap column to desalt and enrich target compounds and a C18 column in second dimension is used for separating other nonpolar compounds. The molecular formulas of impurities were calculated by accurate mass data from the LC/TOF MS.

Experimental

LC Conditions

1st dimension: 1290 Infinity II UHPLC System	
Column 1	ZORBAX NH_2 (4.6 x 250 mm, 5 µm)
Mobile phase	0.08M KH_2PO_4 in water
Flow rate	1.0 mL /min
Oven Temperature	35 ℃
Injection	10 µL
Pump 1	Isocratic for 50 minutes

2nd dimension: 1290 Infinity II UHPLC System	
Column 2	ZORBAX C18 (2.1 x 50 mm, 5 µm)
Mobile phase	A. 20mM $NH_4CH_3CO_2$ inH_2O; B. B. AcN
Flow rate	0.4 mL /min
Pump 1	Gradient elution
Valve	2-Position/6-Port valve
Trap column	PL-SAX Guard (5 x 3 mm)

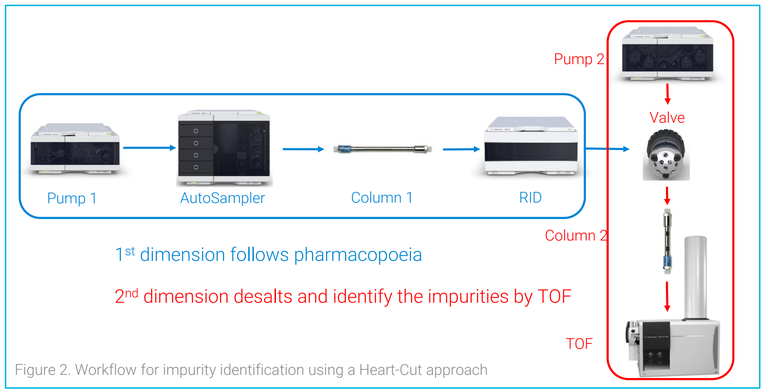

Figure 2. Workflow for impurity identification using a Heart-Cut approach

Results and Discussion

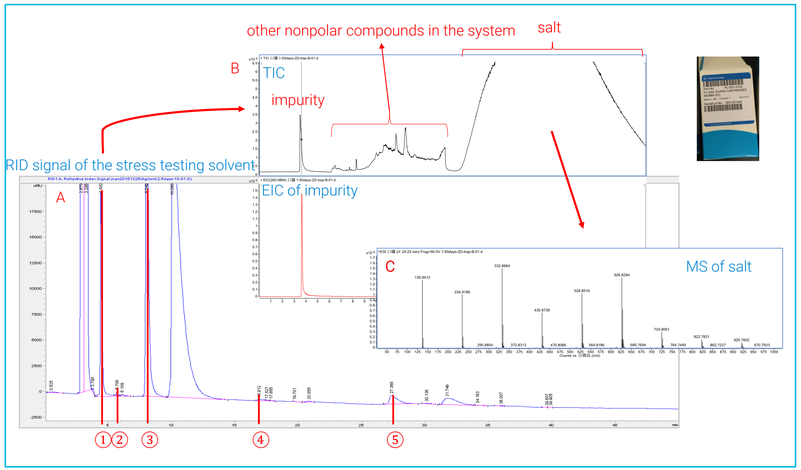

Figure 3. A) The RID signal of the stress testing solvent
B) The TIC and EIC of impurity 1 after desalting and enrichment by the SAX trapping column
C) The mass signal of potassium salt. In regular analysis, this part is switched to waste

MS Conditions

Agilent 6230 TOF Mass Spectrometer	
Ion source	ESI
Ion Polarity	Positive
Capillary voltage	3500 V
Drying gas temperature	325 °C
Drying gas flow	10 L/min (N_2)
Nebulizer pressure	40 psi (N_2)
Spectral rate	2 spectra/s

Elution profile of fosfomycin trometamol using LC-RID analysis

Fosfomycin trometamol was dissolved in mobile phase, incubated at 60 °C for 24 h and placed for 5 days. This solvent was used as stress testing solvent which contained API and several related substances. According to the pharmacopoeia method, more peaks of impurities were observed in the stress testing solvent.

Optimization of the retention time of major impurities and the time of switching valve was performed. As shown in Figure 3, five impurities were diverted to the 2nd dimension with 0.2min trapped in the SAX column. The entire process can be controlled by MassHunter Acquisition as automated methods.

Results and Discussion

Desalt method approach in the 2nd dimension

In the second dimension, several kinds of columns, such as C18, HILIC and ion exchange were tested during method development. With the C18 column, strong ion suppression was observed attributed to no retention for the polar compound. With the HILIC column, it was difficult to distinguish the impurity peak from the complex total ion chromatogram obtained from the MS detector. Additionally, an MS compatible mobile phase for the ion exchange column could not be identified.

Ultimately, a very short strong anion exchange (SAX) column was installed via 6-Port valve after the RID as a trapping column to desalt and enrich related compounds. After desalting by SAX column, the impurity signal is clearly apparent in the TIC. Salts are retained until the end of the analysis in the 2nd dimension; this fraction can be switched to waste without contaminating the mass spectrometer system.

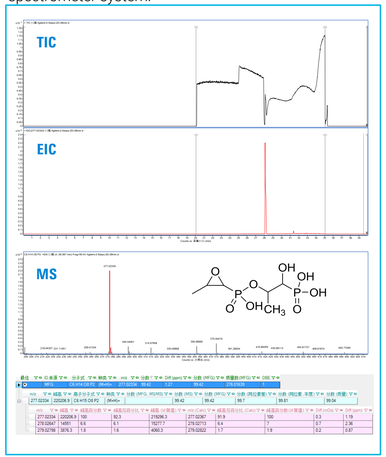

Figure 4. The TIC, EIC and MS spectra of impurity 5. The molecular formula is C6H14O8P2 and the structure proposed refer to literature.

Identification of unknown impurities

Based on retention time, the valve was switched and the specific impurity was delivered to a C18 column, separated using an MS compatible mobile phase from pump 2, and acquired with high resolution accurate mass data by an Agilent 6230 TOF MS.

Fosfomycin and 5 related substances were analyzed and the molecular formulas were calculated with good mass accuracy (<2ppm) and isotope pattern. Four impurities had the same formulas as recorded in the European pharmacopoeia. Their identifications were further confirmed by spiking impurity standards. The molecular formula for the last impurity was C6H14O8P2, which was elucidated to be generated by ring-opening and dehydration reaction of two fosfomycin molecules as described in the reference [4] (Figure 4).

Conclusions

- This workflow uses a Heart Cutting two-dimensional LC/MS method to identify impurities in stress testing solvent of fosfomycin trometamol
- This method eliminates the need to develop an MS compatible LC method for a non-MS compatible pharmacopeia method to perform accurate mass analysis of the impurity of the interest
- In order to desalt the highly hydrophilic fosfomycin related compounds, a very short SAX column was equipped as a trapping column. This enabled separation and detection of the impurities by high resolution accurate mass TOF while diverting the salt fraction to waste for preservation of MS operation

References

[1] British Pharmacopoeia 2009
[2] Chinese Pharmacopoeia 2015
[3] EUROPEAN PHARMACOPOEIA 5.0, Page 1638-1639
[4] Liu C, Lin W, Liu H. Chin. J. Pharm. Anal 2009, 29(12) 2081-2084.

Automated Targeted Screening of Leachables in Pharmaceutical Drug Products Using LC/MSD XT Single Quadrupole System

Syed Salman Lateef, Siji Joseph
Agilent Technologies India Pvt. Ltd, Bangalore, Karnataka, India

ASMS 2017
ThP-435

Agilent
Trusted Answers

Introduction

This work describes a leachable screening methodology for pharmaceutical QA/QC labs. We have previously described analysis of organic non-volatile leachables in Ophthalmic Drug Products (OPD) using an accurate mass LC-QTOF System[1]. Here, compounds from that work were used to illustrate the workflow in a QC environment with a robust and simple to operate single quadrupole MS.

The data analysis processing method was linked to the data acquisition method to automate data analysis. The identified compounds were quantified using a standard addition method and qualifier ions were used to increase the level of confidence for identification. To help identify additional peaks possibly coming from suspected leachables, the acquired spectra were matched against a custom NIST LC/MS library.

Experimental

Sample Preparation

8 target compounds were dissolved in acetonitrile to give a stock solution. The ODP was obtained (from local drug stores in India) and used for the leachable analysis.

Figure 1. Agilent LC/MSD XT

Experimental

Workflow and Instrumentation

The workflow is illustrated in Figure 2. Samples were analyzed in SIM/SCAN mode using an Agilent LC/MSD XT (Liquid Chromatograph/Mass Selective Detector), based on single quadrupole technology, with the Agilent 1260 Infinity II LC system, and OpenLAB CDS Software. The experimental details are given in Table 1.

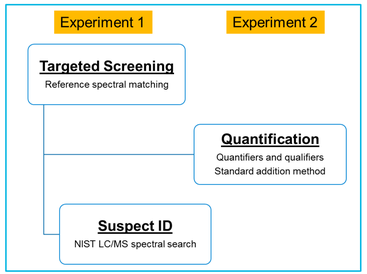

Figure 2. Screening and Quant Workflow

Table 1. LC/MS experimental conditions

Column	**Agilent Poroshell 120 EC-C8, 3.0 x 150 mm, 2.7 µm (p/n 693975-306), operated at 45°C**	
Needle Wash	10 sec (80% methanol/20% water)	
Flow rate/Inj Vol	0.6 mL/min / 2 µL	
Mobile phase	**A: Water, 4.5mM Ammonium Formate + 0.1% Formic acid** **B: 80%MeOH + 20% IPA (v/v), 4.5mM Ammonium Formate + 0.1% Formic acid**	
DAD	**214 ± 4nm, 230 ± 4nm, 254 ± 4nm, and 280 ± 4nm (reference 360 ± 100nm), at 10 Hz**	
Gradient	**Time (min)**	**Mobile phase (B%)**
	0	**7**
	5	**15**
	20	**100**
	25	**100**
	Stop Time: 25 min; Post Time: 5 min	
MSD XT parameters	**Drying gas flow**	**10 L/min**
	Drying gas temperature	**150 °C**
	Nebulizer pressure	**40 psi**
	Capillary voltage	**3500 V (positive and negative modes)**
	Nozzle voltage	**300 (positive and negative modes)**
	Fragmentor voltage	**120 V (Positive mode), 90 (Negative mode)**
	Peak Width	**0.06 min**
	Dwell time	**200 ms**

System Suitability:

The System Suitability test mix containing 3 compounds (chosen from the 8 standards, Table 2) was run to ensure system performance.

Results and Discussion

Table 2. Target compounds

Compound Name	Formula	Predominant charge	UV nm	m/z	SIM m/z	RT
Phthalic anhydride	C8H4O3	[M+H]+	280	149	149	9.73
Methyl-2-benzoyl benzoate	C15H12O3	[M+H]+	280	241.1	209.2	14.59
2,2-Dimethoxy-2-phenyl-acetophenone (Irgacure 561)	C16H16O3	[M+H]+	280	257.1	225.3	16.29
3,5-Ditert-butyl-4-hydroxybenzyl alcohol	C15H24O2	[M-H]- and +	280	235.1 (-)	219.0 (+) 235.1 (-)	17.03
Isopropyl-9H-thioxanthen-9-one, mixture of 2 and 4-isomers	C16H14OS	[M+H]+	280	255.1	255.1	18.31
2-Ethylhexyl 4-(dimethyl-amino) benzoate (Octyldimethyl PABA)	C17H27NO2	[M+H]+	280	278.2	278.2	19.64
1,3-Di-tert butyl benzene	C14H22	-	214	-	-	20.15
Bis (2-ethylhexyl) phthalate	C24H38O4	[M+H]+	280	391.3	391.3	21.13

Setting up the Processing Method:

The separated target compounds with their chromatographic and spectral data (UV, MS –SCAN, MS-SIM) were saved within the processing method (Figure 3).

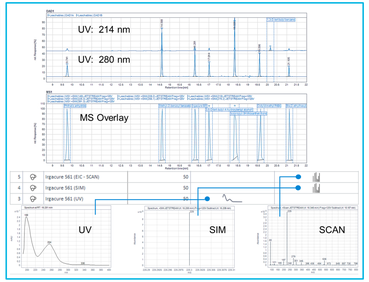

Figure 3. The processing method setup

Automated targeted screening:

- The results report type is selected
- The processing Master method is updated and added to the sequence table for ODP analysis
- Automated reports are generated
- Methyl-2-benzoyl benzoate, and irgacure 561 were identified in the ODP sample

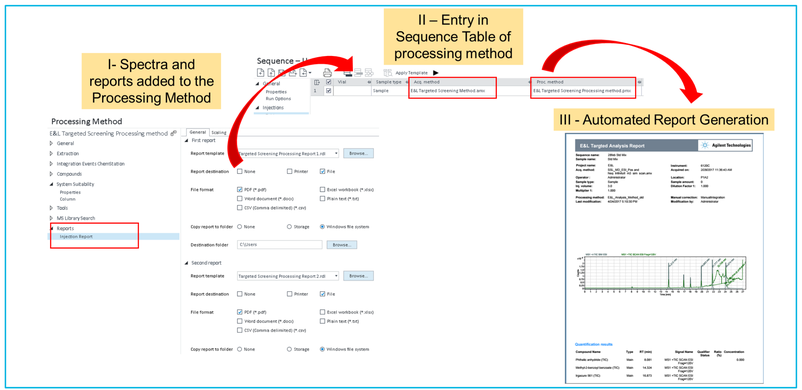

Figure 4. Automated data processing

Results and Discussion

Compliance:

QC laboratories operate under GMP guidelines where data security, integrity, and traceability are in accordance with 21 CFR part 11 or EU Annex 11.

Data Integrity

Data integrity is defined as data being complete, consistent and accurate. To maintain data accuracy in QC labs, application specific calculations are performed by custom calculator within the OpenLAB CDS system.

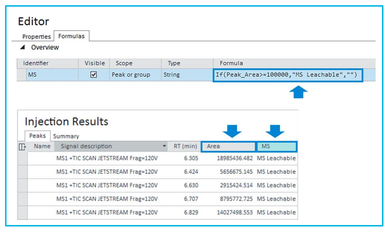

Figure 5. AET setup by custom calculator

The "IF" command was used to display mass spec peaks crossing an arbitrary threshold area value of 100000 as "MS Leachable". In this work, this Analytical Evaluation Threshold (AET) value is arbitrarily set but true AET values for ODP are at least 10x higher.

Quantification:

SIM based quantification using quantifiers and qualifiers of methyl-2-benzoyl benzoate, irgacure 561 and internal standard is shown in Figure 6.

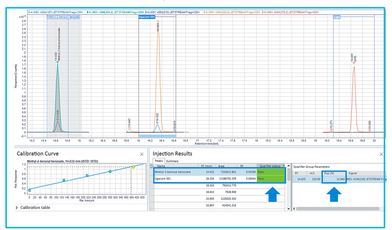

Figure 6. Quantification by standard addition

Qualifier ions increase the confidence of determining the concentration of the target compound in the sample. Concentrations of 148.4 and 140 ng/mL concentration were determined for methyl 2-benzyl benzoate and irgacure 561 respectively.

Suspect Screening:

Suspect peak (labeled as "MS Leachables") from the DP sample were library screened. Its mass spectra was extracted and library searched. Erucamide was identified with a high library matching score.

Figure 7. Suspect screening by library matching

Conclusions

- A rapid and efficient automated targeted screening method for leachables from drug formulations is described using the Agilent LC/MSD XT operating with OpenLAB CDS.
- Quantifier ions together with qualifier ions were used to quantify analytes with added confidence.
- The ability to search unit mass LC/MS spectral libraries, allowed identification of suspect compounds.
- OpenLAB CDS provides data security, integrity, and traceability enables compliance for QC labs.

References

Ref 1: Lateef, S.S., "Extractables and Leachables Detected in Ophthalmic Drug Products Detection and Identification Using High-Resolution LC/MS/MS," Agilent Application Note, 5991-6828EN, 2016.

Analysis of extractable and leachable (E&L) compounds using a novel low-energy EI capable high resolution accurate mass GC/Q-TOF

Kevin Rowland[1], Mark Jordi[1], Kai Chen[2] and Jennifer Sanderson[2]

[1] Jordi Labs, Mansfield, Massachusetts

[2] Agilent Technologies, Inc., Santa Clara, California

ASMS 2017
TP-689

Introduction

Accurate compound identification is critical to the studies of Extractables and Leachables (E&L) [1]. The complexity of E&L extracts, containing chemicals with a wide range of classes and concentrations, poses challenges for compound identification [2]. The GC-amenable portion of E&L studies is conventionally carried out with a unit mass GC/MS in standard EI full scan mode, with compound identification via NIST GC/MS library searching. Limited knowledge can be obtained from this technique for those compounds detected without a convincing library match score.

In this work, we present a novel tool to study E&L compounds with enhanced flexibility and confidence using a high resolution accurate mass GC/Q-TOF equipped with a low-energy EI capable ion source.

Experimental

Instrumental Analysis

The sample extracts and controls were analyzed by an Agilent 7250 GC/Q-TOF system (figure 1), with operational conditions listed in table 1. An injection of *n*-alkanes was used to calibrate the retention index (RI) of the acquisition method.

Figure 1. 7250 GC/Q-TOF system

Experimental

Table 1. GC/Q-TOF operational conditions

Parameter	Value
Column	DB-5 MS UI 15 m x 0.25 mm x 0.25 µm
Inlet	S/SL, 310 °C
Carrier gas	1.5 mL/min Helium
Oven program	50 °C for 5 min 10 °C/min to 320 °C, 10 min
Transferline	280 °C
Source mode	EI, 70 eV, 10-15eV
Source temp	200 °C
Quad temp	150 °C
Spectral range	50 to 1000 m/z

Data Analysis

Compound identification started with MassHunter Unknowns Analysis B.08 using SureMass signal processing and matching against the NIST 14 GC/MS library (figure 2). The MS/MS spectra-based structure elucidation of the candidates for the unknowns was performed using MassHunter Molecular Structure Correlator B.08. Mass Profiler Professional B.13 was used for differential analysis among sample groups.

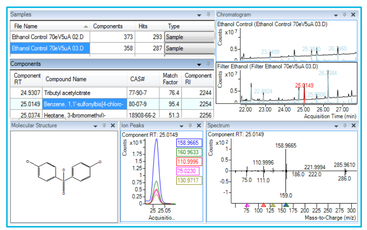

Figure 2. MassHunter Unknowns Analysis software for SureMass peak detection and library matching

Sample Preparation

The components of a model processing unit were extracted using ethanol and water/ethanol (1:1) solutions. The extraction vessels of controls and samples were placed in an oven (50 °C) with shaking at 50 rpm for 72 hours. The leachable extraction of a complete device was performed with a constant circulation of 300 mL of saline solution at 37 °C for 72 hours. Each extract solution (except ethanol) was extracted with equal volume of dichloromethane, and then concentrated 10 times for GC/Q-TOF analysis.

Results and Discussion

Saline Extract vs Control Blank (Leachable Study)

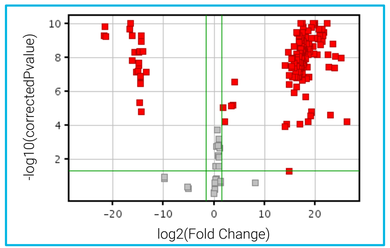

Figure 3. Volcano plot facilitates to reveal compounds significantly present in the saline extract (upper right).

The significance analysis results show 113 compounds present in saline extract of the complete device with a fold change ≥ 3 and a *p*-value ≥ 0.05 compared to the control blank (figure 3). The most abundant components are shown in table 2

Table 2. Compound identification list (top list).

Compound Name	Formula	RI	Mass Diff (mDa)
Caprolactam	C6H11NO	1268	0.2
Phenol	C6H6O	978	0.0
Tri(1,2-propyleneglycol), monomethyl ether	C10H22O4	1315	0.0
Dowanol 62b isomer 1	C10H22O4	1291	-0.2
Dowanol 62b isomer 2	C10H22O4	1294	-0.2
Dowanol 62b isomer 3	C10H22O4	1289	0.0
Tentative ID compound	n.a.	1572	n.a.
Dowanol 62b isomer 4	C10H22O4	1286	-0.1
Benzoic acid, 4-ethoxy-, ethyl ester	C11H14O3	1527	0.1
Tentative ID compound	n.a.	1659	n.a.
Vanillin	C8H8O3	1399	-0.1
Hexanamide	C6H13NO	1144	-0.2
Tentative ID compound	C8H12O3	1403	0.1
7,9-Di-tert-butyl-1-oxaspiro(4,5)deca-6,9-diene-2,8-dione	C17H24O3	1908	-0.2
Tentative ID compound	C15H22O	1476	0.4
Ethylparaben	C9H10O3	1522	0.2
2-Pyrrolidinone, 1-methyl-	C5H9NO	1040	0.3
2,4-Di-tert-butylphenol	C14H22O	1507	0.0
Tentative ID compound	C8H8O	1069	-0.2
2-Imidazolidinone, 1,3-dimethyl-	C5H10N2O	1109	0.3
Acetamide, N-cyclohexyl-	C8H15NO	1292	0.2
Butoxyethoxyethanol	C8H18O3	1187	-0.2
Di-t-butylhydroquinone	C14H22O2	1467	0.0
2-Phenylisopropanol	C9H12O	1088	-0.3
Tentative ID compound	n.a.	1014	n.a.
Benzothiazole	C7H5NS	1232	0.2
Dimethyl phthalate	C10H10O4	1452	0.1
Tentative ID compound	C13H20O2	1349	0.5

Impact of Extraction Solvent (Extractable Study)

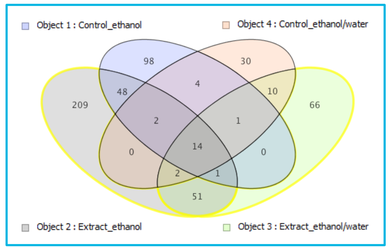

Figure 4. Venn Diagram of extractable compounds from the filter of the device extracted by different solvents.

The extractables from the individual components of the device extracted by ethanol and ethanol/water (1:1) solution to reveal the impact of the extraction solvent were also compared. The Venn Diagram in figure 4 categorizes the components unique to each extraction solvent, and the common ones between the two groups.

Low Energy EI Investigation

The low energy EI experiment increases the possibility of preserving or confirming the molecular ion (M⁺) on the spectrum, as with the example shown in Figure 5.

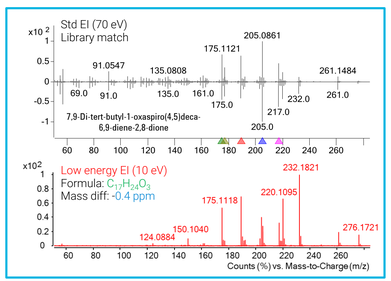

Figure 5. Low energy EI increases the relative abundance of M⁺ on the spectrum of a compound confidently identified with match score of 92.6 (RI: 1908).

Results and Discussion

The workflow to study an unknown compound (common between two solvent extraction groups) with low energy EI and Q-TOF MS/MS is illustrated in figure 6. The possible candidate is a benzenemethanol derivative.

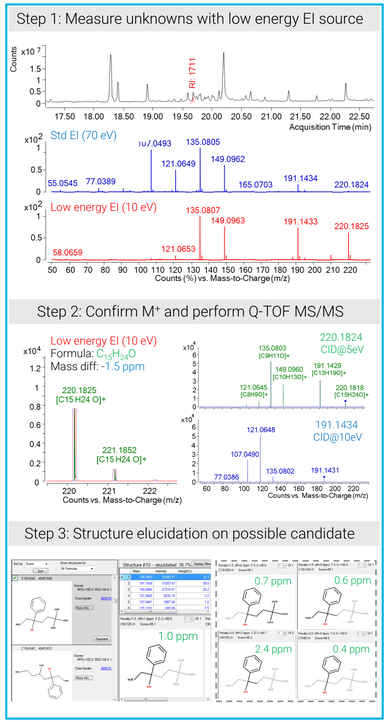

Figure 6. Study of an unknown compound with low energy EI and structure elucidation on a possible candidate using MassHunter Molecular Structure Correlator.

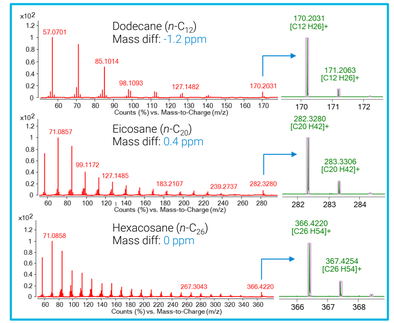

Figure 7. Low energy EI (12 eV) spectra of *n*-alkanes. M⁺ clusters show good mass accuracy and isotopic fidelity.

The low energy EI spectra also helped to confidently identify many alkane compounds which are unique to the ethanol extract with examples shown in Figure 7.

Conclusions

- Low energy EI increases the possibility of preserving or confirming M⁺, and accurate mass MS/MS spectra provide valuable insights in structure elucidation of unknown compounds.
- Accurate mass measurements and retention index calibration can enhance the confidence in compound identification.
- Differential analysis facilitates the comparison study of E&L compounds among sample groups.

References

1 Jenke, D.: Development and Justification of a Risk Evaluation Matrix to Guide Chemical Testing Necessary To Select and Qualify Plastic Components Used in Production Systems for Pharmaceutical Products. PDA J. Pharma. Sci. Technol, **69**, 677–712, (2015).

2 Mire-Sluis, A., Ma, S., Markovic, I., McLeod, L.: Extractable and Leachables. Challenges and Strategies in Biopharmaceutical Development. BioProcess International, Feb (2011).

Manipulation Of Chromatographic Conditions To Maximize The LC/MS Effectiveness

Suresh Babu C.V.[1], Ning Tang[2], Anne Blackwell[3]

[1]Agilent Technologies, India Pvt. Ltd, Bangalore, Karnataka, India
[2]Agilent Technologies, Santa Clara, CA
[3]Agilent Technologies, Wilmington, DE

ASMS 2017
MP-021

Agilent
Trusted Answers

Introduction

For LC/MS-based primary characterization of biomolecules, the correct choice of LC column and method is critical to achieving reproducible separations and high quality MS data. Formic acid ion-pairing agent use in the mobile phase leads to poor chromatographic peak shape with traditional silica based columns.

In this presentation, we have evaluated the performance of polymeric-based reversed phase chromatography for monoclonal antibodies (mAbs) analysis using formic acid modifier. Different sample types such as intact and fragment analysis of various mAbs' were performed to access the separation efficiency. Further, reverse phase LC method for desalting was developed using a polymeric based desalting material and various mAb preparations that contain buffer salts were tested for effective desalting using 2D LC/MS approach.

Experimental

Sample Preparation

Monoclonal antibodies (mAb 1 and mAb 2), and antibody drug conjugate (ADC, mAb 3) were purchased from a local pharmacy and stored according to the manufacturers' instructions. All solvents used were LC/MS grade.

Intact analysis: For intact mAb analysis, mAb samples were diluted to 2 mg/mL using 0.1% formic acid in 3% ACN.

Fragment generation: For reduction: 20 µL of mAb (2 µg/µL) + 5ul DTT (1M), 37 °C for 1 hour. For Papain digestion: 10 µL of mAb (2 µg/µL) + 5 µl digestion buffer (with Cys) + 5 µL of activated papain, 37 °C for 3 hours. For digestion with FabRICATOR: 20 µL of mAb (2 µg/µL) + 0.5 µL FabRICATOR (30 Units), 37 °C for 1 hour.

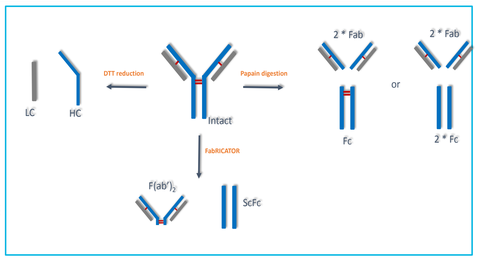

Figure 1: Schematics of mAb fragments generation

LC Parameter	
Column	PLPR-S, 2.1 * 50mm, 5 µm, 1000Å
Inj vol	1 µL
Post time	4 min
Column temp	80 °C
Flow rate	0.6 mL/min
Gradient	0 min – 20% B, 4 min – 20% B, 5 min – 40% B, 10 min – 70% B, 11 min – 90% B, 11.1 min – 20% B

MS Parameter	
Ion mode	Positive ion mode, dual AJS ESI (profile)
Drying gas temp	350 °C
Drying gas flow	8 L/min `
Sheath gas temp	400 °C
Sheath gas flow	11 L/min
Nebulizer	35 psi
Capillary voltage	5,500 V
Fragmentor voltage	300 V
Skimmer voltage	65 V
Oct RF Vpp	750 V
Acquisition	Data were acquired at 2 GHz, MS only mode, mass range 600–4000 m/z (fragments), 2000 – 6000 m/z (intact)
Data analysis	Agilent MassHunter Qualitative Analysis software and Agilent MassHunter BioConfirm software.

Table 1. LC/MS conditions

First-dimensional (IEX)	
Solvent A	Water
Solvent B	NaCl (850.0 mM)
Solvent C	NaH_2PO_4 (41.0 mM)
Solvent D	Na_2HPO_4 (55.0 mM)
Flow rate	0.75 mL/min
Gradient	0 minutes: 30.3 %A, 0.0 %B, 59.6 %C, 10.1 %D 2 minutes: 26.0 %A, 5.0 %B, 56.9 %C, 12.1 %D 8 minutes: 21.5 %A, 10.0 %B, 54.9 %C, 13.6 %D 20 minutes: 13.3 %A, 19.0 %B, 51.9 %C, 15.8 %D 35 minutes: 30.3 %A, 0.0 %B, 59.6 %C, 10.1 %D
1D column	Agilent Bio MAb NP5, 4.6 × 250 mm, PEEK
Second-dimensional (RP)	
Solvent A	0.1% FA
Solvent B	0.1% FA in ACN
Flow rate	0.4 mL/min
Gradient	0 minutes - 5 %B, 0.5minutes – 5 %B, 3minutes – 80 %B, 4 minutes – 80 %B, 4.1 minutes – 5 %B, 6 minutes - 5%B
2D column	Agilent AdvanceBio RP desalting cartridges , 2.1 x 12.5 mm; 10 µm, 1000Å

Figure 2: 2D LC conditions

Results and Discussion

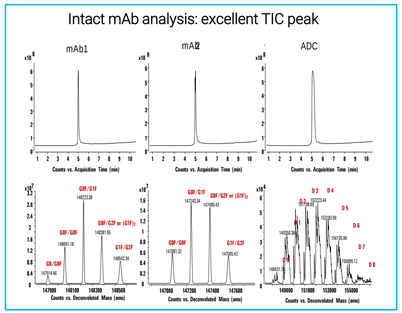

Figure 3. Intact mAb/ADC LC/MS analysis on a PLRP-S, 2.1 x 50 mm, 5 µm, 1000 Å column.

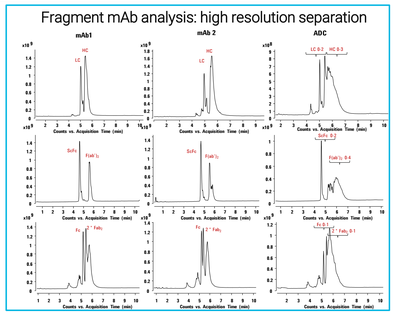

Figure 4. mAb fragment LC/MS analysis on a PLRP-S, 2.1 x 50 mm, 5 µm, 1000 Å column

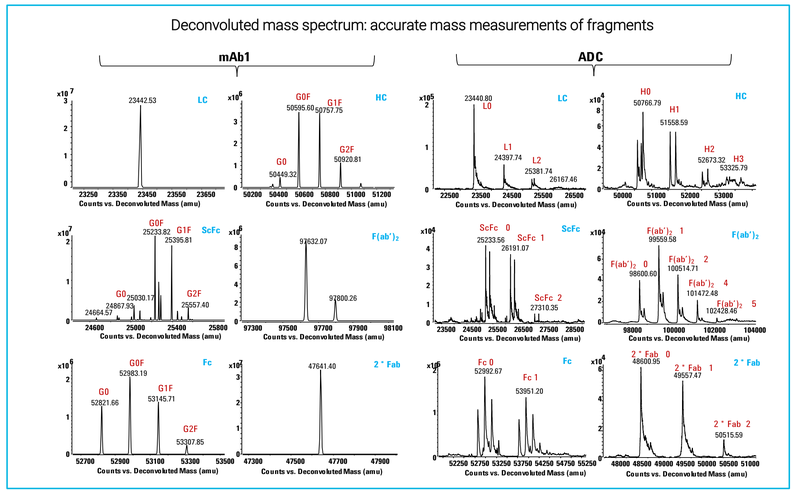

Figure 5. Representative deconvoluted mass spectrum. Top: Reduction; Middle: IdeS digestion Bottom: Papain digestion

Results and Discussion

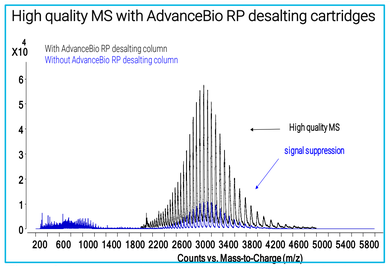

Figure 6. Desalting of mAb1 samples using 2D LC/MS.

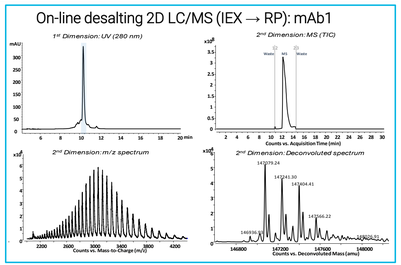

Figure 7. 2D LC/MS profiles of mAb1

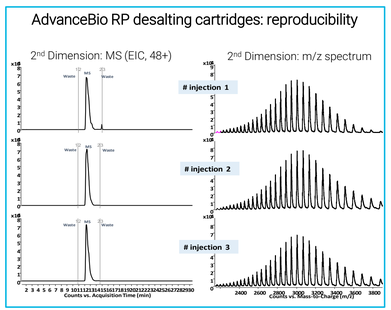

Figure 8. Injection to injection repeatability.

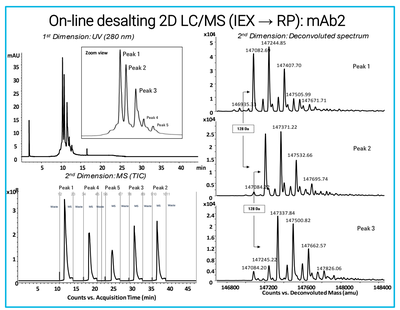

Figure 9. 2D LC/MS of mAb 2 profiles, multiple heart-cutting

Conclusions

- The PLRP-S column demonstrates excellent separation performance for the analysis of mAbs and ADC at both intact and fragment levels.
- The PLRP-S provided better chromatographic performance and high-quality MS response with formic acid-containing mobile phases.
- AdvanceBio desalting cartridges effectively remove salts for better MS sensitivity.

References

- Suresh Babu C.V., "PLRP-S Polymeric Reversed-Phase Column for LC/MS Separation of mAbs and ADC," Agilent Application Note, 5991-7163EN, 2016.
- Suresh Babu C.V., Ravindr G., "Agilent AdvanceBio Desalting-RP Cartridges for Online Desalting in 2D-LC/MS mAb Analysis," Agilent Application Note, 5991-7066EN, 2016.

High throughput platform for screening active constituents in Rhodiola crenulata extract by UHPLC tandem high-resolution mass spectrometry

Tao Bo, Wei Du

Agilent Technologies, No. 3, Wang Jing Bei Lu, Chao Yang District, 100102, Beijing, CHINA

ASMS 2017
MP-120

Agilent
Trusted Answers

Introduction

As an important herbal medicine, Rhodiola crenulata has been widely used as a health food, antidepressant and antifatigue with reinforcing immunity, improving memory, scavenging active-oxygen species, anti-Alzheimer's disease and so on. However, there is few report on systematic analysis of its chemical constituents. Therefore, to develop a sensitive and robust analytical method for identification of chemical constituents in it is necessary and valuable. In our work, a high throughput platform with 30 minute runtime was developed for screening the active constituents in Rhodiola crenulata extract based on UHPLC tandem quadrupole-time of flight mass (Q-TOF) with database search. The workflow of screening bioactive compounds in Rhodiola crenulata was shown below (Figure 1). 46 major active compounds were found and further identified by MS/MS fragmental analysis. This study is significant to interpret material basis for pharmacological effects.

Method

The Rhodiola crenulata extract was dissolved in methanol at 1mg/ml concentration for the LC/MS analysis. All experiments were performed on Agilent QTOF 6545 system coupled to UHPLC1290 platform. The UHPLC and Q-TOF parameters were shown in the table on the right. Home-made dedicated personal compound database and library was utilized with the help of professional software (Agilent Molecular Structure Correlator, MSC) for structure elucidation.

Experimental

Agilent UHPLC 1290 System	
Column	Poroshell EC-C18 2.1X150 mm, 2.7 μm
Mobile phase	A: Water(0.05% Acetic acid); B: ACN, Gradient Elution from 5 to 90 % B in 30 minutes
Flow rate	0.3 mL /min
Oven Temperature	40 °C
Injection	2 μL

Agilent 6545 LC/Q-TOF Mass Spectrometer	
Ion source	AJS
Polarity	Positive/Negative
Ion spray voltage	3500V(Pos) /3000V(Neg)
Dry gas temperature	300°C
Dry gas	6 L/min (N2)
Nebulizer pressure	35 psi (N2)
Sheath Gas Flow	11 L/min (N2)
Sheath Gas Temp	350°C
Acquisition Rate	4Hz MS, 4Hz MS/MS
Collision Energy	10, 20, 40 eV

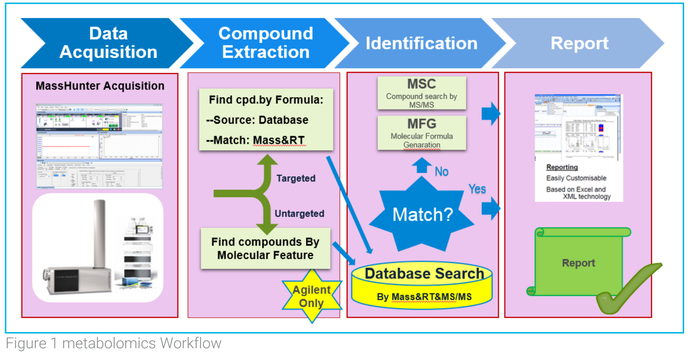

Figure 1 metabolomics Workflow

Results and Discussion

Data Acquisition and Analysis

A high-throughput workflow within 60 min covering sample preparation, chromatographic separation, data acquisition, database search, structure conformation has been well achieved for screening active constitutes in Rhodiola crenulata extract based on UHPLC tandem high-resolution Q-TOF mass spectrometry(Figure 2). AutoMSMS acquisition mode can simultaneously provide MS and MS/MS data for the TCM database searching. Home-made databases including ca.10000 entities for TCM active components identification has been successfully established and applied to the Rhodiola crenulata extract. The MSC software effectively helps the MS/MS elucidation for the structure confirmation of active constitutes found. A total 46 major active compounds were identified with MS/MS fragment confirmation from the Rhodiola crenulata extract, including flavonoids, phenolic acids, terpene and so on (Figure 3).

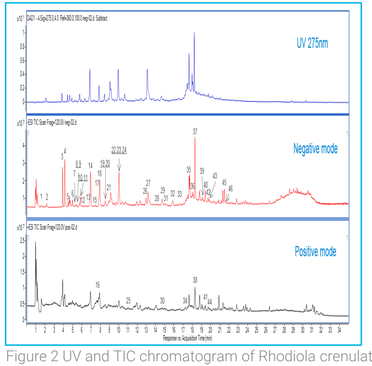

Figure 2 UV and TIC chromatogram of Rhodiola crenulata

No.	Compound	RT (min)	m/z	Polarity	Adduct	Score	Diff (ppm)	MS/MS Fragments
1	Arbutin	1.754	271.082	neg	[M-H]-	98.4	2.84	161.0443,108.0207
2	Gallic acid	2.168	169.0138	neg	[M-H]-	98.4	2.54	125.0247
3	Salidroside	3.912	359.135	neg	[M+CH3COO]-	98.9	0.32	119.0455,89.0235
4	Crenulatin	4.148	307.14	neg	[M+CH3COO]-	99.8	0.59	247.1192,161.0454,101.0241
5	Tyrosol	4.520	137.0603	neg	[M-H]-	96.1	3.41	119.0499,106.0424,93.0345
6	Catechin-(4β-8)-catechin	4.950	577.135	neg	[M-H]-	99.7	0.32	425.0874,407.0775,289.0718
7	Creoside I	5.107	363.1666	neg	[M+CH3COO]-	97.8	1.50	119.0344,89.0246
8	Caffeic acid	5.223	179.0345	neg	[M-H]-	85.5	2.40	135.0451
9	Benzyl-β-D-glucopyranoside	5.248	329.1242	neg	[M+CH3COO]-	99.5	0.42	269.1025
10	Epicatechin	5.720	289.0711	neg	[M-H]-	98.2	1.96	245.0805,109.0285
11	isomer of 6-O-galloyl-salidroside	5.770	451.1245	neg	[M-H]-	98.3	0.24	245.0812,123.0448,109.0290
12	Creoside II	5.952	365.1813	neg	[M+CH3COO]-	99.4	1.29	-
13	Procyanidin B2-3'-O-gallate	6.896	729.1458	neg	[M-H]-	99.0	0.39	407.0771,289.0721,125.0241
14	6-O-galloyl-salidroside	6.946	451.1236	neg	[M-H]-	92.7	1.55	313.0564,169.0147,151.0037,123.0076
15	p-Coumaric acid	7.451	163.0404	neg	[M-H]-	98.6	1.52	119.0502,93.0341
16	2-phenylethyl-1-β-D-glucoside	7.828	285.1331	pos	[M+H]+	99.6	0.47	145.0497,127.0384,85.0284
17	Ethyl gallate	7.914	197.0456	neg	[M-H]-	99.8	0.26	161.0443, 151.0394
18	Vanillic acid	8.055	167.0347	neg	[M-H]-	98.5	1.87	124.0168,108.0216
19	Sachalinoside B	8.502	331.1762	neg	[M-H]-	97.7	0.71	179.0558,119.0347,89.0246
20	Viridoside	8.552	373.1498	neg	[M+CH3COO]-	99.5	0.54	-
21	Ferulic acid	9.020	193.0509	neg	[M-H]-	99.0	1.38	178.0259,134.0362
22	Rhodioloside E	9.927	525.256	neg	[M+CH3COO]-	97.5	1.59	-
23	Catechin	10.009	289.0722	neg	[M-H]-	93.1	1.38	-
24	(-)-Epicatechin-3-O-gallate	10.029	441.0822	neg	[M-H]-	92.6	0.52	289.0706,169.0130
25	isoquercitrin	10.836	465.1024	pos	[M+H]+	99.0	0.82	303.0491
26	n-Hexyl-beta-D-glucopyranoside	12.974	263.15	neg	[M-H]-	99.3	2.71	113.0231,101.0242,71.0136
27	1,2,3,4,6-Pentagalloylglucose	13.197	939.1106	neg	[M-H]-	98.4	0.63	769.0887,617.0773,169.0142
28	Rosiridin	14.092	391.197	neg	[M+CH3COO]-	99.6	0.79	217.0033,161.0457
29	Quercitrin	14.481	447.0935	neg	[M-H]-	98.4	0.2	300.0273,284.0327,255.0301,227.0349
30	Eriodictyol	14.727	289.0706	pos	[M+H]+	99.9	0.23	271.0595,243.0653,153.0175
31	Sachalinoside A	14.970	483.187	neg	[M-H]-	99.5	0.51	285.0398,169.0135,123.0091
32	Rosin	15.864	295.1185	neg	[M-H]-	96.6	2.52	161.0453,133.0663,113.0244,101.0239
33	Rhodiolgin	16.626	463.0882	neg	[M-H]-	98.8	0.02	317.0304,166.9980,139.0041

Results and Discussion

No.	Compound	RT (min)	m/z	Polarity	Adduct	Score	Diff (ppm)	MS/MS Fragments
34	vimalin	17.275	349.126	pos	[M+Na]+	98.9	0.84	-
35	Luteolin-7-O-α-L-rhamnoside	17.657	431.0988	neg	[M-H]-	94.1	1.57	285.0403
36	Rhodiosin	18.025	609.1475	neg	[M-H]-	92.7	0.54	301.0348
37	Rhodiolatuntoside	18.290	447.0933	neg	[M-H]-	99.5	0.08	301.0343
38	Crenuloside	18.294	595.1658	pos	[M+H]+	98.0	0.31	449.1078,303.0490
39	Quercetin	19.168	301.036	neg	[M-H]-	94.6	2.34	178.9984,151.0031,121.0291,107.0128
40	Kaempferol-7-rhamnoside	19.358	431.0977	neg	[M-H]-	97.0	1.23	284.0328,257.0457,151.0035
41	Rhodioloside A	19.438	371.1675	pos	[M+Na]+	92.0	0.34	203.0520,191.1036
42	Creoside V	19.681	449.239	neg	[M-H]-	97.8	1.00	247.1182
43	Denposide A	19.888	507.2447	neg	[M+CH3COO]-	98.6	0.04	-
44	Rhodiooctanoside	19.902	447.2198	pos	[M+H]+	97.8	0.46	-
45	Herbacetin-8-methylether	21.437	315.0509	neg	[M-H]-	97.3	1.11	-
46	Kaempferol	21.619	285.0399	neg	[M-H]-	97.9	1.66	255.0302,227.0340,159.0451,93.0342

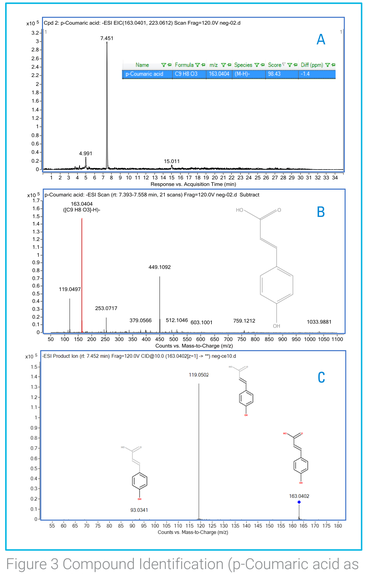

Figure 3 Compound Identification (p-Coumaric acid as an example)
EIC in Rhodiola crenulata sample(A), Mass spectrum(B) and MS/MS fragments elucidation(C)

Conclusions

- 46 major active compounds were identified with MS/MS fragment confirmation from the Rhodiola crenulata extract, including flavonoids, phenolic acids, terpene and so on.
- The established UHPLC-Q-TOF with database search and MS/MS fragmental elucidation provides a high-throughput and robust platform for active compound discovery and quality control in herbal medicine.
- The platform can also be employed to analyzing the chemical constituents in vitro and in vivo for the pharmacological study.

References

1. Fei Han, Characterization of chemical constituents in Rhodiola Crenulate by high-performance liquid chromatography coupled with Fourier-transform ion cyclotron resonance mass spectrometer (HPLC-FT-ICR MS), J. Mass Spectrom. 51(2016), 363–368
2. Fei Han, A rapid and sensitive UHPLC-FT-ICR MS/MS method for identification of chemical constituents in Rhodiola crenulata extract, rat plasma and rat brain after oral administration, Talanta,160 (2016), 183–193

Open Standard for LC/MS Data, Methods, and Results

David W. Peterson, Heiko Fessenmayr,
Agilent Technologies, Inc.

ASMS 2017
ThP-425

Agilent
Trusted Answers

Introduction

Companies and scientists faced with long term data archival and recall requirements must surmount obstacles imposed by changing computational hardware, software, and proprietary vendor data formats. The Pharmaceutical Industry's IQ Consortium has sponsored the Allotrope Foundation (www.allotrope.org) to develop and implement a fully open information standard for the analytical laboratory. Unlike earlier data format standards Allotrope's standards encompass data, methodology, results and extensive sample information. Allotrope member companies from the pharmaceutical industry and Partner Network members (vendors) have been engaged in this effort since 2012. The key concepts behind the Allotrope Data File (ADF) standards employ some of the most recent developments in computer science for organizing complex systems.

- Java and .NET class libraries to read and write the Allotrope standard formats from Microsoft operating systems and any Java virtual machine.
- Use of Web Ontology Language (OWL) www.w3.org to facilitate computer to computer exchange of information and relationships.
- A standard vocabulary of terms, definitions, units of measure to provide consistency across different instruments and vendors.
- Resource Description Framework (RDF) triples to describe "subject-predicate-object" relationships.
- Rigorous definitions for measurement quantities and units of measure - http://www.qudt.org/
- HDF5 Virtual file system from www.hdfgroup.org supported on multiple operating systems.
- ADFs are fully extensible for future applications, company or project specific meta data as well as vendor specific items.
- CMAPs Tool to establish visual representations of sample-predicate-object relationships for discussion and communication to knowledge engineers - http://cmap.ihmc.us/
- Numerous programming development tools to support the technologies using to create, write, and read ADFs.

.

Allotrope Data Container

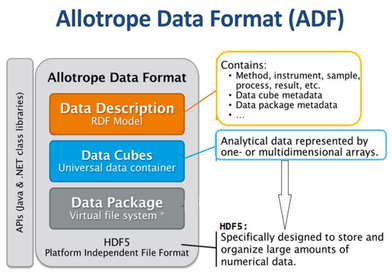

The necessity for these technologies and rigorous development of the ontology and taxonomy becomes apparent when we realize how our definition of a SIM ion in our single quadrupole instrument has changed from a binary format (ChemStation) to an INI file format (ChemStation and MassHunter) and more recently to an XML format (OpenLAB 2). The most common INI format represents SIM ions in a data acquisition method in the following manner.

Ion 1=200.00,100

This terse format does not clearly indicate which number represents the SIM ion and which number is the dwell time. Furthermore, the unit of measure for the dwell time is unstated. The proposed RDF data description being developed is shown below in an *abbreviated* format.

. Run-1- Signal-**SIM-Ion** a «af-c:condition»;
«af-x:has property» «af-x:**m/z**»;
qudt:numericValue "**251**"^^xsd:double ;
qudt:unit qudt-unit:**MassPerCharge**;

Run-1- Signal-**ActualDwell** a «af-c:condition»;
«af-x:has property» «**af-x:event duration**»;
qudt:numericValue "**420.0**"^^xsd:double ;
qudt:unit qudt-unit:**MilliSeconds**;

Results and Discussion

Given the complexity and verbosity of the RDF triples which are intended for computer-to-computer interchange, CMAPs are used as a tool to visualize and communicate the relationships of mass spectrometers within the Allotrope teams and to the knowledge engineers and programmers. The corresponding CMAP for a SIM ion for LC/MS conveys the essence of the SIM ion and its attributes.

.

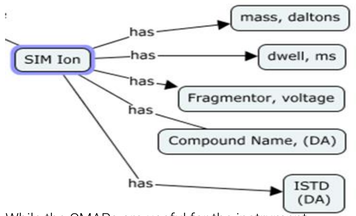

While the CMAPs are useful for the instrument parameters and results that populate the Data Description, the raw data is stored in the Data Cubes. In the case of UV detectors that are sampled at a constant frequency, a simple array in the Data Cube is written. In the case of mass spectral data, there are many types of data and the data varies based on the capability of the instrument. We chose to investigate storage for single quadrupole scanning data. When peak detection is employed, vendors write only the detected peaks into the raw data file resulting in scans that may have no detected masses or hundreds of detected masses. Initial experiments attempted to store each mass spectrum into an individual data cube as a two-dimensional array. When this experiment yielded undesirable results, three arrays were used in a single data cube.

Storage	Mbytes	Creation Time
917 Scan raw File	4	
Separate Data Cubes	26	80 seconds
Single Data Cubes	6	<1 second

Obviously, the overhead to create data cubes is high. When a single data cube is used, the compression algorithms of HD5 may be employed.

.

The data organization for the single cube is shown below.

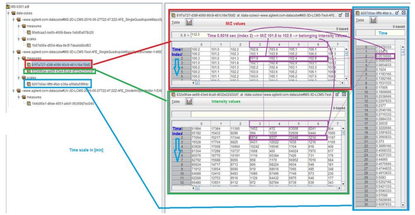

Functional Software Prototype

Ultimately the ADF must be written and read in an environment that is commercially available to the supporters of the Allotrope Foundation. To demonstrate this, a prototype software was developed that supports LC instruments and LC/MS single quadrupole instruments on the ChemStation Edition of OpenLAB. The prototype consists of two components. The first component, the ChemStation2ADF Converter, writes the ADF format with method, raw data, results, instrument traces and other metadata. Once the ADF is created, it is automatically uploaded to an OpenLAB Enterprise Content Management system (ECM) by the Scheduler. The second component, the ADF filter, reads the Data Description from the ADF and places the information into a relational database and which is immediately available to all users through the ECM search and retrieval mechanisms.

Future Activities

- Support other Mass Spectrometer types
- Include qualitative results
- Contribute to the ADF standard for MS
- Read ADFs produced by other vendors

Results and Discussion

Agilent LC-UV and LC/MS Single Quadrupole

Convert ChemStation LC data to ADF / Upload to OpenLAB ECM

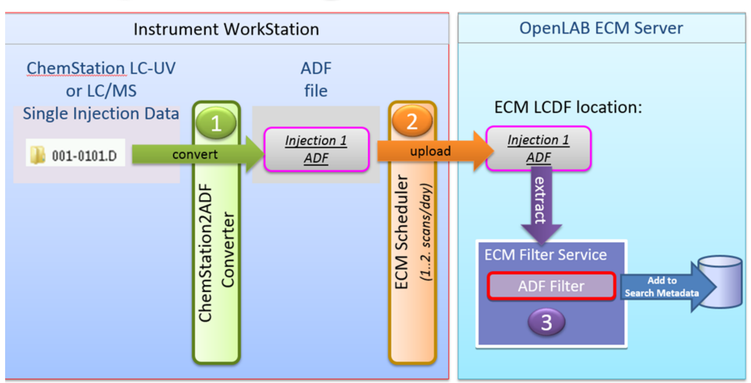

Conclusions

The technologies developed and promoted by the Allotrope Foundation have been demonstrated to work and are in use at several Allotrope member companies.

.

Acknowledgements

The authors acknowledge the contributions and support of the Allotrope Foundation, its Members and Partners as well as several key consultants.

Enhanced Detection of non-covalently bound Enzyme Complexes using a Dedicated Large Molecule Autotune on a Q-TOF Mass Spectrometer

Christian Klein, Huy Bui, Alex Mordehai, Caroline S. Chu, Gregor Overney, William E. Barry
Agilent Technologies Inc., Santa Clara, CA-95051

ASMS 2017
ThP-616

Agilent
Trusted Answers

Introduction

Introduction

The analysis of intact proteins is of great importance to the biopharmaceutical industry. Many released therapeutically relevant drugs are based on monoclonal antibodies.

Nevertheless, for a comprehensive understanding of enzyme complexes different approaches are practiced. The most commonly used method is the infusion of the complexes suspended in high salt containing aqueous buffers at biological pH 7, such as ammonium acetate to maintain their native-like structure in solution. Once in the gas-phase, declustering and desolvation are critical parameters, as described extensively in the literature.

The difference in size, based on collision cross section [1], between a small molecule like acetaminophen and a non-covalent complex as GroEL is about 200.

Due to this large difference, adjustments of the optical rail of the mass spectrometer is a recommended step to accommodate the anticipated different behavior of large molecules.

The previously developed SWARM tune for small molecules has already shown a substantial benefit in small molecule analyte abundance [2], so utilizing the same methodic for large molecules is an extension to the applications based tuning approach in the acquisition software.

Figure 1 shows how multiple elements of the optical rail are tuned simultaneously to find unambiguously the global maximum.

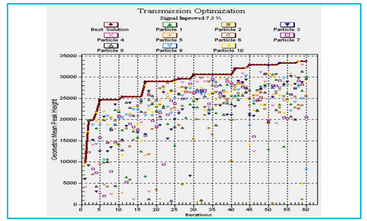

Figure 1: Screenshot from the MassHunter Acquisition UI, showing simultaneously tuning of multiple optical elements. Caption lists various SWARM particles.

Experimental

Experimental conditions: LC-MS

A fully automated System Tune is performed by introducing calibrant solution via the built-in calibrant delivery system. Using a prototype software, the newly developed large molecule Autotune was performed, and the signal abundance of the calibrant ion with the highest *m/z* value compared to the standard System tune.

In a next step, the signal abundance of a chromatographically separated monoclonal antibody was compared under the different tunes. Separation was done at standard flowrates, using a 2.1x50mm PLRPS- column (Agilent Technologies, CA, USA) with formic acid as modifier.

Experimental conditions: native-MS

For native MS analysis, alcohol dehydrogenase was resuspended in 100 mM Ammonium acetate to a final concentration of 1uM. GroEL was prepared according to Campuzano [3] to a final concentration of 1uM GroEL in 200 mM ammonium acetate. All enzymes and chemicals were obtained from (Sigma Aldrich, St. Louis, MO, USA) .

Infusion was performed using a syringe pump at 200 nl/min, using emitter tips with an 8 micron tip size (SIS, Ringoes, NJ, USA). MS analysis was done on a 6545XT AdvanceBio LC/Q-TOF (Agilent Technologies, Santa Clara, CA, USA).

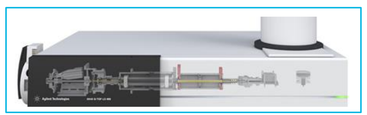

Figure 2: Schematic view of the 6545XT AdvanceBio LC/MS-QTOF.

For fragmentation of GroEL, nitrogen as collision gas was replaced with pure SF_6. Due to SF_6 having different properties, fragmentation can be achieved with much lower energy compared to nitrogen or argon. In addition, a newly designed differential pumping step on the 6545XT AdvanceBio LC/Q-TOF (Figure 2) allowed the use of sulfur hexafluoride.

A prototype software was used to smooth the GroEL fragment spectrum, performing a Savitzky-Golay smoothing of the raw spectra.

Results and Discussion

Most Autotunes of Q-TOF instruments are tunes which are designed to transmit ions in both low and high mass range. We recently demonstrated the benefits of dedicated small molecule tunes, and with this work continue to further develop this tailored strategy. When comparing the standard Autotune to the newly developed large molecule Autotune, we could observe a factor of >3 increase in abundance of 2722 calibrant ion (Figure 3).

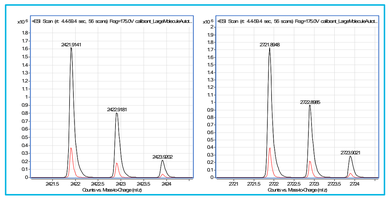

Figure 3: Comparison of high mass calibrant signals using Large Molecule SWARM Autotune (black)and Standard Mass Range SWARM Autotune (red), executed on the same instrument.

The same increase in abundance were observed when using a monoclonal antibody, demonstrating the proof of principle that the changes in the optical rail of the Q-TOF mass spectrometer behave similar for calibrant ions as for intact proteins in a similar *m/z* range. With formic acid as modifier, the most abundant observed charge state was at about *m/z* 3090.

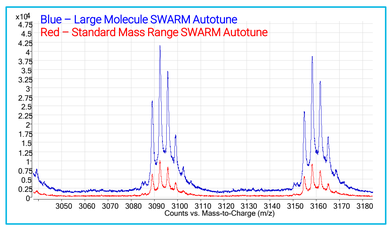

Figure 4: Intact mAb Mass Standard, average mass spectrum using Large Molecule SWARM Autotune and Standard Mass Range SWARM Autotune on the same instrument.

To further explore the utilization of the tune, we analyzed alcohol dehydrogenase (ADH), a 151 kDa tetramer, via nano-infusion under native MS conditions. Using the new tune with an acquisition rate of 1 sec, we had ~4000 counts per spectrum absolute abundance of ADH in the high *m/z range above* 5000. This high abundance makes it possible to fine tune method parameters by solely looking at the real-time acquisition window, compared to the previous need of acquiring and averaging data before decision making (Figure 5). No rolling average or other data manipulation were performed.

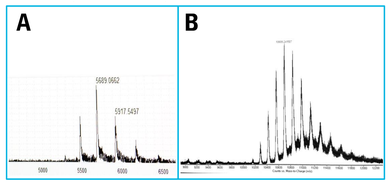

Figure 5: Screenshot from the Acquisition UI acquired at 1 spectra/sec for ADH (A) and GroEL (B).

Using the ion current obtained by the tune, a very fast fine tuning for collision cell pressure and collision energy is possible to obtain best spectra quality.

Figure 6 shows the benefit of the large molecule SWARM Autotune compared to the Standard SWARM Autotune for the Alcohol Dehydrogenase tetramer.

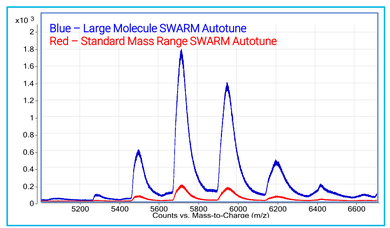

Figure 6: Alcohol Dehydrogenase, average mass spectrum using Large Molecule SWARM Autotune and Standard Mass Range SWARM Autotune executed on the same instrument.

Results and Discussion

In a next step to further explore the functionality and suitability of the newly developed Large Molecule SWARM Autotune we infused GroEL. The tetradecameric complex of in total 802kDa was readily visible in the Acquisition UI. Optimization of the native complex did not show a substantial difference between moderately applied collision energies and pressure. Notably, we used sulfur hexafluoride as collision/cooling gas, and presumably due to the need of ion-cooling lowering the pressure lead to an immediate loss of abundance.

The averaged (non smoothed) spectrum over a 2 min acquisition is shown in Figure 7, showing well resolved charge states between 10500 *m/z* and 11500 *m/z*, as well as more higher *m/z* species up to 14000 *m/z*.

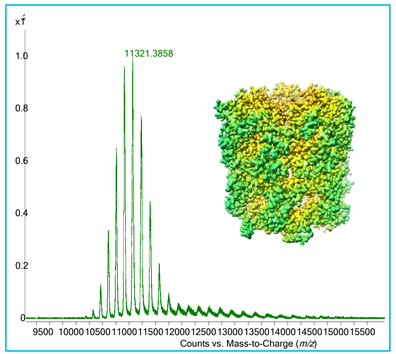

Figure 7: GroEL-14mer, unsmoothed spectrum of 2 min infusion at 200 nl/min of 5pmol GroEL in 200mM Ammonium acetate.

The purpose of using the large sulfur hexafluoride was to induce the ejection of a monomer from the tetradecameric complex, resulting in a tridecameric complex with much higher *m/z* as previously reported on a modified instrument [4]. Here we used the commercially available 6545XT AdvanceBio LC/Q-TOF to demonstrate that with the newly developed Large Molecule Autotune the detection of large complexes with high abundances is possible.

Figure 8 shows the smoothed spectrum of the tridecameric species after successful dissociation from a monomer at the 20,000 *m/z* region.

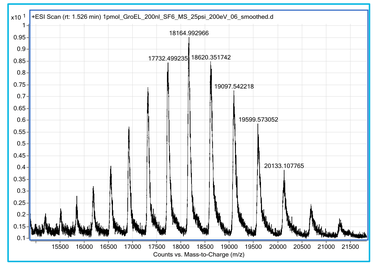

Figure 8: GroEL 13-mer, generated using SF_6 as collision gas at 200eV collision energy.

Conclusions

- Large Molecule SWARM Autotune shows 3-4x increase in large molecule abundance.
- Increased abundance allows to tune instrument via Acquisition UI interaction
- Differential pumping allows maintaining ultra-low pressure in the TOF region despite using SF_6 as collision gas
- Extended mass range on 6545XT AdvanceBio LC/Q-TOF allows for detection of non-covalent complexes at very high *m/z* ratios.

References

[1]Bush Lab, University of Washington http://depts.washington.edu/bushlab/ccsdatabase/

[2]Dorothy Yang, Christian Klein, Crystal Cody and Huy Bui http://www.agilent.com/cs/library/applications/5991-5485EN.pdf

[3]Iain Campuzano and Kevin Giles (2011) Nanoproteomics, chapter 5.

[4]Lorenzen, L., Versluis, C., van Duijn, E., van den Heuvel, R.H.H., Heck A.J.R. (2007) Int. J. Mass Spec.

Comprehensive Characterization on Monoclonal Antibody using a newly developed LC/Q-TOF Instrument

David Wong[1], Chris Klein[1] and Jing Chen[2]

1. Agilent Technologies, Inc., Santa Clara, CA, USA
2. Agilent Technologies, Inc., Madison, WI, USA

ASMS 2017
TP-034

Agilent
Trusted Answers

Overview

This work describes the utilization of the Agilent's 6545XT AdvanceBio LC/Q-TOF system for rapid characterization of Monoclonal Antibody (mAb) samples.

Introduction

Monoclonal antibodies and their derivatives comprise a very important class of biopharmaceutical molecules with a wide range of therapeutic and diagnostic applications. The comprehensive characterization provides not only the complete amino acid sequences of mAbs and their variants, but also the information on their post-translational modifications (PTMs) and locations. However, the lack of automatic workflow in the sample preparation, data processing and result interpretation has been the rate-limiting step for most biopharmaceutical laboratories. In this study, we demonstrate a high throughput workflow that utilizes an automated liquid-handling robot (AssayMAP), an Agilent Infinity II UHPLC system, a newly developed Agilent 6545XT AdvanceBio LC/Q-TOF system, and automated data processing using BioConfirm software for the intact mAb, the mAb subunits and its complete sequence mapping analysis. This system can also be used for the native protein complex analysis (over 800 kDa).

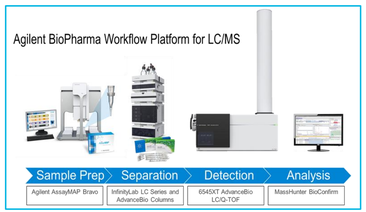

Figure 1. Agilent 6545XT AdvanceBio LC/Q-TOF system.

Experimental

Sample Preparation:

Monoclonal antibody (mAb) standard RM 8671 was purchased from National Institute of Standards and Technology (NIST).

The Agilent AssayMAP Bravo liquid handling system was used to dilute, digest, and desalt the NIST mAb sample. Enzymatic digestions were done using the IdeS protease (Genovis, Inc.) and the Rapid PNGase F (NEB). The digested samples were dried down and resuspended with 0.1 % TFA in DI water.

Approximately 0.5 µg of intact mAb, mAb subunits and mAb digested samples were injected for each LC/MS analysis.

Native GroEL sample was dissolved with 200 mM NH_4OAc into 1 pmol/µL.

LC/MS Analysis:

LC/MS analyses were conducted on an Agilent 1290 Infinity II UHPLC system coupled with an Agilent 6545XT AdvanceBio LC/Q-TOF system equipped with an Agilent Dual Jet Stream ESI source. LC separation for the intact and subunits samples was obtained with Agilent's PLRP-S column (2.1 X 50 mm, 5 µm, 1000Å), while the digested mAb sample was separated by an Agilent AdvanceBio Peptide Mapping column (2.1 X 150 mm, 2.7 µm).

Native protein samples (NIST mAb and GroEL) were infused into the Q-TOF at a flow rate of 200 – 500 nL/min using the 8 µm SilicaTip (PicoTip, New Objective).

Data Analysis:

All MS data of the mAbs were analyzed using the Protein Deconvolution feature of MassHunter BioConfirm B.08.00 software that uses the Maximum Entropy algorithm for accurate molecular mass calculation. Raw data acquired from LC/MS/MS were also processed using the BioConfirm B.08.00 software. This powerful algorithm simplifies downstream data analysis, enabling the automatic identification of peptides and PTMs when compared to a theoretically digested NIST mAb sequence.

Results and Discussion

Workflow 1: Intact mAb Analysis (Agilent App Note: 5991-7813EN)

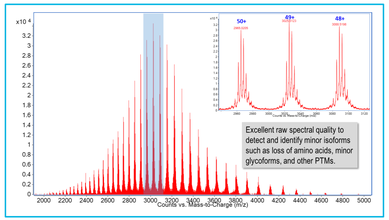

Figure 2. Intact NIST mAb Analysis (0.5 µg injection).

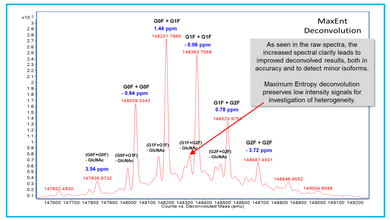

Figure 3. MS Deconvolution of Intact NIST mAb. Mass accuracies for all major glycoforms are: < 5 ppm.

Workflow 2: mAb Subunits Analysis

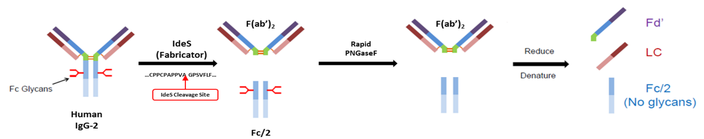

Scheme 1: Sample Preparation Workflow: Enzymatic digestions (IdeS and PNGaseF) and reduction on mAb.

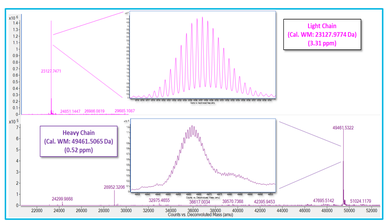

Figure 4. Light and heavy chain of NIST mAb.

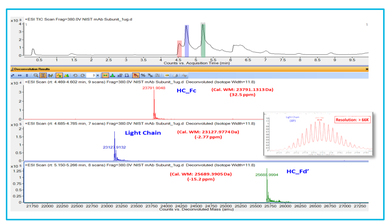

Figure 5. Light chain, Fc and Fd' of heavy chain of NIST mAb. MS resolution: > 66,000 at 2300 *m/z*.

Results and Discussion

Workflow 3: Peptide Sequence Mapping and PTM Identification: (App Note: 5991-7815EN)

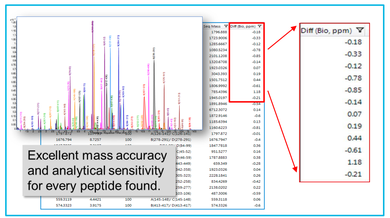

Figure 6. Peptide Mapping and PTM Identification of NIST mAb.

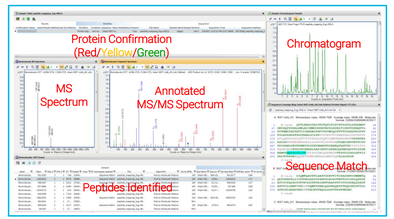

Figure 7. Agilent MassHunter BioConfirm software with representative peptide mapping results and protein sequence coverage.

Workflow 4: Native Protein Analysis:

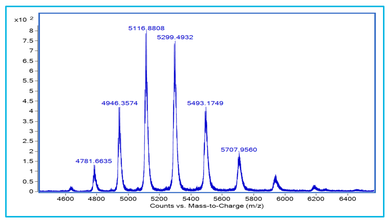

Figure 8. Native MS analysis of intact NIST mAb

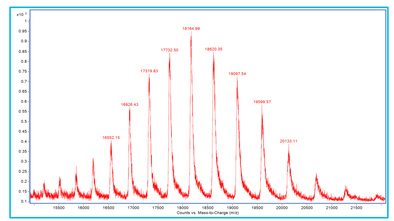

Figure 9. Native MS analysis of GroEL Tridecamer. (Mass range of the 6545XT *m/z*: 30,000 Da)(see Poster ThP 161 for more details)

Workflow 5: mAb Sensitivity Analysis
(App Note: 5991-7814EN)(ASMS Poster: WP 637)

Workflow 6: mAb Glycan Quantitative Analysis
(ASMS Poster: TP 316)

Workflow 7: ADC DAR Analysis
(ASMS Poster: TP 082)

Workflow 8: Host Cell Proteins Analysis
(ASMS Poster: WP 694)

Workflow 9: mAb Disulfide Bonds Analysis
(App Note: 5991-6951EN)

Conclusions

We have demonstrated comprehensive high-throughput mAb analysis workflow solutions integrating automated liquid-handling robot (AssayMAP Bravo), high-performance chromatography technologies, the Agilent 6545XT AdvanceBio LC/Q-TOF, and Agilent MassHunter BioConfirm software for automatic data processing.

Automated Determination of ADC Drug-Antibody Ratios Using an Open Access System

Tanner Stevenson[1], Stephen Madden[1], David Wong[1], Shuai Wu[1], Jade Byrd[1], Robert Williams[1]

[1]Agilent Technologies, Inc. Santa Clara, California

ASMS 2017
TP - 082

Agilent
Trusted Answers

Introduction

Antibody-drug conjugates (ADCs) are an innovative means of targeted drug delivery which are composed of an antibody, a linker, and a cytotoxic drug. One measurement to characterize the efficacy of an ADC sample is the drug-to-antibody ratio (DAR): the average number of drug molecules per antibody[1].

DAR is calculated as a weighted sum of the relative abundances of each drug load species. In order to determine the relative abundances, each species must be individually resolved. LC/MS analysis with spectral deconvolution is a popular method for this analysis, however the process can be complex and tedious. To reduce this complexity, a workflow has been developed consisting of three components: a biopharmaceutical analysis software, a DAR calculator, and an Open Access interface (Figure 1). Together, these components enable a novice user to quickly and accurately determine DAR values with minimal mass spectrometer training. In this study, an array of data from different DAR analyses was studied to compare the accuracy and efficacy of automated DAR calculations using this open access workflow.

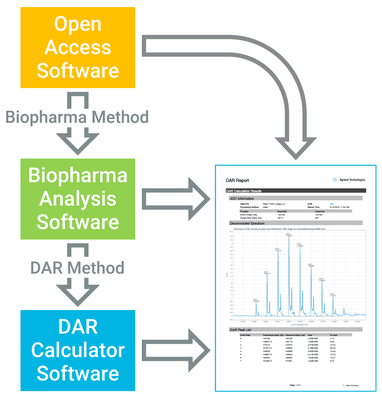

Figure 1. DAR Calculation Open Access Workflow.
Different levels of CAR Calculation automation exist at each step in the workflow

Experimental

Sample Preparation

All DAR analyses used ADC standard (T-DM1) obtained from Genentech that was reconstituted in deionized water. Each analysis used one or more of the following processing techniques: native, deglycosylated, reduced, and reduced deglycosylated. Reduced samples were processed with 35 mM DTT in 10 mM Tris buffer and deglycosylated samples were processed with rapid PNGase F (diluted 1:40) in 10 mM Tris buffer.

LC/MS Analysis

LC/MS analyses were conducted using an Agilent 1290 Infinity II UHPLC connected to either an Agilent 6230 TOF[2] or an Agilent 6545XT AdvanceBio Q-TOF[3], both equipped with an Agilent Dual Jet Stream ESI source. All four sample types were run on the 6230 TOF and native and deglycosylated ADCs were run on the 6545XT Q-TOF. Approximately 1.4 µg of ADC was injected for each run.

Data Analysis

Data analysis was performed both manually and automatically on the same data using the same method parameters. The MassHunter BioConfirm B.08 software was used to extract and deconvolute the data using the Maximum Entropy deconvolution algorithm. The DAR Calculator 1.1 software was used to integrate the peaks of the deconvoluted spectrum and calculate the DAR value using the following formula:

$$DAR = \sum_{i=0}^{n}\left[i \times \left(\frac{A_i}{A_{total}}\right)\right]$$

Where *i* denotes the number of drugs attached to the antibody and *Ai* denotes the area under each DAR species peak cluster, which includes all glycan peaks.

MassHunter Walkup B.02.02 software was used to initiate the sample run with automated analyses. The automatic DAR calculation results were recorded, then the peak integration limits were adjusted as necessary before recording the final DAR. The same data files were then analyzed manually. The accuracy and precision of the automated DAR calculation results were compared between each sample type. Paired two-tailed t-tests were used to compare both the automated and adjusted automated results to the manual results ($p<0.05$).

Results and Discussion

Automated DAR calculation accuracy varied significantly by processing technique (Table 1). Automated results were the most accurate for deglycosylated samples, followed by native and reduced samples. Although the reduced deglycosylated results reported DAR values were accurate, they were significantly different from the manual results. Adjusted automated results were statistically similar to the manual results for all samples except reduced. The accuracy of the adjusted automation results suggests that automated and manual processing of ADCs in BioConfirm can be consistently equivalent. Therefore, it is evident that the discrepancy in the automated results is largely due to the DAR Calculator's operation when identifying peak cluster limits in a noisy signal (see Figure 2).

Table 1. Computed DAR values across all analyses by preparation method

Processing Method		Manual	Automated	Automated Adjusted
Native	DAR	3.5	3.3*	3.5
	CV	2.5%	4.9%	2.3%
Deglycosylated	DAR	3.6	3.6	3.6
	CV	2.7%	2.2%	2.3%
Reduced	DAR	3.2	3.0*	3.3*
	CV	5.8%	6.9%	5.4%
Reduced Deglycosylated	DAR	3.0	3.0*	3.0
	CV	3.1%	2.8%	2.9%

*Results are significantly different from the manual results ($p<0.05$)

Manual Analysis

Manual analysis required a total of 8 steps to reach a DAR value:

1. Initiate the sample run from Walkup
2. Open the data file and method in BioConfirm
3. Extract the peak spectrum
4. Deconvolute the spectrum
5. Export the spectrum to CSV
6. Load the CSV into the DAR Calculator
7. Apply the DAR Calculator method
8. Manually adjust DAR peak limits (if necessary)

T-DM1 has a DAR value of 3.5 on average[4], which indicates the manual results for the intact and deglycosylated samples were accurate. Although the reduced and reduced deglycosylated samples both had average DAR values lower than expected, 3.23 and 3.03 respectively (Table 1), the manual results were used as the comparison baseline for the purposes of this study.

Automated Analysis

Automated analysis required a total of 3 steps to reach a DAR value:

1. Initiate the sample run from Walkup
2. Load the data file into the DAR Calculator
3. Manually adjust DAR peak limits (if necessary)

Deglycosylated and reduced deglycosylated samples had the most accurate automated results, whereas native and reduced samples had DAR values 0.25 less than the manual results, on average. This discrepancy is largely due to variation in automatic placing of peak cluster limits. Automatic peak finding for deglycosylated samples was more accurate because of their cleaner signals (Figure 2). Although the results for non-deglycosylated samples had slightly inaccurate results, the automated workflow still saved significant analysis time by removing all manual steps except DAR peak adjustment.

Results and Discussion

Table 2. DAR Calculation adjustment data across all analyses by preparation method

Processing Method	DAR Adjustment Amount	Percent Adjustment	Percent Adjusted
Native	0.22	6.3%	100%
Deglycosylated	0.02	0.44%	58%
Reduced	0.29	9.1%	100%
Reduced Deglycosylated	0.04	1.3%	94%
All	0.14	4.0%	86%

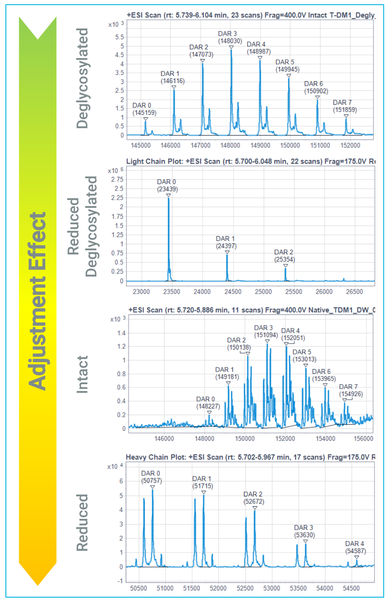

Figure 2. Example Automated DAR Peak Finding Results

Automated Results Adjustment

On average, 86% of data files had to be adjusted, however adjusted amounts varied significantly between samples (Table 2). On the low end, although 58% of deglycosylated samples had to be adjusted, the average DAR adjustment amount was only 0.02. On the high end, all reduced sample's DAR values were adjusted by 0.29 on average. Example spectra needing adjustment can be seen in Figure 2.

Conclusions

- Automating DAR calculations from Walkup significantly reduced analysis time and effort by removing manual data handling steps
- Cleaner deconvoluted signals led to more accurate and precise automated DAR results, while noisier signals required more manual peak limit adjustments
- Although a majority of results required adjusting, the average change in DAR value was only 4%

References

1. Chen, J. et al. "Drug-to-Antibody Ratio (DAR) Calculation of Antibody-Drug Conjugates (ADCs)" Agilent Application Note, 5991-6263EN, 2015.
2. Wong, D. et al. "An Integrated Workflow for Automated Calculation of Antibody-Drug Conjugate (ADC) Drug-to-Antibody Ratio (DAR)" Agilent Application Note, 5991-7366EN, 2016.
3. ASMS Poster MP-132

A Simple Workflow for Monoclonal Antibody N-Glycan Analysis by LC-FLD-SQ

Oscar Potter, Greg Staples, Jordy Hsiao and Te-Wei Chu

Agilent Technologies, 5301 Stevens Creek Blvd, Santa Clara, CA 95051, USA

ASMS 2017
WP-643

Agilent
Trusted Answers

Introduction

Background

Analysis of mAb glycosylation is often performed by enzymatic release of N-glycans followed by labelling with a fluorescent tag and hydrophilic interaction chromatography (HILIC). This allows for accurate relative quantitation of glycans, but often suffers from coelutions and challenging peak assignment.

Fortunately, a mass selective detector (MSD) can be coupled downstream of the fluorescence detector (FLD) so that m/z data is available to assist peak assignment and detect coeluting structures. It is now possible to use a single quadrupole (SQ) MS for this purpose due to two recent advances:
(1) the LC/MSD XT, available with the highly sensitive Agilent Jetstream (AJS) ESI source, which enhances ionization
(2) the InstantPC glycan tag from Prozyme Inc., which dramatically enhances N-glycan ionization efficiency.

We present a HILIC-FLD-MSD workflow that uses these innovations to give robust N-glycan quantitation with high confidence peak assignment and the ability to determine coeluting structures.

Operating the SQ in scan mode provides m/z data for all peaks in the FLD chromatogram, as shown below for a sample of N-glycans from 3 µg of mAb:

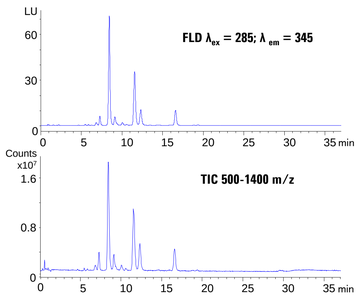

Experimental

Sample Preparation.

All mAb samples were adjusted to 1 µg/µL prior to processing by GlykoPrep®-plus Rapid N-Glycan Sample Preparation with InstantPC (96-ct) from Prozyme Inc. (GPPNG-PC). The sample handling was automated through the use of the AssayMap Bravo Liquid Handling Platform (G5542A). This workflow has the advantage of not requiring any centrifugation or dry down steps.

Samples:

CHO mAb 1 (from our lab)
SiLu™ Lite P/N MSQC4 from Sigma-Aldrich
Nist mAb (NIST, Reference Material 8671).

AssayMap Bravo automated liquid handling platform

Chromatography

Pump: 1260 Infinity II Binary Pump G7112B

Eluent A: 50 mM formic acid adjusted to pH 4.5 with ammonium hydroxide

Eluent B: Acetonitrile

Sampler: G7167A 1260 Infinity II Multisampler with thermostat @ 11 ° C

Column heater: Agilent 1260 Infinity II G7116 TCC @ 40 °C,
with G7116-60015 solvent preheater

Columns were plumbed via 100 µm ID SSTL tubing to a 1260 Infinity Fluorescence Detector (G1321B) with 8 µL flow cell (G1321-60005). The detector was set to λEX @ 285nm, λEm @ 345 nm with PMT gain = 10.

Elution programs were as shown below:

Method A

Time	A	B	Flow
min	%	%	mL/min
0	25	75	0.7
0.5	27	73	0.7
4	28	72	0.7
9	33	67	0.7
9.2	50	50	0.7
9.7	50	50	0.7
10	25	75	0.7
11.5	25	75	0.7
11.8	25	75	0.8
14.5	25	75	0.9
15.3	25	75	0.7
Stoptime = 18 min			

Method B

Time	A	B	Flow
min	%	%	mL/min
0	27	73	0.5
1	28.5	71.5	0.5
9	29.5	70.5	0.5
22	41	59	0.5
22.5	50	50	0.8
23.5	50	50	0.7
23.7	27	73	0.7
25	27	73	0.7
25.5	27	73	0.8
27.5	27	73	0.9
28	27	73	0.5
Stoptime = 30 min			

Method C

Time	A	B	Flow
min	%	%	mL/min
0	22	78	0.6
0.5	26	74	0.6
13	27.5	72.5	0.6
28	39	61	0.6
28.5	50	50	0.5
28.6	50	50	0.4
28.8	22	78	0.4
31	22	78	0.5
31.5	22	78	0.55
33.5	22	78	0.6
Stoptime = 37 minutes			

LC/MSD XT parameters

Ion source: Agilent Jetstream in positive mode
Sheath gas: 300 °C at 10.0 l/min
Dry gas temp: 150 °C at 9.0 l/min
Nebulizer: 35 psig; VCap: 2500 V Nozzle: 500 V
Mass range: 500 – 1400 m/z
Fragmentor: 100 V (low) or 275 V (high)
Gain EMV: 1.0; Step size: 0.10; Peak width: 0.2

Results and Discussion

N-glycan separation

Three methods were developed for the separation of mAb N-glycans. The highest resolution was achieved with a 37 minute cycle time on the 1.8 µm 2.1 x 150 AdvanceBio Glycan Mapping column. This method was used for the remainder of the experiments.

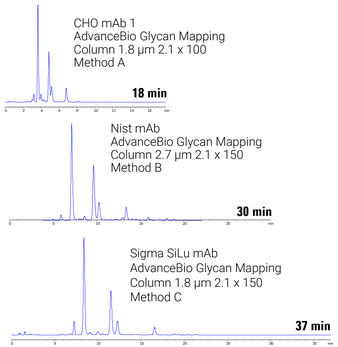

MSD sensitivity

The LC/MSD XT showed excellent sensitivity for InstantPC labelled N-glycans in scan mode. N-glycans were observed almost exclusively as doubly charged ions, predominantly of the form $[M+2H]^{2+}$. Clear signals were observed for N-glycans comprising as little as 0.3% of the glycan profile, as shown below:

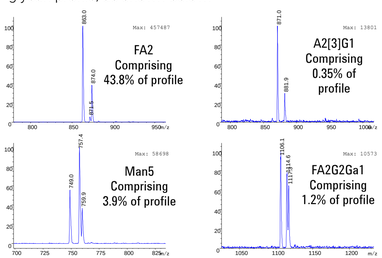

Fragmentation of glycans using the SQ

While MSD parameters were initially optimized to give strong intact signals for the N-glycans, we found that increasing the fragmentor voltage gave rich CID spectra. Therefore, we set the SQ to run scans with alternating high and low fragmentor voltage in order to simultaneously generate intact glycan spectra alongside fragmentation spectra.

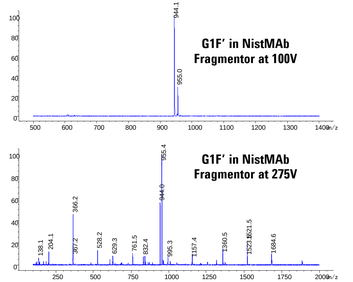

In one case, intact glycan spectra left some ambiguity for the composition and structure assignment, since there were at least two possibilities with the same parent m/z.

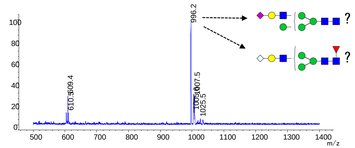

Fortunately, the fragmentation spectra clearly confirmed one of the structures due to the presence of two diagnostic fragment signals.

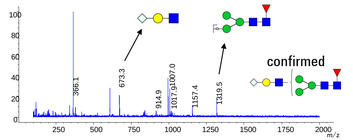

Results and Discussion

Peak assignment

The three mAb N-glycan samples were analyzed using Method C.

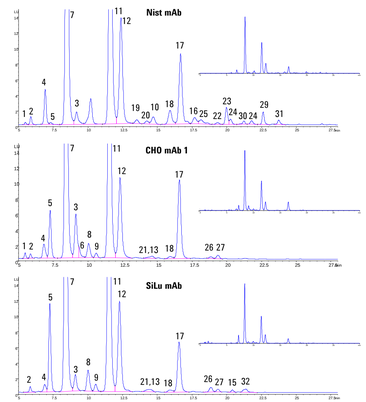

The peaks were integrated and assigned to N-glycan compositions based primarily on $[M+2H]^{2+}$ m/z values.

ID	Observed [M+2H]2+	Proposed Composition	Theoret [M+2H]2+	Proposed Structure Oxford	Proposed Structure Alternative
1	659.9	F1+Core	659.774	F1M3	G0F-2GlcNAc
2	688.4	N1+Core	688.284	A1	G1-GlcNAc
3	748.9	H2+Core	748.798	M5	Man5
4	761.5	N1F1+Core	761.313	FA1	G0F-GlcNAc
5	790.0	N2+Core	789.824	A2	G0
6	842.4	H1N1F1+Core	842.340	FA1G1	G1F-GlcNAc
7	863.0	N2F1+Core	862.853	FA2	G0F
8	871.0	H1N2+Core	870.851	A2[6]G1	G1
9	871.0	H1N2+Core	870.851	A2[3]G1	G1'
10	923.6	H2N1F1+Core	923.366	FAG1Ga1	-
11	944.0	H1N2F1+Core	943.879	FA2[6]G1	G1F
12	944.0	H1N2F1+Core	943.879	FA2[3]G1	G1F'
13	952.0	H2N2+Core	951.877	A2G2	G2
14	964.7	N3F1+Core	964.393	FA2B	G0FB
15	991.9	H5+Core	991.877	M8	Man8
16	996.1	H1N1Sg1F1+Core	995.885	FA1G1Sg1	G1Sg1F-GlcNAc
17	1025.1	H2N2F1+Core	1024.906	FA2G2	G2F
18	1025.1	H2N2F1+Core	1024.906	FA2G1Ga1	G1F+aGal
19	1045.6	H1N3F1+Core	1045.419	FA2[6]B1G1	G1FB
20	1045.7	H1N3F1+Core	1045.419	FA2[3]B1G1	G1FB'
21	1089.5	H1N1F1S1+Core	1089.427	FA1G1S1	G1S1F-GlcNAc
22	1097.7	H1N2F1Sg1+Core	1097.425	FA2G1Sg1	G1Sg1F
23	1106.1	H3N2F1+Core	1105.932	FA2G2Ga1	G2F+aGal
24	1106.1	H3N2F1+Core	1105.932	FA2G2Ga1 iso	G2F+aGal'
25	1126.5	H2N3F1+Core	1126.446	FA2BG2	G2FB
26	1170.4	H2N2F1S1+Core	1170.454	FA2G2S1	A1F
27	1170.4	H2N2F1S1+Core	1170.454	FA2G2S1 iso	A1F iso
28	1178.7	H2N2F1Sg1 + Core	1178.451	FA2G2Sg1	Ag1F
29	1187.1	H4N2F1+Core	1186.959	FA2G2Ga2	G2F+(aGal)2
30	1207.7	H3N3F1+Core	1207.472	FA2BG2Ga1	G2FB+aGal
31	1259.4	H3N2F1Sg1+Core	1259.477	FA2G2Sg1Ga1	Ag1F+aGal
32	1316.2	H2N2F1S2+Core	1316.001	FA2G2S2	A2F

Results

Relative sum abundance of each N-glycan was calculated by integrating the FLD peak area. In the case of a few coeluting structures, the MSD spectrum was integrated across the time period of the FLD peak. The FLD area was then apportioned to both structures according to the combined relative intensity of the doubly charged ions for the two N-glycans that were present in those peaks.

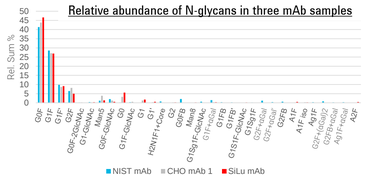

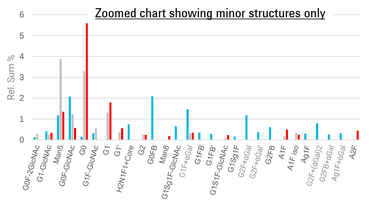

Conclusions

- Glycans are reliably profiled and confidently confirmed with the addition of mass selective detection using the Agilent LC/MSD XT single quadrupole to FLD analysis.
- A method was developed that gave excellent resolution and allowed for the determination of N-glycans with less than 0.3% relative abundance.
- Reliable and sensitive single quadrupole technology provides an affordable solution to glycan profiling.

See also *Comparison of Relative Quantitation of Monoclonal Antibody N-glycans from Fluorescence and MS Detection* https://www.agilent.com/cs/library/applications/5991-6958EN.pdf

Enhanced Analysis of Host Cell Proteins from CHO Cell Cultured mAb Using a Newly Developed Q-TOF Instrument

Linfeng Wu[1], Xinning Jiang[1], Te-Wei Chu[1], Alex Zhu[2], and Jordy J. Hsiao[1]

[1] Agilent Technologies, Santa Clara, CA; [2] Agilent Technologies, Wilmington, DE

ASMS 2017
WP-694

Agilent
Trusted Answers

Introduction

Host cell proteins (HCPs) are process-related impurities during biologics production. Due to their potential to affect product safety and efficacy, identification and quantification of HCPs in drug product is required. Traditionally ELISA is used to monitor the removal of HCPs during bioprocess development. LC/MS analysis has recently emerged as an alternative method that could provide more in-depth characterization of HCPs.

In this study, digest proteins from a purified human IgG1 mAb produced from CHO cells were subjected to one dimensional (1D) LC/MS analysis using the Agilent 6545XT AdvanceBio LC/Q-TOF with a new mode of acquisition, IterativeMS/MS. UPS2 protein standards were spiked in the sample to test HCP analysis. Excellent protein identification and quantification for low level HCPs was achieved by this platform.

Experimental

Sample Preparation

Proteomics Dynamic Range Standard (UPS2, Sigma) was spiked into CHO cell cultured human IgG1 mAb at 1:1000 w/w ratio. Sample without UPS2 spike was prepared in parallel as a negative control. Protein sample was reduced, alkylated and trypsin digested. Digested sample was directly injected for 1D LC/MS experiment.

LC Conditions

Agilent 1290 Infinity II UHPLC with an Agilent AdvanceBio Peptide Plus column (2.7 µm, 2.1x150 mm, PN 675950-902)

LC Parameters	
Mobile phase A	H_2O, 0.1% formic acid
Mobile phase B	90% Acetonitrile, 0.1% formic acid
Flow rate	0.4 mL/min
Gradient	1.0 min → 3% B 50.0 min → 21% B 53.0 min → 90% B 55.0 min → 90% B 55.1 min → 3% B
Stop time	60 min
Column Temperature	60°C

Experimental

MS Conditions

Agilent 6545XT AdvanceBio Q-TOF system with Agilent JetStream source[1].

MS Parameters	
Drying gas temperature	290°C
Drying gas flow	13 L/min
Nebulizer	35 psi
Sheath gas temperature	275°C
Sheath gas flow	12 L/min
Isolation width	Narrow (~1.3m/z)
Acquisition mode	IterativeMS/MS or standard AutoMS/MS as indicated
Dynamic exclusion within run	2 spectra release after 0.2 min
MS mass range	250 -1700 m/z
MS acquisition rate	10 spectra/second
MS/MS mass range	50 - 1700 m/z
MS/MS acquisition rate	3 spectra/second

Data Analysis

Protein database searching was done using Agilent Spectrum Mill Software, and peptide spectral matches were validated by 1% FDR filter.

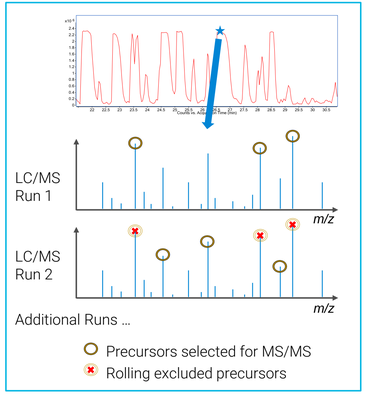

Figure 1. Automated iterative MS/MS

Results and Discussion

Enhanced protein identification by iterative MS/MS

Protein digest was injected for LC/MS experiment using either IterativeMS/MS or a standard AutoMS/MS acquisition with five injections for each method showing the following results:

- Iterative MS/MS acquisition automatically excludes precursors which have been selected for MS/MS in previous runs (Figure 1)
- Iterative MS/MS showed decreased redundant MS/MS spectra and overall increased unique peptide numbers compared to replicate auto MS/MS acquisition (Table 1)

Protein name	Unique peptide #		Spectra #	
	Iterative MS/MS	Auto MS/MS	Iterative MS/MS	Auto MS/MS
mAb heavy chain	42	35	690	1564
mAb light chain	23	21	332	746
Serum albumin	23	18	36	106
Carbonic anhydrase 2	7	6	21	47
Carbonic anhydrase 1	9	6	16	32
Leptin	2	2	5	12
Hemoglobin subunit beta	5	4	8	17
Hemoglobin subunit alpha	3	2	9	15
Ubiquitin	2	3	3	17
Complement C5/C5a anaphylatoxin	1	2	2	8
Small ubiquitin-related modifier 1 (SUMO-1)	3	2	4	3
Peroxiredoxin 1	4	4	8	17
Myoglobin	1	2	1	7

Table 1. Comparison of protein identifications between iterative MS/MS and replicate auto MS/MS

HCP identification sensitivity and proteome coverage

Using UPS2 protein standard as a benchmark and non-spiked mAb as a negative control to assess HCP identification sensitivity and proteome coverage, digest samples were subjected to 1D LC/MS experiment with IterativeMS/MS acquisition. Two injection methods were used (24µg x 5 injections and 32µg x 3 injections) showing the following results:

- Excellent peak chromatography for co-eluting peptides with a broad dynamic range (Figure 2): > 4 orders in peak intensity, >5 orders in protein levels in weight
- Excellent identification of low level HCP (Table 2): 2 unique peptides for the protein at 2.7 ppm level with 3 injections
- Excellent proteome coverage with identification of all the proteins above 7.6 ppm (Table 2)

Protein Accession	Amount (fmoles) in UPS2 vial	Molecular weight (Da)	Protein name	Protein level relative to mAb (w/w, ppm)	Unique peptide #			
					mAb spiked with UPS2 (24µg x 5 inj.)	mAb only (24µg x 5 inj.)	mAb spiked with UPS2 (32µg x 3 inj.)	mAb only (32µg x 3 inj.)
P02768	50000	66,357	Serum albumin	313.0	23	0	19	0
P00918	50000	29,115	Carbonic anhydrase 2	137.3	7	0	5	1
P00915	50000	28,739	Carbonic anhydrase 1	135.6	9	1	6	0
P41159	50000	16,158	Leptin	76.2	2	0	3	0
P68871	50000	15,867	Hemoglobin subunit beta	74.8	5	0	7	1
P69905	50000	15,126	Hemoglobin subunit alpha	71.3	3	0	2	0
P62988	50000	10,597	Ubiquitin	50.0	2	0	5	0
P01031	50000	8,563	Complement C5/C5a anaphylatoxin	40.4	1	0	2	0
P04040	5000	59,625	Catalase	28.1	0	0	2	1
P63165	5000	38,815	Small ubiquitin-related modifier 1 (SUMO-1)	18.3	3	0	0	0
P15559	5000	30,736	NAD(P)H dehydrogenase [quinone] 1	14.5	0	0	2	0
Q06830	5000	21,979	Peroxiredoxin 1	10.4	4	3	3	3
P62937	5000	20,176	Peptidyl-prolyl cis-trans isomerase A	9.5	0	0	1	0
P02144	5000	17,053	Myoglobin	8.0	1	0	1	0
P00167	5000	16,022	Cytochrome b5	7.6	0	0	1	0
P01133	5000	6,353	Pro-epidermal growth factor (EGF)/Epidermal growth factor	3.0	0	0	0	0
P12081	500	58,233	Histidyl-tRNA synthetase, cytoplasmic	2.7	0	0	2	0
P06732	500	43,101	Creatine kinase M-type	2.0	0	0	0	0
P16083	500	25,821	Ribosyldihydronicotinamide dehydrogenase	1.2	0	1	0	0

Table 2. Comparison of UPS2 protein identifications in mAb sample with or without a UPS2 spike. All the UPS2 proteins above 1 ppm were listed to show both identified sensitivity and proteome coverage. A few UPS2 proteins present in non-spike mAb are likely due to protein homologs in the purified mAb, e.g. Peroxiredoxin 1.

Results and Discussion

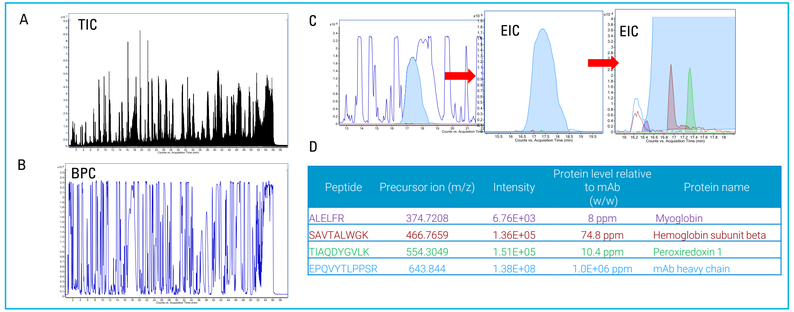

Peptide	Precursor ion (m/z)	Intensity	Protein level relative to mAb (w/w)	Protein name
ALELFR	374.7208	6.76E+03	8 ppm	Myoglobin
SAVTALWGK	466.7659	1.36E+05	74.8 ppm	Hemoglobin subunit beta
TIAQDYGVLK	554.3049	1.51E+05	10.4 ppm	Peroxiredoxin 1
EPQVYTLPPSR	643.844	1.38E+08	1.0E+06 ppm	mAb heavy chain

Figure 2. Total ion chromatography (TIC), base peak chromatography (BPC) and extracted ion chromatography (EIC) of four co-eluting peptides (in color) were shown. High loading capacity (32 µg on-column) was demonstrated by good peak shape of extremely high abundant mAb peptides in A, B and C. Broad dynamic range of peak intensity for co-eluting peptides (> 4 orders) was shown in C and D. The corresponding proteins for co-eluting peptides have an over 5 orders of dynamic range in weight. Peroxiredoxin 1 protein level was underestimated due to presence of homologs in the purified mAb sample.

HCP label-free quantification

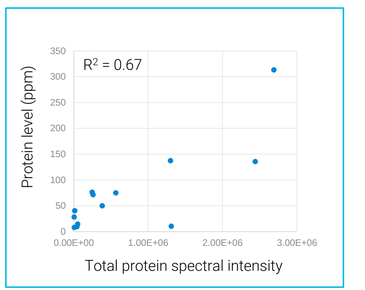

Figure 3. Correlation between protein level in ppm and total protein spectral intensity shows good reliability of label-free quantification for HCPs.

Conclusion

- A host cell protein analysis workflow was demonstrated using the newly developed Agilent 6545XT AdvanceBio LC/Q-TOF
- Simple sample preparation process was used without off-line fractionation or desalting
- 1D LC/MS with data-dependent acquisition was used for accurate protein identification
- Automated IterativeMS/MS acquisition improved protein identification coverage
- Simultaneous protein identification and quantification were shown for low level HCP
- Broad dynamic range allows detection and identification of low level HCP peptides co-eluting with extremely intense mAb peptides

References

[1]Agilent 6545XT AdvanceBio LC/Q-TOF System: Designed for Biopharma. *Agilent Technologies*, publication number 5991-7915EN

Agilent Technologies